UNIVERSITY OF LIVERPOOL

Development of High-Temperature and High-Performance Glass Fibre/PAEK Thermoplastic Prepregs

Thesis submitted in accordance with the requirement of the

University *of* Liverpool for the degree of

Doctor of Philosophy

By

Alireza Moradi

April 2021

DECLARATION

I hereby declare that thesis entitled "*Development of High-Temperature and High-Performance Glass Fibre/PAEK Thermoplastic Prepregs*" is the result of my own work and investigation, except where states otherwise by reference or acknowledgment. This thesis is being submitted in partial fulfilment of the requirements for the degree of PhD. The work presented has not been previously submitted for the award of any other degree of any institution, nor is being submitted concurrently in candidature for any degree or other award.

Alireza Moradi

April 2021

ACKNOWLEDGMENTS

I wish to express my deepest love and gratitude to my parents, Sharareh and Mohammadjavad, my sister, Negar, and my wife, Niloofar, for their unparalleled love and support throughout the entirety of my study. This thesis cannot be completed without their sacrifice and tolerance.

My most sincere gratitude goes to my mentor and supervisor Dr. Zhongwei Guan, who gave me the opportunity to pursue my PhD degree in the University of Liverpool under his guidance. His support, encouragements and feedbacks from the day I expressed my interest to join him in 2016, up until the time of submission of this thesis, has been most kind and valuable.

I also wish to send my warm regards and thanks to all the staff in the School of Engineering who provided their kind assistance in this project, especially Mr. Dave Atkinson, Mr. John Curran, Mr. Derek Neary, Mr. Glen Friel, Mr. Marc Bratley and Mr. Jiji Mathew.

I dedicate this work to God Almighty, who is my strong pillar and creator. Who has made possible and brought me this far. Who is my source of wisdom, knowledge, inspiration and understanding.

I would like to finish off with a verse from the great Persian Sufi mystic, Rumi:

"*Yesterday I was clever, so I wanted to change the world. Today I am wise, so I am changing myself.*"

– **Rumi**

PUBLICATIONS

Moradi, A., and Guan, Z. W., 2020, "Method, product and apparatus," The University of Liverpool, Patent application number GB2016847.2 (Patent pending).

Moradi, A., and Guan, Z. W., 2021, "New technology for lateral spreading of fibre bundles for application in thermoplastic composites," (To be submitted).

Moradi, A., Sun, C., and Guan, Z. W., 2021, "The design and manufacture of a novel thermoplastic prepreg rig based on aqueous impregnation. Part A: Procedure and optimisations," (To be submitted).

Moradi, A., Sun, C., and Guan, Z. W., 2021, "The design and manufacture of a novel thermoplastic prepreg rig based on aqueous impregnation. Part B: Physical and mechanical evaluations," (To be submitted).

Moradi, A., and Guan, Z. W., 2021, "Incorporation of graphene and nanoclay in S2-glass/PAEK composite materials: Physical and mechanical evaluations," (To be submitted).

ABSTRACT

This research project introduces a novel technique of manufacturing thermoplastic prepregs using an aqueous method. Wet powder technology is utilised for this purpose, based on the concept of suspending polymer particles in a liquid carrier and passing fibre reinforcement through a slurry bath containing the aqueous medium so to pick up the resin particles and subsequently, forming a composite material. An in-house unidirectional prepreg production rig is designed and manufactured, based on the concept of drum winding. The prepreg rig benefits from a novel fibre spreading device, designed and manufactured specifically for use with the in-house rig, with ability to adjust the tow/prepreg thickness.

The developed manufacturing method provides grounds for a very effective thermoplastic prepreg production in terms of cost, scale and suitability. Wide range of polymers and fibres can be used with an effective resin impregnation and rapid production. The prepreg rig itself is easily maintained, compact in size, and suitable for laboratory scale research. It also offers the ability to produce high-temperature and high-performance thermoplastic prepregs at considerably low costs.

Numerous physical and mechanical tests are carried out on the manufactured S2-glass fibre/PAEK composite materials with different constituent ratios to evaluate the efficiency of the production line and quality of the manufactured materials. Some notable achievements are the ability to manufacture virtually void-free composite laminates with up to 72 % fibre volume content, and observing low reduction (<16 %) of tensile strength for samples tested in elevated temperatures at 250 °C.

The aqueous manufacturing method allows easy incorporation of nanomaterials inside the resin matrix. Graphene and nanoclay are added into the resin bath to evaluate the changes in physical and mechanical properties of the prepregs and laminates. It is realised that graphene can enhance the tensile properties of the samples by up to 14 %, and flexural properties by up to 38 %, depending on the concentration. Nanoclay is found to deteriorate the tensile strength and only contributes towards higher flexural properties.

TABLE OF CONTENTS

LIST OF FIGURES

LIST OF TABLES

NOMENCLATURE

Abbreviations

0D	Zero Dimensional
1D	One Dimensional
2D	Two Dimensional
3D	Three Dimensional
ACM	Advanced Composite Material
Al	Aluminium
ASTM	American Society for Testing and Materials
BS	Backscattering
CF	Carbon Fibre
CMC	Ceramic Matrix Composites
CNT	Carbon Nanotubes
DC	Direct Current
DP	Diamond Polished
FRP	Fibre-reinforced Polymer
GF	Glass Fibre
HSCT	High Speed Civil Transport
ILSS	Interlaminar Shear Strength
K/E	Kethon/Ether Ratio
L2O	LiquiPowder
LaRC-TPI	Linear Aromatic Condensation-Thermoplastic Imide
Mg	Magnesium
MMC	Metal Matrix Composites
NF	Natural Fibre
NMP	N-Methyl-2-Pyrrolidone
PA	Polyamide
PAEK	Polyarylether Ketone
PAW	Prepreg Areal Weight
PBI	Polybenzimidazoles
PE	Polyethylene

PEEK	Polyether Ether Ketone
PEI	Polyether Imide
PEK	Polyether Ketone
PEKEKK	Polyetherketoneetherketone Ketone
PEKK	Polyether Ketone Ketone
PES	Polyether Sulfone
PMC	Polymer Matrix Composites
PP	Polypropylene
PPA	Polyphthal Amide
PPS	Polyphenylene Sulphide
PSD	Particle Size Distribution
SEI	Secondary Electron Imaging
SEM	Scanning Electron Microscope
SF	Synthetic Fibre
SI	International System of Units
SiO_2	Silicon Dioxide
SMLS	Static Multiple Light Scattering
T	Transmission
T/I	Terephthalic Acid/Isophthalic Acid Ratio
TEX	Linear Density (g/km)
TSI	Turbiscan Stability Index
UD	Unidirectional

Symbols

$\Delta\varepsilon$	Change in Strain
$\Delta\sigma$	Change in Stress
A	Average Cross-sectional Area
b	Sample Width
D	Cylindrical Support Diameter
E_c	Tensile Modulus of Composite
E_{chord}	Tensile Chord Modulus of Elasticity

E_f	Tensile Modulus of Fibre
E_f^{chord}	Flexural Chord Modulus of Elasticity
E_m	Tensile Modulus of Matrix
F_{ilss}	Interlaminar Shear Strength
h	Sample Thickness
L	Support Span Length
L_g	Gauge Length
m_1	Dry Specimen Mass
m_2	Immersed Specimen Mass
m_3	Soaked Specimen Mass
M_f	Fibre Mass
Mi	Specimen Initial Mass
P	Applied Load
P_m	Maximum Load
P_{max}	Maximum Tensile Force
T_g	Glass Transition Temperature
T_m	Melting Temperature
V_c	Composite Volume
V_f	Fibre Volume Content
V_m	Matrix Volume Content
V_v	Void Volume Content
wt%	Percentage by Weight
δ_u	Tensile Failure Displacement
ε_u	Tensile Failure Strain
ρ_c	Composite Density
ρ_f	Fibre Density
ρ_l	Liquid Density
ρ_m	Matrix Density
σ	Flexural Stress
σ_u	Ultimate Tensile Strength

CHAPTER I: INTRODUCTION

1.1 Overview

Composite materials are structural materials consisting of two or more combined individual constituents that are significantly different in physical and chemical properties. These constituents are normally combined in macroscopic level and will remain separate and are not soluble in each other. Usually, one of the constituents acts as the reinforcing phase, with the one embedding the reinforcement is called the matrix. An example of a natural composite is wood, which is typically a fibrous composite with cellulose fibres embedded in lignin matrix. The two constituents together form a much stronger structure [1]. Another example is bone, which is a composite made from hard, however brittle, inorganic hydroxyapatite and a though organic constituent called collagen [2]. One of the earliest man-made composites created by our ancestors is produced by mixing straw with mud. By mixing the two constituents, it is possible to produce bricks that could tolerate both compression and tension. Here, the straw is the reinforcing phase and mud is the matrix.

One can tailor the properties of the composite to meet their demand by carefully choosing the constituents and the manufacturing process. Properties such as resistance to chemicals, heat and weathering can be introduced to the final product by selecting appropriate matrix material. Mechanical properties can be adjusted as required [3].

1.2 Classification

Composite materials are commonly classified by the geometry of the reinforcement or by the type of the matrix. The properties of composite material are a function of the properties of the constituent phases, their relative volumes, and the geometry (shape, size, distribution and orientation) of the reinforcing phase [4]. Composite materials may also be classified according to the function of their matrix. Matrices could be based on polymers, metals or ceramics. In general, polymers and metals are used as the matrix when some ductility is desired. Large usage of polymers as matrix phase compared to metals and ceramics can be attributed to the excellent cost/performance ratio, simple manufacturing methods, and relatively low cost of the raw materials. Ceramic matrices are considered when high-temperature applications are required and adding reinforcing phase to ceramic matrix helps improve the fracture toughness.

1.2.1 Materials for Reinforcement

The reinforcing phase plays the important role to control the load bearing, stiffness and strength properties of the composite material. Reinforcing phase can be categorised into three main forms: fibres, particulates and nanoparticles.

Fibre has a long history in humankind life expanse. For hundreds of years, natural fibres (NFs) like kenaf, bamboo, pine, wool and cotton were used to produce handmade artefacts like mats, bags and ropes. NFs are mainly classified as plant-based, animal-based and mineral-based fibres. [5]. Man-made synthetic fibres (SFs) are made by modification of chemical structures of either minerals or polymers. SFs can be further classified as organic and inorganic, based on their content. These fibres are considered to be one of the important tiers of fibre-reinforced composites and particularly in areas where mechanical, chemical and thermal stability of the composite is vital, such as aerospace and automotive applications [6, 7]. Glass fibre (GF) and carbon fibre (CF) are examples of important SFs.

Particulate composites consist of particles such as aluminium, silicon carbide and gravel, immersed in the matrix phase such as alloys, ceramics or other materials. For most of particulate composites, the reinforcing phase (particles) is harder and stiffer than the matrix phase. For an effective reinforcement, particles should be small in size and evenly distributed throughout the matrix phase. The particles tend to restrain the movement of the matrix phase. The degree of the improvement in mechanical behaviour of the particulate composites therefore depends on strong bonding at the matrix-particulate interface. [8]. An example of particulate composites employed for civil applications is concrete structures, where a high degree of wear resistance is required. Concrete is a composite in which both the reinforcing and matrix phase are ceramic materials.

Nanocomposites are produced from nanomaterials embedded in a matrix material. In nanocomposites, one, two or three dimensions of the nanomaterials shall be on the order of nanometres, whereas accepted range of the nanoparticles to be considered in the nanocomposite should be less than 100 nm. As shown in Figure 1.1, nanomaterials can be classified into three major types depending on their dimension; two-

dimensional (2D) layered, such as graphene and nanoclay, one-dimensional (1D) fibrous, like carbon nanofibres and carbon nanotubes, and zero-dimensional (0D) spherical, with silica nanoparticles and zinc oxide quantum dots being such examples.

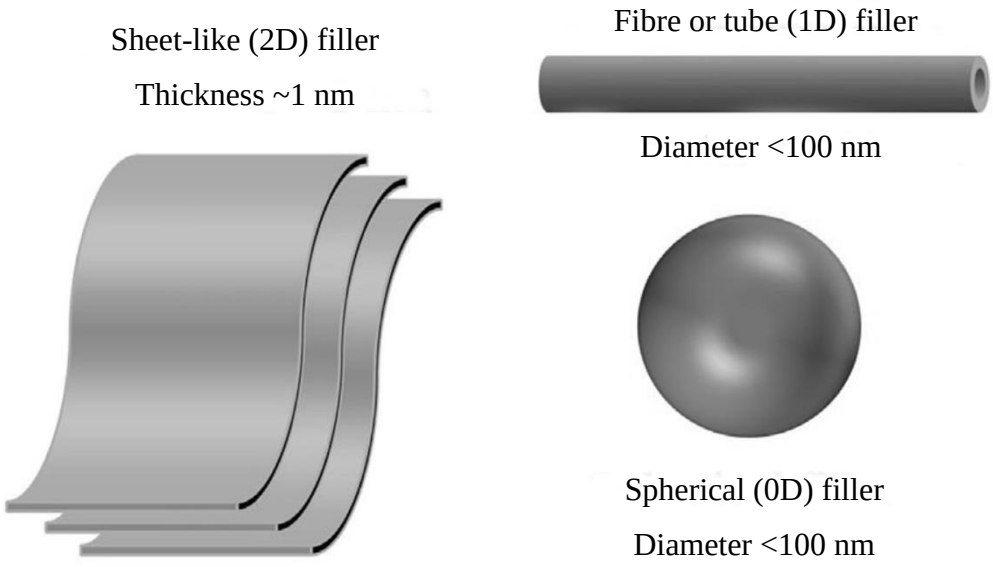

Figure 1.1 Schematic diagrams of three types of nanoscale filler materials [9].

The majority of today's commercial nanocomposites utilise three types of nanomaterials: nanoclays, nanocarbons and nanocrystals. Montmorillonite is the most common type of layered silicate. Montmorillonite consists of ~1 nm thick aluminosilicate layer, surface-substituted with metal cations and stacked in ~10 μm-sized multilayer stacks [10]. Graphene, carbon nanotubes (CNTs) and carbon nanofibres are examples of 2D and 1D nanocarbons. Graphene is a 2D material and is basically a single layer of graphite with carbon atoms arranged in a hexagonal lattice. CNTs are essentially a sheet of graphene that is rolled into a cylindrical hollow structure [11]. Examples of nanocrystals mostly include inorganic oxides such as alumina, silica and zirconia.

1.2.2 Materials for Matrix

As previously mentioned, composites materials can be classified according to the matrix phase. The roles of matrix in composite materials are to keep the reinforcing phase in place, transfer stress between the fillers, provide barrier against harmful

environments such as chemical and moisture, and also protect the surface of the reinforcements. The choice of matrix could be related to factors such as the intended application and the manufacturing method of the composite material. The three major and distinct classes of composites based on their materials for matrix are polymer matrix composites (PMCs), metal matrix composites (MMCs) and ceramic matrix composites (CMCs).

PMCs reinforced with synthetic thin fibres such as carbon, glass and aramid are the most common advanced composites. PMCs contain polymer resins as their matrix phase. The term resin is used to denote a high molecular weight plastic [12]. When heated, the polymer matrix phase undergoes melting or softening, enabling their mixture with the reinforcing phase and forming the final shape of the composite material.

In general, polymer matrices can be divided into two types: thermosetting and thermoplastic. Thermosetting polymers (commonly known as thermosets) are typically liquid in room temperature. they undergo a curing reaction, in which the molecules are chemically joined together by cross-linking to the nearby chains, forming a rigid 3D structure. The most common types of thermosets used in PMCs are epoxy and polyester.

Thermoplastics are typically in solid state and hard in room temperatures but flow under the application of heat and pressure. Unlike thermosets, thermoplastics are not cross-linked. Here, high molecular weight chains are not chemically bond together, as shown in Figure 1.2. They are held in place via weak Van der Waals and hydrogen bonds. They achieve their strength and stiffness through the inherent properties of their monomers and very high molecular weight units. With applying heat, these bonds become weak and eventually break, resulting the molecules to move relative to each other or flow to a new configuration if pressure is applied on them. When cooled, the molecules freeze in their new position and the aforementioned secondary bonds restore, resulting the new shape of the solid polymer. This therefore indicates that unlike thermosets, which once cured the process is not irreversible, thermoplastics can be reheated to become soft, melted and reshaped as many times as required.

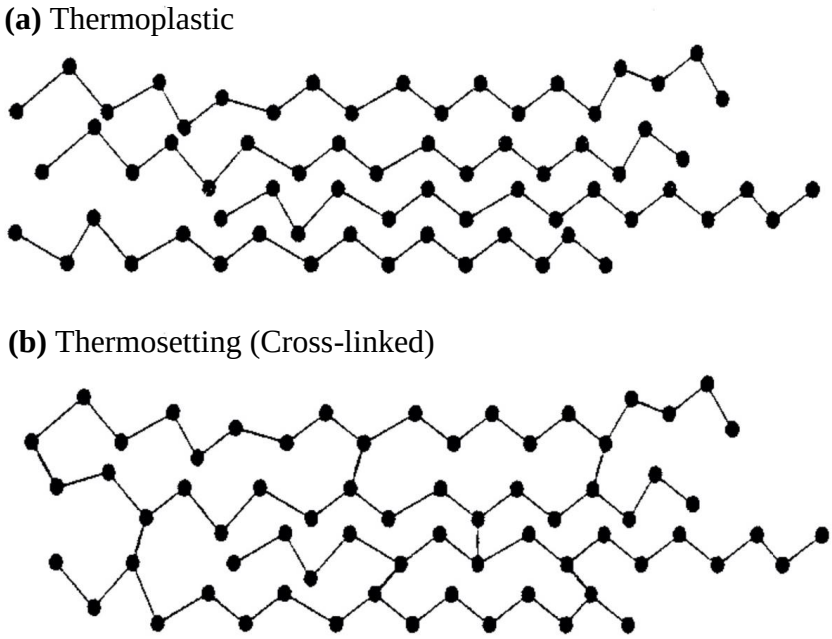

Figure 1.2 Schematic representation of (a) thermoplastic polymer and (b) thermoset polymer chains [13].

Although thermoplastics are less common than thermosets for use in material for matrix, they do have some advantages such as better fracture toughness and impact resistance. Some of these different characteristics are listed in Table 1.1.

Table 1.1 Comparison between thermoplastics and thermoset properties [14].

Thermoplastics	**Thermosets**
Soften on heating and pressure – easy to repair	Decompose on heating
Higher fabrication temperature and viscosities	Lower fabrication temperature
Can be reprocessed	Cannot be reprocessed
High strains to failure	Low strains to failure
Short cure cycles	Long cure cycles
Not tacky and easy to handle	Tacky
Excellent solvent resistance	Fair solvent resistance
Indefinite shelf life	Definite shelf life
Recyclable	Unrecyclable

1.3 Advanced Composite Materials

The term advanced composite material (ACM) is traditionally used for strong and lightweight engineered materials employed in aerospace industries. Due to the dominant usage of fibre-reinforced composites in recent engineering applications, ACMs are often regarded as composite materials with high-performance reinforcement of thin diameter, embedded in a high-grade matrix. Fibre-reinforced polymer matrix composites have become the most important class of composite materials, due to their high specific strength and modulus as well as low manufacturing and materials cost.

1.3.1 Applications

ACMs were primarily developed for aerospace applications to enhance the performance of aircrafts. The first exclusive application of ACMs for military use in aerospace industry can be traced back to 1950s. This changed by early investigations by Boeing in 1970s to implements ACMs for civilian aircrafts, as seen in Figure 1.3(b). The use of composite materials in commercial aircrafts began with a few secondary components, most of which were made from carbon fibre-reinforced epoxy. From 1970s to 1990s, the share of composite material used in aircrafts raised from 5 to 15 wt%, further raising to 25 wt% in 2006 with the introduction of Airbus A380. Early models like the A300 only had few components like the fairings and radome made out of composites; but over time, spoilers, airbrakes, elevators, j-nose, wing ribs, wing box, and many other secondary and primary structures were manufactured from high-performance composite materials. The structural integrity and durability of these early components built the confidence in their capabilities, and consequently promoted further research and development of other structural parts, resulting in a dramatic increase in using ACMs for aircrafts and doubling the share to 50 wt%. The Airbus 350-XWB and Boeing 787 would have 52 and 50 wt% of their components made from high-performance composite materials, respectively, with Boeing 787 having the biggest push by utilising advanced composites for many primary structures including a full composite fuselage, as shown in Figure 1.3(a) [15, 16].

There are other pioneering examples of using larger shares of composite in small size aircrafts. Lear Fan 2100 was a business aircraft built in 1983 with 70 wt% of the

airframe built from carbon fibre and Kevlar-49 epoxy. Many components including main spar, empennage and fuselage was manufactured out of ACMs [17]. Another example is the Virgin Atlantic Global Flyer, a successor to Rutan's aircraft Voyager, which in 1986 became the first plane to fly around the world non-stop, carrying two passengers. The aircraft was almost fully constructed of high-performance and light weight carbon fibre-reinforced epoxy, particularly the structural members. The use of lightweight materials permitted a large 83 wt% of the total 9980 kilogram weight of the aircraft being assigned for fuel only, making it possible to fly around the world in just 67 hours [18].

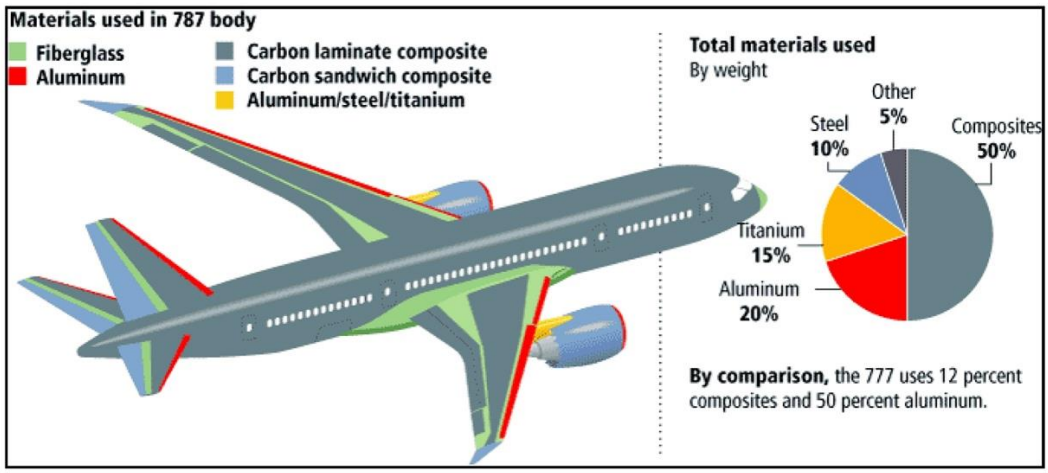

(a)

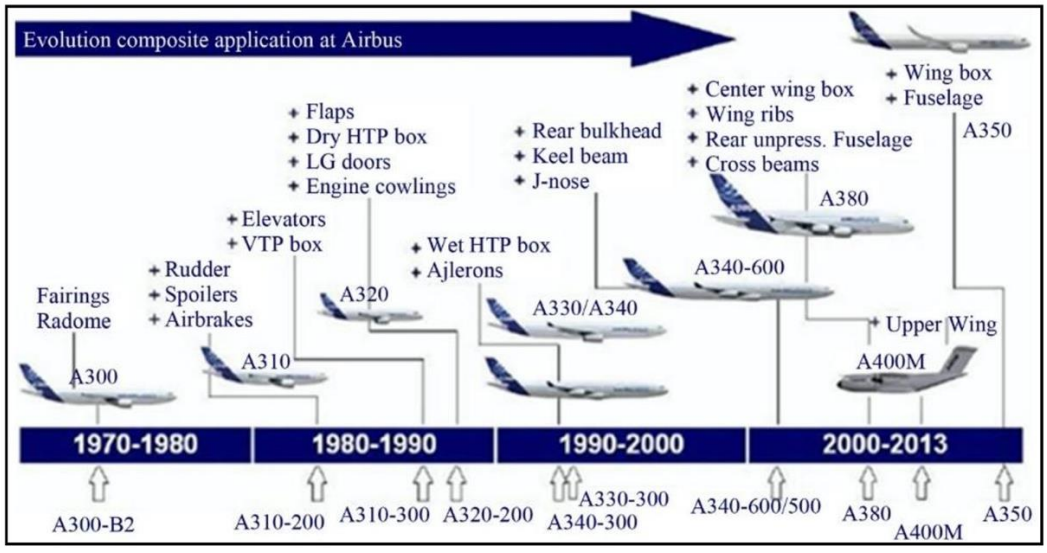

(b)

Figure 1.3 (a) comparison of materials used in Boeing 787 and (b) evolution of composite application in Airbus aircrafts [16].

1.3.2 Advantages and Disadvantages

In recent years, ACMs have become attractive for aerospace, automotive, marine and civil applications due to their exceptional strength and physical properties. They can offer a variety of advantages over conventional engineering materials including metals and ceramics. It however all comes down to specific applications as composites for sure cannot satisfy all engineering requirements and therefore, cannot fully replace all materials. Notable advantages of composites include light weight and low density, high strength to density ratio, high fatigue, impact and corrosion resistance, coupled with improved creep life and controlled (low) thermal expansion.

Composites have great points of interest among engineering materials; however, drawbacks could include relative brittleness with a low toughness (specially in thermoset PMCs), defects such as voids and delamination, high material and manufacturing costs, complex assembling forms, and difficulties in recycling. Repairing of composites is also not a straightforward procedure when compared to for example metals. In engineering applications, essential material choice and parameters could include formability, joinability, affordability, toughness, strength and corrosion resistance, in which composites could face limitations within a few, due to being a relatively new category of materials. Some key limiting factors in using fibre-reinforced composites for aircraft structures would be their relatively high cost and low impact tolerance. Galvanic corrosion is another limiting factor when it comes to using composite materials like carbon fibre epoxy with metals such as aluminium or titanium. Research is underway to tackle such issues; by increasing the capacity of thermoplastic composites for use in fuselage to gain a better impact resistance and better repairability, and also using other high-performance fibres such as glass fibre to eliminate the problems with galvanic corrosion.

1.4 Manufacturing Thermoplastic Composites

The main focus of this study is on the production of thermoplastic polymer composites, based on glass fibre as the reinforcement. As mentioned in Section 1.2.2, thermoplastic matrices can offer a range of benefits in the manufacture of composites when compared to thermosets. The need for low-temperature storage, hard-to-control cure process, and long curing process are among thermosetting composites drawbacks.

In such an environment, high-performance thermoplastic resins are promising alternatives and as the result, interest in thermoplastic composites has increased in aerospace, automotive and marine industries. This can be attributed to their exceptional merits such as infinite shelf life, recyclability, faster manufacturing cycles, inherent toughness, flame retardancy, and much more [19-23].

The manufacturing methods of PMCs with synthetic fibres can vary significantly depending on the utilised polymer matrix and the reinforcing material. However, the main production challenge can be identified as the method of incorporating polymer matrix into the fibres. Unlike the conventional thermosets, thermoplastic polymers are usually in solid state when in room temperature. Here, a number of manufacturing methods have been investigated, which includes melt impregnation, film stacking, fibre commingling, solution impregnation and powder impregnation. Many of the named methods can be implemented for thermoplastic composite production; however, only a few might be suitable for processing high-temperature thermoplastic polymers. In Section 2.3.2, these manufacturing methods are discussed in detail. The advantages and disadvantages of the existing methods are mentioned, and the best techniques are realised and implemented.

1.5 Motivation of the Research

Fibre-reinforced composites have stimulated extensive research work and investigations due to their attractive properties compared to traditional engineering materials. Because of this, they have gained wider and faster development pace. At the same time, gaining a better understanding of these materials is even more crucial, not only to maximise the potential of the existing composites, but also to develop new composite materials and structures with enhanced integrity for use in different engineering applications.

Thermoplastic composites are expected to gradually replace traditional composites utilised in aerospace and automotive applications due to their exceptional advantages and benefits, compared with thermosetting composites. In such a scenario, polyarylether ketone (PAEK) polymers fulfil many of the requirements for production of advanced composite materials due to their exceptional physical and mechanical

properties. It is expected from PAEK composites to become a major alternative to many thermosetting matrices such as epoxy. To date, limited number of studies have been carried out on various PAEK matrices for use in fibre-reinforced composites, with majority of focuses being on CF as the main reinforcement. Therefore, further investigations are crucial to realise the true potential of implementing different PAEKs with different reinforcing fibres.

With such a shift from thermosetting to thermoplastic matrices, realising the most efficient methods of composite production becomes utmost important. The majority of current thermoplastic composite manufacturing methods involve using expensive polymer extruders, which are usually uncapable to process high-temperature matrices such PAEKs. Melt impregnation manufacturing methods bear many barriers in terms of efficient resin impregnation and fibre wet-out, especially for processing polymers with high melt viscosity. This urges the need for an extensive review of the current state of the art and to realise the most efficient prepreg production methods.

1.6 Project Aim and Objectives

There is a need for high-temperature and high-performance prepreg materials for the next generation of fuselage, especially the large size supersonic aircrafts, where the materials have to withstand temperatures between –65 and +200 °C. It is proposed to develop multifunctional high-temperature and high-performance, and low-cost S2-glass/PAEK prepreg materials. The key objectives of this project are:

- To review different methods of producing thermoplastic prepreg and discuss the state of the art.
- To identify an effective and low-cost method of impregnating the fibre reinforcement with PAEK polymer.
- To design and manufacture an in-house prepreg rig with the ability to utilise different types of fibre/matrix and to control prepreg properties.
- To realise the potential of the assembled prepreg rig and undertake parameter optimisations.
- To develop multifunctional high-temperature and high-performance thermoplastic prepreg materials based on S2-glass fibre and PAEK polymers.

- To compare the characteristics of manufactured prepregs with different constituent ratios.
- To physically and mechanically evaluate and compare the properties of the composite laminates manufactured with different constituent ratios.
- To study the effect of nanomaterials on physical and mechanical properties of the laminates.

This research work aims to develop a novel thermoplastic prepreg manufacturing method based on the wet powder impregnation technology, and to achieve an insight on new materials that can satisfy some of the requirements of the new generation of aircrafts, including high service temperature and damage tolerance. Therefore, experimental investigations are carried out to characterise the properties of the newly manufactured composites.

1.7 Thesis Outline

The presented thesis evaluates the potential of the newly developed in-house prepreg rig and the corresponding production materials. The remainder of this thesis will be divided into smaller section, beginning with a comprehensive review of relevant studies to this research, with a focus on different thermoplastic manufacturing methods in Chapter II. Then, Chapter III will include information on the numerous raw constituents utilised during the research project, and will outline the concept, design and manufacturing process of the novel unidirectional drum winding prepreg rig. Different components of the prepreg rig are also described and discussed in detail. In Chapter IV, experimental procedures of manufacturing prepregs will be outlined. This chapter also includes preliminary tests carried out on the prepreg rig for optimisation purposes and also, detailed procedure on how the physical and mechanical tests were performed. Chapter V gathers the results and data obtained from the experimental works. A thorough discussion is followed with each emerging information. Finally, the outcomes of this research work are concluded in Chapter VI and recommendations are set out for future works to come.

1.8 References

[1] Hon, D. N. S., and Shiraishi, N., 2001, Wood and cellulosic chemistry, Marcel Dekker, New York.

[2] Vaz, M. F., Canhao, H., and Fonseca, J. o., 2011, "Bone: A Composite Natural Material," Advances in Composite Materials - Analysis of Natural and Man-Made Materials, IntechOpen.

[3] Park, S., and Seo, M.-K., 2011, Interface science and composites, Elsevier Academic Press, Amsterdam, Boston.

[4] Flinn, R. A., and Trojan, P. K., 1990, Engineering materials and their applications, Houghton Mifflin, Boston.

[5] Puttegowda, M., Rangappa, S. M., Jawaid, M., Shivanna, P., Basavegowda, Y., and Saba, N., 2018, "15 - Potential of natural/synthetic hybrid composites for aerospace applications," Sustainable Composites for Aerospace Applications, M. Jawaid, and M. Thariq, eds., Woodhead Publishing, pp. 315-351.

[6] Pico, D., and Steinmann, W., 2016, "Synthetic Fibres for Composite Applications," Fibrous & Textile Materials for Composite Applications, Springer, Singapore, p. 135.

[7] Sathishkumar, T., Naveen, J., and Satheeshkumar, S., 2014, "Hybrid fiber reinforced polymer composites – a review," Journal of Reinforced Plastics and Composites, 33(5), pp. 454-471.

[8] Chawla, N., and Shen, Y.-L., 2001, "Mechanical Behavior of Particle Reinforced Metal Matrix Composites," Advanced Engineering Materials, 3(6), pp. 357-370.

[9] Fu, S., Sun, Z., Huang, P., Li, Y., and Hu, N., 2019, "Some basic aspects of polymer nanocomposites: A critical review," Nano Materials Science, 1(1), pp. 2-30.

[10] Delory, E., Toma, D., Fernandez, J., Cervantes, P., Ruiz, P., and Meme, S., 2019, "Chapter 4 - Ocean In Situ Sensors Crosscutting Innovations," Challenges and Innovations in Ocean In Situ Sensors, E. Delory, and J. Pearlman, eds., Elsevier, pp. 117-171.

[11] Dhand, V., Rhee, K. Y., Ju Kim, H., and Ho Jung, D., 2013, "A Comprehensive Review of Graphene Nanocomposites: Research Status and Trends," Journal of Nanomaterials, 2013, p. 763953.

[12] Birley, A. W., Haworth, B., and Batchelor, J., 1991, Physics of plastics, Hanser Publishers, Munich.

[13] Gilleo, K., and Ongley, P., 1999, "Pros and cons of thermoplastic and thermoset polymer adhesives in microelectronic assembly applications," Microelectronics International, 16(2), pp. 34-38.

[14] Kaw, A. K., 2006, Mechanics of composite materials, Taylor & Francis, Boca Raton, FL.

[15] Potter, K., and Ward, C., 2010, "17 - In-process composite recycling in the aerospace industry," Management, Recycling and Reuse of Waste Composites, V. Goodship, ed., Woodhead Publishing, pp. 458-494.

[16] Sante, R., 2015, "Fibre Optic Sensors for Structural Health Monitoring of Aircraft Composite Structures: Recent Advances and Applications," Sensors, 15(8), pp. 18666-18713.

[17] Noyes, J. V., 1983, "Composites in the construction of the Lear Fan 2100 aircraft," Composites, 14(2), pp. 129-139.

[18] Pearson, H., 2005, "Round-the-world solo flight takes off," Nature.

[19] Walsh, S. M., Scott, B. R., and Spagnuolo, D. M., 2005, "The Development of a Hybrid Thermoplastic Ballistic Material With Application to Helmets," Army Research Lab Aberdeen Proving Ground, M. D.

[20] Walsh, S. M., Scott, B. R., Spagnuolo, D. M., and Wolbert, J. P., 2006, "Hybridized Thermoplastic Aramids: Enabling Material Technology For Future Force Headgear," Army Research Lab Aberdeen Proving Ground, M. D.

[21] Kulkarni, S. G., Gao, X. L., Horner, S. E., Zheng, J. Q., and David, N. V., 2013, "Ballistic helmets – Their design, materials, and performance against traumatic brain injury," Composite Structures, 101, pp. 313-331.

[22] Vieille, B., Casado, V. M., and Bouvet, C., 2013, "About the impact behavior of woven-ply carbon fiber-reinforced thermoplastic- and thermosetting-composites: A comparative study," Composite Structures, 101, pp. 9-21.

[23] Bandaru, A. K., Chavan, V. V., Ahmad, S., Alagirusamy, R., and Bhatnagar, N., 2016, "Ballistic impact response of Kevlar® reinforced thermoplastic composite armors," International Journal of Impact Engineering, 89, pp. 1-13.

CHAPTER II: LITERATURE REVIEW

2.1 Introduction

This chapter presents a review of the past and state of the art research on fibre-reinforced polymer composites. Reviews include a general overview on different fibre architecture and types, with a focus on glass fibre. Laminated composites will be explained and the use of prepreg will be presented. Other important section of the writing will focus on thermoplastic composites, stating engineering polymers utilised in the making, and finally their manufacturing methods.

2.2 Fibre-reinforced Polymer Composites

Fibre-reinforced polymer (FRP) composites are a category of composites that particularly employs fibres as the reinforcing phase to upgrade the quality of polymer. Fibres in FRPs are more often carbon, glass or aramid, whereas the polymer is usually an epoxy or in general, a thermosetting. In FRP composites, high strength and modulus fibres, which are embedded in the matrix, serve as reinforcement and show high tensile strength and stiffness. Fibre and matrix retain their initial chemical and physical identities. However, the new combination has a series of properties that cannot be achieved with either of the initial materials acting alone. The main load-carrying members are fibres, while the matrix holds the fibres together and transfers shear forces between the fibres. The matrix phase also functions as a coating and protects the material and fibre surface from harsh environment and mechanical abrasion [1, 2]. The fibre reinforcement not only improves the mechanical properties of the polymer, but also enhances acoustical, thermal and electrical properties that are not expected from a simple polymer.

FRPs are utilised pretty much in every kind of cutting-edge engineering structure, especially in automobile and aerospace industry, and are the most common and widely used polymer compositions. The light weight and durability, and higher performance of FRPs compared to most of metal alloys, together with the range of their application, give them advantage over traditional materials. Due to their high specific and lower density properties, FRPs are superior compared to metallic components (strength to weight and modulus to weight ratios).

2.2.1 Laminar Composites

Laminar composites are structures made by stacking and bonding various sheets (often referred to as plies or laminas) one upon the other. A multi-layered structure composed of multiple stacked laminas is termed as a laminate. For the remainder of this chapter, FRP laminates will be emphasised.

2.2.1.1 Lamina

The manufacturing of FRP laminates starts with forming the lamina. Lamina is produced by incorporation large number of reinforcing fibres into a thin layer of resin matrix. Normal lamina thickness ranges between 0.1 to 1 mm. The fibre filaments in a lamina could be continuous or in short lengths. Also, fibres could be oriented in one or more directions, or they could be randomly distributed, as shown in Figure 2.1 [3].

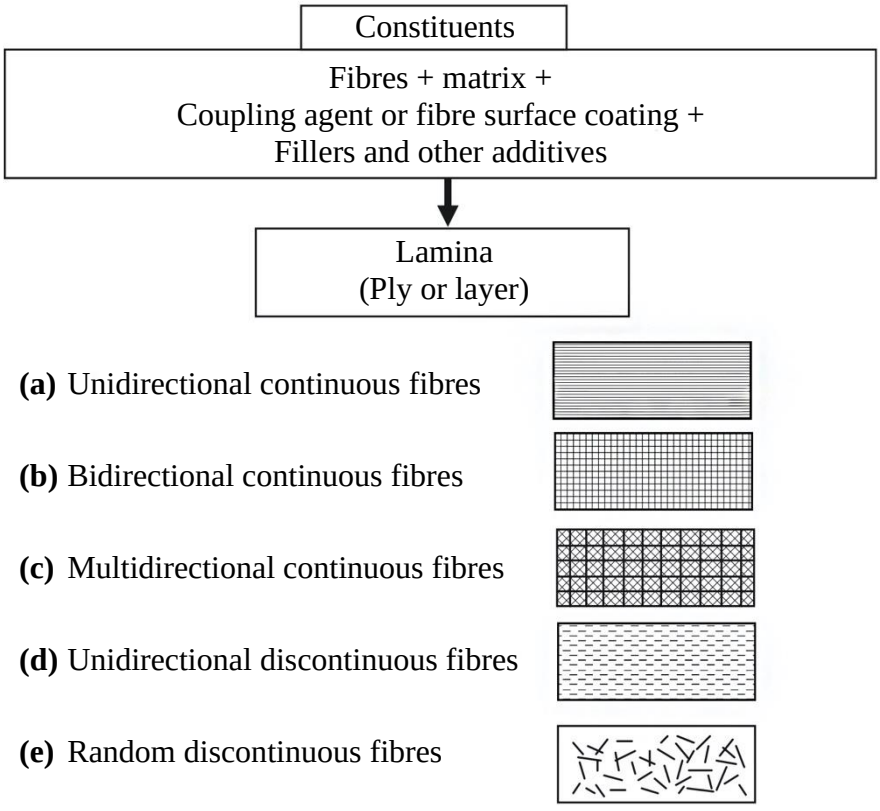

Figure 2.1 Typical fibre architecture of a lamina [3].

If the fibres used in the making are all oriented in the same direction, this arrangement of fibres is called unidirectional (UD). Figure 2.1(a) and (d) represent continuous and

discontinuous UD laminas, respectively. A UD lamina is often called a ply. Continuous long fibres can be used to manufacture bidirectional or multidirectional laminas as illustrated in Figure 2.1(b) and (c). In the bidirectional orientation, fibres are placed in two directions as expected, usually normal to each other. In multidirectional setting, fibre filaments are in more than two headings. The orientation patterns mentioned can be obtained by weaving or other processes utilised within textile industry. Generally, unidirectional and bidirectional are the two most common flat laminas, as shown in Figure 2.2. UD is a 1D configuration, in which all fibres are parallel and aligned in the x (longitudinal) direction. UD lamina possesses highest strength and modulus along the longitudinal axis. However, these values are much lower in transverse direction, since there is no reinforcing fibre (load bearing constituent) along this direction. In bidirectional lamina, the strength and modulus vary along the warp (longitudinal) and weft (transverse) directions and are dependent on the number of fibre strands per unit width. Variety of properties can be achieved by changing the quantity of the fibres in both directions. A bidirectional lamina is called balanced when both directions have equal properties. Bidirectional laminas usually come as a 2D woven form, with warp and weft yarns perpendicularly crimped up and under each other consecutively [3, 4].

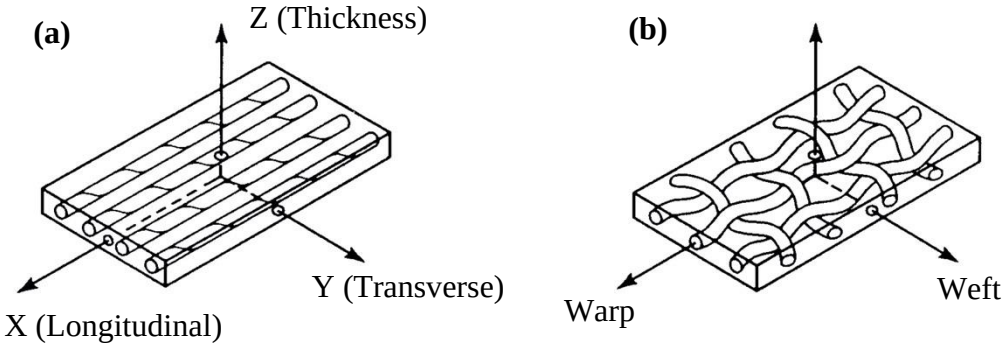

Figure 2.2 Principal types of lamina: (a) 1D unidirectional lamina and (b) 2D bidirectional woven lamina [4].

2.2.1.2 Laminate

As mentioned in Section 2.2.1, a multi-layered structure composed of multiple stacked laminas is termed as a laminate. By stacking and consolidating several plies with various orientations in a specified sequence, a laminate with particular properties

could be formed. Change in fibre orientation and the stacking sequence of the plies can result in generation of wide range of physical and mechanical properties of the final laminate [5].

Conventionally, a 2D system of fibre orientation codes and stacking sequence notations are implemented for continuous FRP composites. The purpose of this system is to provide a simple and understandable description of such practice. The angle between the fibre orientation and the longitudinal axis (x-axis) is measured, with the angles considered positive counter-clockwise, when observing towards the lay-up surface. Measured angles are recorded inside a square bracket and are separated via forward slash symbol. The layout is normally considered from top reference plane going down towards the layers [6, 7].

Figure 2.3 illustrates four classic laminate lay-ups using continuous unidirectional long fibres. Figure 2.3(a) demonstrates a UD laminate, in which all laminas are oriented at 0°. Notation for this stacking sequence is [0°/0°/0°/0°/0°/0°/0°/0°] or $[0°_8]_T$ (T for total laminate). When plies are laid out in an alternative sequence of 0° and 90°, cross-ply laminate is created and, angle-ply laminates will have successive layers switching between the positive and negative value of a certain angle such as ±45° (Figure 2.3(b) and (c), respectively). Multidirectional laminates have multiple laminas in several orientations. Figure 2.3(d) is an example of a multidirectional stacked laminate with a notation code of $[0°/90°/\pm45°]_S$ (S for symmetrical). This specific sequence creates a quasi-isotropic laminate as the orientation of the plies are balanced such that the extensional stiffness of the laminate is constant in all in-plane directions (material behaves like an isotropic material). Plies are normally stacked in a way that fibre orientations are symmetric with respect to the laminate mid-plane. This course of action prevents any out-of-plane bending or twisting [8].

In an FRP laminate, the mechanical properties such as strength and elasticity are improved, which heavily depends on the physical and mechanical properties of both fibre and matrix, their relative volume with respect to each other, and also the length of the fibre and its orientation. However, there are many other factors that affect the quality of a laminar composite [9].

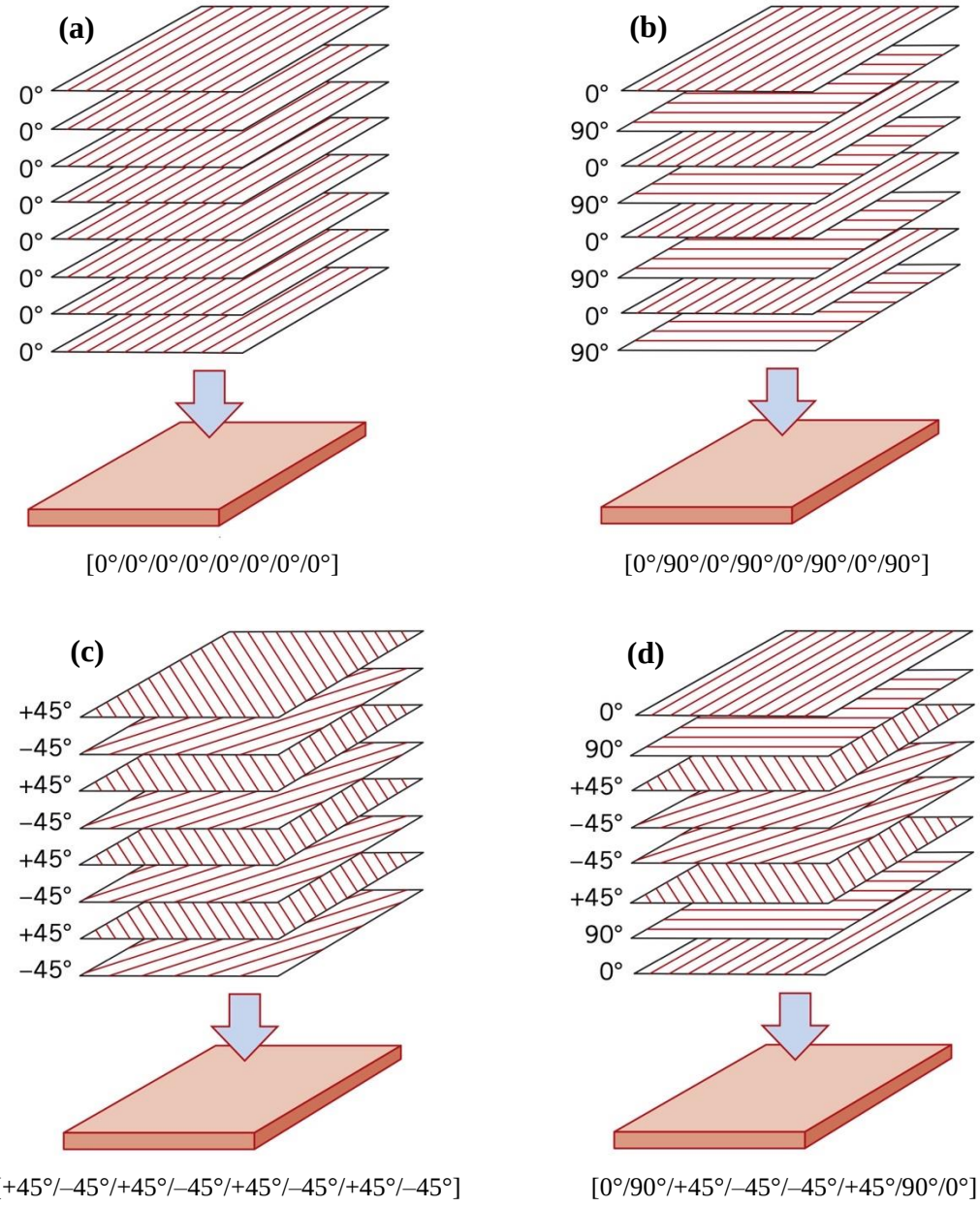

Figure 2.3 Four typical classes of continuous long fibre laminar composites: (a) unidirectional, (b) cross-ply, (c) angle-ply and (d) multidirectional [8].

2.2.1.3 Fibre

The role of fibre phase in FRP composites is to increase the mechanical properties of the matrix. This is achieved by implementing high-performance fibres such as glass and carbon fibre in the matrix phase.

Fibres used in FRPs should be of thin diameters. The experimental strength of fibres is much lower than the theoretical values. This contrast is due to the imperfections

within the fibres. Figure 2.4 shows that as fibre dimeter becomes smaller, the chances of such flaws also decrease. Small diameter fibres also create a larger fibre-matrix interface compared to large diameter fibres, which in practice results in better load transfer between the two phases and consequently better mechanical performance. Finally, the ability of fibres to bend without breaking is essential when manufacturing FRPs, especially when woven fabric is used in the process. Fibres should be flexible so that they could be easily processed when moulding curved composite parts. With a decrease in fibre diameter, the ability of fibre to bend increases [10].

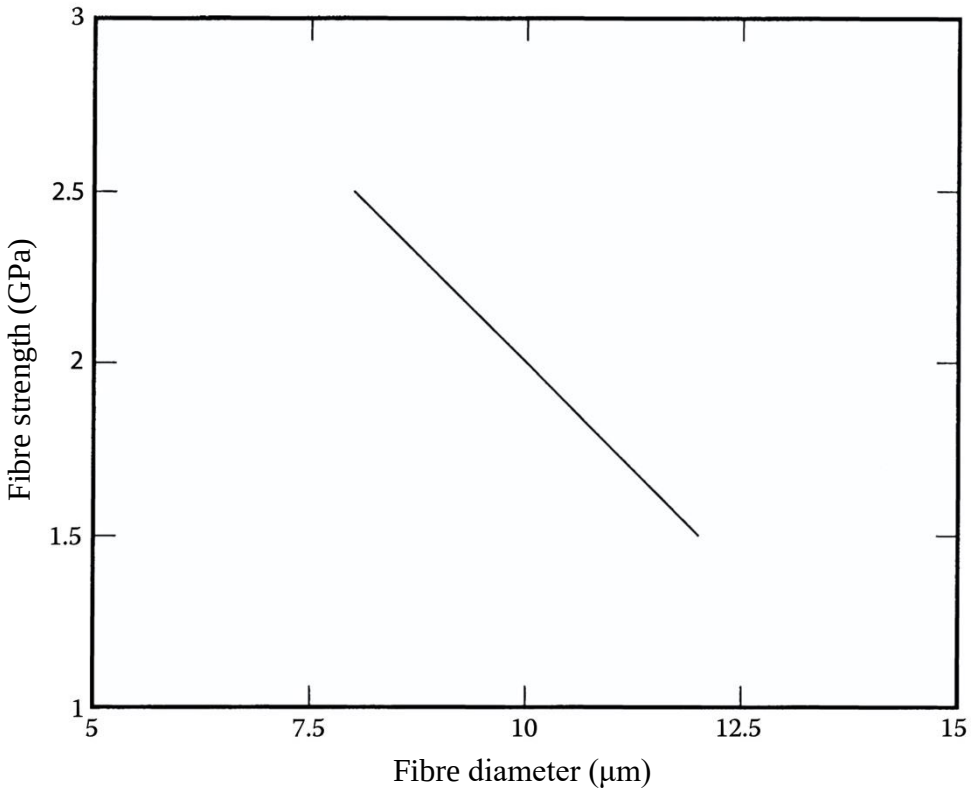

Figure 2.4 Decrease in fibre strength with increase in fibre diameter for carbon fibres [10].

Glass fibre (GF) is the most commonly used fibre in the field of FRP composites. GFs are manufactured from drawing molten glass through tiny platinum holes at the base of a furnace to form fibres with 5 to 24 μm diameter [11]. The fibres are then coated with a thin layer of protective agent comprising lubricant, binder, antistatic etc. The main constituent in GFs composition is SiO_2 (50–65 wt%), incorporated with other oxides such as aluminium, boron, sodium, calcium and iron. Depending on the

chemical compositions of the constituents, GFs with different properties can be achieved. E-glass (E for electrical) is the most common type of GF. E-glass has a good combination of strength, stiffness, electrical insulation, and is the lowest cost in the category. When better chemical corrosion resistance is required, C-glass (C for corrosion) is the option of choice. With an increase in demand for GFs for use in high-performance FRP parts in military components such as missile casings and aircraft pieces, stiffer and stronger GFs are required. S-glass (S for Strength) was developed for such critical applications, obtaining higher strength, modulus, temperature and impact resistance than E-glass. The manufacturing cost of S-glass could be 10 times higher than E-glass, and this have led to the introduction of a lower cost version of S-glass with similar properties, called S2-glass [12, 13].

Once continuous GFs are produced, they should be converted over into an appropriate product for their expected applications. The major final forms are chopped strands, continuous yarn, continuous roving and woven roving, which is also known as woven fabric or cloth, as shown in Figure 2.5.

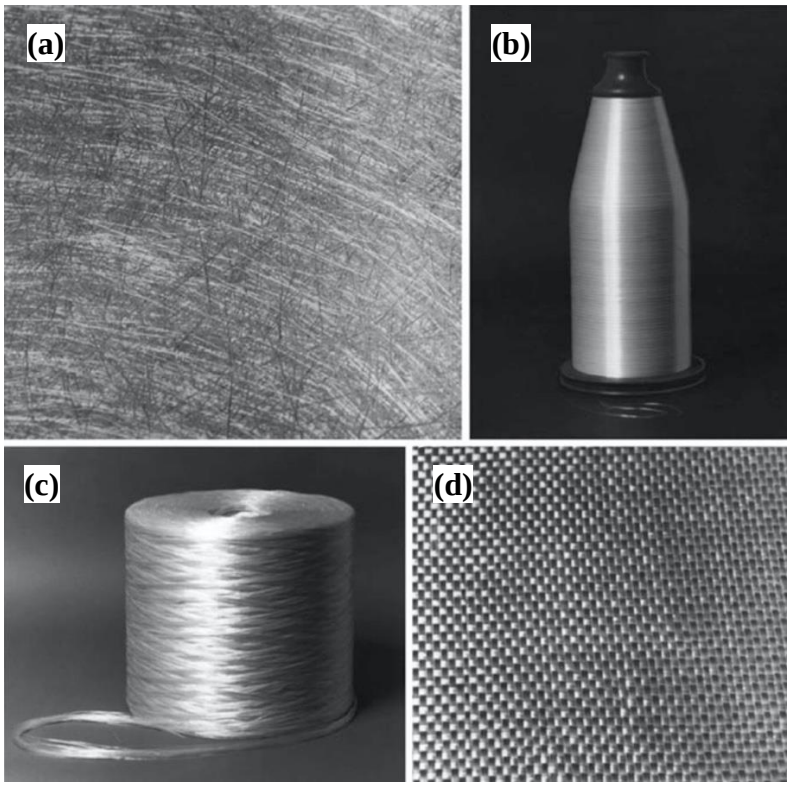

Figure 2.5 Variety of glass fibre forms available: (a) chopped strand, (b) continuous yarn, (c) continuous roving and (d) woven fabric [14].

Continuous fibre roving is the most basic form of GF supplied. Rovings (also commonly known as tows) are formed by gathering untwisted fibre strands as a thick bundle of fibre. Rovings are wound onto a cylindrical package and could be several kilometres long as shown in Figure 2.5(c). Fibre rovings can then be used in variety of weaving processes to construct woven fabrics with different styles such as plain, twill and satin weaves [15].

According to the American society for testing and materials (ASTM) standard D578/D578M-18 [16], GF strands are identified by implementing either an inch-pound system (U.S. customary system) or a TEX/metric system (SI/metric system). The nomenclature associated with this system provides information on continuous filament yarns, discontinuous or staple filament yarns, textured yarns and continuous and discontinuous (chopped) roving. The nomenclature for continuous roving uses an alpha-numeric designation signifying fibre diameter, binder, sizing, TEX (linear density in grams per kilometre) or yield (inverse of linear density in yards per pound), and the manufacturing method of the roving. For instance, letter G is correspondence with filament diameter of approximately 9 microns (8.89–10.15 μm range).

2.2.1.4 Prepreg

Incorporation of fibres into the matrix phase can be achieved by two general methods. The first method involves using the fibre and matrix directly into the manufacturing process to form the final product. Examples of such method are pultrusion and filament winding, in which the fibres are dipped in a resin bath and consequently are passed through a die for pultrusion or are wound around a part in filament winding to form the final structure. In the second method, fibres are firstly incorporated inside the resin phase in a separate process to form a thin sheet like layers that are ready to be moulded in another process. These ready to mould layers are called prepreg.

Prepreg composite materials are becoming increasingly common in the composite industry due to their ease of use, consistent properties, and high-quality surface finish. Prepreg is the term for pre-impregnated reinforcing fibre, which has been impregnated with a resin system. Therefore, the prepreg is ready to be used without the addition of more resin. There are several advantages of using prepregs compared to using

traditional hand layup methods. Perhaps, the convenience of using prepreg is considerable and there will be minimum flaws in the required proportional content of each component. This leads to a stronger, more durable and homogenous composite with far less waste on our hand. Most prepregs are made in specialised sites, which focus on prepregs and consequently, this adds an additional step to the manufacturing chain of prepreg production. Therefore, the cost of prepregs can come as a disadvantage. Also, in thermoset resin prepregs, the resin undergoes a partial curing that changes the resin state from liquid to solid (B-stage), which requires the prepreg to be stored in a cool place to prevent it from cross-linking. The overall shelf life of thermoset prepregs can be very low if stored in room temperatures [17-19].

Prepregs can be tailored for harsh environments that require greater toughness, higher fire resistance, lower flammability and vibration damping by altering the utilised fibre and resin. Fibres such as carbon, glass and aramid are mostly used for preparation of prepregs and they are normally embedded in the resin phase in UD form to produce UD prepreg tapes or in woven/stitched form to produce woven prepreg tapes [20]. The majority of thermoset and thermoplastic resins can be adopted for manufacturing prepregs. The most common type of resin in thermoset prepregs is epoxy due to its high physical and mechanical performance. Other thermosets like vinyl ester and polyester can also be used. Both thermoset and thermoplastic prepregs are classified as prepregs but there are some distinct differences between thermoplastic and thermoset composites. For instance, thermoplastics exhibit pronounced nonlinear mechanical behaviour, especially in high-temperature environments in contrast to thermosets [21].

The typical process of manufacturing UD thermoset prepregs is initiated by pulling and collimating a series of continuous fibre tows, which are hauled off from a rack (commercially known as creel) containing a number of fibre tow bobbins. The fibre collimated tows are then guided through the impregnation stage, in which the fibres are impregnated by a resin matrix, such as epoxy. There are several thermoset impregnation methods such as resin dipping or resin calendaring.

Figure 2.6 illustrates the film calendaring (also known as film impregnation) process of manufacturing thermoset prepregs. In this process, a thin layer of thermoset resin is evenly coated on a release film by the use of a doctor blade. In the second step, the coated film is brought together with the collimated reinforcing fibres that are pulled off from the creel. The combination is then pulled through heat and calendaring/compaction rollers for semi-impregnation of the resin inside fibre filaments. Film calendaring process could be part of a single production line or two separate lines as seen in Figure 2.6. The prepreg is finally wound around a carboard tube and is kept in a refrigerated environment to prevent it from cross-linking. Aerospace grade thermoset prepregs are normally kept in –18 °C and are expired in approximately three months. The prepreg rolls are typically supplied in various width ranging from 0.1 to 3 meters, and also different resin contents and areal weights [22-25].

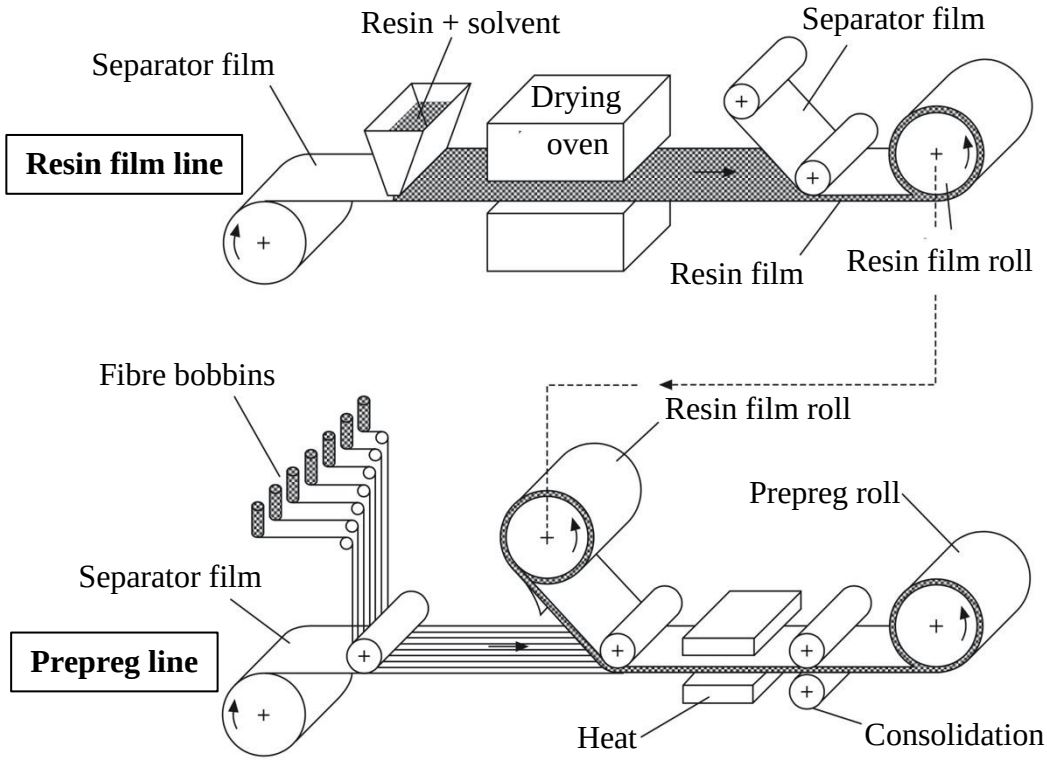

Figure 2.6 Schematic diagram of thermoset prepreg line using film calendaring [19].

2.3 Thermoplastic Composites

The distinctions between thermoset and thermoplastic polymers were previously discussed in Section 1.2.2. It was realised that the use of thermoplastic resin for manufacturing FRPs bring forward a set of valuable advantages. Even though thermosetting matrix composites display interesting mechanical properties, the use of these matrices is limited. The need for low-temperature storage, hard-to-control cure process and long curing process are among thermosetting composites drawbacks. In such an environment, high-performance thermoplastic resins are promising alternatives. Infinite shelf life without the need to refrigerate, faster processing cycles, lightweight, inherent toughness and flame retardancy, higher strength and stiffness, more impacts resistance, more chemical resistant, ability to be remoulded, more environmentally friendly, and the ability to be recycled are among the main benefits of using thermoplastic composites in comparison to their thermosetting counterparts. These distinctions are direct result of the differences between thermoset and thermoplastic resins [26-30]. Following this section, high-performance and engineering plastics will be introduced and the methods of incorporating these matrices between filament fibres to form a prepreg will be reviewed.

2.3.1 Thermoplastic Polymers

Thermoplastics are categorised based on their morphology. These morphologies are crystalline and amorphous. The term crystalline is commonly referred to as semi-crystalline, whereas exists areas of crystallinity, between the amorphous areas. The difference between the two lies in their molecular structure, as shown in Figure 2.7.

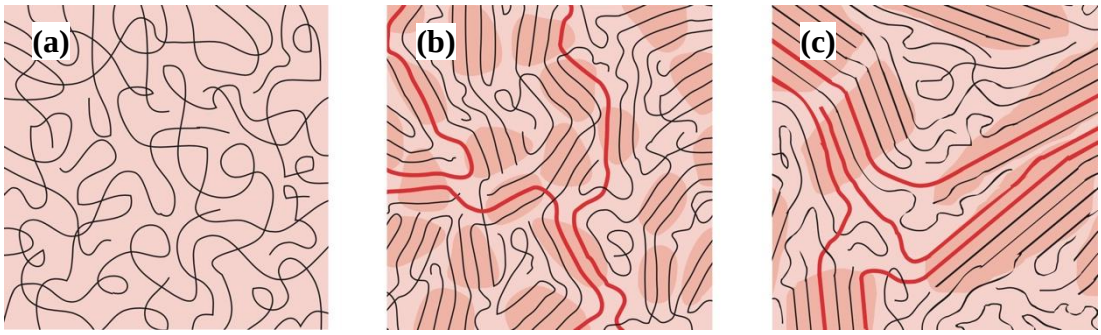

Figure 2.7 The morphology and molecular structure of (a) amorphous, (b) disordered aggregates and (c) semi-crystalline thermoplastics [31].

For visualisation purposes, the order of polymer chains is often compared to cooked spaghetti. As illustrated in Figure 2.7(a), the molecular structure in amorphous thermoplastics is randomly ordered. This results in lack of a defined and sharp melting point, as each intertwined chain could have a different melting temperature (T_m). Amorphous thermoplastics soften gradually with rise in temperature and lose their strength quickly above their glass transition temperature (T_g), even when combined with reinforcing fibres [32, 33]. Because of the varying range of melting point in amorphous resins, these materials are easier to thermoform. They are isotropic in flow and they shrink uniformly in the flow direction. In terms of mechanical properties, amorphous thermoplastics might have better impact resistance; however, they are more prone to physical ageing, stress cracking and fatigue failing. Lack of a defined T_m may also keep them in rubbery state until they reach degradation point [34, 35].

Amorphous thermoplastics were considered as the first choices for manufacturing thermoplastic FRPs. Although the majority of thermoplastics are insoluble by most organic solvents, some amorphous resins can be dissolved due to their randomly oriented molecular structure. This property might be of certain interest especially for manufacturing thermoplastic prepregs, as the thinning of the polymer allows easy impregnation of resin between reinforcing fibres. However, this process is normally coupled with loss and degradation of certain properties. Such composites can be sensitive to solvents when in service. Removing the solvent after the impregnation is also known to be difficult and it has negative effects on the residual strength of the FRP structure such as reduction of the T_g, defects in moulding and other environmental concerns [36].

On the other hand, semi-crystalline thermoplastics have a highly ordered molecular structure, which enables them to acquire a well-defined meting point. The areas of crystallinity are called spherulites and can vary in shape and size. Whereas amorphous materials soften steadily when the temperature rises, semi-crystalline plastics do not show such the performance. They inhibit their solid state until a certain amount of heat is absorbed, and they reach the material's T_m. At their T_m, thermoplastics quickly change into viscous liquid state but this is generally above that of the upper range of amorphous thermoplastics [37, 38].

2.3.1.1 Crystallinity in Thermoplastics

Crystallinity is a thermodynamic event and is controlled by the stability of mobility and free energy of molecules. Factors such as cooling rate and processing temperature can significantly influence the crystalline content, the final morphology, and properties of the semi-crystalline thermoplastic. The crystallinity effect is similar to cross linking, in which the solvent resistance and stiffness increases with an increase in crystalline content. Other factors such as density, optical and mechanical properties can also be altered by the degree of crystallinity [39, 40]. For instance, crystallinity and its morphology can influence the fracture toughness of carbon/PEEK composite. Increased level of crystallinity might enhance the solvent resistance and strength but, it also results in a more brittle material. Reduction of 40 % in fracture toughness of carbon/PEEK has been reported when a cooling rate of 1 °C/min was exercised, versus a fast cooling rate of 50 °C/min [41]. Figure 2.7(b) and (c) represents morphology of semi-crystalline resins with different crystalline contents.

Crystallinity also largely impacts the high-temperature properties of the resin such as the glass transition. Glass transition temperature (T_g) is a temperature in which the amorphous resin or amorphous part of semi-crystalline thermoplastic changes from rigid to rubbery states [42]. Viscoelastic effects come into operation above T_g and this is therefore the lower temperature limit for processing thermoplastics, such as thermoforming [9, 43].

Figure 2.8 displays different regions of polymer viscoelastic behaviour. Generally, there are five regions of viscoelastic behaviour for an amorphous resin but, cross-linking and semi-crystallinity effect can apply changes to this behaviour. It is evident that the modulus values for thermoplastic materials decrease with an increase in temperature. Region II (b–c) is the glass transition region. Once the rise in temperature reaches the T_g, the material experiences a sharp decrease in the modulus. From there on (region III to V), the polymer undergoes substantial plastic deformation until T_m is reached. As mentioned previously, amorphous thermoplastics lack an obvious T_m. In cross-linked polymers the reduction in modulus values is less significant but there is a plateau in the modulus due to the cross-linked network in the rubbery stage. Cross-linked thermosets lack a melting point, as excessive heat pass the T_g leads to

degradation and not melting. Semi-crystalline thermoplastics (dotted line) exhibit both T_g and T_m temperatures. Since the crystalline districts within the polymer network tend to act as a filler stage, the level of the plateau (i.e. modulus) will be administered by the degree of crystallinity. T_m in semi-crystalline resin is attributed to the melting of the crystalline content, whereas T_g is governed by the amorphous region of such materials. The modulus reduction between region I and II depends on the crystallinity content, with higher crystallinity resulting in higher plateau modulus. The flexibility of the polymer in temperatures between T_g and T_m is a result of a rigid crystalline domain embedded in a soft amorphous matrix [43, 44].

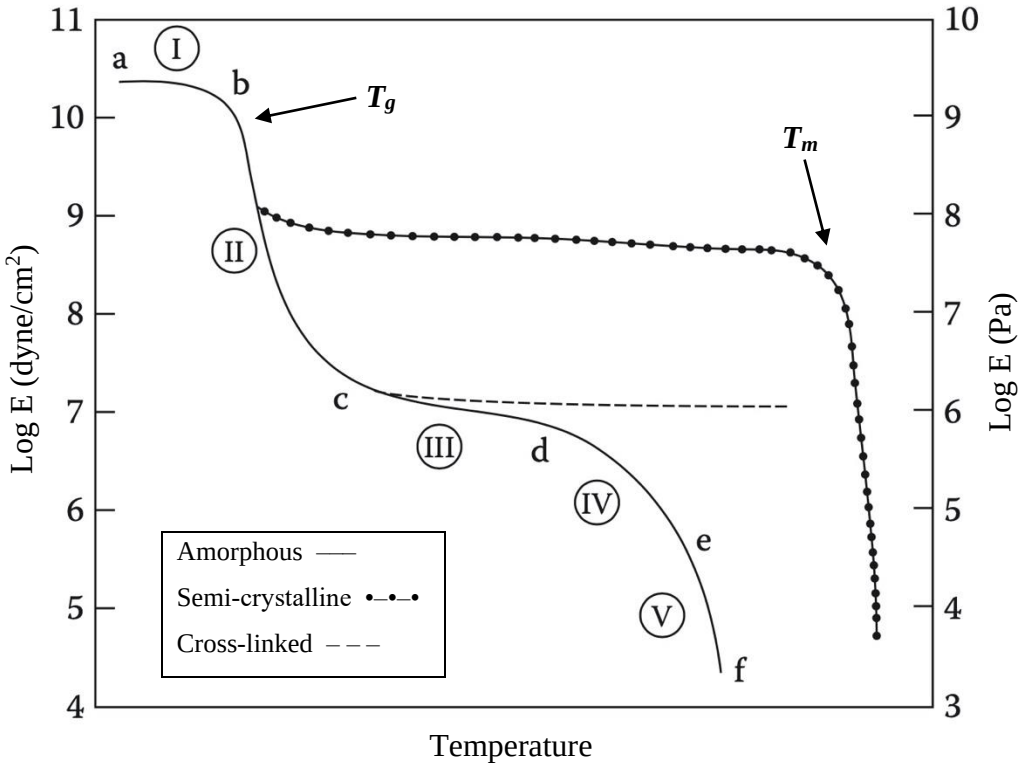

Figure 2.8 Viscoelastic behaviour of a linear amorphous polymer and effects of crystallinity (dotted line) and cross-linking (dashed line) [43].

2.3.1.2 High-temperature Thermoplastics

Candidate materials for production of fuselage and airframe parts for aircrafts are categorised as high-speed civil transport (HSCT) materials. Supersonic aircraft platforms are normally designed to perform at a speed up to Mach 2.0 to 2.4. At such speed, skin temperature of the airframe can rise due to effect of aerodynamic heating at supersonic speed [45]. For instance, as the aircraft speed increases above Mach 1.0,

the temperature begins to rise and reaches 120 °C, while cruising at Mach 2.2. At Mach 2.4, temperatures can reach a range from 150 to 170 °C and even exceed 200 °C at the leading edges of the structure [46]. A satisfactory material shall utilise great maintenance of mechanical and thermal properties at these temperatures.

Thermoplastic matrices display a promising opportunity for aerospace and automotive sectors and potentially can bridge between processability and lightweight high strength FRPs. Many challenges however remain in thermoplastics that need to be addressed to maximise their potential. Traditional thermoplastics show high sensitivity to temperature with very low softening point. For example, commodity polymers such as polyethylene (PE) and polypropylene (PP) have T_m ranging from 100 to 168 °C and a much lower service temperature, making them not suitable for high-temperature applications [47]. Specific properties such as strength and stiffness, and low density of FRPs with such resins systems have encouraged the use of these polymers in various sectors. However, with the increase in demand for high-temperature thermoplastics, other systems are especially required for aerospace industry.

High-temperature thermoplastics are generally characterised by their enhanced heat resistance (>200 °C), their heat distortion and sustainable use in high temperatures. Other properties associated with high-temperature polymers are their durability, toughness and strength, their ability to withstand radiation, ability to be moulded into parts with tights tolerance, and durability [48]. Among many existing high-temperature thermoplastics, only a handful can be utilised for manufacturing high-performance and high-temperature prepregs. Generally, melt processable thermoplastics which resist temperatures above 150 °C are considered as high-temperature polymers [49]. However, melt processability is only one of the many factors reviewed for FRP manufacturing.

Table 2.1 lists some of the primary high-temperature polymers for comparison. Polyether imide (PEI), Polyphenylene sulphide (PPS), Polyether ether ketone (PEEK) and Polyether ketone ketone (PEKK) are amongst the popular choices for manufacturing high-temperature composites. They all function well in elevated

temperatures and have resistance to water or humidity absorption. However, many of the preferred high-temperature engineering thermoplastics are semi-crystalline. Improved thermal stability, toughness, and better deformability are some of the thermal advantageous of semi-crystalline polymers over commercially available amorphous resins. Between T_g and T_m, semi-crystalline polymer consists of a crystalline phase dispersed in a soft amorphous region. Crystallites act as physical crosslinks that retards the movement of polymer chains even above T_g. Although at temperatures above T_g mechanical properties of semi-crystalline thermoplastics are reduced, but this is to a lesser extend compared to amorphous resins. This allows the use of semi-crystalline resins for longer times at higher temperatures [50, 51]. Above the T_g, amorphous thermoplastics exhibit substantial loss of their mechanical properties.

Table 2.1 Thermal characteristics of some high-temperature thermoplastics [39].

Polymer	T_g **(°C)**	T_m **(°C)**	**Processing temperature (°C)**	**Type of morphology**
Polyether imide (PEI)	218	-	316−360	Amorphous
Polyphenylene sulfide (PPS)	88	285	329–343	Crystalline
Polyether ether ketone (PEEK)	143	345	382–399	Crystalline
Polyether ketone ketone (PEKK)	156	310	327–360	Crystalline

In aerospace applications, structural FRP fuselage must be able to tolerate various acidic and fluidic environments in maintenance operations or encountered during the flight. It was previously mentioned that semi-crystalline polymers are more solvent resistant than amorphous polymers due to orderly and densely packed crystallites [52]. Depending on the polymer grade, PEI may be much less chemical resistant than PPS or PEEK. It is reported that the most common PEI grade Ultem 1000, will degrade and hydrolyse in dilute bases. Ultem 1000 is soluble in chlorinated solvents such as methylene chloride and chloroform. Since methylene chloride was used as a paint stripper, it was of significant importance to consider its effect when in contact with primary PEI based composite fuselage parts. Another fluid that has been found to

attack PEI is hydraulic fluid (Skydrol) [39, 48, 53]. Table 2.2 compares the effect of various environmental agents on PEI, PPS, PEEK and PEKK.

Table 2.2 Environmental resistance of selected thermoplastic resins [39].

Environmental agent	PEI	PPS	PEEK	PEKK
Water or humidity	Good	Excellent	Excellent	Excellent
JP-4, JP-5 fuels	Excellent	Excellent	Excellent	Excellent
Hydraulic fluid (Skydrol)	Very poor	Excellent	Excellent	Excellent
Methylene chloride	Poor	Good	Good	Excellent
Methyethyl ketone	Poor	Excellent	Excellent	Excellent
Ethylene glycol	Good	Excellent	Excellent	Excellent

2.3.1.3 PAEK Thermoplastic Family

The polyarylether ketone (PAEK) family of aromatic thermoplastic polymers exhibit an interesting balance and properties for development of multi-functional thermoplastic composites to address many of present limitations. PAEKs are a family of high-performance semi-crystalline (usually) thermoplastics with a unique set of properties such as chemical resistance, thermal stability and great mechanical characteristics over a wide range of temperatures. They also exhibit great combustion resistance and electrical performance. PAEKs are named with regards to their ketone/ether (K/E) ratio, which represents the sequence of ether and ketone chains in the repeating units of polymers. The diphenylene ketone groups provides the high thermal stability and high strength, while the ether linkage account for the flexibility, which also adds thermal stability [54, 55].

There are various combinations of the ketone and ether groups, which are designed to make balance between the heat resistance properties and good processability. The synthesis of the first aromatic PAEK dates back to 1962, which involved electrophilic aromatic substitution of diphenyl ether with phthaloyl chloride [56]. In general, PAEKs can be manufactured using two methods, nucleophilic reaction and electrophilic reaction. In both methods the key point for a homogeneous and steady

reaction is the avoidance of crystallisation and precipitation of the polymer in the solution during the reaction process [57-59].

Figure 2.9 compares the polymer structure of the common PAEK thermoplastics. These polymers have received considerable attention in the past two decades, especially with respect to their high-temperature properties. Both (Polyether ketone) PEK and (Polyetherketoneetherketone ketone) PEKEKK have high T_m of approximately 380 °C, which is quite close to the degradation temperature of PAEKs. This leaves a narrow processing window for these polymers and due to this issue, they are not the ideal choice for melt processing. PEKEKKs are now mainly withdrawn from sale [53]. PEEK and PEKK are considered to be the most widely used and most favourable polymer, particularly in aerospace applications where high-performance light-weight load bearing structures are required in elevated temperature operations. These polymers have also exhibited fantastic resistance to impact energy, and great vibration damping, specifically when coupled with high-performance fibres [60-63].

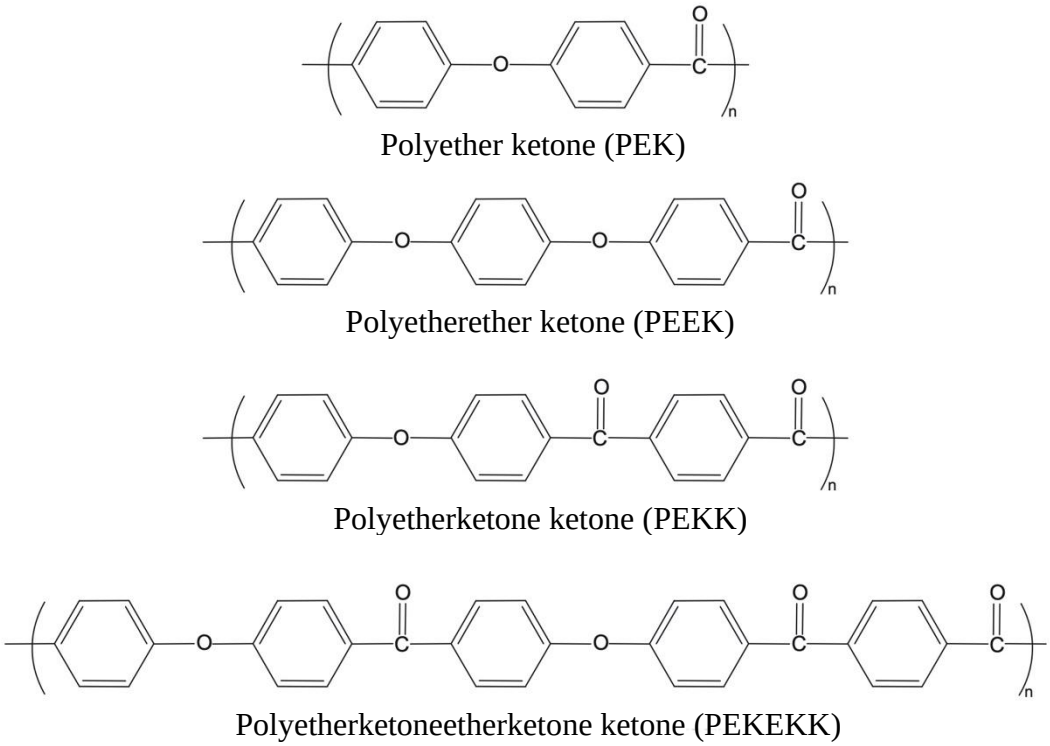

Figure 2.9 Polymer structures of different PAEK thermoplastics [48].

PEEK is a high profile and most widely known and used PAEK. Its properties allow implementation in highly prized engineering applications. PEEK is semi-crystalline with T_m of 335 to 345 °C and T_g of approximately 143 to 145 °C, depending on the polymer grade. The crystallinity rate of PEEK can vary from 40 % (slowly cooled) to amorphous (by rapid quenching). Slow cooling rate is required to provide the essential time for spherulite growth and nucleation. The optimum cooling rate of PEEK is reported to be 0.1 to 11 °C/min, which will yield to 25–35 % crystallinity content [64, 65]. Crystallinity rate can influence numerous physical and mechanical properties of PEEK. Some mechanical properties affected by degree of crystallinity are listed in Table 2.3. It is observed from the table that extra high degree of crystallinity can significantly decrease mode-I fracture toughness but enhance all other mechanical properties.

Table 2.3 Effect of crystallinity on the mechanical properties of neat PEEK 150P [65].

Property	**15 % Crystallinity**	**40 % Crystallinity**	**Change (%)**
Tensile modulus (GPa)	3.4	4.5	32
Tensile strength (MPa)	69.0	96.5	40
Shear modulus (GPa)	1.2	1.4	17
Shear strength (MPa)	41.4	62.0	50
Compression strength (MPa)	151.7	172.4	14
Fracture toughness MI ($MPa.m^{0.5}$)	11.0	3.3	–70

PEEK modulus ranges from 3 to 4 GPa and it can provide a service temperature up to 260 °C. Average fracture toughness of PEEK is 50 to 100 times higher than common epoxies. The polymer exhibits fantastic water absorption properties of less than 0.5 % in room temperature compared to 4 to 5 % for conventional aerospace grade epoxies, and maintains a great serviceability at 125 °C, in which other high-temperature polymers like aromatic polyamides are liable to fail. PEEK also retains great resistance to abrasion and dynamic fatigue, and attacks by most chemical substances except for

highly concentrated sulfuric acid. Such properties have secured PEEK a common place in aerospace and automotive industries [43, 66-68].

PEEK has been replacing metals and other traditional composites due to its lightweight, reduced cost, and resistance to harsh environment. Since PEEK is a polymer resin, mechanical, thermal and physical properties can be upgraded by incorporating reinforcing phases such as carbon fibre and glass fibre. CF/PEEK and GF/PEEK composites are now widely used as structural components in aerospace and aviation industries [69]. Examples of structural parts containing PEEK, and PEEK fibre-reinforced composites include Airbus A320 vertical stabiliser brackets, EH 101 helicopter floor, F-117 rudder assembly, F-22 weapons bay doors, F-22 access covers, OH-58D helicopter horizontal stabiliser, and Rafale engine tunnels [70]. PEEK composites have therefore been studied extensively and become one of the most researched polymer resins. Processing and morphology [71, 72], mechanical performance, delamination and fatigue behaviour of CF/PEEK are among such examples [73-76].

Applications of PEEK are not limited to aerospace industry only. There are wide variety of application across engineering fields in which PEEK is implemented. Semi-crystalline or amorphous PEEK is used to coat and insulate metallic wires. Method includes preparing the surface of the wire via deliberate scratching (for better adhesion) and pulling the wire through PEEK solution or molten PEEK through a die. Other coating methods include thermal spraying and electrophoretic deposition. PEEK coated wires would have better operating temperatures and are protected from external degrading environments such as abrasion or chemicals [77-79].

PEEK is also biocompatible and its superior combination with strength, stiffness and toughness, makes it possible to replace traditional medical materials like titanium. PEEK-based spinal implant received approval in 2013 from United States food and drug administration [80]. PEEK is now being used for dental purposes as well. The fact that mechanical properties of PEEK closely match to that of bone's (bone, enamel and dentin) leads to a lesser stress shielding compared to titanium dental implants. The polymer is mainly used for temporary implant abutments, dental clasps and

frameworks for partial removable dental prostheses [81-83]. Other medical device and instruments with applications in trauma medicine and orthopaedics are manufactured using PEEK including fixators, finger-joint prostheses, osteosynthesis plates, fracture fixation plates and screws [84-86].

Compared to PEEK, PEKK is relatively new to the PAEK family. PEKK can be produced with unique and variable properties depending on different formulations. What gives PEKK an edge compared to other PAEKs is the capacity to synthesise isomeric copolymers to influence the melting temperature T_m of the polymer and extend the melt processing window. By altering the ratios of terephthalic acid (T) and isophthalic acid (I) moieties in the polymer chain, various PEKK copolymers are created. This ratio is commonly known as PEKK T/I ratio. Changing the T/I ratio can introduce a T_m range from 305 to 358 °C and affect the crystallisation rate and crystallinity of PEKK, without substantially changing the T_g. As the isophthaloyl moieties ratio increases, the polymer chains become more disordered and the T_m and crystallinity decreases. For instance, it was reported that PEKK with a T/I ratio of 6/4 has a slow crystallinity kinetics and maintains an amorphous condition [62, 87-89].

PEKK is able to maintain a high degree of chemical resistance as well as its physical properties up to its T_g and it can exhibit multiple crystal forms. The X-ray diffraction pattern of PEKK that has been crystallised by exposure to solvent at room temperature or by low temperature (200 °C) annealing is different from that obtained from slow cooling from the melt or high-temperature annealing [90]. Additionally, PEKK has a slow rate of crystallisation leading to greater dimensional stability, enhanced flow characteristics and reduced moulded-in stresses. Such slow crystallisation rate enables amorphous PEKK films to remain transparent even in elevated operating temperatures, in which PEEK becomes opaque due to crystallisation [91]. PEKK usually has lower processing temperature than PEEK and this is an important point for industrial applications not only because it facilitates composites manufacturing by lowering the power consumption, but also prevent the material degradation [92]. PEKK also exhibits a lower melt viscosity than PEEK, making it easier for injection moulding applications. Higher mechanical values than of PPS and PEI, high toughness and damage tolerance, excellent fire retardancy, low flame, low toxicity and smoke

emission are among other properties of PEKK resin, which makes it a suitable candidate for applications where high-performance FRPs are required [21, 93].

Since the introduction of PEEK and PEKK for the use as the matrix phase in thermoplastic composites, efforts have been made to develop other resin systems based on the PAEK family of aromatic polymers, offering better characteristics package. AE 250 PAEK (also known as engineered PAEK) is one of the most recent resin systems developed by Victrex plc. that is a PEEK based copolymer with much lower T_m of 305 °C but T_g of 149 °C, which maintains mechanical, physical and chemical resistance properties typically compared to PEEK or PEKK. The lower T_m of AE 250 means lower processing temperature, permitting composite parts to be manufactured cheaper and faster, with added perks of implementing out of autoclave processing methods, fast automated lay-up, injection over-moulding and hot stamping, thus eliminating the high use of expensive autoclaves and factories in which houses them. The novel AE 250 is 25–30 % semi-crystalline when press consolidated with a cooling rate of 5–10 °C/min. The lower melting temperature of AE 250 resin widens the processing window whilst still allowing fully crystalline morphology to develop through the cooling phase. A major advantage of AE 250 is that it could be processed with relatively low pressures, opening gates to the production of high-quality parts utilising out of autoclave processing [94].

2.3.2 Manufacturing Methods

The main challenge of manufacturing thermoplastic composites is the incorporation of fibres into the resin matrix. Unlike the conventional thermosets like epoxy that are in a liquid state in room temperature, the thermoplastic polymers are usually solid. Dealing with a liquid resin in room temperature could be more convenient for processing thermoset prepregs with less time consumed and more cost effectiveness. This is mainly due to the fact that thermosets have viscosities less than 100 Pa.s at processing temperature, resulting in high flow rates and consequently better fibre wet-out during the impregnation or prepreg process [95, 96].

In contrast, handling a resin that is provided in a solid form in room temperature could be quite challenging. Poor fibre wetting and impregnation properties of most

thermoplastic resins and their associated processes have been limiting the use of continuous FRPs only to expensive products used in aerospace applications such as CF/PEEK [97]. High melt viscosity of thermoplastics creates a challenge when incorporating the resin phase into the fibre for full impregnation. This issue often is more critical for continuous fibre-reinforced composites. Processing of thermoplastic composites become difficult at viscosities above 550 Pa.s [98]. Poor resin impregnation could lead to sever decline in mechanical properties.

Regardless of the manufacturing process, the first step of thermoplastic prepreg production is resin impregnation. The resin phase must completely surround individual fibre filaments, which are themselves part of a packed bundle. In the impregnation process, the main priority is to guide the resin to a position between individual filaments. It should be ensured that this flow of resin is homogeneous to guarantee a balanced and full impregnation during prepreg production or the full consolidation of the structure. Impregnation is usually followed by application of heat just above the T_m of the polymer to ensure adhesion of the resin to the fibres.

Several impregnation methods have been researched over the years and some of these techniques are now commercially used to produce thermoplastic prepregs. Thermoplastic prepregs can be stored indefinitely and when required, they can be stacked and consolidated to form thicker laminates. Following this section, different methods of producing thermoplastic prepregs will be reviewed and some state-of-the-art ones will be discussed. The review will mostly focus on production method of continuous fibre reinforced prepregs. Some of the most common methods of fibre impregnation for producing thermoplastic composite can be seen in Figure 2.10.

2.3.2.1 Melt Impregnation Process

In melt impregnation (also referred to as hot-melt impregnation), the fibre tow is passed through a bath containing molten polymer. Early appearance of such method dates back to 1976 in US patent US3993726 [99]. Moyer described method involving passing fibre roving through a crosshead extruder to impregnate the rovings with a thermoplastic resin under high pressure. The composite is then pulled through a die to shape a void-free part. Production of at least 30 % fibre by volume was reported in

1985 using the similar method but, preferred thermoplastics were polymers having melting temperature of around 150 °C [100]. The method of pulling reinforcing fibre impregnated with a resin matrix through a die is called pultrusion. A variety of dies cross-sections, such as bar, rod, angle etc., can be implemented to produce the designed shape. Both thermosets and thermoplastics can be pultruded; however, their processing parameters are quite different. Although pultrusion could be a very fast method of production, in conjunction with thermoplastic resins, it can suffer from poor impregnation given the fast production speed and the short window for a full impregnation. Processing temperature, pressure, and the die geometry are some of the key factors considered [101-106].

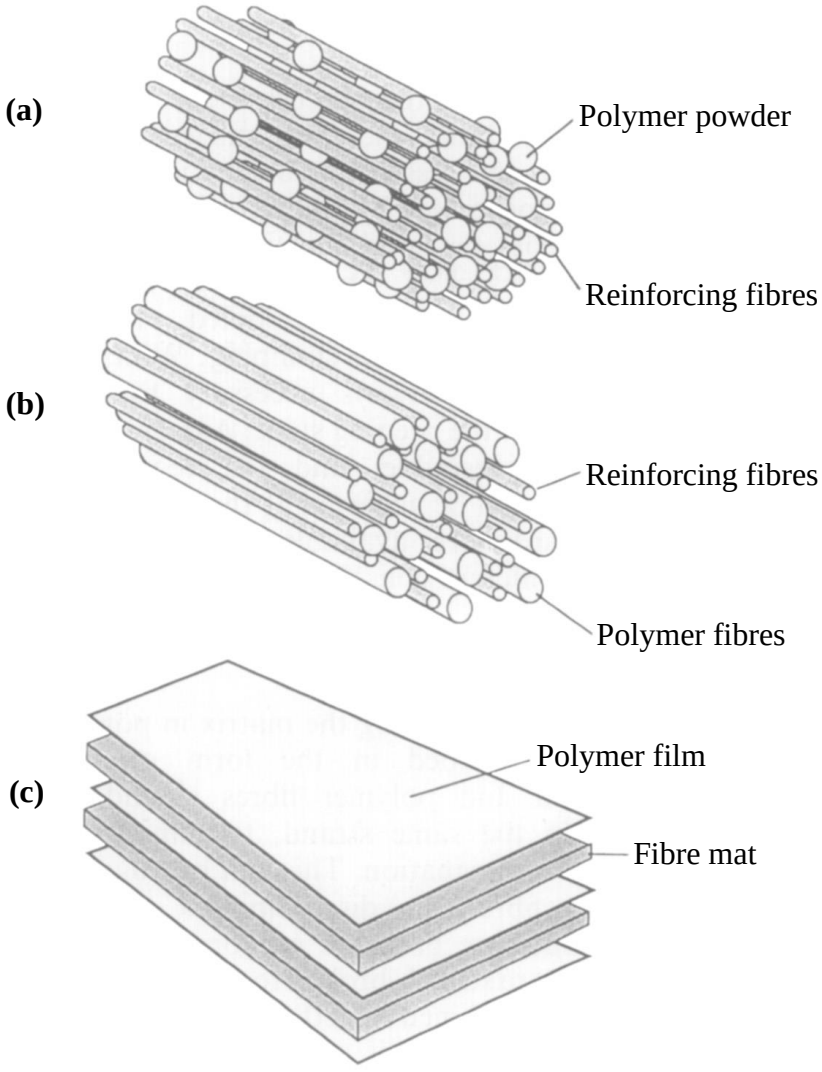

Figure 2.10 Examples of manufacturing method of thermoplastic composite: (a) powder impregnation, (b) fibre co-mingling and (c) film stacking [107].

Since fully polymerised thermoplastic resins have very high molecular weights, their melting viscosities could be two to three times greater than viscosities of common thermosets [108]. This will make impregnation very difficult and as the result, many efforts have been made to assist better impregnation of fibres. Without external forces, impregnation could be limited. It can take up to 6 hours to incorporate a medium viscosity PEEK into a CF roving without the application of pressure [109].

One novel method to increase the impregnation rate is found to be using pin assisted melt process. In this process, the fibre roving is pulled over a single or a series of rollers (pins) to force the molten resin into the fibre bundle. More rollers encourage the impregnation from both sides, consequently resulting in a higher wet-out in case of GF/PP composite [110]. Notable improvement was reported in the impregnation rate by increasing the impregnation time, elevating the resin temperature and increasing the fibre tension for GF/PP production. Heating the rollers and also using vibration seem to have exhibited small improvements as well [111]. However, there are limits to some of these variables. For instance, by increasing the processing temperature it is possible to decrease the polymer viscosity. However, too high temperatures can result in polymer degradation. Also, the shear stress and the frictional stress build-up associated with passing the fibre tow through viscous resin and impregnation rollers can result in filament breakage and excessive fibre abrasion. The passing of fibre tow over the wedge-shaped region located between the fibre roving and the roller can cause pressure to build-up [112, 113].

Since the fibre roving is a packed and concentrated bundle of filaments, it is advantageous to open up the fibre bundle to a spread tow with a wider cross-section. Spreading the fibre tow can increase the surface area of the roving and expose increased number of individual fibres to the resin matrix. This could be achieved by introducing a fibre spread mechanism before guiding the fibres into the resin bath. Examples of such mechanism is spreading rollers [114] and air jets [115]. Marissen et al. [116] developed a significantly modified melt impregnation process by using convex comical shape rotating spreading pins powered by a motor, as shown in Figure 2.11. The manufactured device allowed smooth rotation of the fibre tow around the impregnation pin, thus reducing the pulling force and the viscous drag on the

impregnated bundle. The convex shape of the pins also assisted in better impregnation by spreading the fibre roving, and the conical shape allowed encircling fibres to be removed from the bars. This combination helped maintain the challenging balance between impregnation quality and production speed.

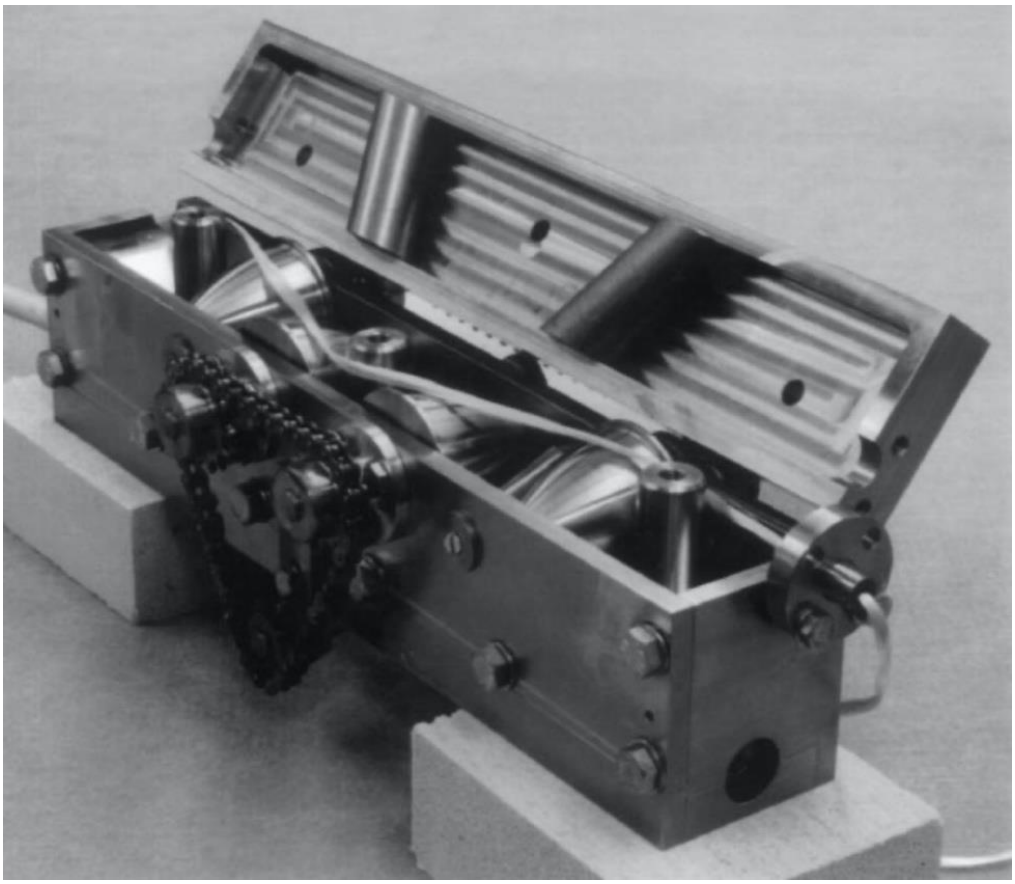

Figure 2.11 Fibre impregnation device consisting of powered conical convex pins for use in melt impregnation process [116].

An inventive impregnation innovation, named impregnation wheel has been created, allowing the production of high-quality impregnated tows or tapes at a considerable speed with an ability to also work with filament winding. The process allowed online melt impregnation of GF with polymers such as PP and PA by utilising a wheel consisting porous ring. Molten resin is squeezed under pressure and impregnates the fibre tow, which is in a tight contact with the outer surface of the ring. The new process offers the possibility of adjusting the fibre volume content by changing the porous ring within the wheel. GF/PP and GF/PA circular tubes were produced with good success using wheel mechanism and filament winding technology [117, 118].

In melt impregnation method, the fibre is generally more prone to damage. This method might work out well for low melting temperature and low viscosity polymers such as PP and nylon 66 but, for high-temperature and high melt viscosity polymers like PAEK family of polymers such as PEEK or PEKK, the penetration of molten polymer into the fibre filaments for a full wet-out of the fibres could be quite challenging. The resin melt viscosity should be as low as possible for a good and uniform impregnation.

2.3.2.2 Film Stacking Process

Due to its relatively ease of production, film stacking method was widely used in early production of thermoplastic composites [119]. In this method layers of lamina containing fibre reinforcement are stacked alternately with pure thermoplastic polymer thin films. The stacked sequence is then heated above the T_m of the resin and pressed to force the polymer resin into the reinforcement layers to form an impregnated composite sheet, as illustrated in Figure 2.10(c). In a sense, film stacking can be categorised as a melt impregnation technique as it involves direct driving of molten resin into fibre reinforcement for impregnation. The applied pressure needs to be sufficient in order to force the polymer flow into the fibres [120, 121].

Despite the convenience of using this method, the long cycle times associated with this process is deemed unattractive on a commercial scale. Also, the effect of higher pressure for better impregnation could be deceiving as high pressures will also force the fibres together and concentrate them, reducing the permeability of the fibre bed. Resin rich areas, limited to woven or random fibre fabrics, and unsuitability for high melt viscosity polymers that result in poor fibre impregnating are also among the disadvantages of using this method [107, 122].

Impregnation methods involving intimate mixing of constituents prior to melting will be discussed in the next few sections. By mixing the two constituents before processing, impregnation can be eased since the distance required for the resin to flow is minimised [123].

2.3.2.3 Fibre Commingling Process

As specified above, a restricting factor for thermoplastic resins is their relatively high melt viscosity compared to thermoset resins. It was also noted that the high viscosity will make the impregnation into the fibre network challenging. An arrangement to tackle this issue is to minimise the flow distance of the resin by commingling the reinforcing fibres with thermoplastic polymer in fibre form, as per Figure 2.10(b). The reinforcement and polymer fibre are commingled, and the resulting hybrid yarn could be used to produce UD tape or could be knitted, woven or filament wound. Despite the form, the commingled yarn is then subjected to heat and pressure so as to melt the polymer resin and wet-out the reinforcing fibre in order to obtain the composite. The difference between this method and direct melt processing is the incorporation of the resin within close vicinity of the reinforcing fibre before melt consolidation [124-126].

Several studies with a focus on yarn manufacturing, commingling process, impregnation and consolidation modelling, and mechanical and physical evaluation of commingled composites have been recorded. The fibre/matrix ratio of commingled yarn can be adjusted by controlling the number of filament fibres in both constituents. Some of the variables that can influence the commingled product include volume fraction of each constituent, density of the matrix, interlacing degree, number of filaments in the fibre bundle and fibres diameter [124, 127-130].

Flexibility is a critical property for composite processing. Compared to other manufacturing methods, commingled yarns are attractive because they exhibit a great degree of flexibility and are readily mouldable to variety of complex shapes [131]. In commingling process high melt viscosity resins such as PEEK could also be processed with a good success. However, comparing the impregnation and mechanism of commingling technique with powder impregnated and sheet impregnated methods for manufacturing CF/PEEK composite shows that higher application of pressure and longer time might be required [132]. Interlacing of the fibre constituents could however be less than perfect and this perhaps might lead to higher impregnation time and resin rich areas, or unimpregnated areas in the composite part [133]. It was reported that de-mingling of commingled prepregs could be possible under tension and can lead to improper mixing of the constituents. Higher tensions during weaving

act on the bottom and the top of the commingled fibre bundle and cause the reinforcing fibre, which is stiffer than the polymer fibre, to shift away from aforementioned areas and create a resin rich area. Nonuniform distribution of constituents can result in insufficient impregnation and therefore affecting the microstructure of the final composite part [132, 134]. Another limitation is fibre commingling is only possible if the thermoplastic resin is available in fibre form. The trick here is to supply polymer fibres with the same diameter as the reinforcing fibre to ensure good distribution of the two fibres. The high cost involved in processing the thermoplastic polymer yarn and commingling it with reinforcing fibre is also an obvious drawback.

Wiegand and Mäder [135] explained a promising online commingling process to overcome some of the aforementioned issues. The proposed approach was implementation of an on-the-line polymer extruder attached to a nozzled spinning device to produce live polymer fibre feed, commingled straight away with the reinforcing fibre, as indicated in Figure 2.12. This technique is superior compared to the traditional air jet texturing as it provides homogeneous distribution of continuous resin and reinforcing filaments, without damaging the fibres. This results in shorter impregnation time and lower void contents, coupled with enhanced mechanical performance. Notable improvements in bonding interface of fibre and matrix were also observed by deploying sizing agent during the commingling process.

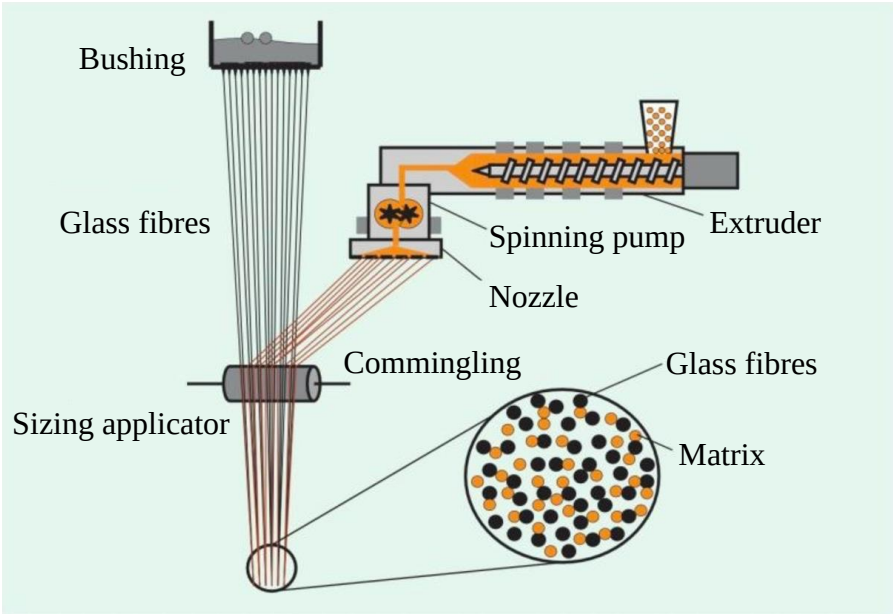

Figure 2.12 Online commingled yarn spinning principle [135].

2.3.2.4 Solution Impregnation Process

One of the methods to avoid the problems associated with high viscosity polymers is using solution processing. By dissolving polymer resin in a suitable solvent, low viscosity solution can be prepared. Thermoplastic prepregs can be manufactured by impregnating fibres with the thinned solution. Low viscosity polymer solution allows easy wet-out of UD or woven fabrics by using many conventional prepreg technologies that are already well stablished for thermosetting resins [136-140].

Early applications of solution processing dates back to 1974 [141]. Typical manufacturing process involves passing the fibre roving through a resin bath containing heated polymer and a plasticiser with certain weight ratios and subsequently, heat melt the impregnated tow to initially evaporate the solvent and then permanently adhere the polymer resin on the fibre. The plasticiser shall be thermally stable up to the T_m of the matrix and at the same time, having a volatility characteristic to enable it to volatilise from the impregnated composite at temperatures above T_m of the resin but below its decomposition temperature, thus providing reduced viscosity compared with the melt viscosity of the polymer alone. This process permits high molecular and high viscosity thermoplastics to be processed given the availability of proper solvent [142, 143].

Solution impregnation is mainly used for amorphous thermoplastics like PEI and polyether sulfone (PES) that are soluble in agents like N-methyl-2-pyrrolidone (NMP). Solvent concentration and temperature can be balanced to supply altogether lower viscosities than that are accessible through the melt impregnation technique. Although in solution impregnation high pressure facilities are not required for good fibre wet-out, in practice there are two major drawbacks in the process. Despite the environmental concerns of using toxic solvents, total removal of the solvent is deemed to be difficult and solvent residuals in the final product can have significant impacts on materials strength, especially at high-temperature applications. High void contents might be created if solvent gets trapped in the consolidated laminate. In the case of amorphous PEI and PES, solvents like NMP could be utilised to thin the polymer. However, in case of solvent resistant semi-crystalline polymers such as PA, more aggressive solvents such as formic acid is required. For highly solvent resistance

polymers like PAEK resins, this is even more challenging, as compatible solvent systems are scarce [144-147].

2.3.2.5 Powder Impregnation Process

Among all the other impregnation techniques, powder impregnation is gaining popularity for having a low-cost manufacturing procedure and great processability. Powder impregnation can be classified into two categories: dry powder impregnation and wet powder impregnation. Both methods include incorporating fine powder of thermoplastic polymer in between fibre filaments for impregnation (as illustrated in Figure 2.10(a)) but vary in the way resin particles are deposited on the fibres. It is desirable to use polymer particles of similar scale to fibre diameter for easy penetration of particles in the fibre bed. This was not always possible due to the limits on milling technologies and the high costs [107]. However, as the powder technology advances and new technologies emerge, decreasing the polymer particle size becomes more effortless and more economically sensible. Many thermoplastic polymers are now available in form of very fine powder, as small as 5 to 10 microns in diameter.

Powder impregnation is also categorised as the tier of methods in which the constituents are mixed prior to melting thus minimising the flow length required for fibre wet-out. In powder processing, impregnation mainly takes place along the fibre direction rather than in transverse direction and this is very beneficial as permeability of the fibre bundle parallel to fibre direction is higher than the perpendicular direction [123, 148, 149].

***Dry powder technology*:** Dry powder impregnation is carried out by passing the fibre tow through a chamber containing the polymer powder. This method was first employed by Price [150], in which the glass fibre roving was passed through a bed of PP powder. Here, polymer particles attached to the fibre filaments due to electrostatic charges.

The majority of dry powder technologies exercise three essential steps: opening up the fibre filaments by spreading the fibre tow, impregnating the fibre, and finally heating the mixture for sintering and coalescence of resin particles on the fibres. The main

distinction in different techniques is the method they employ for attaching the resin particles to the fibres. This is done in a number of different ways as summarised in Table 2.4.

Table 2.4 Summary of available dry powder impregnation technologies.

Method	**Description**
Conventional fluidised bed	Mixing powder with gas to suspend particles.
Electrostatic fluidised bed	Electrostatically charging particles for fibre cling.
Acoustically fluidised bed	Using acoustic energy to suspend particles.
Recirculating fluidised bed	Recirculating particles in a loop for impregnation.
Moisture assisted deposition	Moistening fibres for better particle adhesion.
Electrostatic spray	Spraying electrostatically charged particles on fibre.

Conventional fluidisation involves mixing air into the packed polymer powder in order to loosen up the powder stack in an effort to separate the agglomerated powder into individual particles. This creates an air suspension of particles, helping better penetration of polymer particles between the fibre tow. Factors such as particle size, powder flow pattern, degree of fibre spread and dielectric properties of constituents can influence the deposition [151]. Ganga [152-154] explained in a series of patents a method of impregnating 20 microns in size PA powder by particle fluidisation. Impregnated glass roving where then coated with an outer layer of different or same polymer and melted. Because the melting of the coating layer is done without melting the powder, the resulting material is relatively flexible [155]. Rath et al. [156] successfully fluidised Nylon-12 particles by passing a stream of compressed air in a mechanically agitated powder bed and produced prepregs with fibre volume range of 20 to 50 %. Other works of similar natures with different polymers like PPS and PEEK, and G30-500, AS-4 and IM-7 grades of CF is also carried out [157, 158].

Very fine particles of less than 20 to 30 microns proved hard to fluidise due to interparticle Van der Waal's forces. These forces are effective up to a range of 100 Angstroms and in a conventional fluidisation bed, this will lead to particle

agglomeration and subsequently poor powder impregnation [159, 160]. Difficulties associated with binding and depositing the powder onto the fibre surface can be addressed by grounding the fibre and electrostatically charging the resin powder.

Some researchers have emphasised on implementing electrostatic attraction for achieving even powder impregnation. Early investigations involve electrically charging glass fibres and polymer resin with opposite charges and passing the fibre tow through a gaseous suspension of particles. Electrodes are placed under the distributor to charge the particle gas [161, 162]. Muzzy et al. [163] demonstrated the ability to manufacture AS-4/PEEK, S2-glass/PEEK and AS-4/LaRC-TPI by electrostatically charging and fluidising PEEK or LaRC-TPI powders and depositing the particle on spread tow fibres. The electrostatic charges ensure wide range of particle sizes can be used and attaches to the fibre. Spreading the fibre tow before deposition helps expose more filaments, enhancing the impregnation and producing a composite with better flexibility. Increasing air flow and the voltage or, decreasing particle size can all improve the bed residence time. Compared to AS-4 carbon fibre, non-conductive S2-glass required considerably more time in the deposition chamber for PEEK impregnation [164-167]. Figure 2.13 shows the different steps involved in electrostatic fluidised bed manufacturing process.

A method studied by Iyer and Drzal [168] showcased a controlled and uniform method of powder deposition by using acoustic energy. They utilised an acoustic source in order to subject the powder bed to low frequency vibrations. Different prototype models were manufactured. In this process, acoustic vibrator is used firstly beneath a series of rollers to spread the fibre roving. Similar scale in size particle and fibre was used. Spread fibre was passed through the airborne cloud of particles, which are in close vicinity of an acoustic vibrator. Due to interparticle friction, resin powder is tribo-charged and electrostatically attaches to the filaments. The powder coated tow is then heated for the particles to bond to the fibre. The impregnation rate can be controlled directly via adjusting the amplitude of the vibration [169-171].

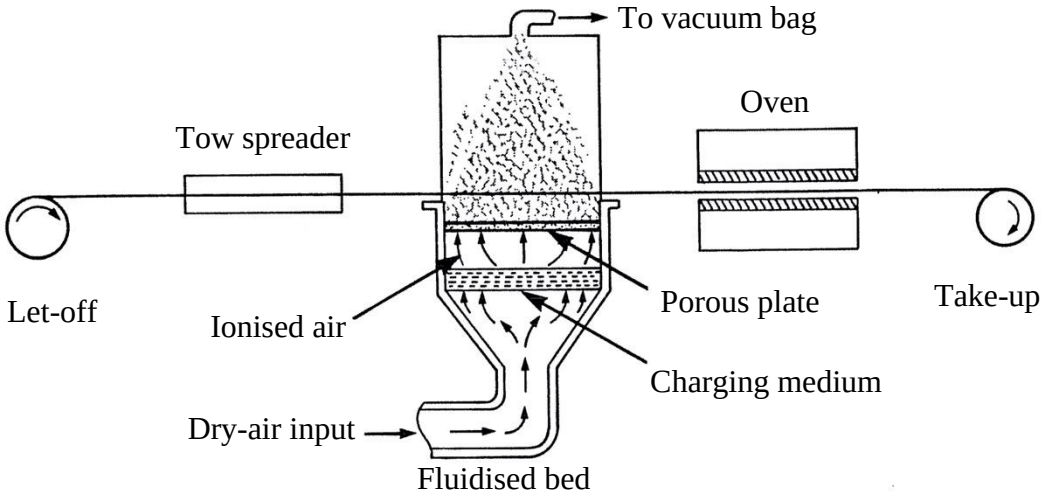

Figure 2.13 Schematic of electrostatic fluidised method for producing continuous composite fibre tow [163].

A NASA-sponsored powder deposition apparatus designed and manufactured at Clemson University implements a recirculating fluidised chamber [172]. As seen in Figure 2.14, fibre bundle is passes through a chamber of polymer particles that are initially fed from a separate channel that mixes particles with nitrogen, sending them on a calculative movement via use of a fan-vacuum system. This way, polymer loss from the chamber is minimised and particles keep on moving through the system, impregnating the fibres in process. Similar approach was tested and improved upon by using a resin control monitoring system that influences the speed of the take-up drum to adjust the amount of polymer particles deposited [173]. However, problems like dust build up in the fan and feed lines, resin contamination, and gas requirements limited the overall functionality and scale of the operation. Some of these problems were later addressed by eliminating the need for precise fibre tension control and utilising better deposition chambers that avoids circulation of the resin particles through the fan interior [174-176].

One way to promote polymer particle adhesion on the fibre is to moisten the spread fibre. This can be achieved by spraying ultra-fine water moistures on the spread fibre [177], or passing the fibre through a chamber with 100 % relative humidity [178]. Powdered polymer is then deposited on the reinforcement and tacked onto via quick application of heat. Drawback with this technique is fibre and polymer agglomeration, resulting in poor impregnation.

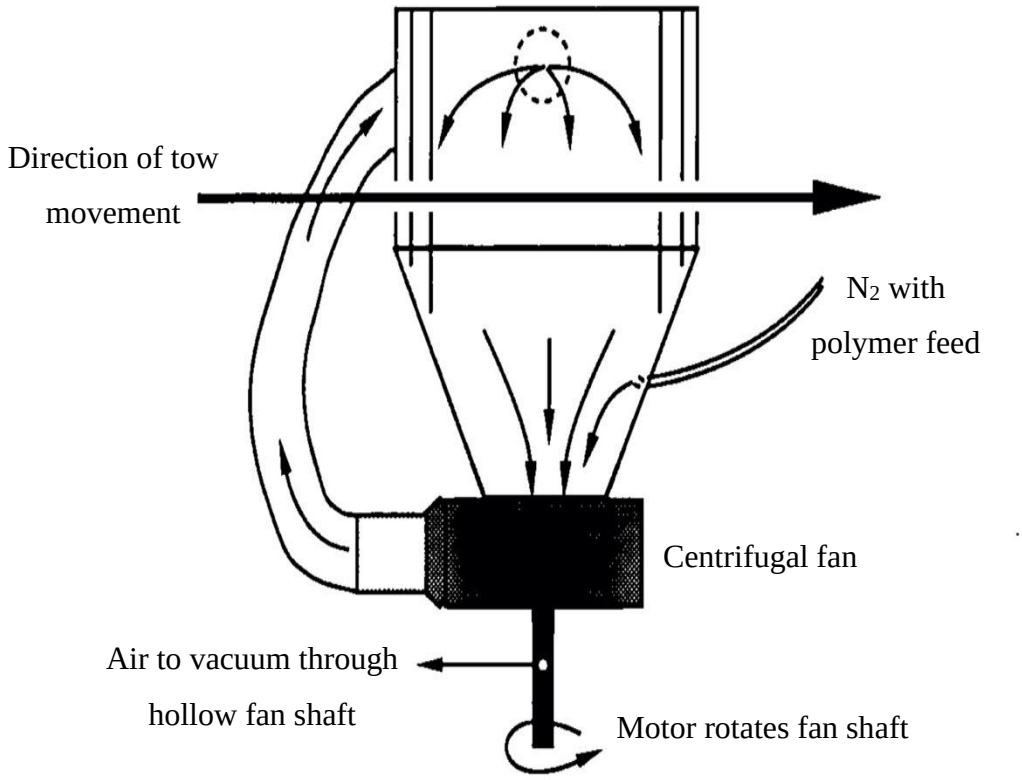

Figure 2.14 Recirculating fluidised chamber mechanism [172].

Electrostatic powder spray of polymer particles on different surfaces were studied throughout the years [179-181], and also been applied for coating fibre reinforcement [182]. Ramani et al. [183] developed an electrostatic spray process that uses both mechanical impregnation and electrostatic adhesion of the resin particles. An electrostatic spray gun is used to create a negative corona field by a corona voltage (–50 to –100 kV) and subsequently coating both sides of a spread fibre bundle. Particles are charged by the ions produced in the corona region. Before the electrostatic coating stage, the fibre tow is heated by a hot nitrogen torch to eliminate the sizing on the fibre, moistened for better electrical conductivity, and passed on a grounded spherical surface for spreading. The method was used to develop GF/PEKK and the effect of fibre velocity, corona voltage and powder mass flow on the degree of powder deposition was investigated [184]. Figure 2.15 demonstrates the electrostatic spray coating setup used in a similar study to produce semi-crystalline polyphthal amide (PPA) carbon fibre composite [185].

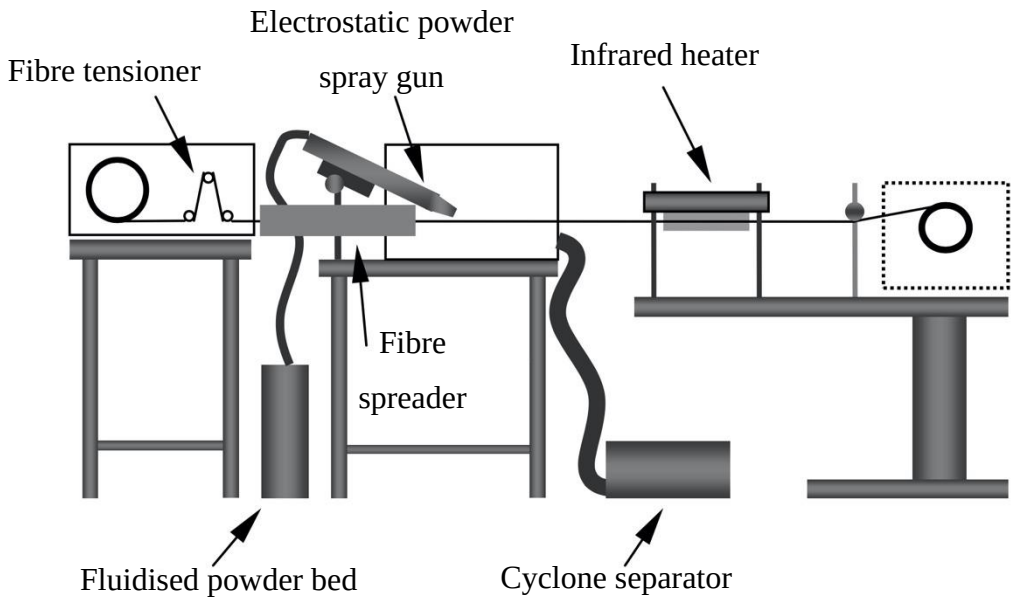

Figure 2.15 Schematic of electrostatic powder spray impregnation process [185].

It is evident that some of the dry powder impregnation technologies offer considerable benefits such as independency of matrix viscosity, avoiding use of toxic solvents, and eliminating secondary processing operations. These techniques however come with a number of drawbacks. Difficulties have been reported in control over fibre volume fraction and most processes require depositing more than necessary powder and removing the extra resin in another procedure. Gas assisted powder flow methods have certain disadvantages such as uneven resin overlay, irregular distribution of particles and the danger of dust explosion. Expensive powder coating equipment could also be concerning and are most employable for conductive fibres like CF and not insulating fibres like GF.

***Wet powder technology*:** The wet powder technology is an alternative to dry powder technique based on the concept of suspending polymer particles in a liquid carrier and passing fibre reinforcement through the slurry tank containing the aqueous medium to pick up the resin particles. Taylor [186] investigated a dispersion of a powdered plastic resin in water, which was made thick by means of water-thickening materials such as; polyethylene oxide and hydroxyethyl cellulose. The dispersion was then applied to fibrous textile to distribute the resin over the fibres. Most methods follow the same procedure but use other composition of liquid carrier [187-189]. PEEK and LaRC-TPI

were reportedly suspended in aqueous solutions of ammonium salts of polyamic acid. Utilising this suspension helped with particle dispersion and as fibre-matrix interface binder. High-performance continuous carbon fibre composites were manufactured with fibre volume content of 36 to 61 % for CF/PEEK, and 38 to 49 % for CF/LaRC-TPI. Various processing conditions including fibre tension and resin concentration can influence the properties of the consolidated laminate [190, 191]. Vodermayer et al. [192] employed an aqueous dispersion containing water, polymer powder and 1 % additive (chremophor surfactant), and further developed a model of powder impregnation of infinite fibres. They stated that with decreasing particle diameter, the powder concentration in the dispersion and consequently the viscosity of the dispersion increases, and concluded that using powders with a particle diameter of about 15 to 20 μm is beneficial. Chary and Hirt [193] created a surfactant solution aqueous foam of the thermoplastic resin by using a nitrogen gas, and deposited the foam on AS-4 carbon fibre. A tube furnace was used to fuse the polymer onto the fibre. In a recent study, Steggall et al. [194, 195] designed a novel powder slurry impregnation method that combined compression moulding with vacuum assisted resin transfer moulding. Slurry of HDPE powder and water was injected in a closed mould containing biaxial glass fabric, and vacuumed down the mould to a collecting pot, impregnating the fabric in process. Composites with an average fibre volume fraction of 65 % were manufactured and a model was developed to predict the void fraction.

Wet powder impregnation offers considerable advantages such as:

- Different particle sizes can be used, which is notably important for impregnating fibre cloth that cannot be spread.
- No polymer solubility limitations compared to solution processing.
- Very low slurry viscosity compared to melt impregnation.
- Easy incorporation of additives and modifying fibre/matrix interface.
- Inexpensive equipment and simple guiding systems without use of die.
- Short melt state time and short resin flow length.
- Easy control over fibre/matrix ratio by adjusting polymer amount in the slurry.
- Easy and safely handling of the process.

Since wet powder technology provides the aforementioned benefits and allows easy addition of nanoparticles in the aqueous suspension, it presents a particularly interesting opportunity and potential to be investigated further, and to be chosen as the method-to-go for this study. Easy addition of nanoparticles within the composite is one of the main agendas of this research.

2.4 Fibre-reinforced Nanocomposites

FRPs provide outstanding mechanical properties combined with many other great characteristics that makes them useful in wide range of applications. However, FRPs sometimes suffer from poor out-of-plane properties due to restrictions of the weak matrix, and polymer resin being the only constituent holding the fibres together. Apart from that, one of the fundamental parameters in FRP composites, affecting mechanical characteristics, is the interface region between the two phases. Sufficient adhesion between the fibre and matrix is required to ensure the load can transfer from matrix to the reinforcing fibres via the interface. Poor interfacial bond can result in poor mechanical performance as the applied load on the composite can easily separate the two phases [196].

In order to tackle some of these issues and improve the transverse and through-the-thickness properties of the composite, FRPs with strong mechanical properties and interface could be fabricated by modifying the fibre or the matrix phase. Composite delamination can be reduced by adding through-the-thickness reinforcement (like 3D fabrics), however such strategies do not affects the fibre/matrix interfacial bond and might compromise the in-plane properties of the laminate and cause fibre waviness [196].

In an attempt to enhance the mechanical properties of FRPs, researchers have recently looked into the modification of the matrix phase by incorporating nanomaterials into the conventional FRP composites to form fibre-reinforced nanocomposites. There is a growing interest in developing multiscale (hierarchical) fibre-reinforced nanocomposites by using two differently scaled reinforcements: microscale fibres and nanoscale fillers. Different types of nanomaterials were mentioned in Section 1.2.1. The motivation behind manufacturing multiscale hierarchical nanocomposites is to

improve upon the performance of conventional FRPs. The presence of nanofillers in the matrix tend to promote better fibre/matrix interfacial adhesion and improve strength, stiffness and thermal properties.

Nanomaterials can be added directly into the matrix or can be applied initially on the reinforcing fibre before resin impregnation. Many types of nanomaterials such as carbon nanotube [197-199], graphene [200-203] and nanoclay [204-207] has been added to FRPs and reported; but, the majority of studies to date are focused on the modification of thermosets and limited data is available for thermoplastic hierarchical nanocomposites. The main reason is the ease of incorporating nanomaterials within thermosets compared to the difficulties associated with mixing such additives with solid in form and high melt viscous thermoplastics. Therefore, fabrication of a homogenous and strong thermoplastic fibre-reinforced nanocomposite depends on uniform dispersion of additives in the polymer matrix and efficient load transfer from polymer matrix to nanomaterials.

In a series of studies, Vlasveld et al. [208-210] reported the mechanical and physical properties of a three-phase nanocomposite consisting of GF or CF reinforcement embedded in a polyamide 6 matrix with layered silicate as the nanoscale reinforcing phase. Polyamide 6 nanocomposite was produced by melt compounding of both constituents with the use of a twin-screw extruder. Film stacking method was used to manufacture nanocomposite laminates. 40 % improvement in flexural and compressive strength was reported in elevated temperatures, which indicated the material can be used in 40 to 50 °C higher than normal temperatures. Clifford and Wan [211] also proved improvement in tensile modulus with applying Halpin-Tsai model to GF/PA clay nanocomposite.

Multifunctional composites can be manufactured by addition of nanocomposites and the composite improvements are not limited to mechanical properties. For instance, nanomaterials can also improve electrical properties of the composite. CF/PEEK with added silver nanowires can enhance through-the-thickness electrical conductivity. Compared to unfilled CF/PEEK, silver nanowire filled CF/PEEK can improve conductivity by a magnitude of four [212].

Nanomaterials can open enormous potential in the field of FRP composites and the potential is uncapped. More specifically, there is a knowledge gap in the field of thermoplastic FRP nanocomposites in general, and also with an emphasis on high-performance thermoplastics like PAEK resins. Depending on the intended application, numerous choices of nonreinforcement are available.

2.5 Fibre Tow Spreading

Spreading the fibre tow is an important aspect in fibre handling and manufacturing prepreg materials. It was previously mentioned that spreading fibre tow helps opening up and exposing fibre filaments for better resin impregnation in prepreg production, especially for thermoplastic composites.

Nowadays, the practice of spreading the reinforcing fibre tow in order to achieve a light, low areal weight and low thickness fibre bundle is called spread tow technology. Spread tow reinforcements are gaining popularity within different industries associated with fibre-reinforced composite materials. Some benefits like relatively straighter fibre orientation, less crimp with woven fabric, and overall better mechanical performance is now understood with these products. The penetration of high viscous resins such as thermoplastics are also proven to be more easily done when using spread tow fabric. Using thin-ply spread tow fabric can also significantly reduce costs by utilising large tows (fibre tows consists of large number of filaments, like 48,000 or 320,000 carbon fibre tows) and help produce even more light-weight components compared with using conventional fabrics.

In a report by Nishikawa et al. [213], plain weave spread tow CF prepreg was used in comparison to conventional plain weave CF composite to determine the fatigue crack constraint in plain-woven composites. Experimental results indicated that the fatigue lives of plain-woven CF reinforced composites using spread tows were longer than those of conventional plain-woven ones. The fatigue crack formation and propagation criterion are affected by tow thickness. With a calculation of results, it was clarified that fatigue crack formulation and propagation was constrained by using spread tows. Thereby, fatigue lives of the composites were improved compared with those of conventional plain-woven fabric composites. Typically, failure of laminated

composites starts with transverse micro-cracking through the thickness of the ply, as the first ply fails, and then delamination damage occurs. Fibre breakage is usually the last stage in the failure mode. However, catastrophic failure can happen without fibre breakage only with micro-cracking and delamination. Sihn et al. [214] concluded from many experiments that thin-ply laminated composites can suppress the micro-cracking and delamination damage without special resin and/or 3D reinforcements. They also stated that the laminate design can be simplified by using higher strain allowable, without the need for a progressive failure analysis. Spread tow enables simple fabric of plain weave structure to be produced with lower crimp angles than conventional fabric of satin weave, and this low crimp angle of a spread-tow fabric reduces the void content and resin rich areas in the thermoplastic composite, resulting in better composite mechanical properties [215]. Figure 2.16 is a schematic drawing of a 12K (12,000 filaments) carbon fibre spread tow. The original width of 12K carbon fibre tow is normally 6 to 7 mm. With spreading the carbon fibre tow, a spread width up to 32 mm can be achieved, without gap introduction between filaments.

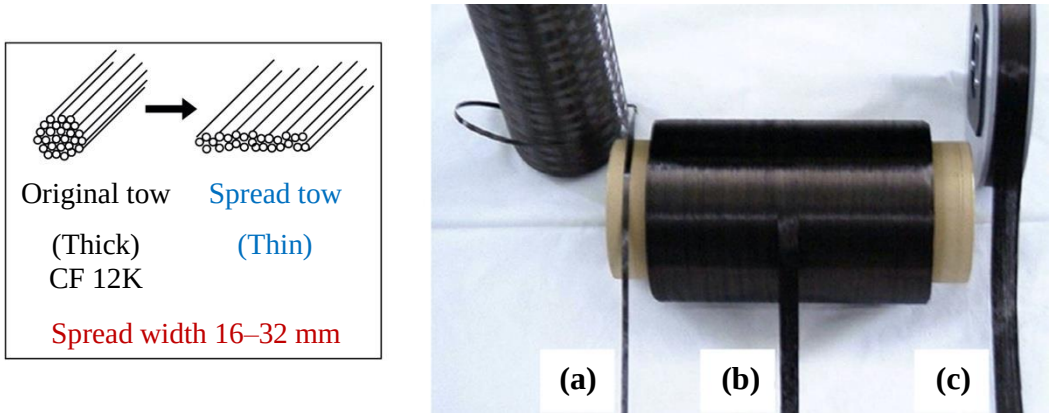

Figure 2.16 12K carbon fibre tow and its spread tow: (a) original tow width: 6 mm, (b) spread tow width: 12 mm and (c) spread tow width: 20 mm [214].

A simple schematic of spread tow process is shown in Figure 2.17. The process starts when the fibre tow is hauled off from the fibre bobbin, going through a spreading device and finally a take-up unit will wind the spread tow on another bobbin for further processing. Spreading devices can be used on their own, just to spread the fibre, or can be integrated in a fibre tow associated process including prepreg production. Lightweight woven fabrics or UD prepregs can be manufactured using spread tow fibres.

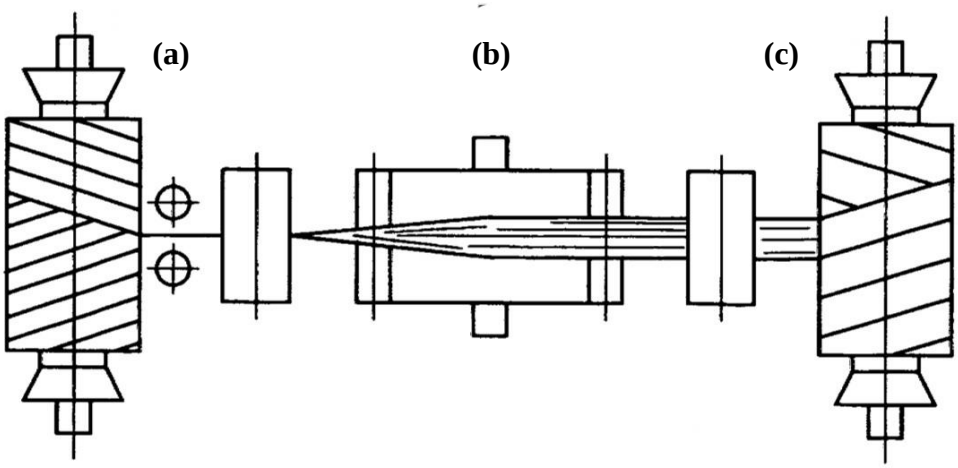

Figure 2.17 Schematic of spread tow process: (a) fibre tow haul of from bobbin, (b) spreading unit and (c) winding unit.

Various methods have been employed to spread fibre tow. The spreading process can be done by direct contact (mechanical) means or through non-contact methods. One direct contact example for spreading fibre tow is the use of spreading pins, in which the fibre tow is passed through a series of rollers to obtain a flat array of separate fibres. In a thorough discussion, Irfan et al. [216] claimed that the spread width using two spreading bars are function of cross-section of the fibre tow, the length of the fibre bundle from the anchor point to the tangential contact point on the first rod, and the angle subtended between the vertical and the anchor point.

Depending on the spreading requirements, both fixed pins [217] and rollers [218] can be utilised as means for lateral spread of the fibre. Occasionally, a form of a reciprocating motion (vibration) is added to a series of spreading rollers to help enhance the opening of the fibre filaments. Depending on the utilised mechanism, the mechanical vibration of rollers could be lateral or perpendicular. For instance, Akase et al. [219] discussed in a patent the opening of carbon fibre tow with the help of axial vibration of at least 1 roller between 2 other non-vibrating rollers. They reported that the non-vibrating roller should be located immediately downstream of the vibrating roller with a distance of 100 mm or less, otherwise, the effect of fibre opening can diminish. A vibration of 3 to 60 Hz was preferred. They reported to have successfully spread 3K CF two to four times the original fibre width. On the downside, they also reported creation of fibre fuzz on the rollers as a result of the lateral (axial) vibration

of the rollers. Fuzzing is occurred when fibres slide laterally on each other, and on the rollers.

Tanaka et al. [220] employed a vibration system in which a series of rollers and a body reciprocated to repetitively touch with, and release from a running fibre tow for spreading, as shown in Figure 2.18. Here, the reciprocating movement of the rollers cause the fibre bundle to experience a tension-free state, as the bundle does not receive any pressure when the vibrating body is in the non-contact state. As the result, fibre tow opens laterally more easily when conveyed through the process (passing on non-moving rollers) due to the lowered tension in the fibre bundle. Up to 30 mm of lateral spread for 12K CF was reported.

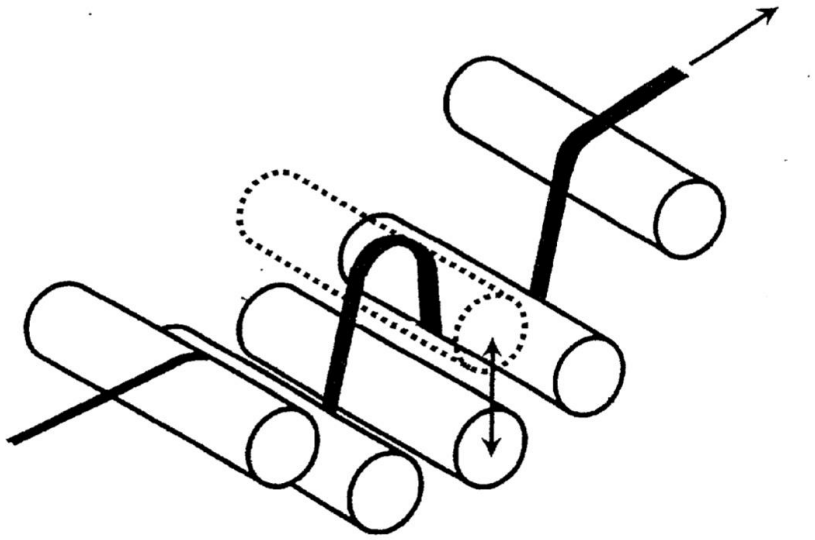

Figure 2.18 Lateral spreading of fibre bundle via reciprocating movement of rollers [220].

A method and system for spreading fibre tow using acoustic energy as a mean of a vibrating device was also patented by Iyer and Drzal [221], in which fibre tow was passed between rollers with the acoustic source placed in bottom. By using the acoustic energy from a speaker, spread tow fibres were produced at high speed with uniform spacing. A speaker powered by a frequency generator was utilised to enhance the degree of fibre spread while the fibre bundle is passed over and under a series of rollers. They reported that for a frequency range of 32 to 39 Hz, the fibres absorb the

most acoustic energy, causing them to spread to their individual filaments. Schematics of the acoustic fibre spreading assembly can be seen in Figure 2.19.

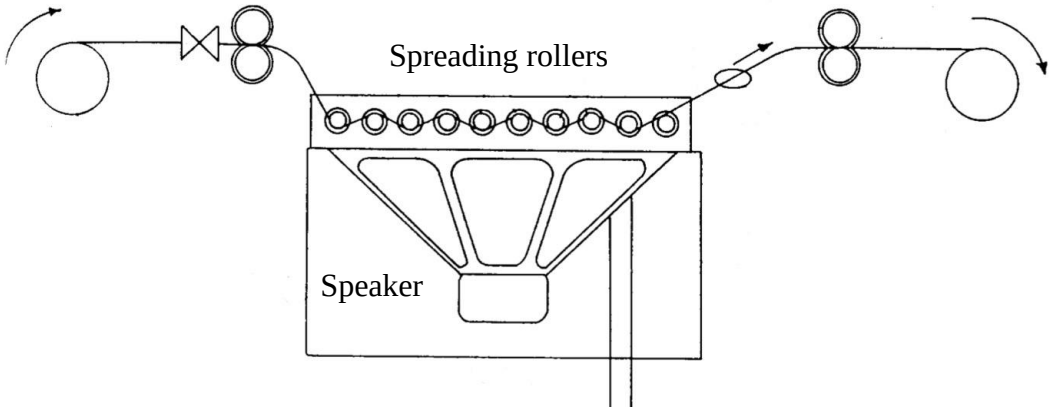

Figure 2.19 Fibre tow spreading via acoustic energy of a speaker [221].

Figure 2.20 illustrates a non-contact method used by Kawabe et al. [222]. They employed a pneumatic spreading technique, which uses air vacuum as a method for spreading the fibre tow. In this technique, the fibre tow is passed over an air duct that sucks the air down using a vacuum pump. Because of the air flow, a difference in air pressure arises in the central portion and both side portion of the fibre so that each fibre gains a force to move outwards, and the fibre bundle opens.

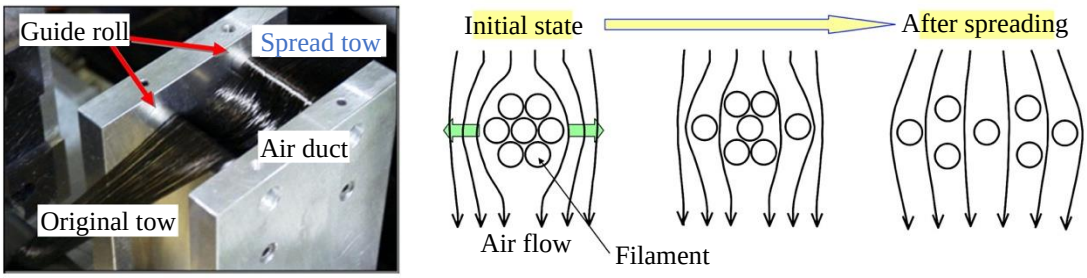

Figure 2.20 Schematic of a pneumatic tow spreading method with the help of airflow [214].

Commercial spread tow products are now manufactured and supplied by a number of companies. The Swedish company Oxeon AB has developed spread tow products, which is commercially known as TeXtreme [223]. As shown in Figure 2.21, the company offers a range of technologies including effective fibre spreading of CF tow

and weaving the spread tow tapes into plain or cross angle TeXtreme fabrics. TeXtreme can be produced in fabric width of 300 to 1500 mm, with standard being 1000 mm.

Additionally, dry UD tapes are made available in a wide variety of widths with areal weight corresponding to the degree of spreading and the type of CF chosen. The areal weight of the spread tow tapes can be adjusted to be as little as 30 g/m^2. Standard tape width is 20 mm, and they benefit from a very good width consistency, and uniform and straight fibre orientation. They can produce dry UD tapes in widths up to 600 mm. TeXtreme spread tow carbon reinforcements can be purchased in dry form, as prepreg or as laminated sheets [224].

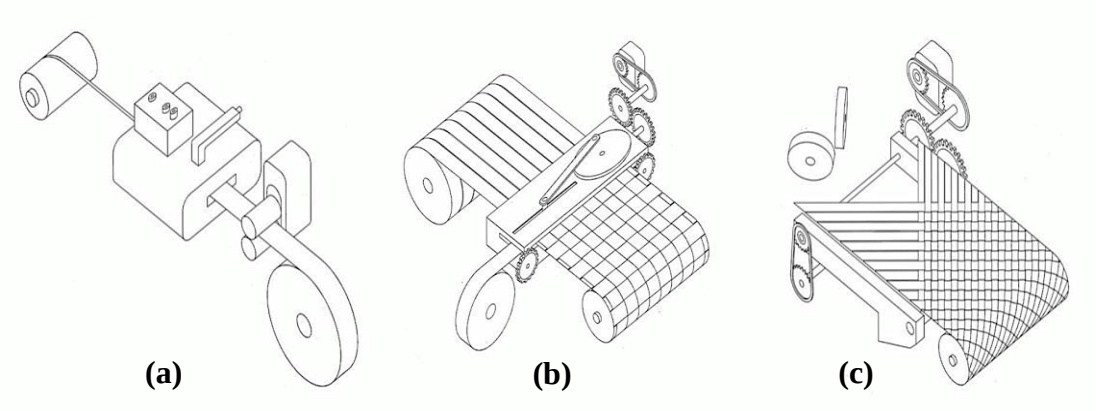

Figure 2.21 Spread tow technologies offered by Oxeon AB: (a) spreading fibre tows into thin tapes, (b) weaving spread tow tapes and (c) cross angle weaving layup of spread tow tapes [223].

Other companies including Sigmatex (UK) and Harmoni Industry (Japan) have also developed methods of manufacturing spread tow fibres and subsequently produce ultra-lightweight spread to fabrics for use in different composite sectors, particularly aerospace industry where reducing the weight of different composite parts is hugely desirable.

2.6 Summary

In this chapter, fibre-reinforced polymer (FRP) composites were introduced. Different types of fibres such as glass and carbon fibre were studied and some of their manufacturing processes were reviewed. Laminated composites were discussed, and

it was explained how laminates are formed from single laminas at which each stacking sequence can have different physical and mechanical properties.

It was noted that prepregs are the best and most widely used form of single ply FRPs, ready to be moulded and worked with. Prepregs can come with different types of matrix phase, usually divided into thermosets and thermoplastics. Benefits of thermoplastics were explained in detail and high-temperature family of PAEK polymers were introduced as a superior option for high-temperature and high-performance prepreg and composite production.

Based on the literature review, various thermoplastic prepreg manufacturing methods were explained. It was come to light that traditional manufacturing methods such as melt impregnation, film stacking, and fibre commingling either require expensive equipment and a costly procedure, or usually are uncapable to process high-temperature matrices such PAEKs. Efficient resin impregnation and fibre wet-out is deemed difficult for polymers with high melt viscosity, which is more evident in melt impregnation prepreg manufacturing techniques. Solution impregnation was discussed as an alternative to melt impregnation methods to tackle the viscosity problem; however, it was realised that this method can degrade the mechanical properties of the polymers, while many polymers including PAEKs would require strong solvents to work with this technique.

It was found that wet powder impregnation technology can eliminate many of the aforementioned problems and provide numerous benefits in comparison to many other traditional methods. Different particle sizes can be utilised and there are no solubility limitations as the polymer powders are only suspended in a liquid carrier. The carrier or the proportion of the constituents can be adjusted accordingly to change the viscosity of the suspension. In addition, different additives can be easily incorporated in the matrix to enhance the properties of the prepreg.

Finally, spread tow fibre technology was discussed and benefits of utilising low-weight plies for manufacturing composite parts were realised. Using thin ply fabrics can increase the fatigue life of the composite, delay and restrain delamination failure,

and reduce the void content and resin rich areas in thermoplastic composites. Different spreading methods can be utilised for opening the fibre bundle, including direct contact or non-contact techniques. It was found that non-contact methods can bring forward additional benefits as there is less contact with guiding rollers, resulting in fewer fibre breakage.

2.7 References

[1] Mallick, P. K., 1993, Fiber-reinforced composites: materials, manufacturing, and design, M. Dekker, New York.

[2] Hull, D., and Clyne, T. W., 1996, An Introduction to Composite Materials, Cambridge University Press, Cambridge.

[3] Mallick, P. K., 2008, Fiber-reinforced composites: materials, manufacturing, and design, CRC Press, Boca Raton Fla., London.

[4] Jones, R. M., 1999, Mechanics of composite materials, Taylor & Francis, Philadelphia, PA.

[5] Daniel, I. M., and Ishai, O., 2006, Engineering mechanics of composite materials, Oxford University Press, New York & Oxford.

[6] ASTM, 2019, "D6507-19 Standard Practice for Fiber Reinforcement Orientation Codes for Composite Materials," ASTM International, West Conshohocken, PA.

[7] Composite Materials, H., 2012, "Composite Materials Handbook, Volume 1 - Polymer Matrix Composites - Guidelines for Characterization of Structural Materials (CMH-17)," SAE International on behalf of CMH-17, a division of Wichita State University.

[8] Callister, W. D., Jr., and Rethwisch, D. G., 2014, Materials science and engineering: An introduction, Wiley, New York.

[9] Smallman, R. E., and Bishop, R. J., 1999, "Chapter 11 - Plastics and composites," Modern Physical Metallurgy and Materials Engineering (Sixth Edition), R. E. Smallman, and R. J. Bishop, eds., Butterworth-Heinemann, Oxford, pp. 351-375.

[10] Kaw, A. K., 2006, Mechanics of composite materials, Taylor & Francis, Boca Raton, FL.

[11] Loos, M., 2015, "Chapter 2 - Composites," Carbon Nanotube Reinforced Composites, M. Loos, ed., William Andrew Publishing, Oxford, pp. 37-72.

[12] Derradji, M., Wang, J., and Liu, W., 2018, "5 - Fiber-Reinforced Phthalonitrile Composites," Phthalonitrile Resins and Composites, William Andrew Publishing, pp. 241-294.

[13] Middleton, B., 2016, "3 - Composites: Manufacture and Application," Design and Manufacture of Plastic Components for Multifunctionality, William Andrew Publishing, Oxford, pp. 53-101.

[14] Chawla, K. K., 2019, Composite materials : science and engineering, Springer, Verlag, New York.

[15] Soutis, C., 2005, "Fibre reinforced composites in aircraft construction," Progress in Aerospace Sciences, 41(2), pp. 143-151.

[16] ASTM, 2018, "D578/D578M-18 Standard Specification for Glass Fiber Strands," ASTM International, West Conshohocken, PA.

[17] Bader, M. G., 2002, "Selection of composite materials and manufacturing routes for cost-effective performance," Composites Part A: Applied Science and Manufacturing, 33(7), pp. 913-934.

[18] Jiang, B., Huang, Y. D., He, S., Xing, L. X., and Wang, H. L., 2015, "Quality analysis and control strategies for epoxy resin and prepreg," TrAC Trends in Analytical Chemistry, 74, pp. 68-78.

[19] Pansart, S., 2013, "6 - Prepreg processing of advanced fibre-reinforced polymer (FRP) composites," Advanced Fibre-Reinforced Polymer (FRP) Composites for Structural Applications, J. Bai, ed., Woodhead Publishing, pp. 125-154.

[20] Heth, J., 2000, "From art to science: A prepreg overview," High-Performance Composites, 8, pp. 32-36.

[21] Sun, C. T., Chung, I., and Chang, I. Y., 1992, "Modeling of elastic-plastic behavior of LDF™ and continuous fiber reinforced AS-4/PEKK composites," Composites Science and Technology, 43(4), pp. 339-345.

[22] Buck, M., 2005, "Widest thermoplastic prepreg tapes produced," Reinforced Plastics, 49(2), p. 16.

[23] McIlhagger, A., Archer, E., and McIlhagger, R., 2015, "3 - Manufacturing processes for composite materials and components for aerospace applications," Polymer Composites in the Aerospace Industry, P. E. Irving, and C. Soutis, eds., Woodhead Publishing, pp. 53-75.

[24] Molyneux, M., Murray, P., and P. Murray, B., 1983, "Prepreg, tape and fabric technology for advanced composites," Composites, 14(2), pp. 87-91.

[25] Stewart, R., 2009, "New prepreg materials offer versatility, top performance," Reinforced Plastics, 53(5), pp. 28-33.

[26] Walsh, S. M., Scott, B. R., and Spagnuolo, D. M., 2005, "The Development of a Hybrid Thermoplastic Ballistic Material With Application to Helmets," Army Research Lab Aberdeen Proving Ground, M. D.

[27] Walsh, S. M., Scott, B. R., Spagnuolo, D. M., and Wolbert, J. P., 2006, "Hybridized Thermoplastic Aramids: Enabling Material Technology For Future Force Headgear," Army Research Lab Aberdeen Proving Ground, M. D.

[28] Kulkarni, S. G., Gao, X. L., Horner, S. E., Zheng, J. Q., and David, N. V., 2013, "Ballistic helmets – Their design, materials, and performance against traumatic brain injury," Composite Structures, 101, pp. 313-331.

[29] Vieille, B., Casado, V. M., and Bouvet, C., 2013, "About the impact behavior of woven-ply carbon fiber-reinforced thermoplastic- and thermosetting-composites: A comparative study," Composite Structures, 101, pp. 9-21.

[30] Bandaru, A. K., Chavan, V. V., Ahmad, S., Alagirusamy, R., and Bhatnagar, N., 2016, "Ballistic impact response of Kevlar® reinforced thermoplastic composite armors," International Journal of Impact Engineering, 89, pp. 1-13.

[31] Noriega, R., Rivnay, J., Vandewal, K., Koch, F. P. V., Stingelin, N., Smith, P., Toney, M. F., and Salleo, A., 2013, "A general relationship between disorder, aggregation and charge transport in conjugated polymers," Nature Materials, 12(11), pp. 1038-1044.

[32] Ashbee, K. H. G., 1989, Fundamental principles of fiber reinforced composites, Technomic, United States.

[33] Packham, D. E., 1994, "Physics of plastics: Processing, properties and materials engineering," Polymer International, 33(1), pp. 115-116.

[34] Kausch, H. H., and Legras, R., 1993, Advanced thermoplastic composites : characterization and processing, Oxford University Press, USA.

[35] Snook, S., 1994, Engineering plastics and elastomers : a design guide, Institute of Materials, London.

[36] Cogswell, F. N., 1992, Thermoplastic aromatic polymer composites : a study of the structure, processing and properties of carbon fibre reinforced polyetherketone and related materials, Butterworth Architecture, Oxford.

[37] Jones, I., 2013, "10 - Laser welding of plastics," Handbook of Laser Welding Technologies, S. Katayama, ed., Woodhead Publishing, pp. 280-301.

[38] Gilbert, M., 2017, "Chapter 3 - States of Aggregation in Polymers," Brydson's Plastics Materials (Eighth Edition), M. Gilbert, ed., Butterworth-Heinemann, pp. 39-57.

[39] Miracle, D. B., and Donaldson, S. L., 2001, "18. Thermoplastic Resins," ASM Handbook, Volume 21 - Composites, ASM International.

[40] Brazel, C. S., and Rosen, S. L., 2012, Fundamental Principles of Polymeric Materials, John Wiley & Sons, Incorporated, Somerset, United States.

[41] Li, T. Q., Zhang, M. Q., Zhang, K., and Zeng, H. M., 2000, "The dependence of the fracture toughness of thermoplastic composite laminates on interfacial interaction," Composites Science and Technology, 60(3), pp. 465-476.

[42] ISO, 2020, "BS EN ISO 11357-2:2020 Plastics. Differential scanning calorimetry (DSC). Determination of glass transition temperature and step height," BSI Standards Limited.

[43] Chanda, M., 2017, Plastics Technology Handbook, Taylor & Francis Group, Milton, United Kingdom.

[44] Béland, S., 1990, High performance thermoplastic resins and their composites, Noyes Publications, Park Ridge, NJ.

[45] National-Research-Council, 1996, Accelerated Aging of Materials and Structures: The Effects of Long-Term Elevated-Temperature Exposure, The National Academies Press, Washington, DC.

[46] Huda, Z., and Edi, P., 2013, "Materials selection in design of structures and engines of supersonic aircrafts: A review," Materials & Design, 46, pp. 552-560.

[47] Sastri, V. R., 2014, "6 - Commodity Thermoplastics: Polyvinyl Chloride, Polyolefins, and Polystyrene," Plastics in Medical Devices (Second Edition), V. R. Sastri, ed., William Andrew Publishing, Oxford, pp. 73-120.

[48] Sastri, V. R., 2014, "8 - High-Temperature Engineering Thermoplastics: Polysulfones, Polyimides, Polysulfides, Polyketones, Liquid Crystalline Polymers, and Fluoropolymers," Plastics in Medical Devices (Second Edition), V. R. Sastri, ed., William Andrew Publishing, Oxford, pp. 173-213.

[49] UL, 2018, "Standard for Polymeric Materials - Long Term Property Evaluations 5th Edition," UL Standards.

[50] Rubinstein, M., and Colby, R. H., 2003, Polymer physics, Oxford University Press, Oxford & New York.

[51] Clum, J. A., 2009, "Essentials of Polymer Science and Engineering, by Paul C. Painter and Michael M. Coleman,"United States, p. 239.

[52] Lesser, D., and Banister, B., 1989, "Amorphous thermoplastic matrix composites for new applications," 21st International SAMPE Technical Conference, pp. 507-513.

[53] Kyriacos, D., 2017, "Chapter 21 - High-Temperature Engineering Thermoplastics," Brydson's Plastics Materials (Eighth Edition), M. Gilbert, ed., Butterworth-Heinemann, pp. 545-615.

[54] Vasconcelos, G. d. C., Mazur, R. L., Botelho, E. C., Rezende, M. C., and Costa, M. L., 2010, "Evaluation of crystallization kinetics of poly (ether-ketone-ketone) and poly (ether-ether-ketone) by DSC," Journal of Aerospace Technology and Management, 2, pp. 155-162.

[55] Urakawa, O., 2014, "Polyaryletherketone," Encyclopedia of Polymeric Nanomaterials.

[56] Bonner, J. W. H., 1962, "Aromatic polyketones and preparation thereof," EI Du Pont de Nemours and Co, United States patent US3065205.

[57] Parker, D., Bussink, J., Grampel, H., Wheatley, G., Dorf, E. U., Ostlinning, E., and Reinking, K., 2012, "Polymers, High-Temperature," Ullmann's Encyclopedia of Industrial Chemistry, Wiley-VCH, Weinheim.

[58] Attwood, T. E., Dawson, P. C., Freeman, J. L., Hoy, L. R. J., Rose, J. B., and Staniland, P. A., 1981, "Synthesis and properties of polyaryletherketones," Polymer, 22(8), pp. 1096-1103.

[59] Kemmish, D., 2010, Update on the technology and applications of polyaryletherketones, iSmithers Rapra Publishing.

[60] Bersee, H. E. N., 2010, "Composite Aerospace Manufacturing Processes," Encyclopedia of Aerospace Engineering, pp. 1-16.

[61] Chang, I. Y., and Lees, J. K., 1988, "Recent Development in Thermoplastic Composites: A Review of Matrix Systems and Processing Methods," Journal of Thermoplastic Composite Materials, 1(3), pp. 277-296.

[62] Sung Chun, Y., and Weiss, R. A., 2004, "Thermal behavior of poly(ether ketone ketone)/thermoplastic polyimide blends," Journal of Applied Polymer Science, 94(3), pp. 1227-1235.

[63] Gan, D., Lu, S., Song, C., and Wang, Z., 2001, "Morphologies, Mechanical Properties and Wear of Poly(ether ketone ketone) (PEKK) and its Composites Reinforced with Mica," Macromolecular Materials and Engineering, 286(5), pp. 296-301.

[64] Campbell, F. C., 2004, "10. Thermoplastic Composites: An Unfulfilled Promise," Manufacturing Processes for Advanced Composites, Elsevier.

[65] Talbott, M. F., Springer, G. S., and Berglund, L. A., 1987, "The Effects of Crystallinity on the Mechanical Properties of PEEK Polymer and Graphite Fiber Reinforced PEEK," Journal of Composite Materials, 21(11), pp. 1056-1081.

[66] Ma, R., and Tang, T., 2014, "Current strategies to improve the bioactivity of PEEK," International Journla of Molecular Science, 15(4), pp. 5426-5445.

[67] Platt, D. K., 2003, Engineering and High Performance Plastics, Smithers Rapra Press.

[68] Ma, C.-C. M., and Yur, S.-W., 1991, "Environmental effects on the water absorption and mechanical properties of carbon fiber reinforced PPS and PEEK composites. Part II," Polymer Engineering & Science, 31(1), pp. 34-39.

[69] Díez-Pascual, A. M., Ashrafi, B., Naffakh, M., González-Domínguez, J. M., Johnston, A., Simard, B., Martínez, M. T., and Gómez-Fatou, M. A., 2011, "Influence of carbon nanotubes on the thermal, electrical and mechanical properties of poly(ether ether ketone)/glass fiber laminates," Carbon, 49(8), pp. 2817-2833.

[70] Miracle, D. B., and Donaldson, S. L., "ASM Handbook, Volume 21 - Composites," ASM International.

[71] Cogswell, F. N., 1987, "The Processing Science of Thermoplastic Structural Composites," International Polymer Processing, 1(4), pp. 157-165.

[72] Cogswell, F. N., 1991, "The experience of thermoplastic structural composites during processing," Composites Manufacturing, 2(3), pp. 208-216.

[73] Leach, D. C., and Moore, D. R., 1985, "Toughness of aromatic polymer composites reinforced with carbon fibres," Composites Science and Technology, 23(2), pp. 131-161.

[74] Dr Carlile, D. C. L. D. R. M. N. Z., 1989, Mechanical Properties of the Carbon Fiber/PEEK Composite APC-2/AS-4 for Structural Applications, ASTM International, West Conshohocken, PA.

[75] Jar, P. Y. B., Mulone, R., Davies, P., and Kausch, H. H., 1993, "A study of the effect of forming temperature on the mechanical behaviour of carbon-fibre/peek composites," Composites Science and Technology, 46(1), pp. 7-19.

[76] El Kadi, H., and Denault, J., 2001, "Effects of Processing Conditions on the Mechanical Behavior of Carbon-Fiber-Reinforced PEEK," Journal of Thermoplastic Composite Materials, 14(1), pp. 34-53.

[77] Boccaccini, A. R., Peters, C., Roether, J. A., Eifler, D., Misra, S. K., and Minay, E. J., 2006, "Electrophoretic deposition of polyetheretherketone (PEEK) and PEEK/Bioglass® coatings on NiTi shape memory alloy wires," Journal of Materials Science, 41(24), pp. 8152-8159.

[78] Sheiko, N., Kékicheff, P., Marie, P., Schmutz, M., Jacomine, L., and Perrin-Schmitt, F., 2016, "PEEK (polyether-ether-ketone)-coated nitinol wire: Film stability for biocompatibility applications," Applied Surface Science, 389, pp. 651-665.

[79] Kruk, A., Zimowski, S., Łukaszczyk, A., Cieniek, Ł., and Moskalewicz, T., 2019, "The influence of heat treatment on the microstructure, surface topography and selected properties of PEEK coatings electrophoretically deposited on the Ti-6Al-4V alloy," Progress in Organic Coatings, 133, pp. 180-190.

[80] Parsipanny, N. J., 2013, "VESTAKEEP® PEEK-Based Spinal Implant Receives FDA 510(k) Approval," https://corporate.evonik.us/en/vestakeep-peek-based-spinal-implant-receives-fda-510k-approval-102637.html (Last accessed 30.04.21).

[81] Goldberg, A. J., Burstone, C. J., Hadjinikolaou, I., and Jancar, J., 1994, "Screening of matrices and fibers for reinforced thermoplastics intended for dental applications," Journal of Biomedical Materials Research, 28(2), pp. 167-173.

[82] Fuhrmann, G., Steiner, M., Freitag-Wolf, S., and Kern, M., 2014, "Resin bonding to three types of polyaryletherketones (PAEKs)—Durability and influence of surface conditioning," Dental Materials, 30(3), pp. 357-363.

[83] Najeeb, S., Zafar, M. S., Khurshid, Z., and Siddiqui, F., 2016, "Applications of polyetheretherketone (PEEK) in oral implantology and prosthodontics," Journal of Prosthodontic Research, 60(1), pp. 12-19.

[84] Kwarteng, K. B., and Stark, C., "Carbon fiber reinforced PEEK (APC-2/AS-4) composites for orthopaedic implants," Materials Science.

[85] Kurtz, S. M., and Devine, J. N., 2007, "PEEK biomaterials in trauma, orthopedic, and spinal implants," Biomaterials, 28(32), pp. 4845-4869.

[86] Nakahara, I., Takao, M., Bandoh, S., Bertollo, N., Walsh, W. R., and Sugano, N., 2012, "Novel surface modifications of carbon fiber-reinforced polyetheretherketone hip stem in an ovine model," Artif Organs, 36(1), pp. 62-70.

[87] Cortes, L. Q., Lonjon, A., Dantras, E., and Lacabanne, C., 2014, "High-performance thermoplastic composites poly(ether ketone ketone)/silver nanowires: Morphological, mechanical and electrical properties," Journal of Non-Crystalline Solids, 391, pp. 106-111.

[88] Quiroga Cortés, L., Caussé, N., Dantras, E., Lonjon, A., and Lacabanne, C., 2016, "Morphology and dynamical mechanical properties of poly ether ketone ketone (PEKK) with meta phenyl links," Journal of Applied Polymer Science, 133(19), p. 43396.

[89] Arkema, 2018, "PEKK – Polyether Ketone Ketone Kepstan® PEKK," https://www.extrememateriales-arkema.cn /export /sites /technicalpolymers /.content /medias /downloads /brochures /kepstan-brochures /kepstan-br-general.pdf (Last accessed 30.04.21).

[90] Avakian, P., Gardner, K. H., and Matheson Jr., R. R., 1990, "A comment on crystallization in PEKK and PEEK resins," Journal of Polymer Science Part C: Polymer Letters, 28(8), pp. 243-246.

[91] Urwyler, P., Zhao, X., Pascual, A., Schift, H., and M¸ller, B., 2014, "Tailoring surface nanostructures on polyaryletherketones for load-bearing implants," European Journal of Nanomedicine, 6, pp. 37 - 46.

[92] Bai, J. M., Leach, D., and Pratte, J., 2005, "Properties of poly(etherketone-ketone) composites," JEC Composites Magazine, 42(15), pp. 64-66.

[93] Mazur, R. L., Cândido, G. M., Rezende, M. C., and Botelho, E. C., 2016, "Accelerated aging effects on carbon fiber PEKK composites manufactured by hot compression molding," Journal of Thermoplastic Composite Materials, 29(10), pp. 1429-1442.

[94] Green, S., 2019, "VICTREX AE 250 – A Novel polyaryletherketone polymer suited to automated tape placement and out of autoclave processing," https://www.victrex.com/~/media /whitepapers/victrex-ae-250---technical-paper-camx-2018.pdf (Last accessed 30.04.21).

[95] Domínguez, J. C., 2018, "Chapter 4 - Rheology and curing process of thermosets," Thermosets (Second Edition), Q. Guo, ed., Elsevier, pp. 115-146.

[96] Ra, S., and Lee, H., 2007, "Nano Sized Patterning on the Thermoset Materials Using Thermal Curing Nano-Imprinting Technology," Solid State Phenomena, 121-123, pp. 681-684.

[97] d'Hooghe, E. L., and Edwards, C. M., 2000, "Thermoplastic Composite Technology; Tougher Than You Think," Advanced Materials, 12(23), pp. 1865-1868.

[98] Smith, C. P., 1988, "High Performance Polymers," ChemTech, 18(5), pp. 290-291.

[99] Moyer, R. L., 1976, "Methods of making continuous length reinforced plastic articles," Hercules LLC, United States patent US3993726.

[100] N.Cogswell, F., Hezzell, D. J., and Williams, P. J., 1985, "Fibre reinforced compositions and methods for producing such compositions," SABIC Innovative Plastics US LLC, United States patent US4559262.

[101] Åström, B. T., 1992, "Development and application of a process model for thermoplastic pultrusion," Composites Manufacturing, 3(3), pp. 189-197.

[102] Tomas åström, B., Larsson, P. H., and Byron Pipes, R., 1991, "Development of a facility for pultrusion of thermoplastic-matrix composites," Composites Manufacturing, 2(2), pp. 114-123.

[103] Carlsson, A., and Tomas Åström, B., 1998, "Experimental investigation of pultrusion of glass fibre reinforced polypropylene composites," Composites Part A: Applied Science and Manufacturing, 29(5), pp. 585-593.

[104] Kim, D.-H., Lee, W. I., and Friedrich, K., 2001, "A model for a thermoplastic pultrusion process using commingled yarns," Composites Science and Technology, 61(8), pp. 1065-1077.

[105] Åstroöm, B. T., and Pipes, R. B., 1993, "A modeling approach to thermoplastic pultrusion. II: Verification of models," Polymer Composites, 14(3), pp. 184-194.

[106] Larock, J. A., Hahn, H. T., and Evans, D. J., 1989, "Pultrusion Processes for Thermoplastic Composites," Journal of Thermoplastic Composite Materials, 2(3), pp. 216-229.

[107] Gibson, A. G., and Månson, J. A., 1992, "Impregnation technology for thermoplastic matrix composites," Composites Manufacturing, 3(4), pp. 223-233.

[108] Miracle, D. B., and Donaldson, S. L., 2001, "69. Thermoplastic Composites Manufacturing," ASM Handbook, Volume 21 - Composites, ASM International.

[109] Lee, W. I., and Springer, G. S., 1987, "A Model of the Manufacturing Process of Thermoplastic Matrix Composites," Journal of Composite Materials, 21(11), pp. 1017-1055.

[110] Gaymans, R. J., and Wevers, E., 1998, "Impregnation of a glass fibre roving with a polypropylene melt in a pin assisted process," Composites Part A: Applied Science and Manufacturing, 29(5), pp. 663-670.

[111] Peltonen, P., Lahteenkorva, K., Paakkonen, E. J., Jarvela, P. K., and Tormala, P., 1992, "The Influence of Melt Impregnation Parameters on the Degree of Impregnation of a Polypropylene/Glass Fibre Prepreg," Journal of Thermoplastic Composite Materials, 5(4), pp. 318-343.

[112] Bates, P. J., Kendall, J., Taylor, D., and Cunningham, M., 2002, "Pressure build-up during melt impregnation," Composites Science and Technology, 62(3), pp. 379-384.

[113] Bates, P. J., and Charrier, J. M., 2000, "Pulling tension monitoring during the melt impregnation of glass roving," Polymer Composites, 21(1), pp. 104-113.

[114] Xian, G., Pu, H.-T., Yi, X.-S., and Pan, Y., 2006, "Parametric Optmisation of Pin-assisted-melt Impregnation of Glass Fiber/Polypropylene by Taguchi Method," Journal of Composite Materials, 40(23), pp. 2087-2097.

[115] Muzzy, J. D., 1988, "Processing of Advanced Thermoplastic Composites," Proceedings of Manufacturing International '88. The Manufacturing Science of Composites, T. G. Gutowski, ed., ASME, New York, NY, pp. 27-39.

[116] Marissen, R., Th. van der Drift, L., and Sterk, J., 2000, "Technology for rapid impregnation of fibre bundles with a molten thermoplastic polymer," Composites Science and Technology, 60(10), pp. 2029-2034.

[117] Henninger, F., and Friedrich, K., 2002, "Thermoplastic filament winding with online-impregnation. Part A: process technology and operating efficiency," Composites Part A: Applied Science and Manufacturing, 33(11), pp. 1479-1486.

[118] Henninger, F., Hoffmann, J., and Friedrich, K., 2002, "Thermoplastic filament winding with online-impregnation. Part B. Experimental study of processing parameters," Composites Part A: Applied Science and Manufacturing, 33(12), pp. 1684-1695.

[119] Hogan, P., "The production and uses of film stacked composites for the aerospace industry," Proc. Proc. SAMPE Conf., Society for the Advancement of Material and Process Engineering, New York, USA.

[120] Ali, R., Iannace, S., and Nicolais, L., 2003, "Effects of processing conditions on the impregnation of glass fibre mat in extrusion/calendering and film stacking operations," Composites Science and Technology, 63(15), pp. 2217-2222.

[121] Cender, T. A., Simacek, P., and Advani, S. G., 2013, "Resin film impregnation in fabric prepregs with dual length scale permeability," Composites Part A: Applied Science and Manufacturing, 53, pp. 118-128.

[122] Wang, X., Mayer, C., and Neitzel, M., 1997, "Some issues on impregnation in manufacturing of thermoplastic composites by using a double belt press," Polymer Composites, 18(6), pp. 701-710.

[123] Grouve, W. J. B., and Akkerman, R., 2010, "Consolidation process model for film stacking glass/PPS laminates," Plastics, Rubber and Composites, 39(3-5), pp. 208-215.

[124] Offermann, P., Diestel, D., Choi, B. D., Mäder, E., and Hübner, T., 2002, "Advancement of comingling hybrid yarns for thermoplastic fiber reinforced composites," 45, pp. 12-14.

[125] Bates, P., and Ekhator, I., 2004, "Continuous Consolidation of Commingled Glass and Polypropylene Roving," Journal of Reinforced Plastics and Composites, 23(13), pp. 1409-1424.

[126] Bhat, G. S., 1997, "Plastics: Materials and Processing by A. Brent Strong," Materials and Manufacturing Processes, 12(3), pp. 560-562.

[127] Alagirusamy, R., and Ogale, V., 2005, "Development and Characterization of GF/PET, GF/Nylon, and GF/PP Commingled Yarns for Thermoplastic Composites," Journal of Thermoplastic Composite Materials, 18(3), pp. 269-285.

[128] Bernet, N., Michaud, V., Bourban, P. E., and Manson, J. A. E., 1999, "An Impregnation Model for the Consolidation of Thermoplastic Composites Made from Commingled Yarns," Journal of Composite Materials, 33(8), pp. 751-772.

[129] Klinkmüller, V., Um, M. K., Steffens, M., Friedrich, K., and Kim, B. S., 1994, "A new model for impregnation mechanisms in different GF/PP commingled yarns," Applied Composite Materials, 1(5), pp. 351-371.

[130] Wakeman, M. D., Zingraff, L., Bourban, P. E., Månson, J. A. E., and Blanchard, P., 2006, "Stamp forming of carbon fibre/PA12 composites – A comparison of a reactive impregnation process and a commingled yarn system," Composites Science and Technology, 66(1), pp. 19-35.

[131] Van West, B. P., Pipes, R. B., Keefe, M., and Advani, S. G., 1991, "The draping and consolidation of commingled fabrics," Composites Manufacturing, 2(1), pp. 10-22.

[132] Ye, L., Friedrich, K., Kästel, J., and Mai, Y.-W., 1995, "Consolidation of unidirectional CF/PEEK composites from commingled yarn prepreg," Composites Science and Technology, 54(4), pp. 349-358.

[133] Van West, B. P., Pipes, R. B., and Advani, S. G., 1991, "The consolidation of commingled thermoplastic fabrics," Polymer Composites, 12(6), pp. 417-427.

[134] Long, A. C., Wilks, C. E., and Rudd, C. D., 2001, "Experimental characterisation of the consolidation of a commingled glass/polypropylene composite," Composites Science and Technology, 61(11), pp. 1591-1603.

[135] Wiegand, N., and Mäder, E., 2017, "Commingled Yarn Spinning for Thermoplastic/Glass Fiber Composites," Fibers, 5(3), p. 26.

[136] Larson, N. W. K., Rasnack, W., Hoekstra, N., Boland, C., Leone, E., Santos, I., Healy, K., Chawla, T. S., and Shoepe, S., "Development of a Solvent-Based Prepreg Treater," Proc. 122nd ASEE Annual Conference & Exposition, Seattle, WA, pp. 1-20.

[137] Akbar, S., Ding, C., Yousaf, I., and Khan, H. M., 2008, "E-Glass/Phenolic Prepreg Processing by Solvent Impregnation," Polymers and Polymer Composites, 16, pp. 19-26.

[138] Xu, A., Bao, L., Nishida, M., and Yamanaka, A., 2013, "Molding of PBO fabric reinforced thermoplastic composite to achieve high fiber volume fraction," Polymer Composites, 34(6), pp. 953-958.

[139] Liu, B., Xu, A., and Bao, L., 2017, "Preparation of carbon fiber-reinforced thermoplastics with high fiber volume fraction and high heat-resistant properties," Journal of Thermoplastic Composite Materials, 30(5), pp. 724-737.

[140] Rommel, M., "Process development and mechanical properties of IM7/LaRC PETI-5 composites," Proc. Intl. SAMPE Tech. Conf. Ser., pp. 1-13.

[141] Turton, C., and Mcainsh, J., 1974, "Thermoplastic compositions," Imperial Chemical Industries Ltd, United States patent US3785916.

[142] Cogswell, F. N., and Staniland, P. A., 1985, "Method of producing fibre-reinforced composition," Imperial Chemical Industries Ltd and Cytec Technology Corp, United States patent US4541884.

[143] Cogswell, F. N., and Measuria, U., 1986, "Reinforced fibre products," Imperial Chemical Industries Ltd, United States patent US4624886.

[144] Savadori, A., and Cutolo, D., 1993, "Impregnation, flow and deformation during processing of advanced thermoplastic composites," Makromolekulare Chemie. Macromolecular Symposia, 68(1), pp. 109-131.

[145] Wu, G. M., and Schultz, J. M., 2000, "Processing and properties of solution impregnated carbon fiber reinforced polyethersulfone composites," Polymer Composites, 21(2), pp. 223-230.

[146] Goodman, K. E., and Loos, A. C., 1990, "Thermoplastic Prepreg Manufacture," Journal of Thermoplastic Composite Materials, 3(1), pp. 34-40.

[147] Hou, T. H., Belvin, H. L., and Johnston, N. J., 2001, "Automated Tow Placed LARC™-PETI-5 Composites," High Performance Polymers, 13(4), pp. 323-336.

[148] Williams, J. G., Morris, C. E. M., and Ennis, B. C., 1974, "Liquid flow through aligned fiber beds," Polymer Engineering & Science, 14(6), pp. 413-419.

[149] Åström, B. T., Pipes, R. B., and Advani, S. G., 1992, "On Flow through Aligned Fiber Beds and Its Application to Composites Processing," Journal of Composite Materials, 26(9), pp. 1351-1373.

[150] Price, R., 1973, "Production of impregnated rovings," Imperial Chemical Industries Ltd, United States patent US3742106.

[151] Padaki, S., and Drzal, L. T., 1997, "A Consolidation Model for Polymer Powder Impregnated Tapes," Journal of Composite Materials, 31(21), pp. 2202-2227.

[152] Ganga, R. A., 1986, "Flexible composite material and process for producing same," Arkema France SA, United States patent US4614678.

[153] Ganga, R. A., 1987, "Apparatus for producing flexible composite material," Arkema France SA, United States patent US4713139.

[154] Leone, M., Carbone, R. F., and Ganga, R. A., 1994, "Composite material the characteristics of which can be modulated by preimpregnation of a continuous fiber," Francais Etat and Arkema France SA, United States patent US5275883.

[155] Connor, M., Toll, S., Månson, J. A. E., and Gibson, A. G., 1995, "A Model for the Consolidation of Aligned Thermoplastic Powder Impregnated Composites," Journal of Thermoplastic Composite Materials, 8(2), pp. 138-162.

[156] Rath, M., Kreuzberger, S., and Hinrichsen, G., 1998, "Manufacture of aramid fibre reinforced nylon-12 by dry powder impregnation process," Composites Part A: Applied Science and Manufacturing, 29(8), pp. 933-938.

[157] Bucher, R. A., and Hinkley, J. A., 1992, "Fiber/Matrix Adhesion in Graphite/PEKK Composites," Journal of Thermoplastic Composite Materials, 5(1), pp. 2-13.

[158] Bullions, T., Loos, A., and McGrath, J., "Advanced composites manufactured via dry powder prepregging," Proc. Proceedings of the International Conference on Composite Materials.

[159] Geldart, D., Harnby, N., and Wong, A. C., 1984, "Fluidization of cohesive powders," Powder Technology, 37(1), pp. 25-37.

[160] Iyer, S. R., and Drzal, L. T., 1989, "Behavior of cohesive powders in narrow-diameter fluidized beds," Powder Technology, 57(2), pp. 127-133.

[161] Brown, A., and Moran, R., 1974, "Apparatus for impregnating strands, webs, fabrics and the like," Owens Corning Corp, Owens Corning Fiberglas Corp, United States patent US3817211.

[162] Brown, A. W., and Moran, R. J., 1975, "Method for electrostatically impregnating strand,"United States patent US3919437.

[163] Muzzy, J. D., Varughese, B., Thammongkol, V., and Tincher, W., 1989, "Electrostatic prepregging of thermoplastic matrices," SAMPE Journal, 25(5), pp. 15-21.

[164] Muzzy, J. D., and Varughese, B., 1992, "Flexible multiply towpreg and method of production therefor," Georgia Tech Research Corp, United States patent US5094883.

[165] Muzzy, J. D., and Varughese, B., 1992, "Flexible multiply towpreg," Georgia Tech Research Corp, United States patent US5171630.

[166] Muzzy, J. D., and Colton, J. S., 1993, "Non-woven flexible multiply towpreg fabric," Georgia Tech Research Corp, United States patent US5198281.

[167] Muzzy, J. D., and Colton, J. S., 1994, "Flexible multiply towpreg tape from powder fusion coated towpreg and method for production thereof," Georgia Tech Research Corp, United States patent US5296064.

[168] Iyer, S. R., and Drzal, L. T., 1990, "Manufacture of Powder-Impregnated Thermoplastic Composites," Journal of Thermoplastic Composite Materials, 3(4), pp. 325-355.

[169] Iyer, S., Drzal, L. T., and Jayaraman, K., 1992, "Method coating fibers with particles by fluidization in a gas," Michigan State University, United States patent US5102690.

[170] Iyer, S., Drzal, L. T., and Jayaraman, K., 1992, "Method for fiber coating with particles," Michigan State University, United States patent US5123373.

[171] Iyer, S., and Drzal, L. T., 1992, "Method for fiber coating with particles," Michigan State University, United States patent US5128199.

[172] Allen, L. E., Edie, D. D., Lickfield, G. C., and McCollum, J. R., 1988, "Thermoplastic Coated Carbon Fibers for Textile Preforms," Journal of Thermoplastic Composite Materials, 1(4), pp. 371-379.

[173] Baucom, R. M., Snoha, J. J., and Marchello, J. M., 1991, "Process for application of powder particles to filamentary materials," National Aeronautics and Space Administration (NASA), United States patent US5057338.

[174] Silva, J. F. M. G. D., Nunes, J. P. L. G., Silva, L. A. R. D., and Marques, A. T., 2002, "Equipment to produce continuously powder coated thermoplastic matrix prepregs (towpregs)," Universidade Do Minho, WIPO patent WO2002006027.

[175] Nunes, J. P., Silva, J. F., Marques, A. T., Crainic, N., and Cabral-Fonseca, S., 2003, "Production of Powder-Coated Towpregs and Composites," Journal of Thermoplastic Composite Materials, 16(3), pp. 231-248.

[176] van Hattum, F. W. J., Nunes, J. P., and Bernardo, C. A., 2005, "A theoretical and experimental study of new towpreg-based long fibre thermoplastic composites," Composites Part A: Applied Science and Manufacturing, 36(1), pp. 25-32.

[177] Ogden, A. L., Hyer, M. W., Wilkes, G. L., and Loos, A. C., 1992, "The Development of an Alternative Thermoplastic Powder Prepregging Technique," Journal of Thermoplastic Composite Materials, 5(1), pp. 14-31.

[178] Throne, J. L., 1994, "Method of depositing and fusing polymer particles onto moistened continuous filaments," University of Akron, United States patent US5364657.

[179] Gillette, D. J., 1982, "Method and apparatus for electrostatic coating with controlled particle cloud," Electronic Equipment Corp, United States patent US4330567.

[180] Kittle, K., and Falcone, M., 2006, "Powder coating process," Akzo Nobel Coatings International BV, United States patent US20060062929.

[181] Kittle, K., and Falcone, M., 2004, "Powder coating process with electrostatically charged fluidised bed," Akzo Nobel Coatings International BV, United States patent US20040126487.

[182] Throne, J. L., and Ogden, A. L., 1994, "Method of depositing and fusing charged polymer particles on continuous filaments," University of Akron, United States patent US5370911.

[183] Ramani, K., Woolard, D. E., and Duvall, M. S., 1995, "An electrostatic powder spray process for manufacturing thermoplastic composites," Polymer Composites, 16(6), pp. 459-469.

[184] Woolard, D. E., and Ramani, K., 1995, "Electric field modeling for electrostatic powder coating of a continuous fiber bundle," Journal of Electrostatics, 35(4), pp. 373-387.

[185] Zaniboni, C., and Ermanni, P., 2006, "An Electrostatic Powder Spray Process for Manufacturing Polyphthalamide High Performance Composite," 8th International Conference on Flow Processes in Composite Materials (FPCM8), Douai, France.

[186] Taylor, G. J., 1981, "Method of impregnating a fibrous textile material with a plastic resin," BP Corp North America Inc, United States patent US4292105.

[187] Chabrier, G., Moine, G., Maurion, R., and Szabo, R., 1986, "Process for manufacturing profiled strips in fiber-loaded thermoplastic resin, installation for the implementation thereof and profiled strips obtained," Coflexip SA, Spie Batignolles SA, United States patent US4626306.

[188] O'Connor, J. E., 1987, "Reinforced plastic," Phoenixx TPC Inc, United States patent US4680224.

[189] Dyksterhouse, R., and Dyksterhouse, J., 1990, "Production of improved preimpregnated material comprising a particulate thermoplastic polymer suitable for use in the formation of substantially void-free fiber-reinforced composite article," Cytec Technology Corp, United States patent US4894105.

[190] Texier, A., Davis, R. M., Lyon, K. R., Gungor, A., McGrath, J. E., Marand, H., and Riffle, J. S., 1993, "Fabrication of PEEK/carbon fibre composites by aqueous suspension prepregging," Polymer, 34(4), pp. 896-906.

[191] Yu, T. H., and Davis, R. M., 1993, "The Effect of Processing Conditions on the Properties of Carbon Fiber-LaRC TPI Composites Made by Suspension Prepregging," Journal of Thermoplastic Composite Materials, 6(1), pp. 62-90.

[192] Vodermayer, A. M., Kaerger, J. C., and Hinrichsen, G., 1993, "Manufacture of high performance fibre-reinforced thermoplastics by aqueous powder impregnation," Composites Manufacturing, 4(3), pp. 123-132.

[193] Chary, R. R., and Hirt, D. E., 1994, "Coating carbon fibers with a thermoplastic polyimide using aqueous foam," Polymer Composites, 15(4), pp. 306-311.

[194] Steggall, C., Simacek, P., Advani, S. G., and Yarlagadda, S., "A model for thermoplastic melt impregnation of fiber bundles during consolidation of powder-impregnated continuous fiber composites," Proc. The 9th International Conference on Flow Processes in Composite Materials.

[195] Steggall-Murphy, C., Simacek, P., Advani, S. G., Yarlagadda, S., and Walsh, S., 2010, "A model for thermoplastic melt impregnation of fiber bundles during consolidation of powder-impregnated continuous fiber composites," Composites Part A: Applied Science and Manufacturing, 41(1), pp. 93-100.

[196] Khan, S. U., and Kim, J. K., 2011, "Impact and delamination failure of multiscale carbon nanotube-fiber reinforced polymer composites: A review," International Journal of Aeronautical and Space Sciences, 12(2), pp. 115-133.

[197] Bekyarova, E., Thostenson, E. T., Yu, A., Kim, H., Gao, J., Tang, J., Hahn, H. T., Chou, T. W., Itkis, M. E., and Haddon, R. C., 2007, "Multiscale Carbon

Nanotube−Carbon Fiber Reinforcement for Advanced Epoxy Composites," Langmuir, 23(7), pp. 3970-3974.

[198] Siddiqui, N. A., Khan, S. U., Ma, P. C., Li, C. Y., and Kim, J.-K., 2011, "Manufacturing and characterization of carbon fibre/epoxy composite prepregs containing carbon nanotubes," Composites Part A: Applied Science and Manufacturing, 42(10), pp. 1412-1420.

[199] Kwon, Y. J., Kim, Y., Jeon, H., Cho, S., Lee, W., and Lee, J. U., 2017, "Graphene/carbon nanotube hybrid as a multi-functional interfacial reinforcement for carbon fiber-reinforced composites," Composites Part B: Engineering, 122, pp. 23-30.

[200] Wang, X., Song, L., Pornwannchai, W., Hu, Y., and Kandola, B., 2013, "The effect of graphene presence in flame retarded epoxy resin matrix on the mechanical and flammability properties of glass fiber-reinforced composites," Composites Part A: Applied Science and Manufacturing, 53, pp. 88-96.

[201] Jia, J., Du, X., Chen, C., Sun, X., Mai, Y.-W., and Kim, J.-K., 2015, "3D network graphene interlayer for excellent interlaminar toughness and strength in fiber reinforced composites," Carbon, 95, pp. 978-986.

[202] Qin, W., Vautard, F., Drzal, L. T., and Yu, J., 2015, "Mechanical and electrical properties of carbon fiber composites with incorporation of graphene nanoplatelets at the fiber–matrix interphase," Composites Part B: Engineering, 69, pp. 335-341.

[203] Vázquez-Moreno, J. M., Sánchez-Hidalgo, R., Sanz-Horcajo, E., Viña, J., Verdejo, R., and López-Manchado, M. A., 2019, "Preparation and Mechanical Properties of Graphene/Carbon Fiber-Reinforced Hierarchical Polymer Composites," Journal of Composites Science, 3(1), p. 30.

[204] Haque, A., Shamsuzzoha, M., Hussain, F., and Dean, D., 2003, "S2-Glass/Epoxy Polymer Nanocomposites: Manufacturing, Structures, Thermal and Mechanical Properties," Journal of Composite Materials, 37(20), pp. 1821-1837.

[205] Kornmann, X., Rees, M., Thomann, Y., Necola, A., Barbezat, M., and Thomann, R., 2005, "Epoxy-layered silicate nanocomposites as matrix in glass fibre-reinforced composites," Composites Science and Technology, 65(14), pp. 2259-2268.

[206] Subramaniyan, A. K., and Sun, C. T., 2006, "Enhancing compressive strength of unidirectional polymeric composites using nanoclay," Composites Part A: Applied Science and Manufacturing, 37(12), pp. 2257-2268.

[207] Sharma, B., Mahajan, S., Chhibber, R., and Mehta, R., 2012, "Glass Fiber Reinforced Polymer-Clay Nanocomposites: Processing, Structure and Hygrothermal Effects on Mechanical Properties," Procedia Chemistry, 4, pp. 39-46.

[208] Vlasveld, D. P. N., Parlevliet, P. P., Bersee, H. E. N., and Picken, S. J., 2005, "Fibre–matrix adhesion in glass-fibre reinforced polyamide-6 silicate nanocomposites," Composites Part A: Applied Science and Manufacturing, 36(1), pp. 1-11.

[209] Vlasveld, D. P. N., Bersee, H. E. N., and Picken, S. J., 2005, "Nanocomposite matrix for increased fibre composite strength," Polymer, 46(23), pp. 10269-10278.

[210] Vlasveld, D. P. N., Daud, W., Bersee, H. E. N., and Picken, S. J., 2007, "Continuous fibre composites with a nanocomposite matrix: Improvement of flexural and compressive strength at elevated temperatures," Composites Part A: Applied Science and Manufacturing, 38(3), pp. 730-738.

[211] Clifford, M. J., and Wan, T., 2010, "Fibre reinforced nanocomposites: Mechanical properties of PA6/clay and glass fibre/PA6/clay nanocomposites," Polymer, 51(2), pp. 535-539.

[212] Cortes, L. Q., Racagel, S., Lonjon, A., Dantras, E., and Lacabanne, C., 2016, "Electrically conductive carbon fiber / PEKK / silver nanowires multifunctional composites," Composites Science and Technology, 137, pp. 159-166.

[213] Nishikawa, Y., Okubo, K., Fujii, T., and Kawabe, K., 2006, "Fatigue crack constraint in plain-woven CFRP using newly-developed spread tows," International Journal of Fatigue, 28(10), pp. 1248-1253.

[214] Sihn, S., Kim, R. Y., Kawabe, K., and Tsai, S. W., 2007, "Experimental studies of thin-ply laminated composites," Composites Science and Technology, 67(6), pp. 996-1008.

[215] El-Dessouky, H. M., and Lawrence, C. A., 2013, "Ultra-lightweight carbon fibre/thermoplastic composite material using spread tow technology," Composites Part B: Engineering, 50, pp. 91-97.

[216] Irfan, M. S., Machavaram, V. R., Mahendran, R. S., Shotton-Gale, N., Wait, C. F., Paget, M. A., Hudson, M., and Fernando, G. F., 2012, "Lateral spreading of a fiber bundle via mechanical means," Journal of Composite Materials, 46(3), pp. 311-330.

[217] Calkins, R. W., 1991, "Fiber impregnation process," Garlock Sealing Technologies LLC, United States patent US4994303.

[218] Nakagawa, N., and Ohsora, Y., 1992, "Fiber separator for producing fiber reinforced metallic or resin body," Ube Industries Ltd, United States patent US5101542.

[219] Akase, D., Matsumae, H., Hanano, T., and Sekido, T., 2000, "Method and apparatus for opening reinforcing fiber bundle and method of manufacturing prepreg," Toray Industries Inc, United States patent US6094791.

[220] Tanaka, K., Ohtani, H., Matsumae, H., Tsuji, S., and Akase, D., 2004, "Production device and method for opened fiber bundle and prepreg production method," Toray Industries Inc, United States patent US6743392.

[221] Iyer, S., and Drzal, L. T., 1991, "Method and system for spreading a tow of fibers," Michigan State University, United States patent US5042111.

[222] Kawabe, K., Matsuo, T., and Maekawa, Z.-i., 1998, "New Technology for Opening Various Reinforcing Fiber Tows," Journal of the Society of Materials Science, Japan, 47(7), pp. 727-734.

[223] El-Dessouky, H. M., 2017, "Advanced Composite Materials: Properties and Applications," 6 Spread Tow Technology for Ultra Lightweight CFRP Composites: Potential and Possibilities, De Gruyter Open Poland, pp. 323-348.

[224] Borg, C., 2015, "An introduction to spread tow reinforcements: Part 1 – Manufacture and properties," Reinforced Plastics, 59(4), pp. 194-198.

CHAPTER III: DEVELOP IN-HOUSE RIG TO MANUFACTURE THERMOPLASTIC PREPREGS

3.1 Introduction

This chapter presents an overview on the concept, design and manufacturing processes of a novel thermoplastic prepreg rig. The idea of manufacturing high-performance and high-temperature thermoplastic prepregs in a lab scale production will be discussed, together with evaluation of the proposed method. Initially, the concept of the method is examined, followed by a list of materials that were used throughout the research project. Then, initial testing on the rig was carried out. Here, two thermoplastic prepreg manufacturing rigs were proposed and manufactured, that is, woven prepreg and UD prepreg rigs, with a special focus on the UD manufacturing line.

3.2 The Concept

The first challenging step of this project is to employ and investigate the practicality of an effective method of thermoplastic resin impregnation, and subsequently prepreg production. The main derivatives affecting the choice for a suitable manufacturing method are charted in Figure 3.1. For this purpose, three main factors including suitability, cost and scale are taken into account.

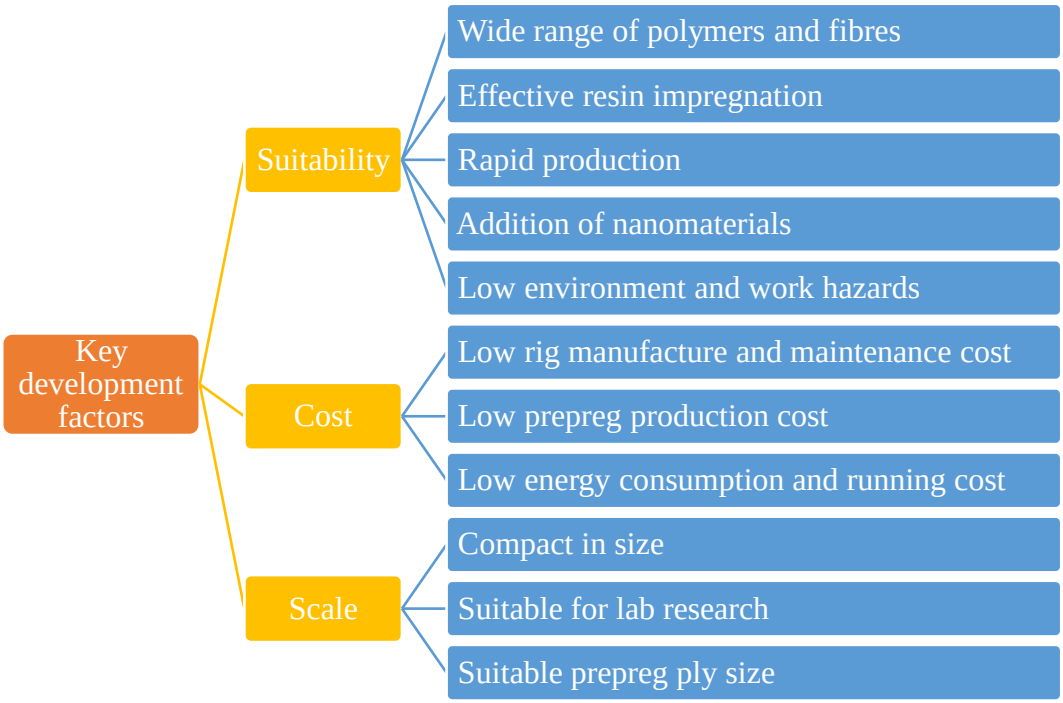

Figure 3.1 Key factors considered for the manufacturing process and rig development.

Upon research and investigation on different production methods, the most suitable impregnation technique to serve the purpose of this project would be wet powder impregnation. Although aqueous impregnation technique might add on an extra step to the production line when compared to dry powder technology, it is an effective and low-cost method. Not only it eliminates the need for expensive coating or melting devices, but it also allows impregnation for variety of reinforcements using a range of polymer particle sizes. It is also safe and does not involve hazardous solution agents. Therefore, the main focus would be on this method.

Another aspect of the project is to investigate the effect of adding nanomaterials in the matrix phase on the mechanical properties of composite laminates. This urges a need for a homogenous blend of polymer resin and any other additive material. In this instance, wet powder impregnation is promoted and appears to be the most suitable option. In wet powder impregnation, as long as a suitable liquid carrier is implemented, it is assumed that any additive material can be thoroughly mixed with polymer powder, to form a homogenous suspension. With dry powder impregnation method, additive materials could not be mixed thoroughly to form a homogenous resin and it is deemed hard to coat the reinforcing fibres evenly. The extend of effectiveness of wet powder impregnation method is therefore focused on this study.

Based on the wet impregnation method, the proposed rig concept should also be cost effective in the making and material production. It should be compact in size and suitable for lab scale research and development purposes.

3.3 Materials

In this section the raw materials used in the project are described and their technical data sheets are listed. The materials include different reinforcing fibres and polymers, liquid carrier and nanomaterials. The focus is however on S2-glass reinforced PAEK composites. Information on the material data sheets were directly obtained from the manufacturers or from their online database. Efforts were made to collect as much information as possible on each material.

3.3.1 Reinforcing Fibre

Three types of reinforcing fibres, namely, woven E-glass tape, S2-glass tow and carbon fibre (CF) tow, were used throughout this project.

3.3.1.1 Woven E-glass Tape

The first reinforcement type is a plain weave E-glass fibre tape that was supplied by Matrix Composite Materials Company Ltd. (UK). Properties of the E-glass tape is listed in Table 3.1.

Table 3.1 Properties of the E-glass fibre tape.

Property	**Description or value**
Weave type	Plain weave
Warp and weft yarn	EC9-136
Sizing	Amino silane
Areal weight (g/m^2)	200
Tape width (mm)	100
Tape thickness (mm)	0.20

3.3.1.2 S2-Glass Fibre Tow

S2-glass is the high-end class of glass fibres and can offer up to 85 % more tensile strength, after impregnated with resin, than conventional glass fibres. S2-glass fibre offers enhanced weight performance and provides better cost performance compared to aramid and carbon fibre. S2-glass has higher level of silica compared to standard glass fibres, which offers higher tensile and compressive strength, better toughness, and high temperature and impact resistance [1, 2].

S2-glass fibre roving was supplied by AGY LLC. (USA), which is the sole supplier of this material. The grade of the S2-glass fibre roving used was 933-AA-750. The 933 version is designed for use in aerospace and defence applications. This grade consists of numerous G filament (9 microns) continuous glass strands. The strands are without mechanical twist and are treated with a thermally stable inorganic sizing

suitable for high-temperature matrices such as PAEKs. Here, the 933 version is recorded as having a poor broken filament resistance. Grade 933-AA-750 has a linear density of 675 g/1000m (TEX) and would approximately have 4200 filaments bundled together. The apparent thickness and width of the received fibre roving was measured 0.20 mm and 2.5 mm, respectively. Table 3.2 shows the technical data sheet of the product.

Table 3.2 Properties of S2-glass fibre roving grade 933-AA-750.

Properties	**Description or value**
Fibre properties	
Tensile strength (MPa)	4890
Tensile modulus (GPa)	89
Strain (%)	5.7
Density (g/cm^3)	2.47
Filament diameter (μm)	9 (G)
Roving properties	
Yield (g/1000m)	675
End count	10
Number of filaments	4150–4200
Sizing type / Amount (%)	933 / 0.23
Twist	Never twisted

3.3.1.3 Carbon Fibre Tow

Grade AKSACA 3K A-38 continuous carbon fibre tow was supplied from DowAksa Ltd. (Turkey). CF was not the primary reinforcing fibre in this project and the use of CF was just to demonstrate the ability of using different fibre rovings in manufacturing CF based composites using the thermoplastic prepreg rig developed. Properties of the received CF are shown in Table 3.3.

Table 3.3 Properties of 3K A-38 carbon fibre tow.

Properties	Description or value
Fibre properties	
Tensile strength (MPa)	3800
Tensile modulus (GPa)	240
Strain (%)	1.6
Density (g/cm^3)	1.78
Roving properties	
Yield (g/1000m)	200
Number of filaments	3K or 3000
Sizing type / Amount (%)	D012 / 1.0–1.5
Twist	Never twisted

3.3.2 Thermoplastic Polymers

Several thermoplastic polymers in the form of fine powder were used in this research either for evaluation or testing purposes. In case of supplying PAEK resins, options were limited as there are only a few companies who manufacture and supply these polymers, specifically in form of fine powder. Further down the line it is realised that not all PAEKs are suitable for manufacturing thermoplastic composites using the in-house prepreg rig and the PAEK grade heavily impacts the process.

3.3.2.1 Polypropylene (PP)

In order to evaluate wet powder impregnation method, polypropylene (PP) polymer powder was used as an alternative to PAEK and for use in the woven prepreg test rig. PP powder is commercially available and costs notably less than PAEKs, making it ideal for trial runs and testing.

PP in form of fine powder was provided by Goonvean Fibres Ltd. (UK) with specification as listed in Table 3.4.

Table 3.4 Characteristics of polypropylene powder.

Property	**Description or value**
Particle size (μm)	(D_{50})~55–75, (D_{95}) <90
Melting point (°C)	159–171
Density (g/cm^3)	0.90–0.91

3.3.2.2 Polyaryl ether ketone (PAEK)

PAEK family of thermoplastics was the main polymer employed for the manufacture of high-performance and high-temperature prepregs. Three different grades of PAEK as disclosed in Table 3.5 were investigated. PAEK grades are listed in order of their receipt and utilisation during the project.

The first set of PAEK polymers was polyether ketone (PEK) grade G-PAEK 1100PF, and also a PEK and polybenzimidazole (PBI) blend branded as GAZOLE 6200PF, and was obtained from Gharda Chemicals Ltd. (India). GAZOLE 6000 series are PEK/PBI blends with high thermal and chemical stability. PBI is a high-performance thermoplastic polymer with a glass transition temperature (T_g) exceeding 400 °C and impressive mechanical properties [3]. Melt processing of PBI however can be extremely challenging and requires a very high pressure.

AE 250 PAEK (also known as engineered PAEK) is one of the most recent resin systems developed by Victrex plc. (UK). It is a PEEK based copolymer with much lower melting temperature (T_m) of 305 °C compared to PEK and a T_g of 149 °C. AE 250 can maintain mechanical, physical and chemical properties typically compared to PEK, PEEK or PEKK.

The lower T_m of AE 250 means reducing processing temperature by 40 to 60 °C, permitting composite parts to be manufactured cheaply and fast with added perks of implementing out of autoclave processing, fast automated lay-up, injection over-moulding and hot stamping, thus eliminating the high use of expensive autoclaves and factories, where houses them. The novel AE 250 is 25–30 % semi-crystalline when

press consolidated with a cooling rate of 5–10 °C/min. The lower melting temperature of AE 250 resin widens the processing window, whilst still allowing fully crystalline morphology to develop throughout the cooling phase. A major advantage of AE 250 is that it can be processed with a relatively low pressure, opening gates to the production of high-quality parts utilising out of autoclave processing [4].

Table 3.5 Characteristics of different PAEK powder systems: (a) mechanical properties and (b) thermal and physical properties.

(a)

Supplier / Grade	**Chemical structure**	**Tensile strength (MPa)**	**Tensile modulus (GPa)**	**Tensile elongation (%)**	**Flexural strength (MPa)**	**Flexural modulus (GPa)**
Gharda G-PAEK 1100PF	PEK	110	4.2	20–25	185	4.1
GAZOLE 6200PF	PEK/PBI	90	5.6	2	150	6.1
Victrex AE 250	PAEK	90	3.5	15	150	3.3

(b)

Supplier / Grade	**Melting point (°C)**	**Glass transition (°C)**	**Melt viscosity (Pa.s)**	**Density (g/cm^3)**	**Particle size (µm)**
Gharda G-PAEK 1100PF	372	152	300–350 @400 °C	1.30	(D_{50}) <10
GAZOLE 6200PF	372	152	300–350 @400 °C	1.30	-
Victrex AE 250	305	149	200 @400 °C	1.28	(D_{50}) <10

AE 250 is later found to be the most suitable resin system for manufacturing thermoplastic prepreg and is chosen as the main polymer for this research.

3.3.3 Liquid Carrier

Due to the low surface energy of PAEKs, they are normally not very well dispersed in water, if at all. Water alone cannot usually wet out the PAEK powder fully and this therefore urges the need for a dispersing agent in order to improve the separation of the particles, and to prevent their sedimentation or agglomeration in the slurry.

For this purpose, a liquid carrier from Tech Line Coatings Inc. (USA) with a tradename of LiquiPowder (L2O) was used. Although L2O is a commercially available product, access to information on the ingredients of the base blend is limited due to the presence of non-disclosure agreements and commercial confidentiality. However, the manufacturer advised few key details.

While electrostatic application can be used to coat a variety of irregular shapes, dry powder does have problems entering porous materials such as fibre strands. Also applying powder to a non-conductive surface is a challenge. Wood, plastics, ceramics and other non-metallic or non-conductive substrates are difficult to coat, especially with electrostatic methods. Moistening non-conductive surfaces to get the powder to stick is only of minimal benefit as it is difficult to properly apply the powder at the desired level in this manner. Moreover, once the water has evaporated the powder is very easily dislodged.

L2O is a water-based and non-hazardous dispersion system that virtually allows any powder to be suspended in a slurry. L2O contains a blend of dispersing and water-thickening agents that promotes homogenous suspension of PAEK particles in the slurry for prolonged periods without settling and helps preventing particle clumping. Resinous ingredients in L2O provide great initial bond between PAEK particles and glass fibre filaments, holding the particles firmly on the fibres even after the water base is dried and evaporated. Heat melting the PAEK subsequently results in permanent bond on reinforcing fibres. The basic powder is all that remains after curing, in a way that L2O characteristics are effective for bonding. Everything in the

liquid carrier leaves the composite upon melting the PAEK, and only the actual polymer remains.

3.3.4 Nanomaterials

In the later stages of this study the effect of nanomaterials in manufacturing of S2-glass fibre reinforced PAEK prepregs is investigated. Two nanomaterials were used in the project.

3.3.4.1 Graphene

Graphene in nanoscale powder was supplied by Versarien plc. (UK) under the trademark of Nanene, which is a high quality, low defect, few-layer and high carbon purity graphene. It has a 2D flake like structure with high lateral dimension, which can create large interfaces within the composite matrix. Table 3.6 gives the properties of Nanene.

Table 3.6 Properties of graphene (Nanene) nanoparticles.

Property	**Description or value**
Layers ≤5, ≤10, >10 (%)	60, 90, 10
Apparent thickness (nm)	<3.5, 10 layers
Lateral dimension (μm)	<10
Bulk density (g/cm^3)	0.1857
Surface area (m^2/g)	45

3.3.4.2 Nanoclay

Montmorillonite nanoclay in very fine powder form with a stock number NS6130-09-902 was received from Nanoshel LLC. (USA) with material specifications as seen in Table 3.7.

Table 3.7 Properties of montmorillonite clay nanoparticles.

Property	**Description or value**
Average particle size (nm)	~1
Bulk density (g/cm^3)	0.7609
Density (g/cm^3)	2.6
Surface area (m^2/cm^3)	0.09–1.8

3.4 Evaluation of Wet Powder Technology

The first step before starting to develop and design a concept was to evaluate if this method could be implemented and possibly work. The impregnation and powder adhesion to the glass fibre was the greatest concern and thus, initial focus was to determine the suitability of the L2O carrier. For this purpose, L2O was mixed with a small and undefined amount of PP powder to form a powder slurry. Since the purpose of this trial was solely to evaluate the potential of L2O as a favourable dispersing agent, no PP/L2O ratio was defined.

Initial observations suggested that L2O could disperse and suspend the powder well given the fact that they were only manually stirred with a stick. The mixture was then brushed over a piece of glass fibre fabric to observe the adhesion of powder on glass fabric. Powder slurry seemed to have successfully wetted the glass fibre and after leaving the fabric to dry for a few hours, PP powder did not fell off the glass fabric even when gently shaken. The process is showed in Figure 3.2.

The first impressions on L2O indicated that it could be a promising candidate for use in the prepreg manufacturing process. However, in order to fully understand its potential and operational abilities in practice, it should be utilised in an established prepreg manufacture rig. For this purpose, two thermoplastic prepreg manufacturing rig was proposed and manufactured.

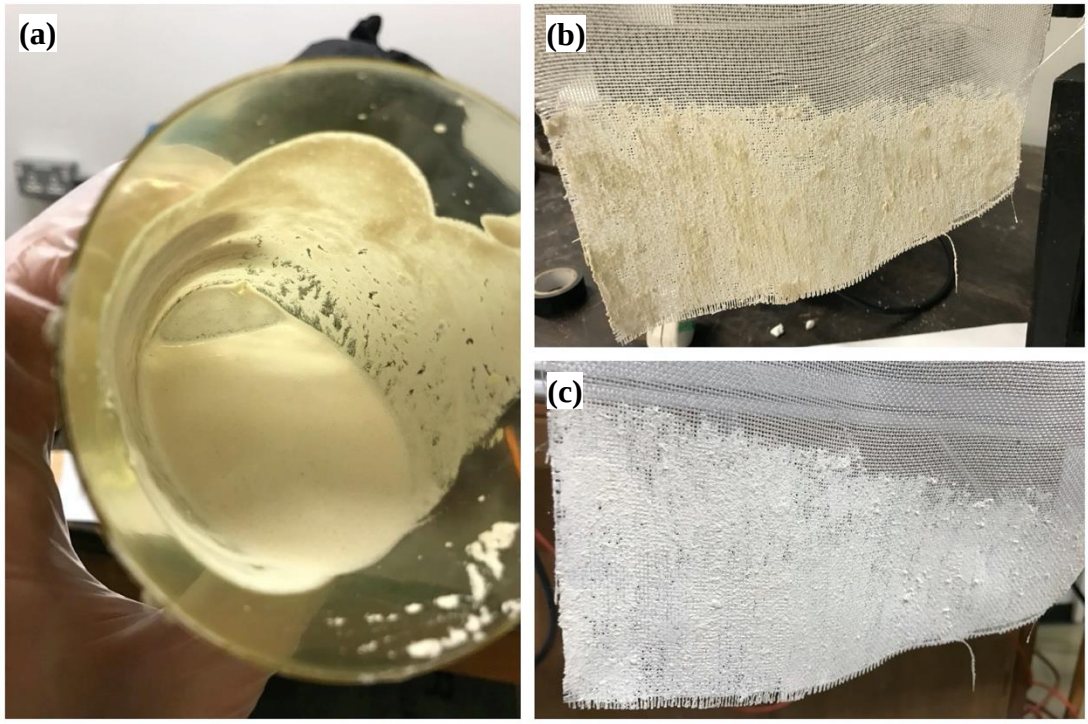

Figure 3.2 L2O carrier suitability test: (a) L2O and PEKK mixture, (b) brushed mixture on glass fabric surface and (c) dried powder attached to glass fabric.

3.5 Woven Prepreg Test Rig

The concept of a woven fabric prepreg rig was emerged from observing the success rate of the proposed wet impregnation method and base materials in production. As the result, the concept of a woven prepreg rig was developed as highlighted in Figure 3.3. The concept is based on wet impregnation of a woven glass fabric when dipped and passed through a powder slurry bath, followed by heating and melting of the polymer for permanent bond on the fabric.

This automated prepreg line consists of five steps as illustrated in Figure 3.4. Raw materials used for this step include:

- Woven E-glass (as in Section 3.3.1.1)
- Polypropylene powder (as in Section 3.3.2.1)
- L2O carrier (as in Section 3.3.3)

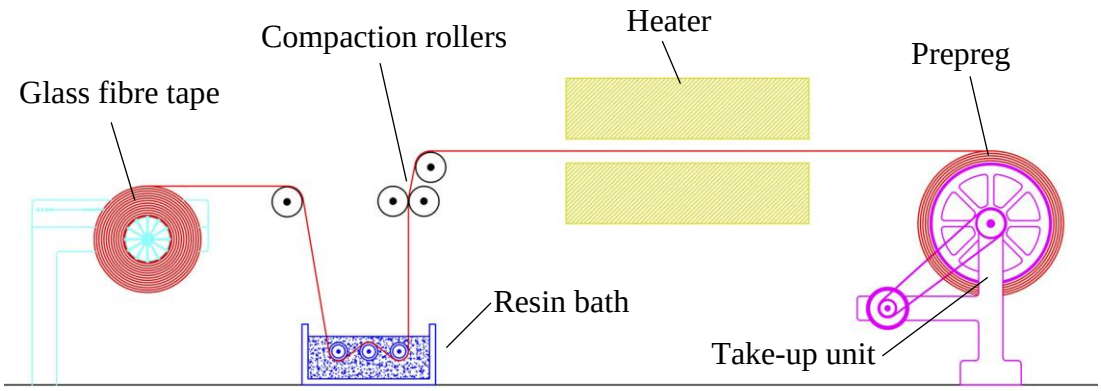

Figure 3.3 Concept of the woven prepreg test rig.

The process commences when woven glass fibre tape is drawn from the package holder and is guided through the resin bath, in which the PP powder is suspended in the L2O liquid carrier. The resin bath houses three rollers. Powder slurry is squeezed between glass fibre tape and rollers so as to impregnate the fabric with the resin system.

After the glass fibre picks up the resin, the glass tape passes through a set of metering rollers. As shown in Figure 3.4(c), the rollers are placed parallel with each other and the gap between them is adjustable via a screw thread micrometre gauge. The wet glass tape is passed and nipped between the metering rollers. Employment of this mechanism not only helps pinch the wetted fabric, but also controls the amount of resin that passes through. In this way, the amount of resin that passes through and adheres to glass tape can be controlled and the excessive resin can fall back in the resin bath container. It is observed that the resin powder is uniformly deposited on glass fibre after the glass tape exits the metering rollers.

The next step is when the impregnated glass tape is passed between two infrared heaters to help evaporating the carrier and consequently melting the PP resin for permanent adhesion on the glass tape. Finally, the prepreg composite material is taken up and wound on a spool connected to a geared motor. The trick here is to adjust the winding speed so that the wet prepreg finds enough time for water evaporation and subsequently reaching the melting temperature of PP during the run through the

heating unit. By the time the prepreg reaches the take-up unit, PP resin should also cool down to temperatures below its T_m. This can be achieved by introducing an external cooling system or simply by extending the traveling distance of prepreg between the heaters and winding unit.

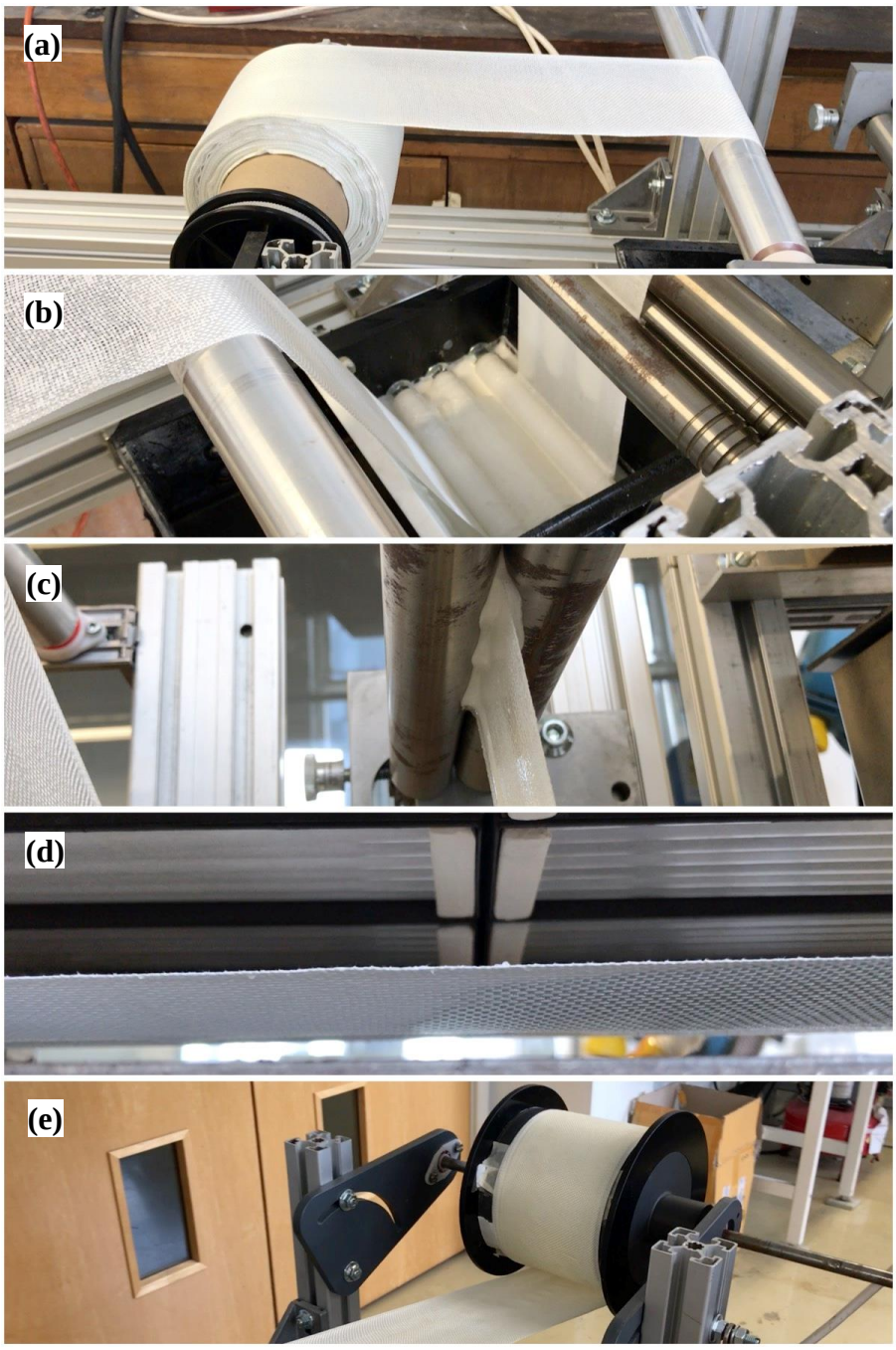

Figure 3.4 Woven prepreg test rig comprising: (a) package holder, (b) resin bath, (c) metering rollers, (d) heating unit and (e) take-up unit.

The manufactured prepreg is shown in Figure 3.5. The manufacturing process demonstrates efficient and even deposition of PP powder on the glass fibre fabric. The resulting prepreg material had a uniform thickness of approximately 0.25 mm.

Figure 3.5 Woven glass fibre/PP prepreg manufactured by the trial rig.

Testing on woven prepreg manufacture rig was terminated at this point and no further analysis on the different processing parameters or prepreg material characterisation were performed. This is due to the fact that main focus of this study was on producing UD prepreg and not woven prepreg.

By undertaking the woven prepreg manufacture trials, it was concluded that the proposed wet impregnation manufacturing technique is indeed effective and promising. Woven glass fabric was successfully impregnated with PP resin and woven glass fibre prepreg was manufactured. This was a solid indicator that this method can be levelled up to UD prepreg manufacture and somehow ticked off one of the key development factors in the concept, suitability and operational abilities.

3.6 Drum Winding Unidirectional Prepreg Rig

The main objective of the project was to develop a technique to manufacture thermoplastic UD prepregs, with a special focus on S2-glass/PAEK composites. This involves impregnation of continuous fibre roving in order to produce towpreg.

Towpreg is a bundle of fibres, which are impregnated with polymer resin. Multiple towpregs can be placed parallel to each other to form a UD tape, i.e. UD prepreg. Common industrial practice of manufacturing UD prepreg involves pulling multiple fibre tows from a creel that holds multiple fibre bobbins. Fibre tows are then guided through the levelling process, converged and ultimately placed parallel to each other before entering the resin impregnation process. Depending on the desired width of the prepreg tape, number of fibre bobbins required can vary. For instance, if one needs to produce a 100 mm wide UD prepreg tape, given that the width of fibre roving used is 4 mm, a creel with 25 individual fibre bobbins would be required (if there is no fibre spreading involved). This method would therefore require multiple guiding systems and substantial investment in raw materials.

It was previously discussed that cost and scale are two of the key development factors in mind for the design of the prepreg rig. Based on the wet impregnation method, the proposed rig in concept should be cost effective in manufacturing line and material production. It should be compact in size and suitable for lab scale research and development purposes.

3.6.1 Concept of Drum Winding Unidirectional Prepreg Rig

Fibres tend to function better when held straight. Crimp in fibre is normally not desired in high-performance composites, like components for aerospace industry. To benefit from ultimate mechanical performance, and freedom of placing composite reinforcement in the desired orientation, UD prepreg rig is desired. A UD prepreg is one in which a majority of fibres run in one direction only, which is normally the 0° direction. UD prepregs offer the ability to place reinforcement in the structure exactly where it is needed and where stress tends to be high. On top of this, fibres in UD prepregs are straight, therefore UD prepregs are classified as non-crimp materials. This results in highest possible fibre/matrix properties in fabrication of different composite components.

Several fundamental criteria shall be met in order to design and manufacture an effective laboratory scale UD thermoplastic prepreg rig, which are:

- Control the resin to fibre ratio, i.e. fibre volume content.
- Control the thickness and fibre spread.

By fulfilling these criteria, prepregs with different physical properties can be produced and the effect of different settings on the mechanical behaviour of the composite can be investigated. The UD prepreg rig in a laboratory scale should be cost effective, without the need for expensive tools and textile equipment. It should provide measures to control the fibre volume content and tools to control the thickness of the prepreg and degree of fibre spread. For this purpose, drum winding of continuous fibre roving based on wet impregnation technology is proposed and developed.

The concept of utilising a winding drum for manufacture of UD prepreg originates from a common industry practice of manufacturing composite materials, namely filament winding. In filament winding, single or multiple continuous fibre rovings are initially soaked with thermosetting resin by passing through a resin bath, and subsequently winding around a rotating mandrel/drum or any other desired shape, in order to form a composite material based on the geometry of the winding object. Fibre roving delivery system placed on a carriage actuates horizontally in line with the axis of the rotating mandrel while placing the wet fibre in the desired angle or pattern. The winding process is controlled by the fibre feeding mechanism and the rate of rotation of the mandrel [5]. Filament winding is primarily used with circular or oval hollow sections and it is traditionally used to produce tanks, pressure vessels and pipes. Schematics of filament winding process are shown in Figure 3.6.

Based on the function of the filament winding process, it was realised that this method could be implemented for producing UD thermoplastic prepreg. Imagine thermosetting resin inside the resin bath of typical filament winding machine is replaced with a suspension of polymer powder in a liquid carrier and the horizontal actuation setting of the carriage is in harmony with the winding speed in such a way that the fibre tow is just wound close to the previous array, next to each other, parallel on the winding drum. This way a sheet of wet UD prepreg is placed on the drum. All required would then be to consolidate the polymer and remove the wound layer from the drum to have a UD prepreg.

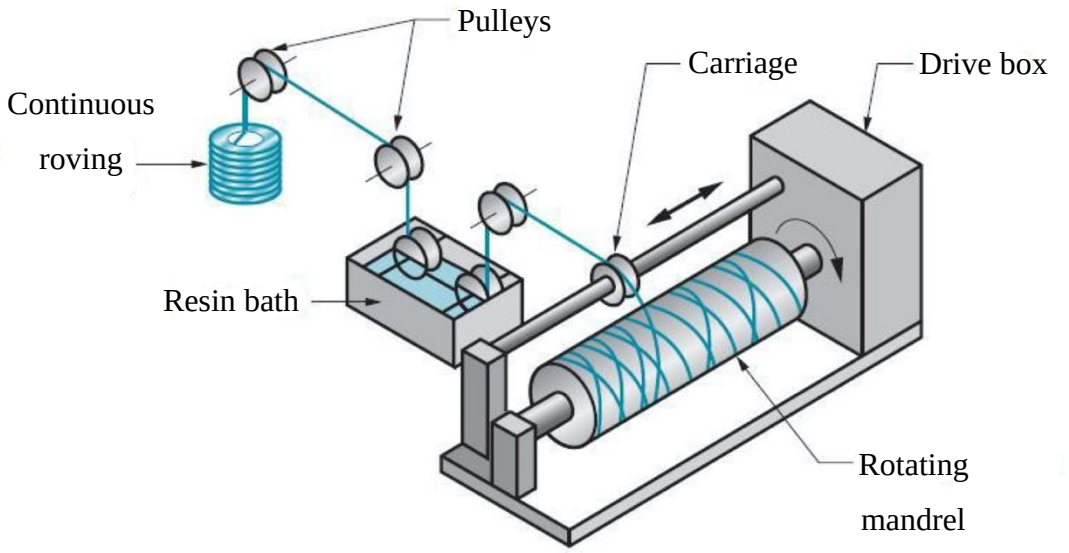

Figure 3.6 Example of a filament winding process [6].

3.6.2 Design

Early design concepts of the UD drum winding rig were based on the above thoughts. It was acknowledged that the proposed method would have certain merits and limits identified as:

Merits

- Novelty of the process
- Low quantity of raw material
- Compact in size
- Cost effective

Limits

- Noncontinuous production
- Prepreg size limit

The proposed method eliminates the use of multiple fibre bobbins on a creel and enables the production of prepreg with a single fibre bobbin. This significantly reduces the production cost and at the same time minimises the size of the prepreg rig. However, this method comes with a few limits. The size of the prepreg obviously depends on the size of the winding drum, that is, the wider the drum in diameter and length, the wider the prepreg size. Also, the production of UD prepreg would not be continuous. Once the winding is completed (single run of the linear actuator from one

side of the drum to the other), the machine stops to cut off the fibre roving from the drum and subsequently introduces heat to evaporate the water from the wet prepreg and melt the polymer. Finally, the prepreg is removed by cutting it across the length of the drum. The process can then start over. Despite these limits the proposed process seems ideal for small scale research and development purposes. Figure 3.7 is a simple illustration of the prepreg rig design concept. The design consists of a number of primary components sketched in different colours.

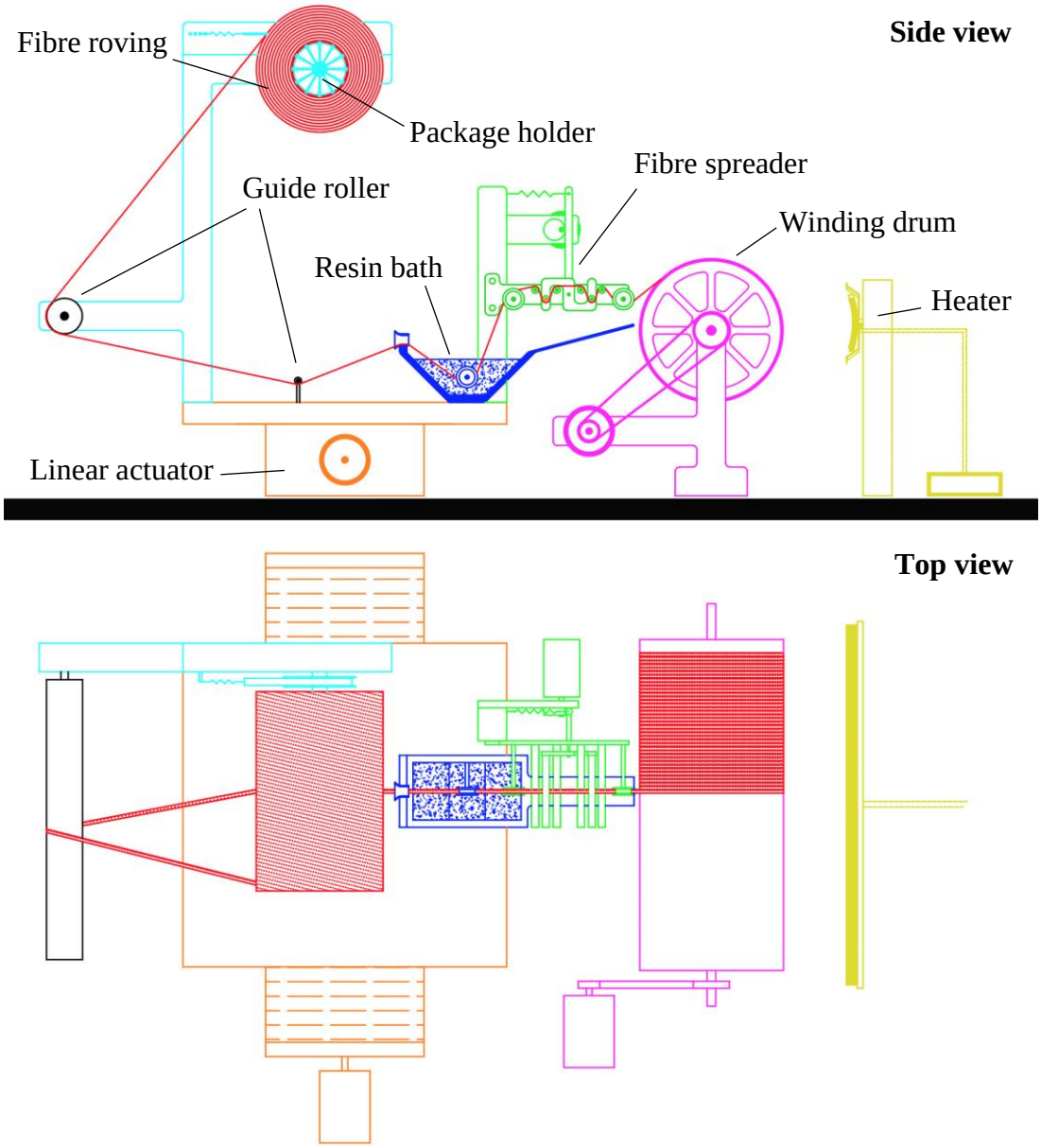

Figure 3.7 Design concept of drum winding thermoplastic prepreg rig.

The first component is the package holder (cyan). The package holder is where the fibre bobbin is mounted on. The package holder compartment along with the resin bath (blue) and the fibre spreader (green) are installed on a solid carriage plate, which is attached to a linear actuator (orange). As the fibre tow (red) is hauled off from the package holder, it passes a series of guiding rollers (black). It then passes through a guiding eyelet and is dipped in the resin bath, containing the PAEK slurry. The fibre tow is soaked in powder slurry as it exits the resin bath. After which, the wet fibre tow is passed on a series of rollers and enters the fibre spreader system. The rollers are a part of a new fibre spreading mechanism, which will be discussed later. In this stage, forces exerted on the fibre tow from the rollers causes the powder slurry to fully penetrate the fibre tow for resin impregnation. The fibre tow is also spread at this stage.

The concept of the proposed manufacturing method is to wind the impregnated fibre tow on a winding drum (pink) to manufacture a UD thermoplastic prepreg. The linear actuator unit is chosen in correspondence to the size of the winding drum and therefore, the actuator is able to horizontally travel the whole length of the drum. It is evident that the speed in which the linear actuator travels horizontally should be regulated with the rotating speed of the winding drum, so that the wet fibre tow is positioned next and parallel to each other, after each revolution of the drum, with perhaps small overlap. After the winding process is complete, the heater (yellow) is introduced to the system. The heat initially helps evaporating the water (including L2O carrier) in fibre tow and later melt the PAEK powder for permanent adhesion.

3.6.3 Rig Assembly

Initial experiments indicated that the proposed manufacturing method could potentially produce UD thermoplastic prepreg. With the above concept in mind, numerous parts were purchased, or designed and manufactured in-house. Figure 3.8 shows the assembled drum winding UD prepreg rig and the manufacturing processes. The designed and manufactured test rig is composed of several parts. For a better understanding, different parts of the rig are discussed in four sections. The prepreg manufacture process is also briefly explained.

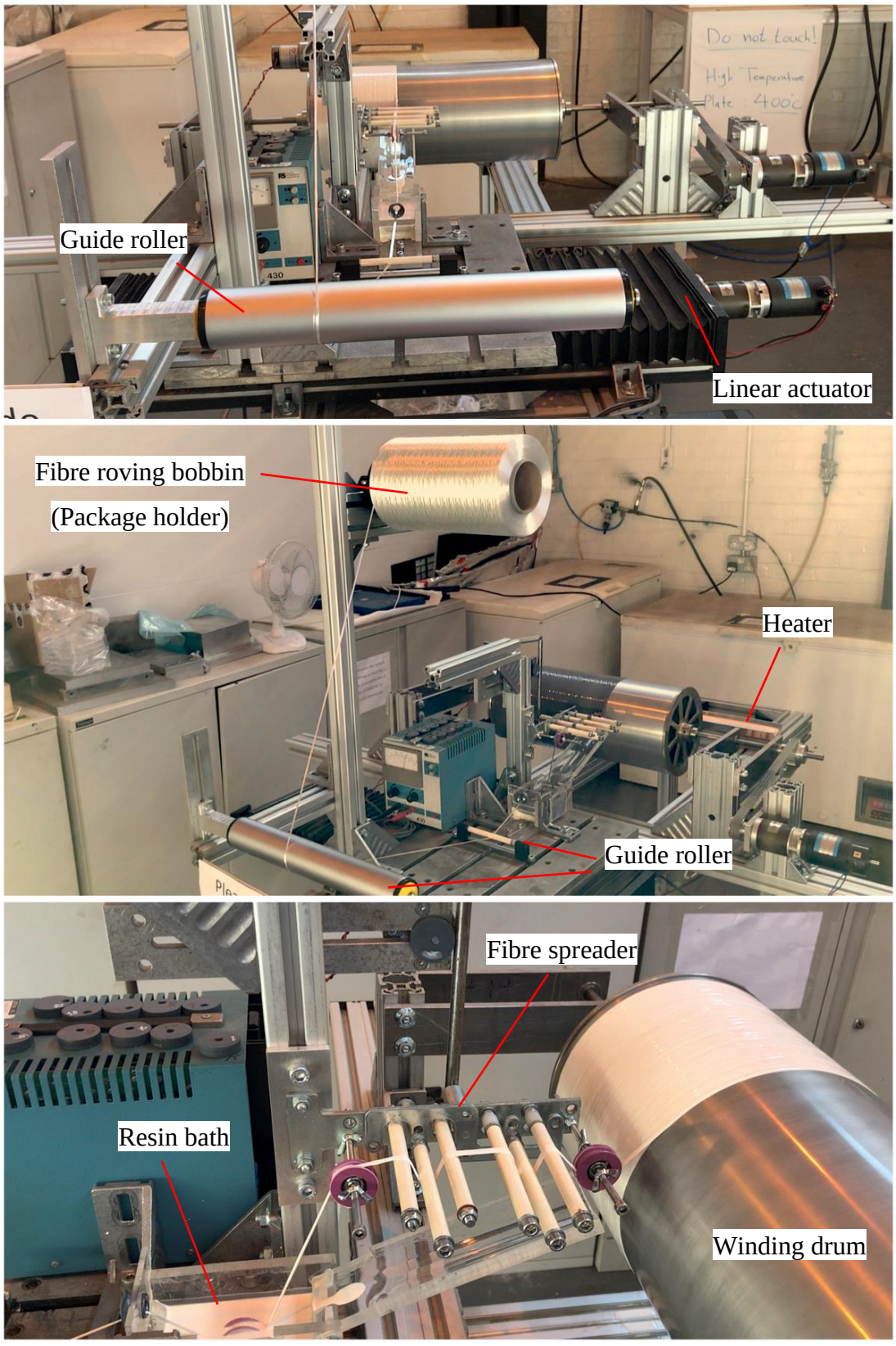

Figure 3.8 Assembled drum winding thermoplastic prepreg rig comprising several parts.

All assembled parts of the rig are installed on cuboid aluminium structural frames. The frames sit on two pairs of wheels for portability. The wheels can be locked so that the frame does not move for prepreg processing. The frame is manufactured from 40 x 80L mm IR aluminium profiles with 8 mm slot for part fixtures. The 8 mm slot on the aluminium profiles allows M8 T-slot nut or screw to be used for different part installations. In order to assemble the frames, aluminium profiles are connected using angle brackets.

3.6.3.1 Linear Actuator and Mounted Parts

The first major part of the rig is the linear actuator, which itself houses many other parts. The linear actuator is a device that converts circular motion into linear movement. The most common types of linear actuators are belt-driven actuators and ball screw actuators.

A ball screw transforms rotational motion into linear motion with the help of a threaded shaft. The threaded shaft provides a helical runway for the ball bearing, acting as a screw. The electric motor mounted on one side of the actuator body is connected to the threaded shaft via a coupling. The ball screw is attached to a plate, which is mounted on two sliding shafts. When the DC motor connected to the threaded shaft starts rotation, the actuator plate moves linearly. Ball screws have better positioning accuracy compared to belt drives. They are also more reliable with repeatability and this is often a very critical factor in precision applications such as filament winding. Therefore, a rigid ball screw drive mechanism is a better choice. A ball screw linear actuator with 500 mm stroke length was used.

A bigger plate is mounted on the actuator plate so as to house other components. The package holder and evidently the fibre roving bobbin are mounted on this plate. The package holder part was supplied by Cygnet Texkimp Ltd. (UK), as shown in Figure 3.9. The main part of the package holder is a housing tube, which accommodates the inner diameter of the fibre bobbin carboard tube that normally comes in a standard size of approximately 76 mm in diameter. The tube itself is loaded on a bearing, attached to a large pulley. A leather band is set around the surface of the pulley to one end and is attached to a spring to the other end. As fibre tow is pulled, the tube (and

the attached pulley) starts rotating. The pulley and band mechanism provides control over the tension in the hauled off fibre roving. The resistance between the leather band and the pulley causes friction and results in controlled and constant tension in the fibre roving. The tension can be controlled with adjusting the spring level attached to the main package holder frame, with 5 different options available. Experiments with handling fibre roving indicates that there should be a distance of at least 500 mm from fibre bobbin to the next fibre guiding equipment. This distance is sufficient for the fibre tow to have a smooth run on the upcoming metal roller so as to avoid any fibre twists. Fibre twists are not desirable due to affecting the fibre spread and orientation, and therefore changing the physical properties of the final prepreg product. The S2-glass roving used in the experiment was grade 933-AA-750 from AGY. The fibre bundle has approximately 4200 individual filaments and a width of 2.5 to 3.0 mm.

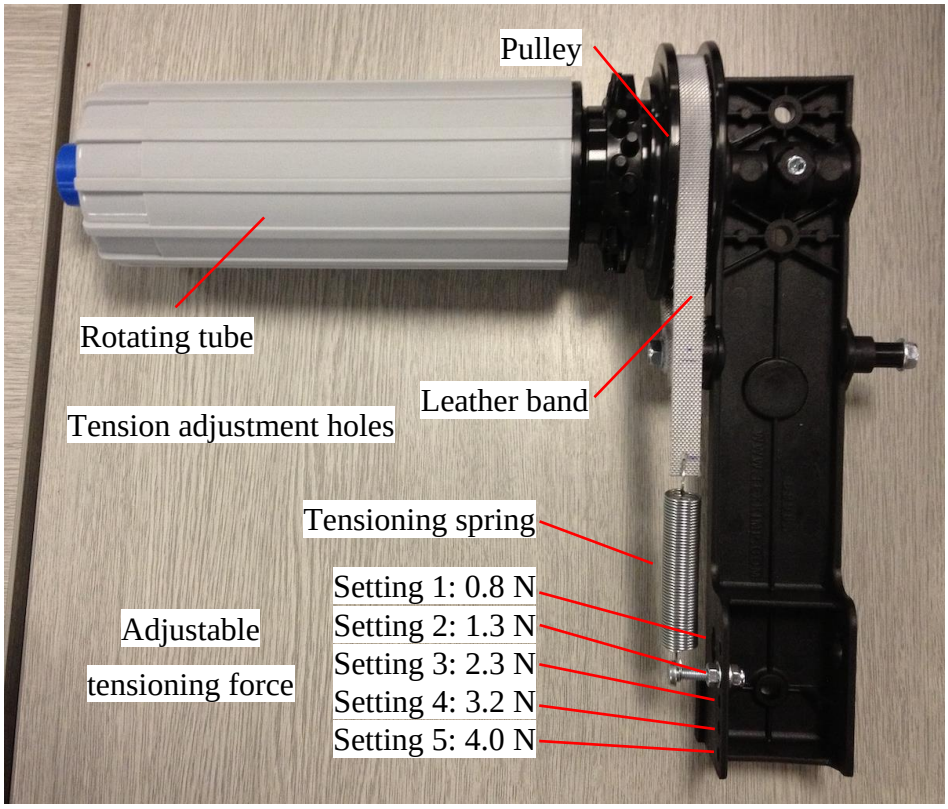

Figure 3.9 Package holder apparatus and tensioning force options.

As the fibre is hauled off from the package holder, it is guided down towards a metal roller. The fibre roving is originally wound transversal around a carboard tube with a constant angle and it is passed on a rotating roller as it unwinds to prevent fibre twist.

The guide roller is installed at least 500 mm away from the fibre bobbin to allow full transverse of the fibre tow around the roller and to prevent fibre twist.

The guiding surfaces of such processing equipment are usually treated so as to prevent the brittle fibres from sticking to them. This particular metal roller utilises a special Topocrom coating and was obtained from TEXMER GmbH & Co. KG (Germany), as shown in Figure 3.10. A Topocrom surface has a number of hemispherical structures with a shape of domes. The smoothness of the surface of these domes helps the filament to slide very easily, and also the air pockets trapped between these structures act as a cushion, enhancing the tendency of the fibre to glide over, therefore reducing the chances of fibre sticking on the surface. Topocrom coating is known to help with fewer fibre breakage, less formation of dust on fibre guiding parts, and to have a high abrasion, wear and corrosion resistance. The resistance to wear property is very beneficial as the glass fibres are very abrasive when they are in contact with other surfaces.

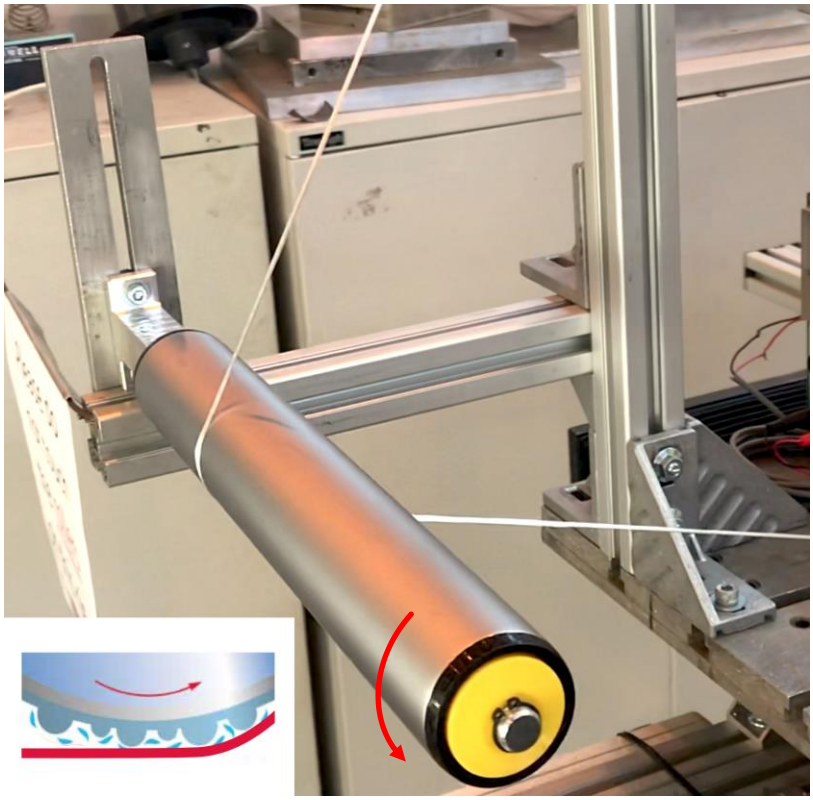

Figure 3.10 Topocrom coated guide roller.

After the Topocrom coated rollers, the fibre bundle enters the resin bath compartment. The main body of the resin bath is made of transparent acrylic. This gives the ability to observe the level of the resin in the bath. There are two fibre guiding equipment items installed on the resin bath. The first guiding part is ceramic eyelet. The fibre tow enters this ceramic eyelet just after gliding on the Topocrom roller. It is recommended that any change in fibre direct (guiding the fibre) is made using an eyelet with a large radius to reduce the possibility of breaking the filaments on a tight bend. An eyelet with a flange (entry) diameter of 22 mm and exit diameter of 10 mm was therefore implemented. As the fibre is hauling off from the package holder, the fibre glides over the metal roller, swinging horizontally from one end of the roller to another. The big radius on the flange side of the ceramic eyelet helps the fibre to swing easily without any fibre twists and at the same time, centring the fibre bundle for entering the resin bath as it exits the eyelet. The smoothness of the process is absolutely essential for processing brittle fibres such as S2-glass. Ceramic guides are quite popular for handling reinforcing fibres due to their inherent resistance to wear and abrasion. As previously mentioned, wear resistance is of crucial importance due to the abrasive properties of fibres, notably glass fibre. For composites and especially glass fibre, a diamond polished (DP) surface is recommended for ceramic guides, which will reduce the breakage of the fragile glass filaments. Therefore, all the ceramic compartments used for processing the fibre are DP finished. All ceramic guides were supplied by Ascotex Ltd. (UK).

A DP ceramic bearing roller is fitted inside the resin bath. This roller has a flat groove with a depth of 4 mm and width of 5 mm. The grooved guide roller helps centring the fibre further in the resin bath for the next stage of the process. The ceramic roller has a metal shielded bearing in order to prevent derbies and particularly polymer powder from entering the bearing. The choice of a rotating guide roller is due to a number of factors. Firstly, the rotation of the ceramic bearing inside the resin bath helps reduce the tension inside the fibre bundle and therefore resulting in fewer fibre breakage. The rotation of this bearing also helps the powder resin not to settle and also helps preventing resin agglomeration on the roller.

3.6.3.2 Fibre Spreader Assembly

While soaked in PAEK slurry, S2-glass exits the resin bath onto the fibre spreader system. A spreading mechanism was designed based on the direct contact method (mechanical method); i.e. use of spreading pins in which the fibre tow is passed through a series of rollers to obtain a flat array of separate fibres. The fibre spreader assembly is meant to provide control over the spread of fibre (prepreg thickness) and help impregnate the fibres with PAEK resin. The idea here is to pass the fibre tow above and below a series of ceramic rollers in order to push the PAEK particles inside the fibre bundle. The forces exerted on the fibre bundle by the rollers help the PAEK slurry to diffuse fibre filaments and therefore, impregnate the fibre bundle. These forces also help individual glass filaments to slide on each other, spreading the fibre bundle and reducing the thickness of the towpreg. The tow is also spread further with the PAEK particles acting as spacers between filaments when they penetrate the fibre bundle.

Kawabe and Matsuo [7] concluded that fibre tow is spread better and easier when the coefficient of friction between the rollers and fibre tow is small. As shown in Figure 3.11, they established a relationship between the forces exerted from fibre filaments on each other in the lateral direction (F_{x+}) and the friction forces on the filaments from the roller in the lateral direction (F_{x-}) in a finite fibre model. They divided the fibre layers into numerous steps (n) and considered the external forces acting on a triangular section (fibre A, B and E), including the force from top layers on fibre E (F_{EY}), force from the roller on fibre A (F_{AY}) and friction force on fibre A (F_{ART}) in equilibrium. When F_{x+} is greater than F_{x-}, the maximum friction force becomes less than the fibre opening force, and this subsequently results in lateral spreading of the fibre bundle on the roller.

Experiments suggested that the roller diameter, number of rollers, distance between the rollers, and the contact angle between the fibre and the rollers can also affect the degree of the fibre spread. In summary, roller diameters of 12, 18 and 24 mm were tested with no significant difference in the spread width. Five rollers showed better spread results than two, however resulted in tension increase in the fibre bundle.

Higher contact angles significantly increased the spreading degree and fixed rollers demonstrated enhanced fibre spread compared to rotating rollers.

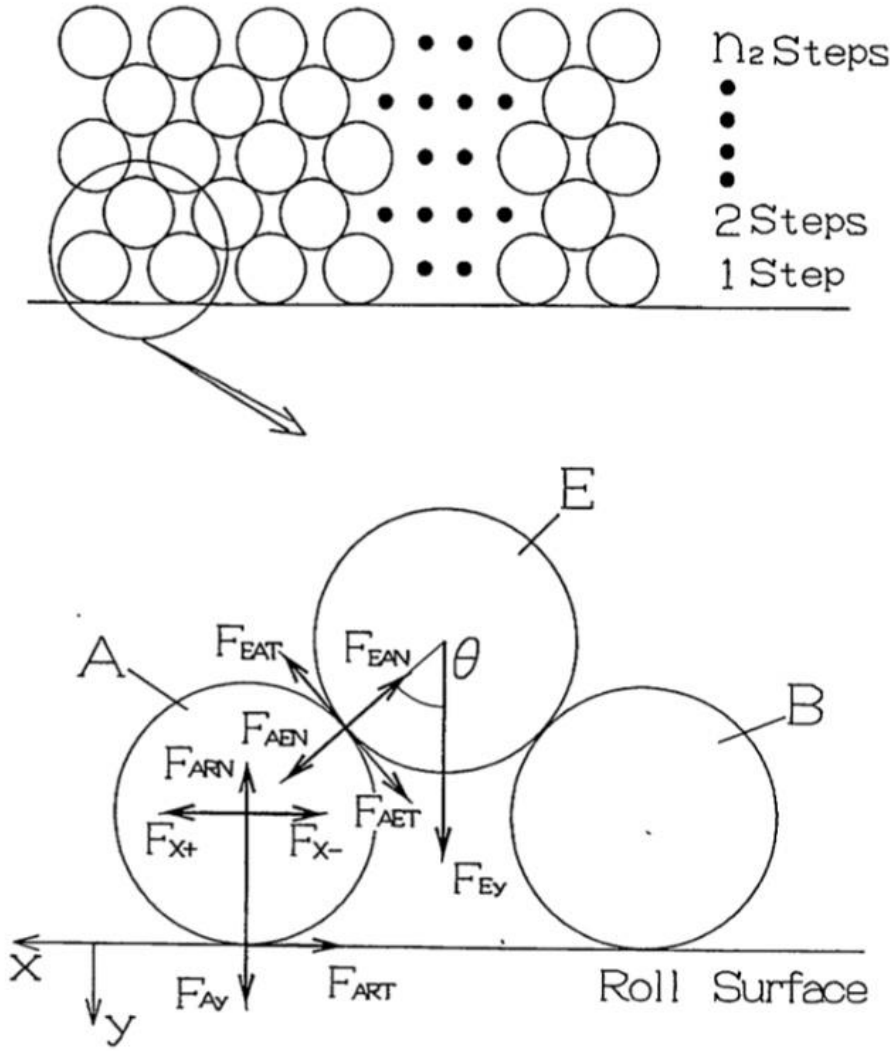

Figure 3.11 Mechanical process involved in lateral spread of fibre tow on a cylindrical roller [7].

As suggested by Irfan et al. [8], one method of spreading fibre tow is passing the fibre over spreading rollers. The force exerted on the fibre tow from the rollers will cause the fibre to spread. In their experiment, they manually applied a reciprocating motion on the fibre tow, held between a set of rollers. They referred each reciprocating motion of the fibre tow as one tension-cycle, as shown in Figure 3.12. They concluded that six such tension-cycles were necessary to obtain equilibrium in the degree of fibre

spreading. They also stated that releasing the tension in the bundle and re-apply the tension-cycle can enhance the degree of lateral spreading.

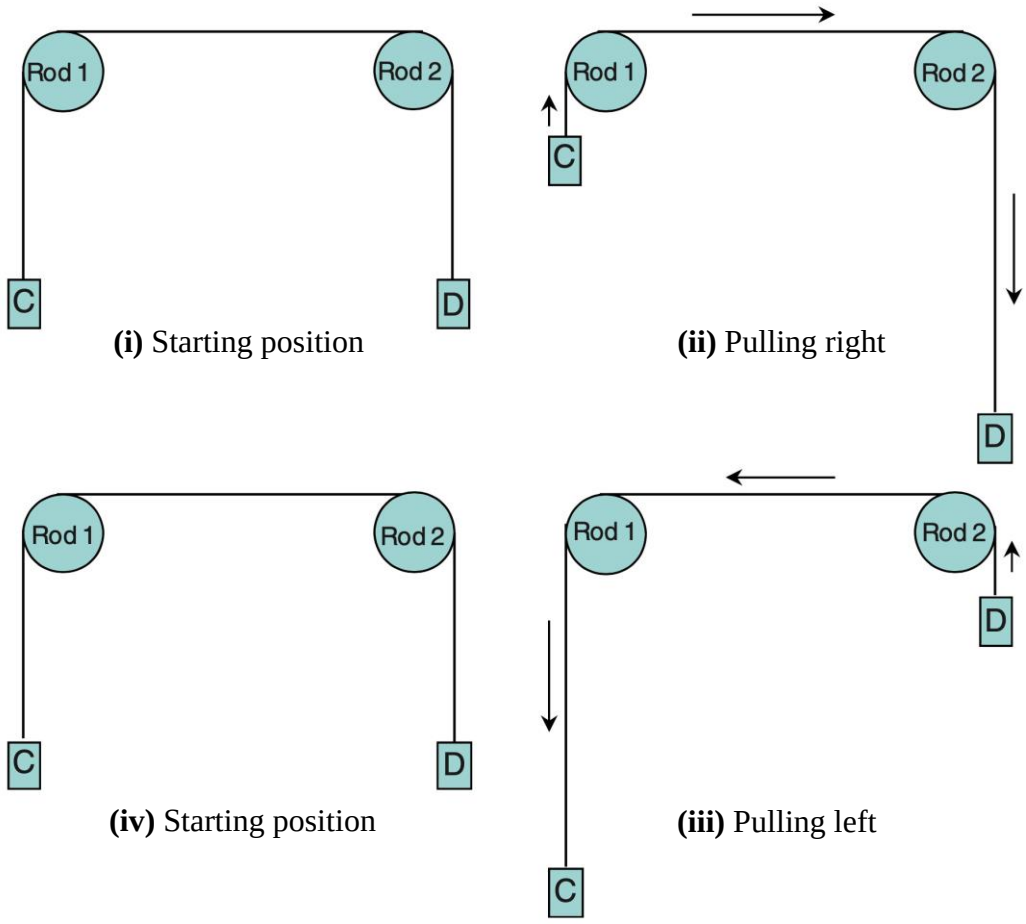

Figure 3.12 Schematic illustration of a single tension-cycle involving the motion of the fibre bundle over two rods [8].

The design of the novel fibre spreader device is based on some of the findings in aforementioned studies. Schematic design and function of the fibre spreader is shown in Figure 3.13. The fibre spreader employs a reciprocating mechanism to create a vibration in a set of rollers. This device employs the manual technique shown in Figure 3.12 for creating a tension-cycle and enhances it by automating the movement. The spreading device not only has the reciprocating motion, but also by drawing the fibre tow from bobbin faster than the winding unit, it can constantly keep the fibre tow passing through the spreading unit in a low tension and then tension-free state. This results in a higher fibre spread, as suggested by above mentioned studies.

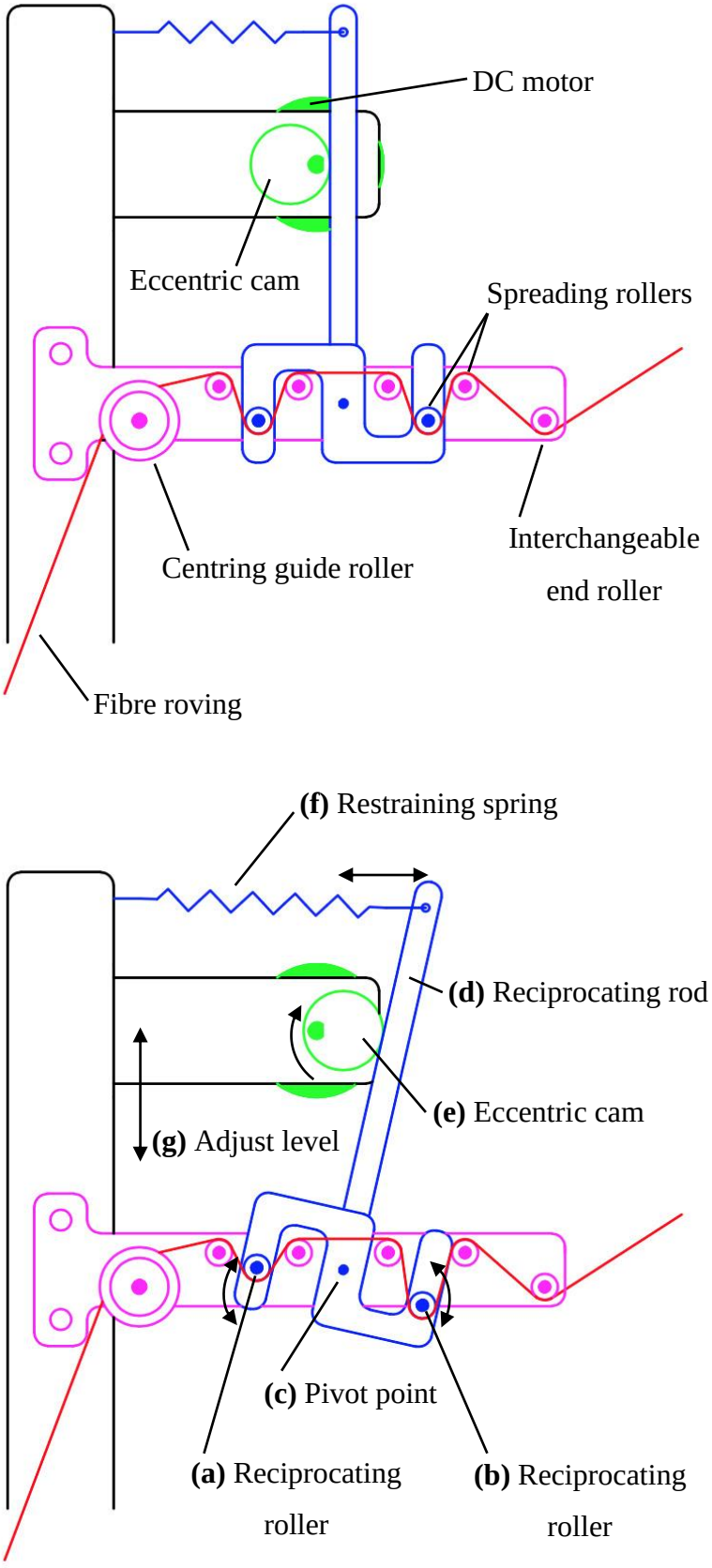

Figure 3.13 Schematics of the fibre spreader assembly consisting of three different parts.

The fibre spreader consists of three main parts. The first two parts (pink and blue) are comprised of series of DP rollers. The pink part is static and is bolted to an aluminium profile, which is installed on the linear actuator part as discussed before. The blue part is dynamic and is connected to the pink part via a shafted bearing. The shaft is extended to the other end of the bearing and is connected to a long rod. The rod is in contact to the third part of the fibre spreader (green), which is an eccentric cam connected to a DC motor.

The fibre spreader includes several DP ceramic rollers. The pink static part houses 6 rollers in total. The first one is a rotating guide roller (bearing) same as the one implemented inside the resin bath. This is a flat groove with a depth of 4 mm and width of 5 mm. This ceramic guiding roller helps centring the impregnated fibre tow for the spreading stage. The static part has four more 10 mm diameter DP finish ceramic rollers further down the line for impregnation and fibre spread. At the end of the process there is an interchangeable roller that can be adjusted according to the spreading needs. Three options were envisioned: 5 and 10 mm in width rollers, and an open casual roller. These interchangeable guide options can be seen in Figure 3.14.

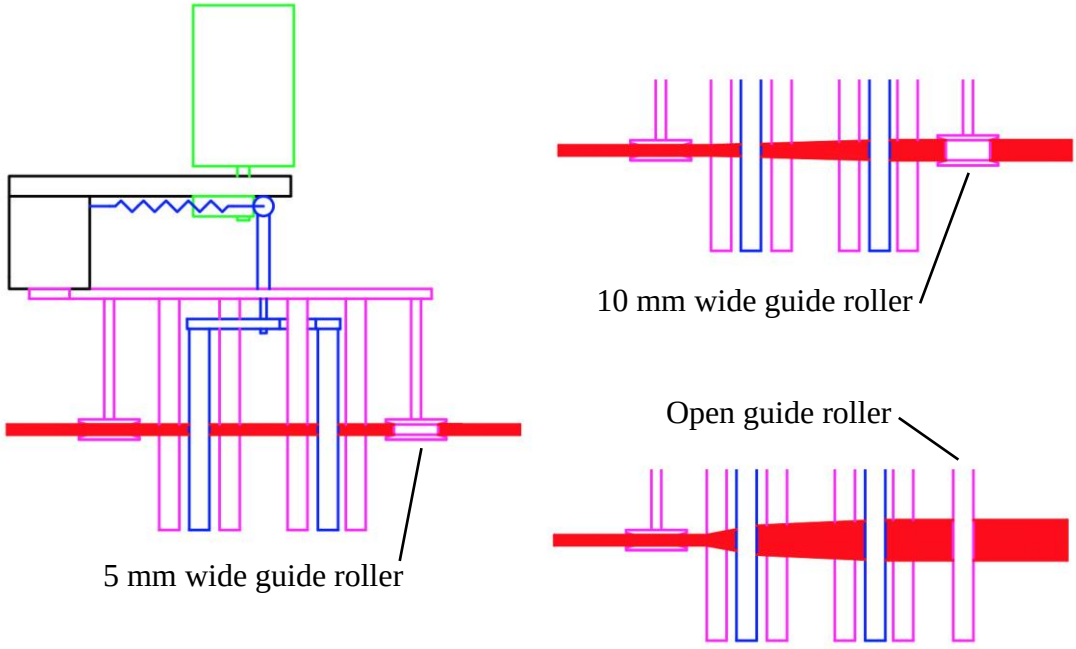

Figure 3.14 Top view schematics of the fibre spreader assembly showcasing different options for the interchangeable end roller.

The blue dynamic part also accommodates two 10 mm diameter DP ceramic rollers that are responsible for creating the spreading tension-cycle mechanism. All 10 mm diameter rollers are adjustable to be fixed or rotating.

As illustrated in Figure 3.13, the process begins when the impregnated tow glides over the centring roller. As mentioned before, all the rollers, except (a) and (b), are fixed on the static part (pink) of the fibre spreader assembly. Rollers (a) and (b) however are mounted on a separate dynamic plate (blue). The sequence begins when fibre tow is passed over the first roller and goes below roller (a), coming up and over two consecutive rollers, passes below roller (b) and goes over and under two more rollers. The spreading process begins when the eccentric cam (e) connected to a DC motor starts rotating. By the means of this rotation, rod (d) starts a reciprocating motion as shown. Rod (d) is connected to the dynamic plate, which accommodates rollers (a) and (b) and because of this, rollers (a) and (b) start their own reciprocating motion around the pivot point (c). The rod (d) and therefore the dynamic plate is restrained via spring (f). This helps rod (d) and eccentric cam (e) to always stay in contact and the process continues after each motion frequency. The reciprocating motion of rollers (a) and (b) will generate the tension-cycle needed and causes the fibre tow to spread laterally, specifically between rollers (a) and (b). Each motion frequency therefore resembles one tension-cycle that was pointed out in the above aforementioned studies.

Two factors in the fibre spreader assembly can be controlled: the frequency and the amplitude of the motion. The frequency of the tension-cycle can be adjusted via controlling the speed of the DC motor. The motion amplitude of rollers (a) and (b) can be changed with using eccentric cams with different off-sets or adjusting the level (g) of the eccentric cam. For instance, lower levels (g) will result in higher amplitudes of rollers (a) and (b).

Besides spreading the fibre tow and adjusting the thickness of the prepreg, the fibre spreader assembly is also responsible for an effective PAEK powder impregnation. It is also evident that the fibre tow will spread further when polymer particles are diffused into the fibre tow and act as spacers. It is therefore believed the amount of fibre spread of dry bundle and wet bundle would be different.

3.6.3.3 Winding Drum

Another major part of the prepreg manufacturing rig is the winding drum. As showed in Figure 3.15, an aluminium tube is used as the main body of the winding drum. The aluminium drum has an outer diameter of 200 mm, wall thickness of 3 mm and a length of 460 mm. The drum length is chosen just under the stoke of the linear actuator to ensure full transverse movement. The drum is capped by two sets of holders at both ends. Both ends of the drum are mounted on a set of bearings via a 12 mm diameter stainless steel shaft.

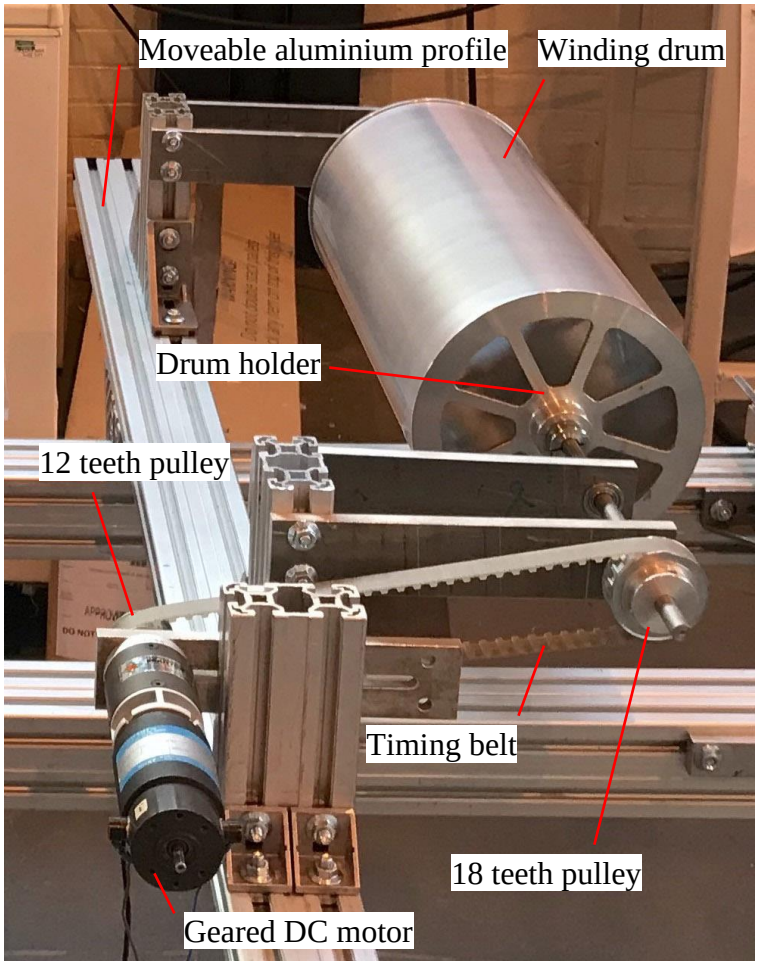

Figure 3.15 The winding drum rotating via the belt and pulley assembly.

One side of the stainless steel shaft is connected to a precision timing belt pulley with 18 teeth. This pulley is part of the mechanism that rotates the winding drum. This pulley is connected to another pulley with 12 teeth via a timing belt. This set of pulleys will create a speed ration of 2:3. The second pulley is coupled to a geared DC motor, mounted on the aluminium profile that also holds the drum. This aluminium profile is

adjustable and can slide horizontally along the length of the prepreg rig. The winding initiates when the DC motor starts revolution and transfers the power to the pulley system. Size and the number of teeth on both pulleys can be changed and adjusted to fulfil the requirements of the winding speed.

Since the impregnated fibre is intended to be wound directly on the surface of the winding drum and subsequently melt, the surface of the drum is treated. The drum is firstly sanded down to 500 and 1000 grit to obtain an even surface. It is then polished to a finer surface of 2500 and 5000 grit for a smoother surface. The polymer is heated and melted on the surface of the drum to form a consolidated prepreg. Therefore, the surface of the drum is further treated. To avoid PAEK polymer stick on the winding drum after heat melting, the surface of the drum is treated with special release agent. The drum is initially treated with Chemlease 15 mould sealer in order to seal the surface of the drum to reduce the porosity and provide a beneficial base coat for all types of release agents. After sealing the surface of the drum from porosities, the drum is coated with Zyvax TakeOff release agent. This is a semi-permanent, water-based release agent utilised in this project that can be used for all major resin systems in composite industry. Zyvax TakeOff provides the minimal transfer of the release agent onto the composite part and is capable of providing multiple releases with one application of the product. It can also tolerate high processing temperatures without release agent cross-linking. It has the ability to be applied to hot mould surfaces, so as to provide quicker processing times. The combination of a smooth surface finish and use of seal/release agent ensures smooth release of the prepreg material after heat melting of the PAEK polymer. Chemlease 15 sealer and Zyvax TakeOff release agent was supplied from Chem-Trend L.P. (USA).

3.6.3.4 Controllers and Heater

The transverse speed of the linear actuator and the winding speed of the drum can be adjusted using the speed controller unit showed in Figure 3.16. Both speeds are assigned in percentage with 0 % being stop/off and 100 % being full speed of the DC motors mounted on the linear actuator (Traverse) and the winding drum (Drum). These percentages are interpreted in mm/s for the transverse speed and in revolutions per minute (rpm) for winding speed as per Table 3.8.

Table 3.8 Interpretation of speed settings on the controller to conventional measurement units.

Controller setting	Transverse speed (mm/s)	Drum speed (rpm)
0 %	0.00	0.0
10 %	0.07	0.0
20 %	0.29	0.9
30 %	0.56	2.6
40 %	0.79	4.6
50 %	1.03	6.7
60 %	1.28	9.0
70 %	1.49	11.7
80 %	1.75	14.0
90 %	1.96	16.5
100 %	2.13	19.0

Figure 3.16 Controller for adjusting the speeds of the linear actuator (Traverse) and the winding drum (Drum).

The transverse speed vs the winding speed should be regulated to accommodate slight fibre-overlap when the winding process begins. This overlap is crucial due to the fact that there are minor changes in the width of fibre tow when reaching the winding drum

for processing. Small overlap proves beneficial by not allowing gaps between fibre tows when the winding process initiates. The winding speed shall be selected in a way that the resin slurry does not start to run freely on the winding drum. The spreading rollers would squeeze the excess resin off the fibre bundle. However, if very high winding speed is selected, excess slurry cannot find enough time to drip off the rollers. It is therefore best to set the winding speed first and then adjust the linear motion in conjunction to that.

The frequency and amplitude of the fibre spreader motion can be adjusted using the speed controller unit and the eccentric cams showed in Figure 3.17(a) and (b), respectively.

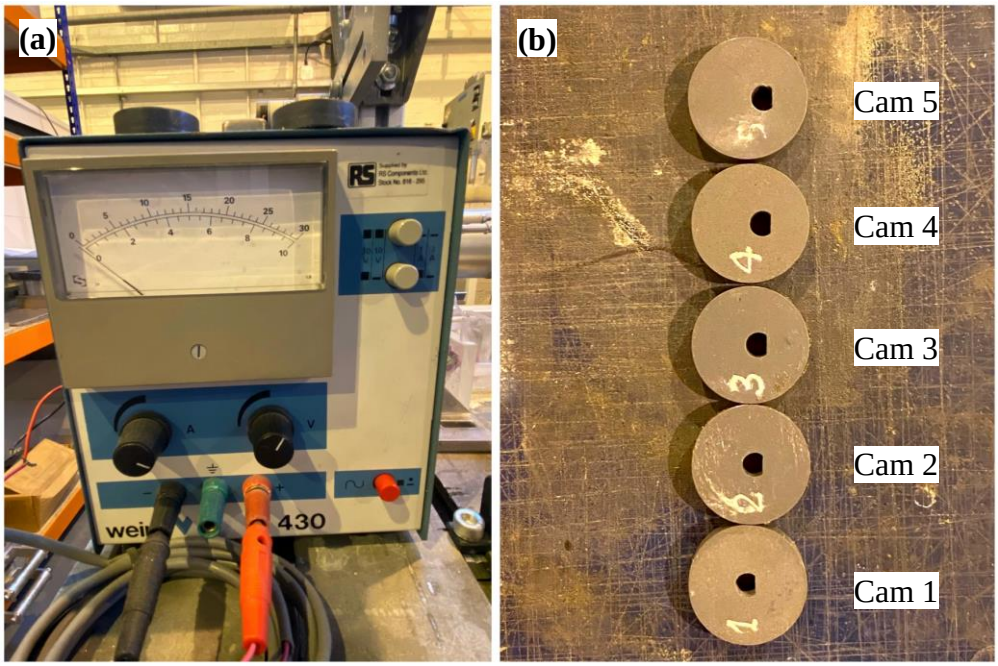

Figure 3.17 Fibre spreader controls: (a) the voltage controller adjusting the frequency and (b) off-set cams responsible for adjusting the amplitude.

The rotational speed (frequency) of the cam can be controlled by adjusting the voltage of the DC motor embedded on the fibre spreader assembly. For controlling the amplitude of the vibration, five plastic cams with 30 mm diameter were machined. The pivot point was selected 1 to 5 mm off-set from the central point to produce the different eccentric effect of each cam.

Table 3.9 lists the frequency and amplitude ranges available for testing. The amplitude of the movement is measured from the corresponding movement of the rod part of the fibre spreader that is in contact with the cam.

Table 3.9 The frequency and amplitude setting of the fibre spreader device.

Frequency		**Amplitude**	
Voltage setting	***Value (Hz)***	***Cam number***	***Value (mm)***
5	1.0	1	2
10	2.3	2	4
15	3.7	3	6
20	5.0	4	8
25	6.3	5	10
30	7.7		

The last major part of the prepreg line is the heating unit, as shown in Figure 3.18. After the winding is complete, the transverse motor is turned off and the impregnated fibre tow is cut off from the drum for the final stage of the process, heat melting. The drum is moved towards the end of the prepreg line, where the heating unit is located. The heating unit consists of two paired ceramic heaters. While still rotating, the winding drum is positioned above the ceramic heaters set to 400 °C where the wet prepreg is heated for at least 1 hour until a majority of water/L2O residues leave the wet prepreg, so as to obtain a dry prepreg. After which, the drum is dismantled from the rig and is placed inside an oven for final heat melting and permanent adhesion of PAEK on S2-glass fibres. The prepreg is heated up to 310 °C in the oven, slightly above the T_m of PAEK, at a ramp rate of 10 °C/min. If any, the remaining residues will leave the prepreg while the drum is being heated inside the oven.

After consolidation, the winding drum is cooled down and removed from the oven. The prepreg sheet is then cut from the drum. This is done by cutting the prepreg with a sharp blade along a small groove that is machined across the whole length of the drum.

Figure 3.18 The heating unit comprising: (a) two ceramic heaters and (b) temperature controller.

3.7 Summary

In this chapter, the concept of wet powder impregnation was discussed and practicality of an effective method of thermoplastic resin impregnation and subsequently thermoplastic prepreg production was investigated. Wet powder technology was realised as being capable to fulfil three main rig development requirements including suitability, cost and scale.

All the raw materials used during the project was described and their technical data sheets were listed. The materials included different reinforcing fibres and polymers, liquid carrier and nanomaterials. Also, some preliminary tests were carried out to understand and evaluate the effectiveness of the liquid carrier for prepreg production.

Two novel in-house rigs were designed and developed: a woven rig for manufacturing continuous woven fabric prepreg, and a drum winding rig capable of manufacturing UD prepregs. The novel drum winding rig was chosen as the main focus of this project,

due to the fact that UD prepreg is more appealing in order to benefit from ultimate mechanical performance the composite, and freedom of placing composite reinforcement in the desired orientation.

The design of the drum winding prepreg rig was based on the concept of filament winding, i.e. impregnated fibres being wound on a drum to produce UD prepreg sheets. Different parts involved in the design and manufacture of the drum winding rig were produced and the function of each component was discussed. Here, an innovative fibre spreader assembly was also designed and manufactured, in order to control the thickness of the produced prepregs.

Common industrial practice of manufacturing UD prepreg would require multiple fibre bobbins, creels, guides, rollers, etc. and thus, requiring a substantial investment. The proposed thermoplastic prepreg manufacturing process based on drum winding was therefore found ideal for research and development purposes, due to factors such as fast processing times and low running costs.

3.8 References

[1] AGY, 2004, "Advanced Materials: Solutions for demanding applications," https://www.agy.com/wp-content /uploads /2014/03 /Advanced_Materials_Brochure-Technical.pdf (Last accessed 30.04.21).

[2] AGY, 2004, "High Strength Solutions To Your Toughest Reinforcement Challenges," https://www.agy.com /wp-content /uploads/2014/03/S2_Glass_Fibers-Technical.pdf (Last accessed 30.04.21).

[3] Mustarelli, P., Quartarone, E., and Magistris, A., 2009, "Fuel Cells – Proton-Exchange Membrane Fuel Cells | Membranes: Polybenzimidazole," Encyclopedia of Electrochemical Power Sources, J. Garche, ed., Elsevier, Amsterdam, pp. 734-740.

[4] Green, S., 2019, "VICTREX AE 250 – A Novel polyaryletherketone polymer suited to automated tape placement and out of autoclave processing," https://www.victrex.com/~/media /whitepapers/victrex-ae-250---technical-paper-camx-2018.pdf (Last accessed 30.04.21).

[5] Minsch, N., Herrmann, F. H., Gereke, T., Nocke, A., and Cherif, C., 2017, "Analysis of Filament Winding Processes and Potential Equipment Technologies," Procedia CIRP, 66, pp. 125-130.

[6] Ma, Q., Rejab, R., Mat Sahat, I., Manoj Kumar, N., and Merzuki, M., 2019, "Robotic filament winding technique (RFWT) in industrial application: A review of state of the art and future perspectives," 5, pp. 1668-1676.

[7] Kazumasa, K., and Tatsuki, M., 1998, "Technology for Spreading Tow and Its Application to Composite Materials Part 2 : Spreading Tow by Roll Method," Sen'i Kikai Gakkaishi (Journal of the Textile Machinery Society of Japan), 51(2), p. 65.

[8] Irfan, M. S., Machavaram, V. R., Mahendran, R. S., Shotton-Gale, N., Wait, C. F., Paget, M. A., Hudson, M., and Fernando, G. F., 2012, "Lateral spreading of a fiber bundle via mechanical means," Journal of Composite Materials, 46(3), pp. 311-330.

CHAPTER IV: EXPERIMENTAL PROCEDURE

4.1 Introduction

This chapter presents the procedure on how the experimental programmes were carried out. Several preliminary tests are performed in order to evaluate the possible potentials of the prepreg rig and to determine the optimum settings. Upon establishing a consistent production method, experimental work is carried out to produce S2-glass/PAEK (polyarylether ketone) prepreg product. Three sets of different prepreg resin contents are investigated and the resulting prepregs are physically evaluated. Prepreg materials are subsequently laminated with consideration of temperature, time duration and pressure. Different laminate samples are produced, and specimens are machined and cut in order to evaluate physical properties such as fibre volume and void content. Mechanical assessments such as tensile, flexural and interlaminar shear tests are undertaken to measure the mechanical properties of the produced laminates. After identifying the optimum prepreg and laminating settings, multiscale (hierarchical) fibre-reinforced nanocomposites are manufactured and are compared to their laminate counterparts with no added nanomaterial.

4.2 Preliminary Experiments for Method Evaluation and Optimisation

The proposed thermoplastic prepreg production method and rig are novel, and this therefore urges the need for numerous trials and optimisations. For an effective investigation of the prepreg rig, different variables that affect the properties of the prepreg are identified as:

- PAEK–L2O ratio
- Fibre tension
- Winding speed
- Fibre spreader frequency and amplitude
- Fixed or rotating roller
- Interchangeable end roller

These variables consequently affect the properties of the final prepreg materials. Initial tests were designed to investigate resin systems with different PAEK content and the effectiveness of the liquid carrier. Different tests are also carried out to identify the effects of other variables on the amount of powder pick-up by the fibre tow and the

degree of fibre spread. These tests are also crucial to evaluate the consistency of the production method and the resulting prepreg materials. The tests are divided into two sections: PAEK–L2O and rig setting tests.

4.2.1 PAEK–L2O Slurry Preparation and Tests

For preparing the resin slurry, PAEK powder was weighed and added to the weighed L2O for mixture. Ratios prepared were 10, 20, 30 and 40 % of PAEK to 90, 80, 70 and 60 % of L2O by weight, respectively. For instance, 20 grams of PAEK powder was added to 180 grams of L2O to produce 10 - 90 % ratio slurry. In the case of adding nano additives to the slurry for production of hierarchical prepregs, nanomaterial was added 0.5, 1.0, 2.5 and 5.0 part per hundred of PAEK by weight. For instance, 1 gram of graphene was added to 20 grams of PAEK and 180 grams of L2O in order to produce a 5.0 wt% graphene slurry of 10 - 90 % PAEK–L2O ratio.

Constituents were placed in a closed mixing pot and mixed using an overhead lab stirrer for 30 minutes on a low speed of 500 rpm followed by 30 minutes of a higher speed of 1000 rpm. Generally, slow stirring speeds are chosen to avoid creation of heavy foams and introduction of air bubbles inside the slurry. The slurry is then transferred into a degassing chamber where it is degassed for 60 minutes under a vacuum pressure of 0.8 Pa. The slurry is slowly stirred using a magnetic stirrer while being degassed to avoid possible particle sedimentation.

The PAEK slurries prepared were tested for particle size distribution (PSD). Laser diffraction technique, via a sequential combination of measurements using blue (432 nm) and red (633 nm) laser light sources on a Malvern Mastersizer 3000, was implemented for analysing particle sizes in different suspensions. It should be noted that as the particle size decreases, the scattering angle increases, and the scattered light becomes more diffuse. In order to achieve a good lighting background for fine particles, low obscuration rate was used to avoid multiple scattering. Usually, 5 to 10 % obscuration is recommended for fine particle measurements.

Here, 10 wt% slurry samples were further diluted by adding 10 part by weight de-ionised water, as the original slurries are too dense on their own for PSD

measurements. Here, Hydro SV liquid dispersion unit was utilised, which comprises a sample cuvette that holds the sample and dispersant liquid together. The cuvette was loaded with approximately 6 mL of dispersing liquid (de-ionised water or L2O) and a magnetic stirrer bar was placed into the cuvette. The cuvette is then inserted into the cuvette holder within the Hydro SV cell. The magnetic stirrer was set to 1200 rpm.

The refractive and absorption index of PAEK was set to 1.58 and 0.1, respectively. The refractive indices of de-ionised water and L2O were measured using an Anton Paar refractometer and the values were recorded as 1.33 and 1.34, respectively. Once the setup is ready, aqueous samples are fed directly into the dispersion unit until an obscuration rate of approximately 10 % is achieved. The dispersion is then stirred inside the cuvette for 30 minutes before starting the measurements. Particle size traces were recorded against the volume density of the size population. Figure 4.1 illustrates some of the equipment involved in PSD measurement.

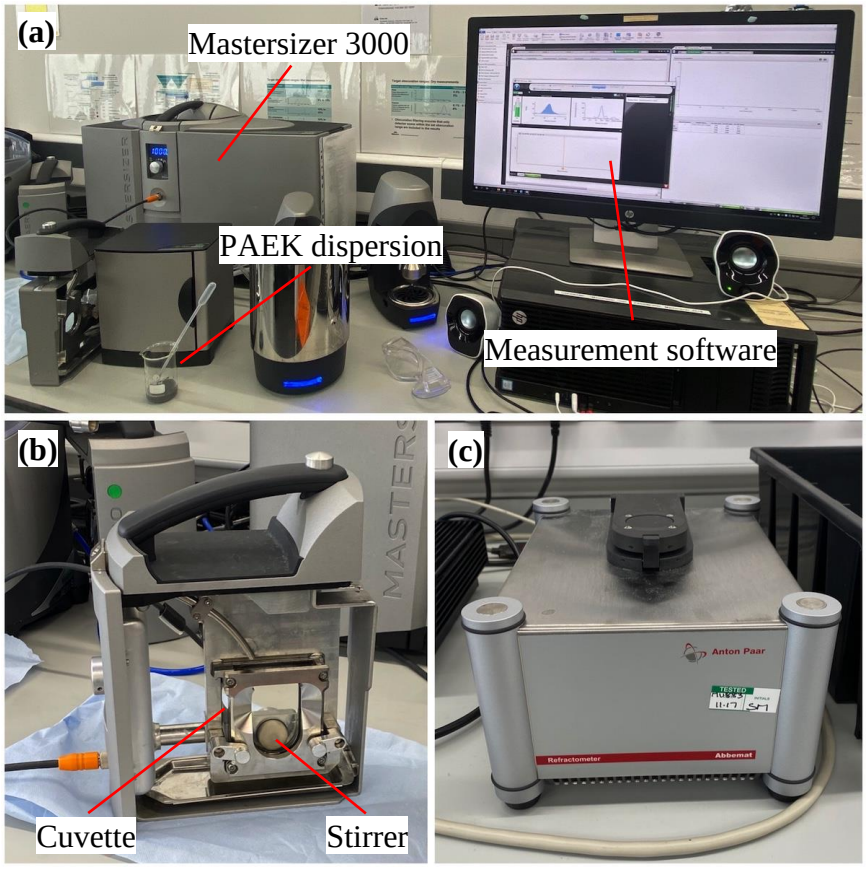

Figure 4.1 Particle size distribution measurements: (a) Mastersizer 3000 setup, (b) Hydro SV dispersion unit and (c) Anton Paar refractometer.

For a better understanding of colloidal stability and sedimentation properties of the prepared slurries, the turbidity of selected samples was measured using a Formulaction Turbiscan AGS, as seen in Figure 4.2. Turbiscan AGS uses a pulsed near infrared light source (wavelength of 880 nm) for measurements. The transmission (T) detector (at 180°) receives the light, which goes through the sample, while the backscattering (BS) detector (at 45°) receives the light scattered backward by the sample.

Here, 20 mL of the prepared and readily agitated (magnetic stirrer for 30 minutes) sample slurries were dispensed into screw-top glass vials and were mounted into the electrically controlled temperature blocks. The temperature of all the blocks were set to 25 °C (room temperature), to represent the ambient temperature of the prepreg rig working area. Both transmitted and backscattered light were measured over the whole height of the vials every 5 minutes for a duration of 120 minutes (25 cycles). This duration shall give an extended overview of the turbidity behaviour of PAEK slurries when put inside the resin bath, and undergoing the prepreg production process.

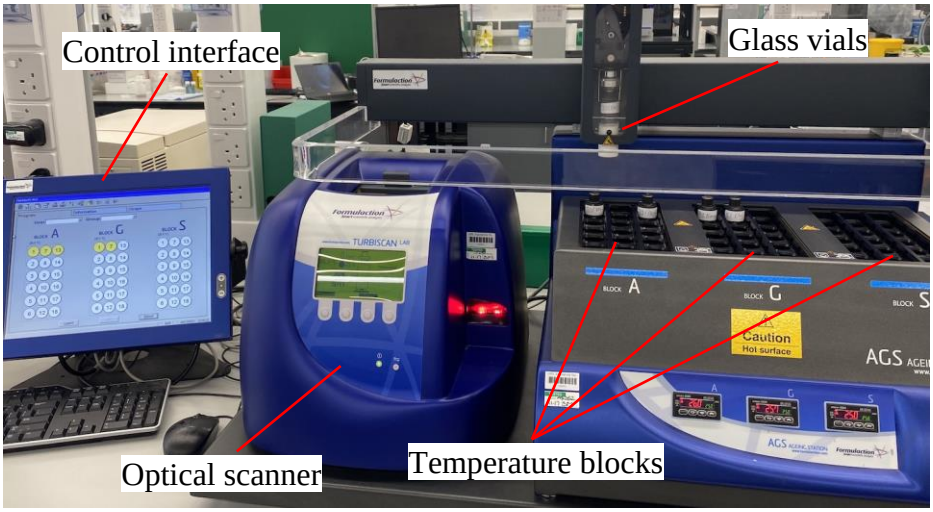

Figure 4.2 Turbiscan AGS unit comprised of different parts for measuring turbidity.

4.2.2 Prepreg Rig Settings and Tests

Apart from the PAEK–L2O ratio, other factors contributing to changes in prepreg properties are various settings that are adjustable on the prepreg rig. It is reported that impregnation and fibre spreading depends on several factors and variables regardless of the process and method used [1-4]. As there are so many parameter variables, it is difficult to assess and optimise the parameters with traditional one-factor-at-a-time

method since one cannot identify interactions between the parameters. The goal here is to identify a range in which each setting can be adjusted to and consequently optimise each for the best synchronisation. Ultimately, it is preferred to only deal with one variable to customise different prepregs with different fibre volume content. Therefore, the PAEK–L2O ratio is chosen as the best option for controlling the fibre volume and it is proposed to keep other identified variables affecting the prepreg constant.

PAEK–L2O ratio was discussed as one of the parameters and the interchangeable end roller is identified as a tool only to control the amount of fibre spread. This therefore leaves us with four more variables: fibre tension and winding speed (winding tests) and, fibre spreader frequency, amplitude and also fixed or rotating rollers (fibre spread tests). Here, 20 wt% PAEK slurry was chosen in following tests as a moderate value and benchmark.

4.2.2.1 Winding Tests

While the linear actuator plate is placed far right or left of the actuation stroke, S2-glass tow is pulled through all the guide parts of the prepreg rig and is affixed on the far right or left side of the winding drum using an adhesive tape. The PAEK slurry prepared is then added to the resin bath. In the winding tests, two variables are being investigated: fibre tension and winding speed. The fibre spreader is turned off and the spreading rollers are set to rotating. Open guide roller is chosen for the interchangeable end roller.

The process starts with the revolution of the drum at a desired speed for 3 rounds without initiating the linear actuator, positioning 3 layers of fibre tow on top of each other. This ensures the fibre tow is wound tight on the drum and prevents tow slippage. After 3 revolutions, the transverse run (linear actuator) is initiated to process the winding. The transverse speed is adjusted in a fashion to allow slight fibre-overlap when the winding process begins.

Winding speed is varied from 0.9 to 19.0 rpm and the initial tensioning force is adjusted on the package holder via the pulley and band mechanism, varying from

setting 1 to 5 (0.8 to 4.0 N), with 1 being the lowest tensioning force and 5 being the highest. This test is to visually observe the resin bath, impregnated tow, fibre waviness, fibre breakage etc. For instance, the winding speed shall be selected in a way that the resin slurry does not start to run freely on the winding drum. The spreading rollers would squeeze the excess resin off the fibre bundle, however, if very high winding speeds are selected, excess slurry cannot find enough time to drip off the rollers. It is therefore best to set the winding speed first and then adjust the linear motion in conjunction to that for production of the prepreg.

4.2.2.2 Fibre Spread Tests

In the fibre spread tests, the effects of fibre spreader frequency, amplitude and also fixed or rotating rollers on the degree of fibre spread are investigated. Fibre spread tests are carried out after the rig is optimised for the optimum fibre tension and winding speed (winding tests), suitable for manufacture of the final prepreg material.

Similar to the winding tests, the linear actuator plate is positioned at the starting point to the right or left of the stroke. The glass fibre tow is guided through the rig and is affixed on the winding drum via an adhesive tape. The PAEK slurry prepared is then added to the resin bath. The frequency and amplitude of the fibre spreader are set to a desired level. A frequency range of 1.0 to 7.7 Hz and amplitude of 2 to 10 mm were studied. The spreading rollers are set to rotating and an open guide roller is chosen for the interchangeable end roller. Once the best setting for frequency and amplitude is realised, the effects of fixed rollers on the fibre spread are evaluated and compared to the time when rotating rollers are implemented.

To ensure the fibre tow stays firm on the drum without slippage, the drum starts the revolution for 3 rounds without starting the linear actuator to lay 3 layers of fibre on top of each other. The speed of the winding drum is set to the prime established speed identified in the winding test. Fibre tension is kept constant and is set in accordance with the prime setting found in winding tests. The transverse run is then initiated to begin the winding process. The transverse speed is adjusted in a way to accommodate significant (20 to 30 mm) gap between the wound tows on the winding drum. This

allows enough space between each revolution for observation and setting change purposes.

The impregnated fibre tow is wound 20 rounds on the drum with significant gaps between each revolution. After the winding process is completed, the tow is wound for another 3 rounds while the linear actuator is turned off, positioning another 3 layers of fibre tow on top of each other. This ensures the fibre tow is wound tight on the far end side of the drum and prevents tow slippage. The impregnated fibre tow is then cut off from the drum.

Finally, the drum is positioned above the ceramic heaters in order to evaporate the water residues. At this stage, the drum is still rotating, ensuring that the heat is distributed evenly on the impregnated fibre tow. The heater is set to 400 °C and the drum is heated for 1 hour. This setting is found to be ideal for extracting water residues from the wet composite. Once the product is dry and the drum is stopped, the fibre width (degree of fibre spread) is measured using a vernier calliper for all 20 rounds and the mean value is obtained.

4.2.2.3 Resin Pick-up Test

The resin pick-up test is designed to investigate if the amount of resin picked up by the fibre tow remains constant throughout the winding. The test is crucial for the final prepreg production in order to ensure the prepreg material produced has consistent physical properties. This test is carried out using the optimum rig settings found in Section 4.2.2.1 and 4.2.2.2, i.e. the winding tests and fibre spread tests.

In the resin pick-up test, the only variable affecting the amount of PAEK deposited on S2-glass fibres is set to be the PAEK–L2O ratio. To investigate this, 4 different PAEK–L2O ratios are prepared and investigated, i.e. 10, 20, 30 and 40 wt% PAEK slurry.

The linear actuator plate is set to the starting point of the stroke and the S2-glass tow is affixed on the drum after going through guiding tools. The PAEK slurry prepared is then added to the resin bath. The fibre spreader is turned on and the frequency and

amplitude are set to 5.0 Hz and 6 mm, respectively. These values are identified as being optimum in the fibre spread tests. The spreading rollers are set to rotating and 5 mm guide roller is chosen for the interchangeable end roller.

Three layers of fibre is wound on top of each other to prevent slippage after the revolution of the drum at 7.8 rpm, without starting the linear actuation. Initial fibre tensioning force is kept constant and is set to option 2 (1.3 N), the prime value identified in the winding tests. The transverse run is then initiated to begin the winding process. The transverse speed is adjusted in a way to accommodate significant (20 to 30 mm) gap between the wound tows on the winding drum. About 10 meters of the impregnated fibre tow is wound around the drum, which requires approximately 16 revolutions of the drum. Example of this process is illustrated in Figure 4.3.

Figure 4.3 Winding impregnated fibre tow on the drum for the resin pick-up test.

After the winding process is completed, the tow is wound for another 3 rounds while the linear actuator is turned off, positioning another 3 layers of fibre tow on top of each other. This ensures the fibre tow is wound tight on the far end side of the drum

and prevents tow slippage. The fibre tow is then cut off from the drum after completion of the winding process.

The drum is then positioned above the ceramic heaters in order to evaporate the water residues. Similar to the fibre spread tests, the drum continues to rotate while being heated so as to ensure even distribution of heat on surface of the drum. The heater is set to 400 °C and the wet composite is heated for 1 hour in order to extract water residues from the wet towpreg. The drum rotation is stopped when the fibre tow is dried. After which, the fibre tow is cut from the drum by initially removing the final 3 layers on top of each other. The wound fibre tow sample is then cut into 1-meter-long specimens for a total of 10 specimens.

As seen in Figure 4.4, cut specimens are then positioned into individual pots and placed inside an oven heated at 150 °C for a further 1 hour. Desiccant silica gel is also placed inside the oven as a drying agent to help absorbing any remaining moisture in specimens. The sample fibre tows are then weighed immediately after they are removed from the oven to avoid moisture absorption. The weight of all 10 specimens is recorded and compared. The investigation here is to primarily identify whether the resin-pick up by the fibre tow is consistent throughout the winding process or not.

Figure 4.4 Drying process of impregnated fibre tow specimens for resin pick-up test.

4.3 Unidirectional S2-Glass/PAEK Prepreg

The preliminary experiments indicate that the proposed manufacturing method could be used to produce UD thermoplastic prepreg. Once the winding tests and fibre spread tests are completed, the optimised setting for each variable that affects the properties of the prepreg is obtained. As mentioned before, it is preferred to only deal with one variable to customise different prepregs with different fibre volume contents. Therefore, PAEK–L2O ratio is chosen as the best option to control the fibre volume, while it is proposed to keep other identified variables constant.

For manufacturing UD thermoplastic prepregs, the only variable affecting the amount of PAEK deposited on the S2-glass fibre (or carbon fibre trial) is set to be the PAEK–L2O ratio. For this purpose, 3 different PAEK–L2O ratios are prepared and investigated, which include 10, 20 and 30 wt% slurries.

This time, all the prime values influencing the properties of the prepreg are identified. The linear actuator is placed far right or left of the actuation stroke and the glass fibre tow is passed through all guiding tools and subsequently affixed on the winding drum, similar to the tests mentioned previously in Section 4.2.2. The PAEK slurry prepared is then added to the resin bath. The frequency and amplitude of the fibre spreader are set to 5.0 Hz and 6 mm, respectively. The spreading rollers are set to rotating and 5 mm guide roller is chosen for the interchangeable end roller. The 5 mm guide roller is selected in order to limit the fibre spread to 5 mm in all three PAEK slurry ratios, for consistency of the prepreg production.

The speed of the winding drum is set to 7.8 rpm and 3 layers of fibre tow is wound on the drum while the linear actuator is stationary to make sure the fibre tow is tightly wound on the drum and to avoid slippage. Option 2 (1.3 N) is chosen for the fibre tension and is kept constant throughout the winding process. The linear actuator is subsequently turned on to initiate the winding process. The transverse speed should be regulated to accommodate slight fibre-overlap when the winding process begins. This overlap is crucial, due to the fact that there are minor changes in the width of fibre tow when reaching the winding drum. Small overlap proves beneficial by not allowing gaps between fibre tows when the winding process initiates. A transverse

speed of 0.29 mm/s (20 % setting) is found to correlate well with the 5 mm interchangeable end roller.

Identical to Section 4.2.2.3, when the linear actuator reaches the end of its stroke and completes the winding process, it is turned off while the drum winds for another 3 rounds to fully secure the impregnated fibre on the drum. After that, the fibre tow is cut off from the drum. Subsequently, the rotating drum is shifted towards the heating unit where it is heated via the ceramic heaters at 400 °C in order to evaporate the water residues. The prepreg is heated for 1 hour above the ceramic heaters. Finally, the drum is stopped when the prepreg is dry. The far end fibre tow is fixed on the prepreg by melting it using a soldering iron. This ensures the wound fibre tow does not unwound and remains secured under tension.

In the next stage the winding drum is placed inside an oven set at a temperature slightly above the melting temperature of the polymer. For instance, the oven is set to 310–330 °C when AE 250 polymer is used for manufacturing the prepreg. A type-K thermocouple is positioned at the centre of the drum in close proximity of the prepreg material to observe the changes in temperature. Desiccant silica gel is also placed inside the oven as a drying agent to help absorbing any remaining moisture in specimens. The drum is heated until the type-K thermocouple reads a temperature equal or greater than the melting temperature of the polymer. In this stage the polymer particles are melted and adhered permanently on the fibre tow, forming the final prepreg material. Once the melting process is completed, the oven is turned off and the material is cooled down with a cooling rate of 5–10 °C/min. The drum is then removed from the oven and the prepreg is cut from the drum. This is done by cutting the prepreg with a sharp blade along the small groove situated across the whole length of the drum.

Finally, the prepreg sheet is laid down on a flat surface and is cut to the desired dimensions using a sharp blade. The prepreg plies are then ready for further processing including lamination. Figure 4.5 showcases some of the steps and processes involved in manufacturing the prepreg material.

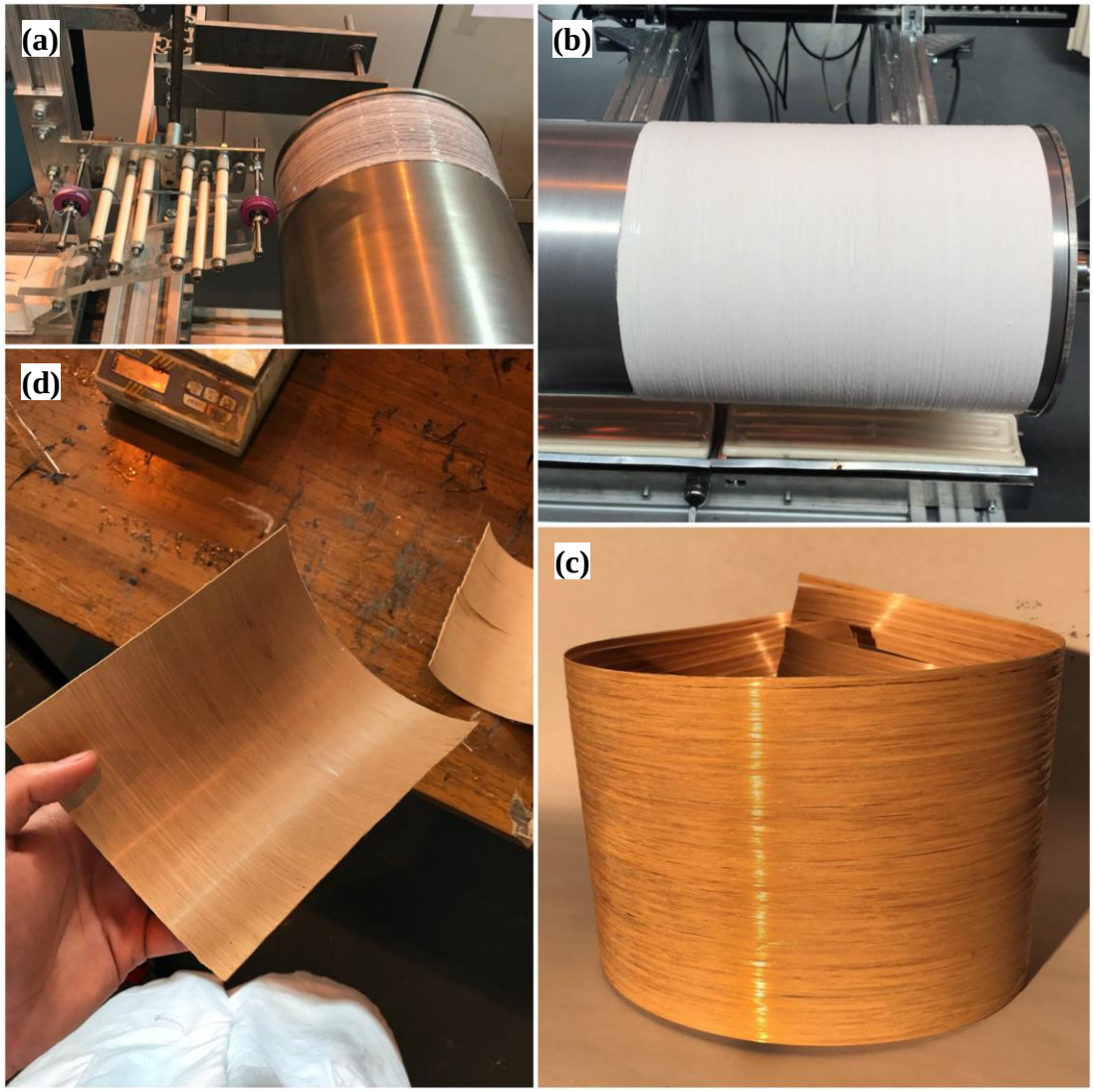

Figure 4.5 The process of manufacturing S2-glass/PAEK prepreg: (a) winding, (b) drying and melting, (c) removing and (d) cutting to desired dimensions.

4.4 Sample Preparation

After the prepreg material is ready and cut from the drum, the sheet can be cut further into smaller pieces as required. Prepregs can be tested for evaluating physical properties of the samples and to determine the consistency of the production line.

Prepreg plies can also be stacked on each other and heat-pressed to form composite laminates. Properties of manufactured laminates including the ratio of the constituents and the void content is further determined. Micrographs of different samples are generated, and a series of mechanical tests are performed for evaluations.

4.4.1 Test of Physical Properties of the Prepreg

Two important properties, namely prepreg areal weight (PAW) and thickness are measured to identify the physical properties of the prepregs and the consistency of the production line.

For this purpose, small ply pieces with dimensions of 100 x 100 mm are cut from the original prepreg sheet produced. Usually, a prepreg sheet with a length of 450 mm is wound around the drum. However, since both ends of the wound prepreg sheet is cut and disposed of, an effective prepreg sheet of approximately 400 mm long is obtained. Given the diameter of the winding drum (200 mm), the consumable prepreg sheet size taken off the drum is approximately 400 x 628 mm. This indicates that a full run of the winding drum will result in an effective prepreg sheet size of 400 x 628 mm, through which 24 single ply prepreg pieces of 100 x 100 mm can be obtained, as the examples shown in Figure 4.6.

Figure 4.6 Single ply prepreg samples cut with dimensions of 100 x 100 mm.

Mass per unit area of specimens is calculated and recorded in g/m^2. This is carried out by measuring the weight of each specimen and dividing it by its area as per Equation 4.1.

$$Prepreg\ Areal\ Weight\ (PAW) = \frac{Mass}{Area} \qquad \textit{Equation 4.1}$$

Thickness of each specimen is also individually measured using a vernier calliper from all sides and the mean value is recorded. It is noteworthy to mention that multiple batches of prepregs with same PAEK–L2O ratios and rig settings were manufactured to observe if the prepreg rig produces the same quality prepreg after each run.

4.4.2 Lamination

Among the composite laminate manufacturing processes available, hot compression moulding (out-of-autoclave method) is often used because of its ability to reach high temperature and pressure during the consolidation of the fibre by the polymer matrix, thus resulting in a void-free composite part and uniformly dispersed fibres [5]. Hot compression moulding is fast, and there is no need for expensive autoclave equipment. A Meyer model APV 3530/16 heat press machine was used for manufacturing laminates.

Prepreg pieces are stacked on each other and consolidated to form a composite laminate. Plies can be laid down inside a mould in any desired sequence but, for comparison purposes, prepreg plies are laid at 0° to form UD laminates. Two picture frame moulds are designed and manufactured from mild steel for producing laminates, as showed in Figure 4.7(a). The first mould has a dimension of 100 x 100 mm and the second one is 50 x 200 mm, both having same laminating area of 10,000 mm^2.

Figure 4.7(b) and (c) illustrates the moulding procedure for laminating. Prepreg plies are stacked between a pair of 2 mm thick mirror-finish stainless steel plates before entering the picture frame mould in order to achieve a smooth laminate finish with minimum surface defects. Use of stainless steel plates also helps protecting the mould. To avoid prepregs stick on the moulding surface after the PAEK melting, the surface

of the stainless steel plates are treated with a special release agent. They are initially treated with Chemlease 15 mould sealer in order to seal the surface to reduce the porosity and provide a beneficial base coat for all types of release agents. After sealing the surface from porosities, the plates are coated with Zyvax TakeOff release agent. This is a semi-permanent, water-based release agent utilised in this project that can be used for all major resin systems in composite industry. Zyvax TakeOff provides the minimal transfer of the release agent onto the composite part and is capable of providing multiple releases with one application of the product. It can also tolerate high processing temperatures without release agent cross-linking. It has the ability to be applied to hot mould surfaces, so as to provide quicker processing times. The combination of a smooth surface finish and use of seal/release agent ensure smooth release of the laminate after the melting of the PAEK polymer. Chemlease 15 sealer and Zyvax TakeOff release agent were supplied by Chem-Trend L.P. (USA).

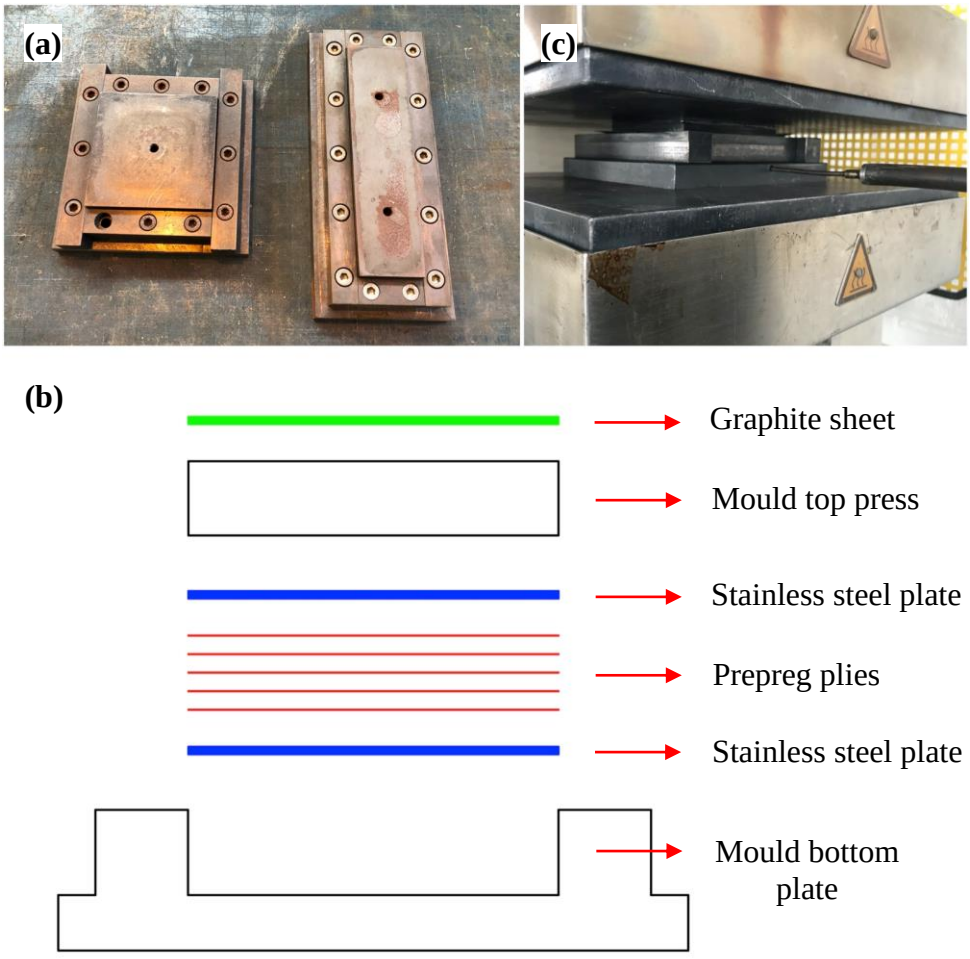

Figure 4.7 Composite lamination process: (a) moulding tools, (b) moulding sequence and (c) controlled heat pressing.

Before placing the moulded plies inside the heat press machine for hot compression moulding, a 2 mm graphite sheet is positioned on the top of the mould (the male part on the top press). The use of graphite sheet accommodates slight variations in heat press platen alignment and helps producing laminates with low thickness variation. Flexicarb RGS1 graphite sheet was supplied by Flexitallic Ltd. (UK). The mould is then placed between the two heating platens and is heat pressed. As demonstrated in Figure 4.7 (c), a type-K thermocouple is inserted mid-way inside the mould within close proximity of prepreg plies in order to observe the temperature of the material.

The typical cure cycle used for composite lamination is shown in Figure 4.8. As can be seen from the figure, the composite material is heated to a temperature above the T_m of the PAEK resin and then is pressed for 10 to 30 minutes. The consolidated laminate is subsequently cooled down at a rate of 5–10 °C/min while maintaining the pressure until below the resin's T_g. After which, the mould is opened, and the laminate is removed.

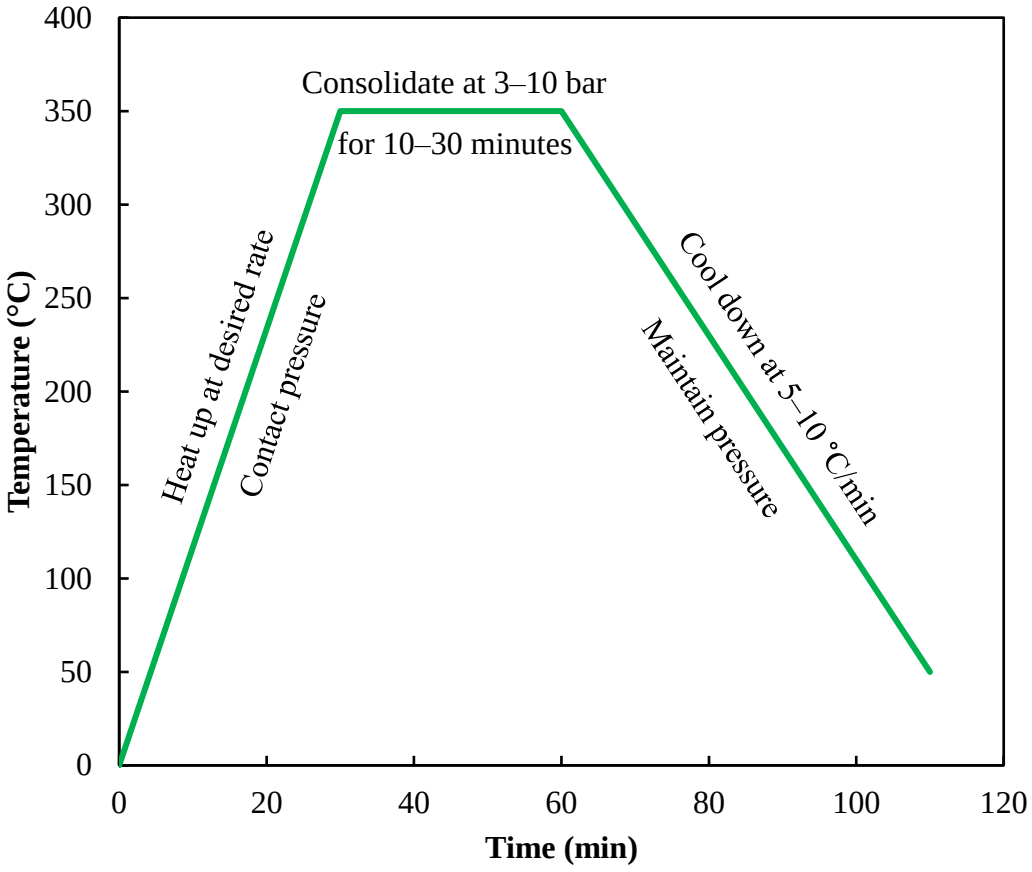

Figure 4.8 Typical cycle used for consolidating thermoplastic composite laminates.

In order to identify the optimum prepregs and processing settings, a thorough characterisation of laminates with different PAEK–L2O ratios is required. For this purpose, three different sets of prepregs were manufactured with different PAEK–L2O ratios of 10, 20 and 30 wt%, as previously mentioned.

In hot compression moulding, there are three parameters which affect the properties of the consolidated laminates, i.e. time, temperature and pressure. Each of these parameters is responsible for properties such as thickness, fibre volume and void content. It is therefore desired to optimise these parameters for each prepreg setting. In order to limit the number of samples required for this study, it was decided only to vary the processing pressure and time, and to keep the processing temperature constant. The processing temperature was kept constant at 350 °C for AE 250 PAEK. Three processing pressure settings of 3.5, 7.0 and 10.5 bar were used. Also, the processing time under pressure varied from 10, 20 and 30 minutes. Therefore, for each prepreg resin content, 9 laminates were manufactured. Since prepregs with three resin contents were produced, a total of 27 laminates were manufactured and compared, as charted in Figure 4.9.

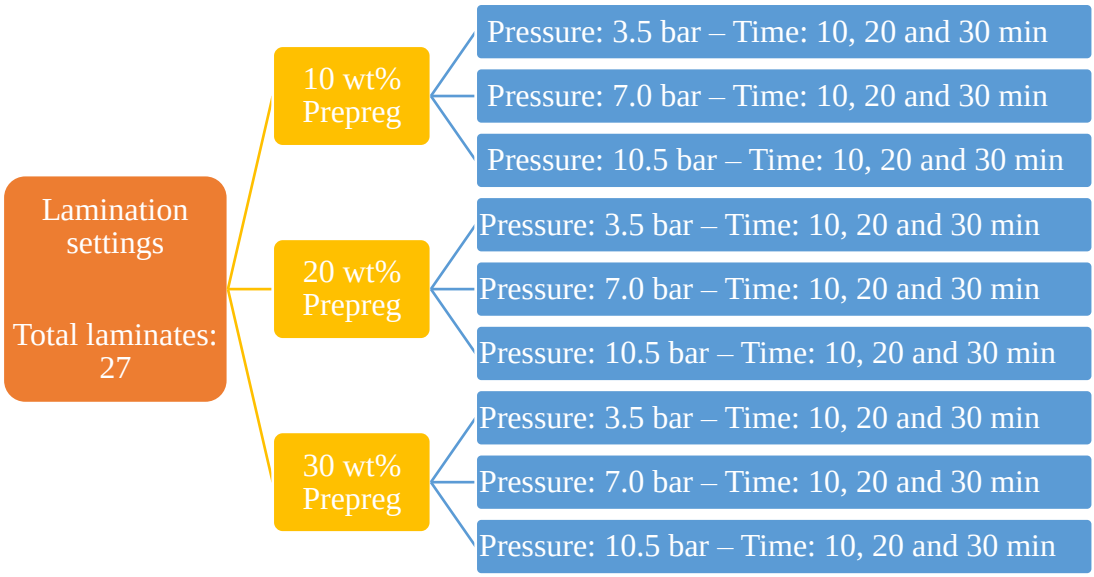

Figure 4.9 Processing parameters to manufacture 27 laminates to determine the optimum prepreg settings.

The manufacture and testing of these 27 laminates will determine the optimum prepreg and its corresponding laminate processing settings, i.e. pressure and time. The identification of the optimum prepreg will ease the advancement of this study by only implementing these optimum settings and utilising the best prepreg for further tests and investigations.

4.4.3 Fibre Volume and Void Content

A quantitative description of the proportions of composite constituents is necessary in order to specify the composite material. For the purpose of physical illustration, constituents are necessarily quantified in terms of their volume fraction. It is evident from Equation 4.2 that volume fraction sum V_c of all constituents, including fibre volume V_f, matrix volume V_m and the void volume V_v is equal to 1 (or 100 %).

$$\sum V_c = 1$$
$$V_c = V_f + V_m + V_v = 1 \qquad \textit{Equation 4.2}$$

Fibre volume and void content are important factors when manufacturing and comparing different FRPs. These values determine the ratio of the reinforcement compared to the resin matrix and consequently determine the mechanical and physical properties of the manufactured composite. Usually, higher fibre volume content and lower void content leads to a stronger and more durable composite.

ASTM D3171-15 [6] was adopted and implemented in order to determine the constituent contents of the composite materials produced. However, the first step of determining fibre volume content and subsequently the void content is to calculate the density of the composite samples. Measurement of the density was carried out in accordance with ASTM D792-13 [7]. Figure 4.10 demonstrates the practice of determining the density of the composite. The container is filled with liquid (usually distilled water) to a level where the bottom pan of the scale balance is submerged. Firstly, the dry mass of the specimen is measured in the top pan and recorded. The sample is then placed in the bottom pan submerged in liquid. The composite is left submerged for several minutes to allow any liquid into possible pores. Once the

reading has stabilised, the mass of the sample in the bottom pan is recorded. Sample is then removed from the water and dried using a non-absorbent material (like latex glove) until there is no surface water on the specimen. Finally, the sample is weighed again in the top pan after submersion in liquid.

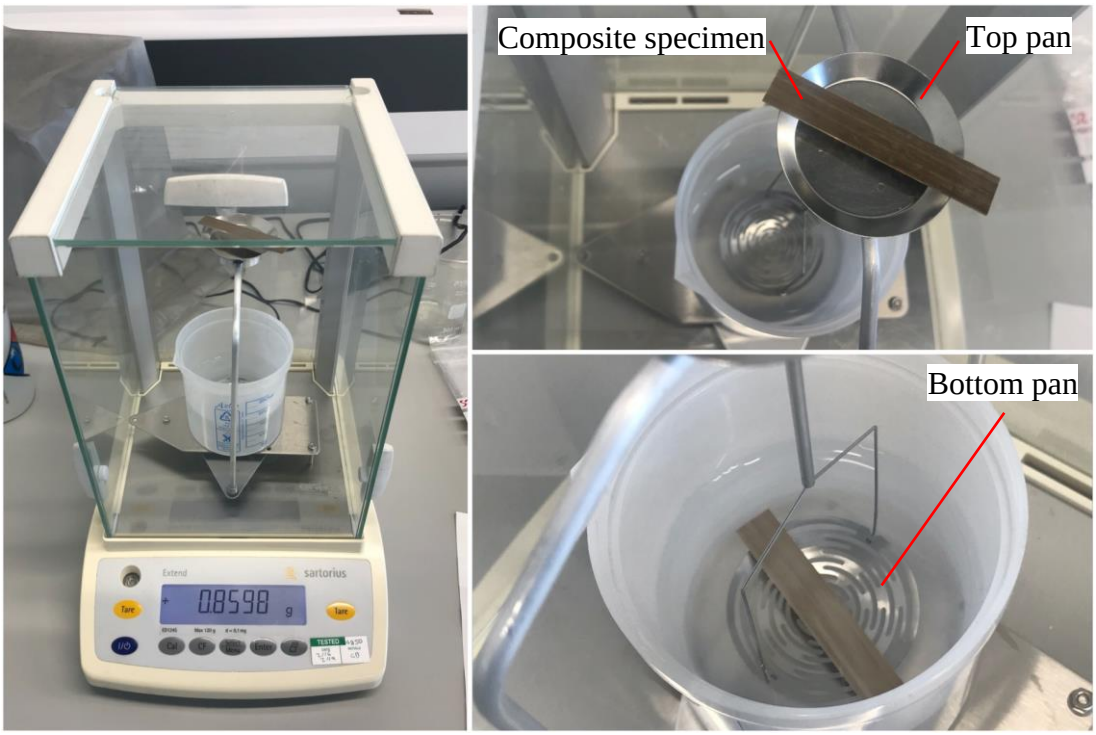

Figure 4.10 The process of determining density of the composite samples.

Density ρ_c of the sample is calculated using Equation 4.3 where m_1 is the mass of the dry specimen, m_2 is the apparent mass of the immersed specimen, m_3 is mass of the soaked specimen and ρ_l is the density of the liquid. Typical density of water at the time of the test at 21.4 °C is 0.99791 g/cm^3.

$$\rho_c = \frac{m_1}{m_3 - m_2} \times \rho_l \qquad \textit{Equation 4.3}$$

The Procedure G from test method I of the ASTM D3171-15 [6] was used to determine the volume of constituents and the void content. In this method, the resin matrix of the composite is removed in a furnace by combustion. The weight percent of the reinforcement is calculated, and from this value, if densities of both the composite and the reinforcement are known, the volume percent is calculated. An additional

calculation for void volume can be conducted if the density of the matrix is known or determined.

The Procedure G, matrix burn-off in a muffle furnace, is used for reinforcements such as glass, or ceramic that are not affected by high-temperature environments. In this method, the specimen with known mass and density (from the previous test) is placed in a desiccated pre-weighed crucible. The crucible should be cleaned by heating it to 500 to 600 °C or more in a muffle furnace and cooled in a desiccator before weighing. The crucible is positioned inside a preheated muffle furnace and is heated at 600 °C for 3 hours. The crucible is then removed from the furnace and the sample is turned around while fibre bundles are opened up using a tweezer for a more efficient ignition of the matrix. Such the operation is to make sure all the PAEK resin ignites and oxidises, and the only constituent left inside the crucible is the reinforcing fibre. The crucible is placed inside the muffle furnace once again and the sample is heated at 600 °C for another 3 hours. In the next stage the crucible is removed from furnace and is immediately transferred inside a desiccator for cooling down to room temperature. Specimen is then weighed while still in the crucible. The weight of the fibre is obtained by subtracting the crucible mass from the weight of crucible with the sample inside.

The Fibre volume V_f and matrix volume V_m content is determined in percentage using Equation 4.4, where M_f is mass of the fibre, M_i initial mass of the specimen, ρ_f density of the reinforcement, ρ_m density of the matrix and ρ_c the density of the specimen.

$$V_f = (\frac{M_f}{M_i}) \times \frac{\rho_c}{\rho_f} \times 100 \qquad \textit{Equation 4.4}$$

$$V_m = \frac{(M_i - M_f)}{M_i} \times \frac{\rho_c}{\rho_m} \times 100$$

The void volume V_v is calculated in percentage in accordance with Equation 4.5.

$$V_v = 100 - (V_f + V_m) \qquad \textit{Equation 4.5}$$

Figure 4.11 exhibits the burnt-off samples in the fibre volume and void content test after removal from the furnace. As can be seen in the figure, PAEK matrix completely departs the composite sample, leaving only the reinforcing fibre inside the crucible.

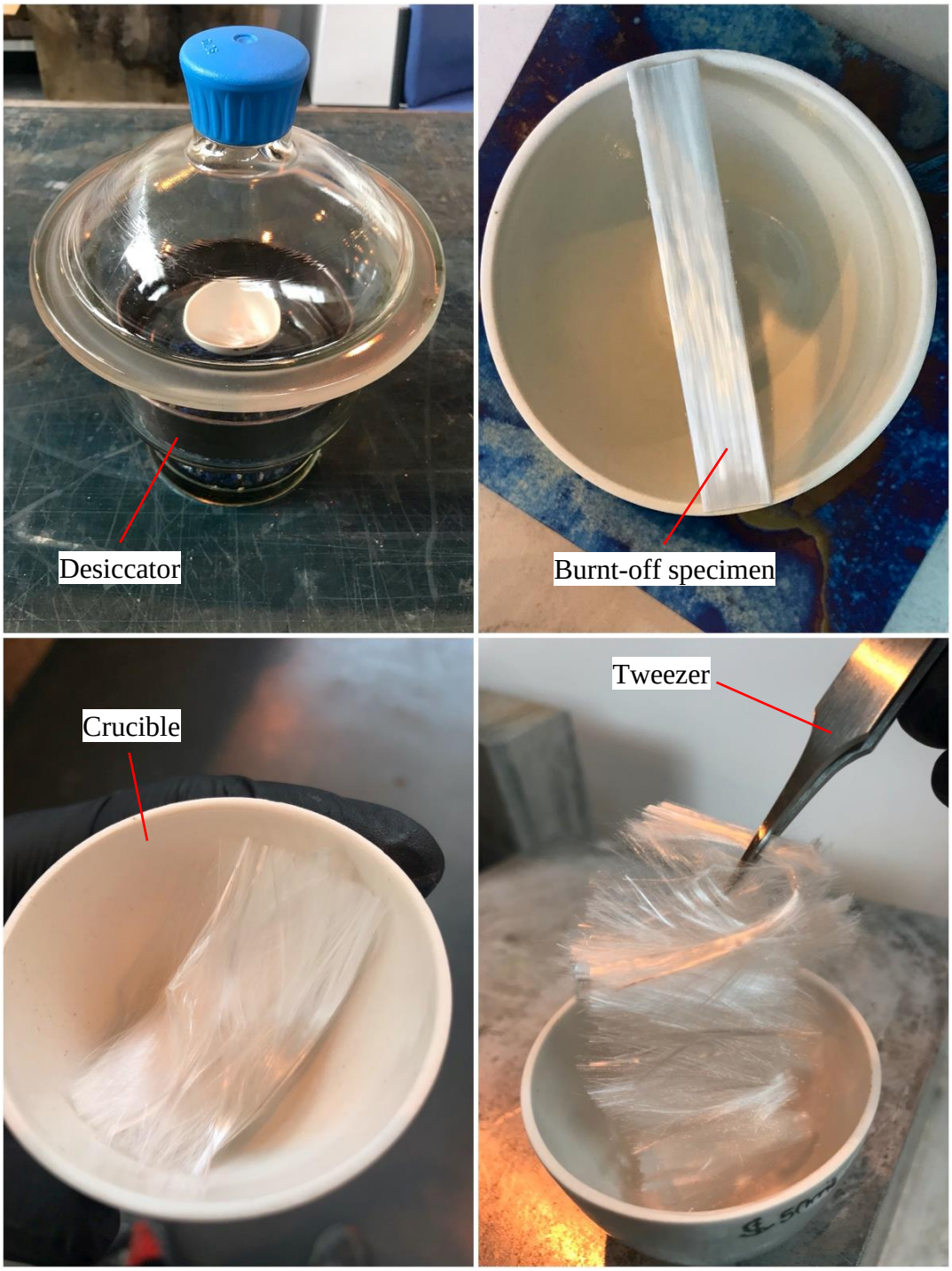

Figure 4.11 Composite sample matrix burn-off for determining fibre volume and void content.

4.4.4 Microimaging of Samples

Transverse and longitudinal cross-sections of prepregs and laminates were observed to understand certain properties of the material, where appropriate. The selected cross-sections were sequentially cleaned in an ultrasonic bath with hot water and detergent, three times and each time for 20 minutes, in order to ensure the removal of any oil or hydrophobic residues from the cutting and handling operations. This procedure minimises the interference with the infiltration of the mounting resin into the specimen. Figure 4.12 shows the steps taken for preparing such samples for microimaging.

The clean and dry cross-sections were secured in spiral steel mounting-clips as appropriate and placed in standard 32 mm diameter pre-greased circular moulds, as shown in Figure 4.12(a). The use of the mounting clips assured the correct orientation of specimens, perpendicular to the base, in each mount. EPO-SET supplied by MetPrep Ltd. (UK), which is an appropriate low-viscosity and room temperature curing epoxy mounting resin, was employed for the mounting of the samples.

The cured and mounted specimens were removed from their moulds and cleaned as before to remove residual mould-release compound, as shown in Figure 4.12(b). The specimens were then surface refined by standard materialographic procedure using sequentially finer grades of silicon carbide grit-paper with water lubrication from a particle-size of 150 μm (P120 mesh) down to 8 μm (P2500 mesh) on a Struers Knuth-Rotor 2 polishing machine, as shown in Figure 4.12(c). As seen in Figure 4.12(d), the finely-ground specimens were then polished on a Metaserv universal polisher, firstly using a water-based slurry of 1 μm alumina on a napped synthetic-fibre cloth grade MEMPHIS by MetPrep Ltd. (UK), and finally using a 40 nm aqueous silica suspension grade OPUS by MetPrep Ltd. (UK), on a similar cloth substrate, employing the carousel-type automatic polishing machine, operating at approximately 150 rpm. Specimens were finally washed in detergent and distilled water, to remove any residual polish, and dried using ethanol in a current of hot air.

Micrographs were collected using Nikon EPIPHOT metallurgical inverted optical microscope. Model Infinity 2-2c camera from Lumenera Corporation was utilised for

capturing the images. The main magnification ratios for capturing the images were 50, 100, 200, 400 and 600 X.

Figure 4.12 The procedure of polishing samples for microimaging: (a) mounting specimens inside 32 mm round moulds, (b) cleaning cured samples in ultrasonic bath, (c) surface grinding, (d) fine polishing and (e) prepared samples.

For a better understanding of the physical and mechanical properties of the composite samples and their corresponding failure modes, fractography was carried out on selected fractured specimens. Two image capturing equipment were used: optical microscope with reflected brightfield lighting using crossed-polarising filter, and scanning electron microscope (SEM).

Fine shards of the failed specimens, 50–70 mm in length, were carefully mounted onto standard (25 x 75 mm) glass microscope slides, using strips of double-sided adhesive tape. Mounting each specimen flat and parallel with the plane of the slide was essential, in order to exploit the very limited depth-of-field available in visible-light microscopy.

The resultant slide-mounted specimens were analysed using reflected brightfield lighting, on a Leitz Metalloplan optical microscope, fitted with Leitz PL objective lenses. Subsequent micrographs were captured employing the same lighting set-up and crossed-polarising filter technique, using an Infinity 2-3C CCD digital camera in conjunction with Infinity Capture 6.0 software from Lumenera Corporation.

Being partly crystalline in microstructure, the PAEK matrix interacts optically with polarised light, resulting in false-colour birefringence fringes. This phenomenon was found to be exhibited, by even the thinnest of polymer films, making this technique very useful for rapidly diagnosing the presence of such material. In contrast, being amorphous, the glass fibre filaments do not undergo this special interaction with polarised light; instead, the incident light is simply reflected in the usual manner, with no noticeable change in colour. Hence, this technique was found to be invaluable for discriminating between coated and uncoated glass fibres.

Secondary Electron Images (SEI) of the failed specimens were recorded using a JEOL JSM6610 scanning electron microscope. Similar failed specimen shards, this time around 5–10 mm in length, were mounted on films of conductive carbon tape, onto standard 10 mm diameter SEM stubs. In order to render the fracture surfaces electrically conductive, the resultant fibre mounts were plasma-coated with a nano-film of pure silver metal, using an Edwards SP150 sputter-coating unit from Edwards Vacuum. Enhancing the specimen's surface electrical conductivity facilitates superior and low-noise image formation in the SEM, by dissipating any residual primary electron charge. Specimens catastrophically failed were also mounted vertically onto standard 10 mm diameter SEM stubs, using conductive silver paint. These mounts were rendered electrically conductive, as previously mentioned, by sputter-coating technique.

4.5 Mechanical Property Tests

A number of mechanical tests were carried out in order to determine the mechanical properties of the produced laminates. The tensile test was the first to be carried out and will determine the optimum prepreg setting, i.e. which PAEK–L2O ratio prepreg will produce laminates with the highest tensile strength. Flexural and interlaminar shear tests were also performed on the optimum laminates.

4.5.1 Tensile Test

Tensile tests were carried out according to ASTM D3039/D3039M-14 [8]. The manufactured composite laminates were extracted from the moulding tool after hot compression. Before machining laminates to desired sizes for producing tensile coupons, composite laminates were tabbed. E-glass sheets with a thickness of 1.6 mm were used as the tabbing material. Tabbing is especially essential for testing UD composites in order to promote the failure in the gauge length of the sample and not the grips. Where appropriate, E-glass sheets were angle grinded to produce a 10° bevel. The bevel angle feathers smooth transition of load into the coupon. For this purpose, a tab jig device was designed and manufactured as seen in Figure 4.13(a). The glass sheet cut is positioned inside both sides of the jig. The jig is subsequently placed on the top of a sanding belt in order to grind off the E-glass sheet and produce the bevelled tabs as showed in Figure 4.13(b).

As seen in Figure 4.14(a), the two ends of the laminates were keyed from both sides with a 300 grit sandpaper and washed in hot water and detergent to ensure that any oil or hydrophobic residues were removed from the handling operations. Otherwise, these may interfere with the adhesion of the subsequent sample to tabbing material. The mechanical abrasion on the laminate surface promotes better adhesion of the tab. Epoxy adhesive film grade XA120 with a thickness of 0.2 mm was supplied from Easy Composites Ltd. (UK) and were used to bond the tabs to the laminates. Four layers of the epoxy resin film were sandwiched between the laminate and the tab. The tabbed laminate was then put inside a release film bag and was vacuumed under a vacuum pressure of 0.8 Pa, while it was cured inside the oven. Recommended initial cure cycle for the film resin is 8 hours at 90 °C (ramp rate 2 °C/min). Where the maximum T_g is required, a post cure of 120 °C for 1 hour should be followed (ramp rate 0.3 °C/min).

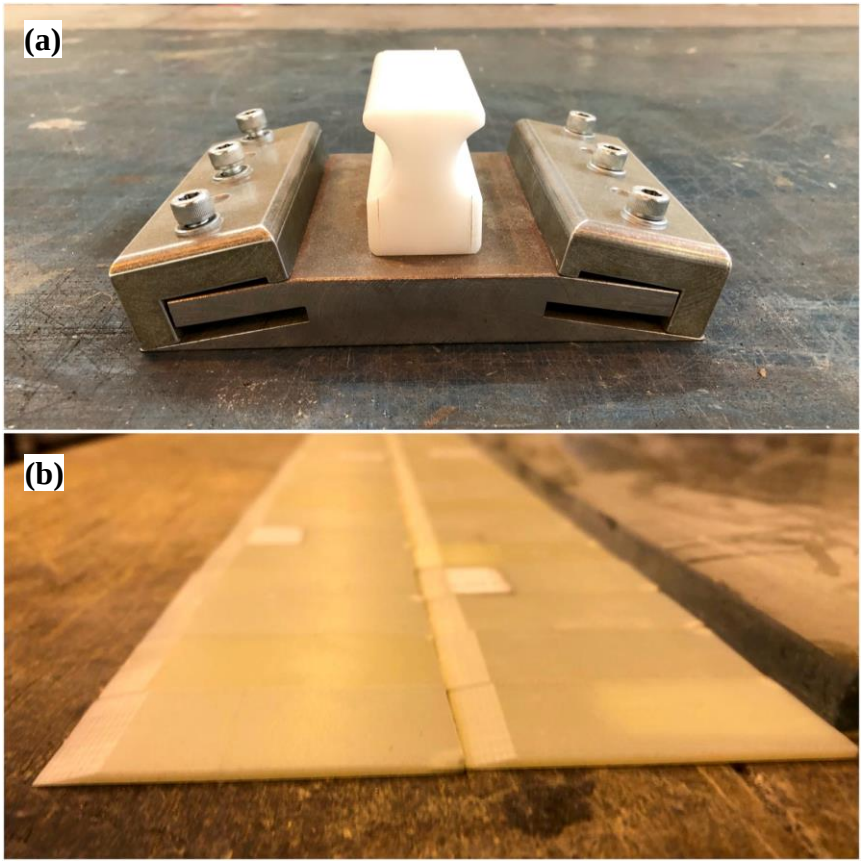

Figure 4.13 The designed and manufactured jig for producing bevelled tabs.

Once the E-glass tab is affixed on the composite, the laminates are cut along the fibre direction (0° direction) using a lubricated diamond tip blade saw to produce short or long UD tensile coupons as seen in Figure 4.14(b) and (c), respectively. Long samples were specifically produced for high-temperature tensile tests.

Quasi-static tensile tests were conducted using an Instron model 5985 universal testing machine. Strain response of composite samples were recorded using an extensometer with a gauge length of 10 mm attached to the middle section of the tensile coupon. The test was carried out with a constant crosshead speed of 2 mm/min and the load–displacement data were recorded to understand the mechanical behaviour of the samples. Figure 4.15(a) shows an example of the tensile test conducted in practice.

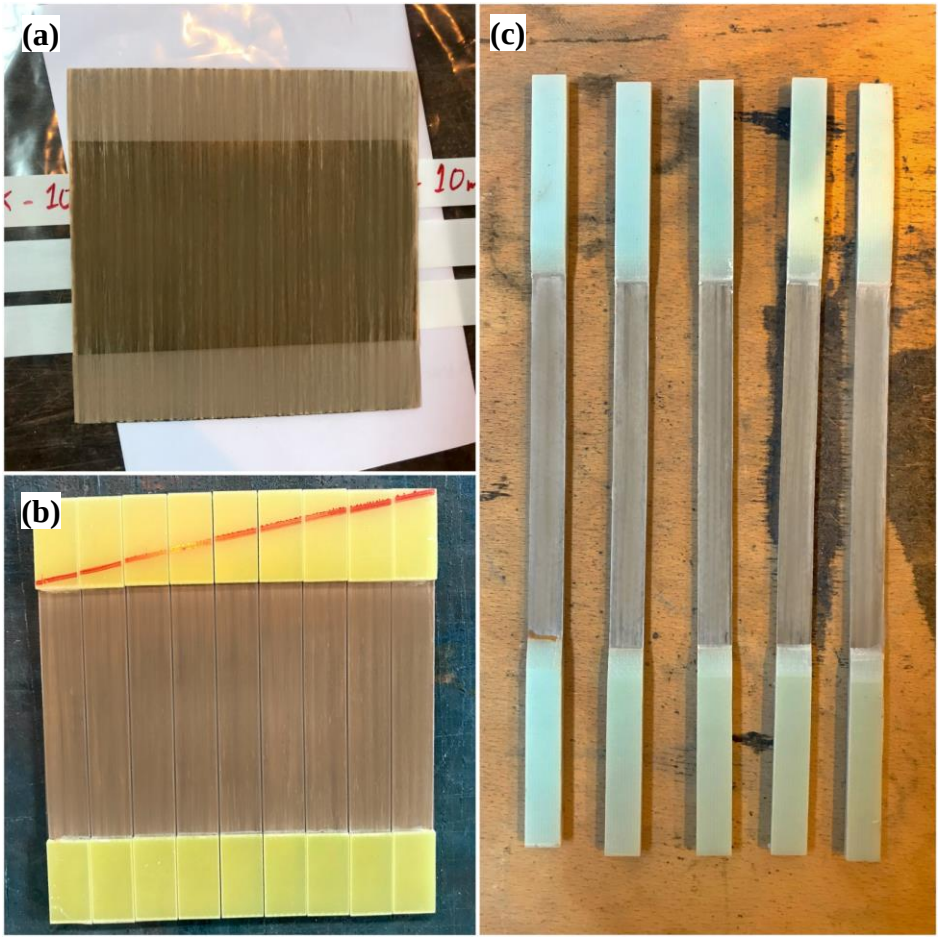

Figure 4.14 Fabrication of tensile coupons: (a) keyed laminate, (b) tabbed laminate and (c) cut tensile specimens.

In the case of tensile testing of UD coupons under high temperatures, coupons were inserted inside a temperature-controlled chamber. The heated chamber was designed and manufactured from an aluminium alloy housing several heating elements. The outer surface of the chamber is insulated with flame retardant super wool 607 fibre to reduce heat loss. As illustrated in Figure 4.15(b), a type-K thermocouple was attached to the centre of the sample using a Kapton tape to monitor the temperature of the composite. The chamber was then sealed, and the specimen was heated to the desired temperature as per Figure 4.15(c). The required temperature is maintained within ±3° variation and the sample is soaked in heat for at least 10 minutes before the test starts.

By conducting this test, the influence of elevated temperatures on the tensile strength of the composite samples could be understood. Samples were therefore tested in room temperature, 100, 150, 200 and 250 °C, respectively.

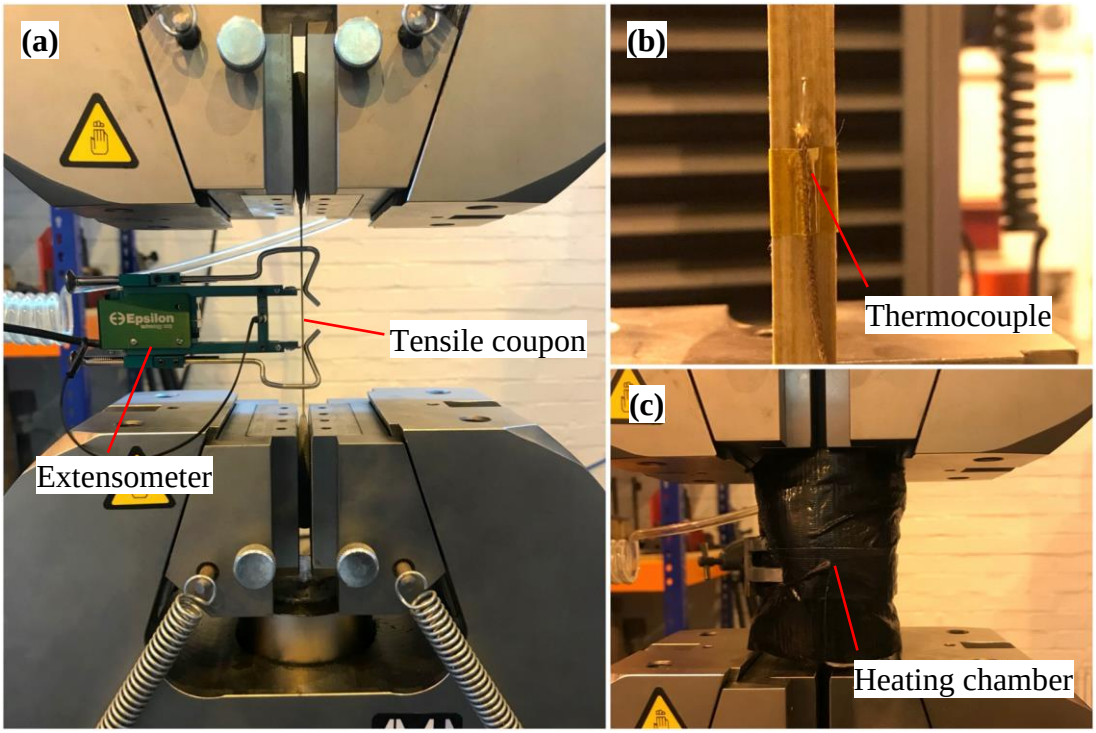

Figure 4.15 Tensile test setups and procedure.

At least five samples were tested for each laminate specification and the results were recorded. Here, tensile strength and modulus, and also failure strain were calculated from the load-displacement data where appropriate. The ultimate tensile strength σ_u can be calculated using the following equation:

$$\sigma_u = \frac{P_{max}}{A} \qquad \textit{Equation 4.6}$$

where P_{max} is the maximum force before failure and A is an average cross-sectional area of the sample. Tensile chord modulus of elasticity, E_{chord}, with a strain range of 0.1 to 0.3 %, was measured in order to calculate the tensile modulus using the following equation:

$$E_{chord} = \frac{\Delta\sigma}{\Delta\varepsilon} \qquad \textit{Equation 4.7}$$

where $\Delta\sigma$ is difference in the applied tensile stress between the two strain points and $\Delta\varepsilon$ is the corresponding strain increment (nominally 0.2 %).

Failure strain ε_u is determined by tensile strain from the indicated displacement at failure point using the following equation:

$$\varepsilon_u = \frac{\delta_u}{L_g} \qquad \textit{Equation 4.8}$$

where δ_u is the extensometer displacement at failure and L_g is extensometer gauge length.

4.5.2 Flexural Test

Flexural tests were carried out according to ASTM D7264/D7264M-15 [9]. Procedure A (three-point bending) of the test standard was adopted, as illustrated in Figure 4.16.

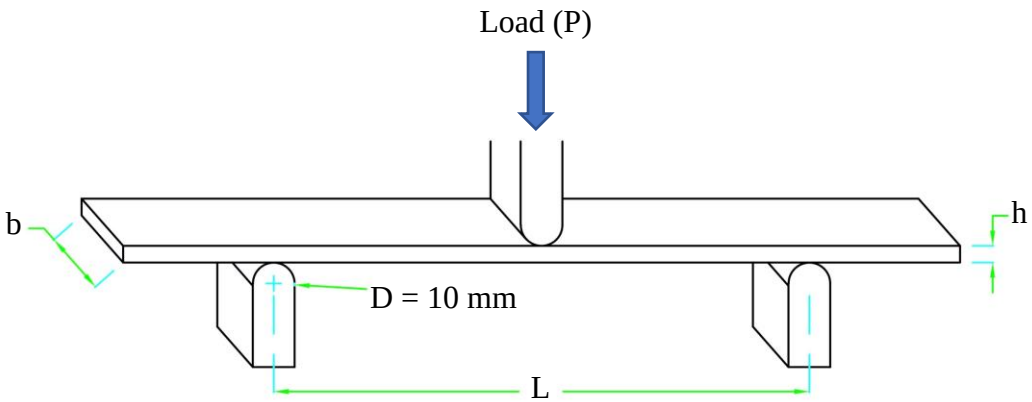

Figure 4.16 Schematics of the flexural test procedure A (three-point bending).

Composite samples were cut into specimens with thickness of h and width of b. Recommended dimensions are 4 mm for the thickness and 13 mm for the width. The length of the sample shall be at least 20 % more than the span length of L. Specimens were mounted on the fixture as shown in Figure 4.16. A span to thickness ratio of 32:1 was chosen. That is, for 4 mm thick samples, the distance between the two bottom support pins was 128 mm. Both support pins and the loading nose were cylindrical rods manufactured from hardened steel with a diameter (D) of 10 mm.

Quasi-static flexural tests were conducted using an Instron model 5985 universal testing machine. Force P is applied to the specimen by the movement of the loading nose at the mid-span with crosshead speed of 1 mm/min, resulting specimen deflection at the centre of span. The load–deflection data is captured until failure occurs on one of the extreme fibres.

At least five samples were tested for each laminate specification and the results were recorded. Here, flexural strength and flexural modulus were calculated from the load-displacement data. The flexural stress σ can be calculated using the following equation:

$$\sigma = \frac{3PL}{2bh^2} \qquad \textit{Equation 4.9}$$

The flexural strength is equal to the maximum stress at the outer surface corresponding to the peak applied force prior to failure. Flexural chord modulus of elasticity E_f^{chord} was implemented in order to calculate the flexural modulus using the following equation:

$$E_f^{chord} = \frac{\Delta\sigma}{\Delta\varepsilon} \qquad \textit{Equation 4.10}$$

where $\Delta\sigma$ is difference in the flexural stress between the two strain points and $\Delta\varepsilon$ is the corresponding strain increment (nominally 0.2 %).

4.5.3 Interlaminar Shear Test

Interlaminar shear tests were carried out according to ASTM D2344/D2344M-16 [10]. Flat specimen configuration of the test standard was practiced as illustrated in Figure 4.17.

Samples were machined into specimens with thickness of h and width of b. Recommended dimensions are 6 mm for the thickness and 12 mm for the width. The length of the sample shall overhang the span length L from both sides by at least the

specimen's thickness. Recommended specimen length is 40 mm. Specimens were mounted on the fixture as shown in the Figure 4.17. A span to thickness ratio of 4:1 was chosen. That is, for 6 mm thick samples, the distance between the two bottom support pins was 24 mm. Both support pins and the loading nose were cylindrical rods manufactured from hardened steel with a diameter (D) of 3 mm and 6 mm, respectively.

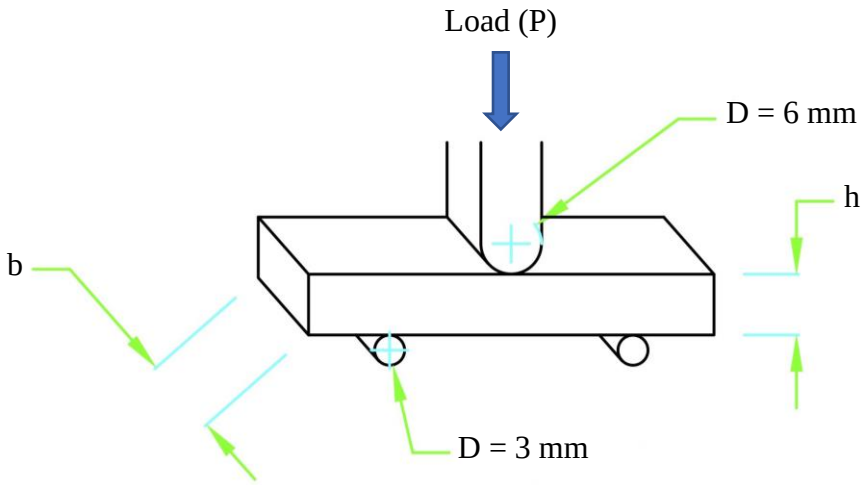

Figure 4.17 Schematics of the Interlaminar shear test using flat specimen configuration.

Quasi-static interlaminar shear tests were conducted using an Instron model 5985 universal testing machine. Force *P* is applied to the specimen by the movement of the loading nose at the mid-span with crosshead speed of 1 mm/min, resulting shear stress on planes midway between the loading nose and support points. The load is applied to the specimen while data is being recorded. The test continues until a 30 % drop-off is observed in the load.

At least five samples were tested for each laminate specification and the results were recorded. Here, short-beam strength was calculated from the maximum load observed during the test. The interlaminar shear strength (ILSS) F_{ilss} can be calculated using the following equation:

$$F_{ilss} = 0.75\frac{P_m}{bh} \qquad \textit{Equation 4.11}$$

where P_m is the maximum load observed during the test.

4.6 Summary

In this chapter, experimental procedures of numerous physical and mechanical tests were explained. Initially, a series of preliminary experiments were proposed and carried out to understand the effectiveness of different parameters of the prepreg rig. Different variables such as the PAEK–L2O ratio, tension of the fibre, winding and actuating speed, fibre spreader settings, and different guide rollers were investigated. The preliminary tests were designed in a fashion to identify the effect of each parameter on the properties of the produced prepregs.

Once the optimum setting is established for each parameter, experimental work was carried out to produce S2-glass/PAEK prepreg. The preliminary experiments indicated that the proposed manufacturing method could potentially be used to produce UD thermoplastic prepreg. For manufacturing prepreg materials, it was decided to deal only with one variable to customise prepregs with different fibre volume content. Therefore, PAEK–L2O ratio was chosen as the best option to control the volume of constituents. For this purpose, three different PAEK–L2O ratios of 10, 20 and 30 wt% of PAEK in slurry were prepared and investigated.

The manufactured prepreg materials were subsequently observed visually and tested for their physical properties. Prepreg areal weight and thickness of the prepregs were measured, and cross-sectional micrographs were produced to understand the effectiveness of the proposed wet powder impregnation method, and the extent of polymer particle infusion into the fibre bundle, shedding light on homogeneity of fibre/matrix distribution.

Laminated composites were manufactured accordingly, taking into consideration three processing variables: temperature, time and pressure. Different laminate samples were produced, and specimens were machined and cut in order to evaluate physical

properties such as fibre volume and void content. Additionally, mechanical assessments such as tensile, flexural and interlaminar shear tests were undertaken to measure the mechanical properties of the laminates. Finally, multiscale (hierarchical) fibre-reinforced nanocomposites were manufactured by adding graphene and nanoclay into the resin bath. They were then compared to their laminate counterparts without adding nanomaterials.

4.7 References

[1] Ramani, K., Woolard, D. E., and Duvall, M. S., 1995, "An electrostatic powder spray process for manufacturing thermoplastic composites," Polymer Composites, 16(6), pp. 459-469.

[2] Henninger, F., Hoffmann, J., and Friedrich, K., 2002, "Thermoplastic filament winding with online-impregnation. Part B. Experimental study of processing parameters," Composites Part A: Applied Science and Manufacturing, 33(12), pp. 1684-1695.

[3] Xian, G., Pu, H.-T., Yi, X.-S., and Pan, Y., 2006, "Parametric Optmisation of Pin-assisted-melt Impregnation of Glass Fiber/Polypropylene by Taguchi Method," Journal of Composite Materials, 40(23), pp. 2087-2097.

[4] Kazumasa, K., and Tatsuki, M., 1998, "Technology for Spreading Tow and Its Application to Composite Materials Part 2 : Spreading Tow by Roll Method," Sen'i Kikai Gakkaishi (Journal of the Textile Machinery Society of Japan), 51(2), p. 65.

[5] Mazur, R. L., Cândido, G. M., Rezende, M. C., and Botelho, E. C., 2016, "Accelerated aging effects on carbon fiber PEKK composites manufactured by hot compression molding," Journal of Thermoplastic Composite Materials, 29(10), pp. 1429-1442.

[6] ASTM, 2015, "D3171-15 Standard Test Methods for Constituent Content of Composite Materials," ASTM International, West Conshohocken, PA.

[7] ASTM, 2013, "D792-13 Standard Test Methods for Density and Specific Gravity (Relative Density) of Plastics by Displacement," ASTM International, West Conshohocken, PA.

[8] ASTM, 2014, "D3039/D3039M-14 Standard Test Method for Tensile Properties of Polymer Matrix Composite Materials," ASTM International, West Conshohocken, PA.

[9] ASTM, 2015, "D7264/D7264M-15 Standard Test Method for Flexural Properties of Polymer Matrix Composite Materials," ASTM International, West Conshohocken, PA.

[10] ASTM, 2016, "D2344/D2344M-16 Standard Test Method for Short-Beam Strength of Polymer Matrix Composite Materials and Their Laminates," ASTM International, West Conshohocken, PA.

CHAPTER V: RESULTS AND DISCUSSION

5.1 Introduction

This chapter presents the experimental results obtained during the prepreg rig trials, manufacturing process and from testing the prepreg and laminate composite materials. Initially, results from preliminary tests are discussed, which include the effectiveness of the L2O carrier and different settings on the prepreg rig such as the winding speed and fibre tension. Subsequently, different settings of the fibre spreading assembly are tested and discussed, followed by completion of the resin penetration trial and improved tests. The manufactured prepreg materials are tested for their physical properties and the effects of different PAEK–L2O ratios on areal weight and thickness are discussed. Results from physical and mechanical properties of the manufactured laminate composites are tabulated and compared. The effects of different processing pressure and time on the properties of the composite laminates are investigated and cross-sectional micrographs of different laminates are compared. Tensile test results are discussed along with outcome of the shear and flexural evaluations. High-temperature tensile tests are also carried out and the tensile results are discussed and compared with the ones obtained in room temperature. Finally, the effects of nanomaterials on mechanical behaviour of laminates are elaborated.

5.2 Preliminary Results for Method Evaluation and Optimisation

In this section results from a number of preliminary tests are compared. The tests include the experiments with PAEK–L2O ratio, and settings of the prepreg rig and the fibre spreading device. Resin take-up test is also discussed and the consistency of the production, specifically the amount of PAEK resin collected by the fibre tow is investigated.

5.2.1 AE 250 PAEK–L2O Slurry Test Results

A selection of prepared suspensions was tested for particle size distribution, and stability measurements of particles in L2O carrier. The obtained results from the experiments were analysed to investigate the suitability of L2O as a carrier to segregate and suspend polymer and additive particles.

5.2.1.1 Particle Size Distribution Measurements

Laser diffraction method was used to measure the particle size and particle size distribution (PSD) of PAEK slurries. The intensity of the scattered light is measured and analysed to calculate the size of the particles that created the scattering pattern.

Figure 5.1 shows the average PSD graphs (5 measurements) for PAEK slurries with de-ionised water and L2O as the dispersing agent. Two different calculations are provided: volume density for the size of each band and the cumulative percentage below each size band.

By comparing the volume distributions, it can be seen that the dominant average particle diameter measurements for both carriers are approximately 10 microns. However, this value is lower for when water is used as the dispersing agent. It can be observed that the corresponding volume graph for water as the dispersant has two peaks, one at approximately 10 microns and another at around 200 microns. This indicates that two dominant average particle sizes exist in the water suspension. In other words, PAEK clusters of 200-micron in size are formed in the slurry, and water as the carrier is not fully capable of separating PAEK particles.

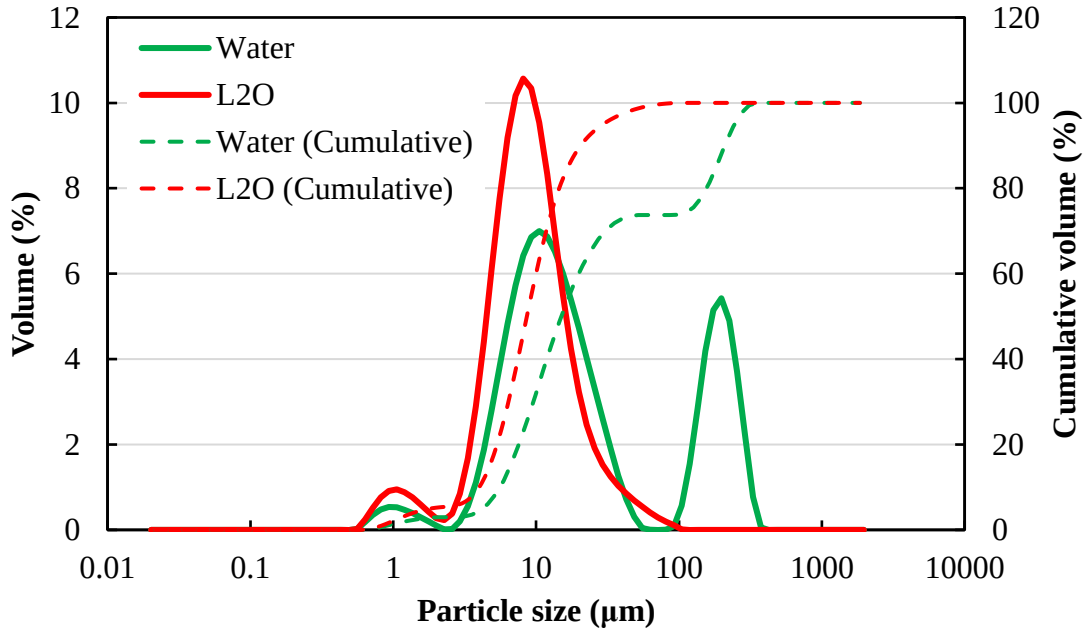

Figure 5.1 Particle size distributions of PAEK powder dispersed in water and L2O.

For a better understanding, mass median diameter percentile readings can be used for analysis. Table 5.1 compares the Dv_{10}, Dv_{50} and Dv_{90} values for when water and L2O are used as the carrier. Here, for instance, Dv_{50} indicates the size of PAEK particle below which 50 % of the sample lies, and the "v" in the expression shows that this refers to the volume distribution. By studying the Dv_{50} of both carriers, it can be seen that 50 % of the measured particle sizes are 8.60 μm or less when L2O is used as the dispersant, compared to 15.01 μm for when water is used, which is almost double the value. Here, approximately 60 % of all measured particle sizes, with L2O in use, are 10 microns or under, which is particularly important for the impregnation stage of prepreg production. Additionally, 90 % of the measured particles in L2O were 20.34 μm in size or under, compared to 209.17 μm for when in water.

Table 5.1 Comparison of standard mass median diameters for water and L2O as the carrier and PAEK particles as the dispersed phase.

	Mass median diameter (μm)		
Carrier	***Dv_{10}***	***Dv_{50}***	***Dv_{90}***
Water	5.56	15.01	209.17
L2O	3.98	8.60	20.34

It is clear that L2O has a better performance in micronizing PAEK particles compared to water only. Maximum particle size range discovered in L2O carrier was between 200–250 microns, which only accounted for 0.02 % of the volume population. At least 99.9 % of all scanned particles were recorded as under 150 microns ($Dv_{99.9}$ <150 μm). In contrast, particles in water can be as large as 400 microns, although only small percentage.

PAEK slurries with the added 5 wt% Nanene and nanoclay were also tested in 10 wt% PAEK samples. The addition of nanomaterials did not have any significant impact on the PSD measurements. That said, the Dv_{10}, Dv_{50} and Dv_{90} values for when Nanene was utilised was noticeably lower compared to normal 10 wt% samples, and were recorded as 3.45, 7.78 and 15.32 μm, respectively. Since this was not the case with

when nanoclay was added to the slurry (almost same PSD data as normal slurries), the decline in the average PSD can be attributed to the high light absorption index of Nanene particles that are black in colour and prevent light to scatter. Although the addition of Nanene particles in the overall volume might have decreased the PSD values for all ranges, $Dv_{99.9}$ for these samples were recorded as 39 μm, which seems quite unrealistic.

5.2.1.2 Turbidity Measurements

Experiments were carried out on selected colloidal PAEK systems to understand the stability (particles remaining suspended in L2O at equilibrium) of 10, 20 and 30 wt% PAEK slurries. Additionally, 5 wt% Nanene and nanoclay PAEK slurries were also studied as the highest tier of added nanomaterials in this project. Obviously, the goal here is to identify if the stability is hindered by sedimentation or aggregation phenomena for the duration of the test, which was 25 cycles with 5-minute intervals between each cycle (120 minutes in total).

Figure 5.2 illustrates a visual macroscopic fingerprint of 10, 20 and 30 wt% slurry samples over a 120-minute period using static multiple light scattering (SMLS) technology. Here, two synchronous optical sensors receive respectively light transmitted through the sample (180° from the incident light, transmission sensor), and light backscattered by the sample (45° from the incident radiation, backscattering detector). Transmission (T) and backscattering (BS) data are acquired every 40 μm. The captured data provides the transmitted and backscattered light flux in percentage relative to standards (suspension of monodisperse spheres and silicone oil), as a function of the sample height (in mm). Usually, backscattering data is used to analyse opaque and concentrated dispersions, which is the case in PAEK–L2O samples.

The mean BS value measured during the first scan of the middle part of the vials (14 to 29 mm) for 10, 20 and 30 wt% sample were 88.1, 93.8 and 95.1 %, respectively. This is a direct indication that slurries with higher PAEK concentration would have a higher BS value. This is typical as higher particle concentrations will result in more light being backscattered.

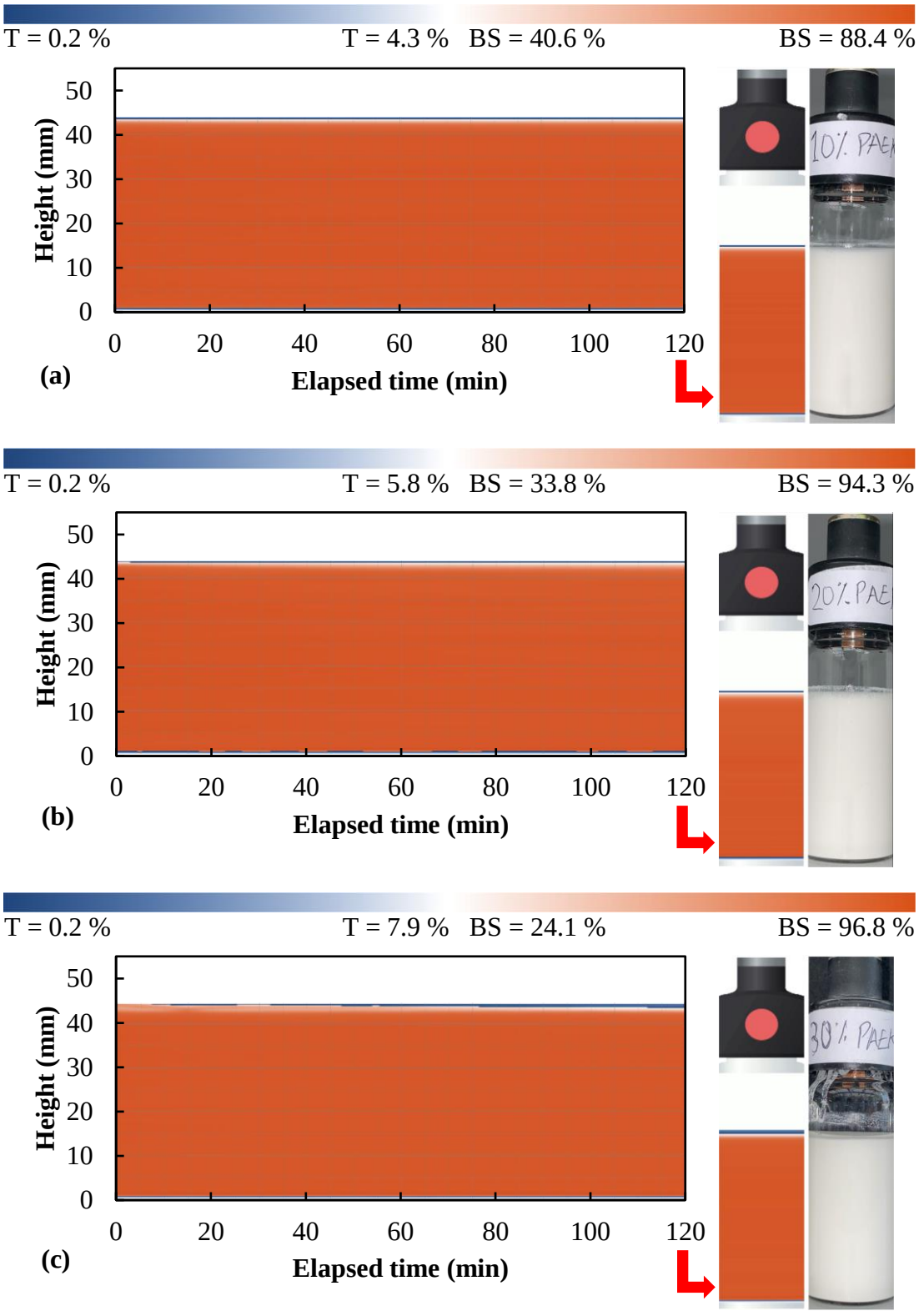

Figure 5.2 Visual stability of samples over the height of filled vials after two hours for: (a) 10 wt%, (b) 20 wt% and (c) 30 wt% PAEK slurries.

The main instabilities observed with colloidal systems are usually of two types: particle migration and particle size increase. Local variations of the concentration of

particles in the sample will initiate variations of the T or BS level measured. At the same time, global variations of the particle size in the sample will also affect these values. When analysing turbidity profiles, the scanned height of the sample can be separated into three parts: bottom, middle and top. Variations in the top and bottom of the sample are linked to migration phenomena, while variations in the middle section are usually due to changes in particle size.

It is observed from Figure 5.2 that all three samples have a relatively good colloidal stability for a duration of 120 minutes. The variations in BS of the middle part of the samples for the last cycle (after 120 minutes), compared to the initial middle scan for all three samples, were observed to be less than 1 %. This therefore demonstrates no significant evidence of change in particle sizes, i.e. particle flocculation.

Sedimentation is encountered when the density of the dispersed phase is greater than the density of the continuous phase. By studying the variations in the concentration of the PAEK phase between the top and the bottom of the sample, sedimentation can be detected. As evident from Figure 5.2, there are traces of decrease in BS (and increase in T) at the top of the samples due to a decrease in the particle concentration. The mean BS values of the top part of the samples in vial (35 to 43 mm) for the last cycle (after 120 minutes), compared to the first scan, are decreased by 1.8, 6.0 and 12.9 % for 10, 20 and 30 wt% samples, respectively. These values suggest that 10 wt% suspensions are quite stable for a duration of 120 minutes. Stability for 20 and 30 wt% samples are slightly lower compared to 10 wt% samples. Also, the phase separation (clarification) in 30 wt% samples are more obvious. This incident is expected as PAEK concentration in 20 and 30 wt% samples are higher compared to 10 wt% samples and consequently, results in a faster migration of the particles to the bottom of the vial.

Figure 5.3 shows delta BS traces of the final scan for 10, 20 and 30 w% samples with respect to the height of the vial. For a better visualisation of the results and to amplify the variations, delta values can be implemented. Here, delta consists of subtracting the reference scan (by default the first one) from the other scans and using this reference scan as a blank value.

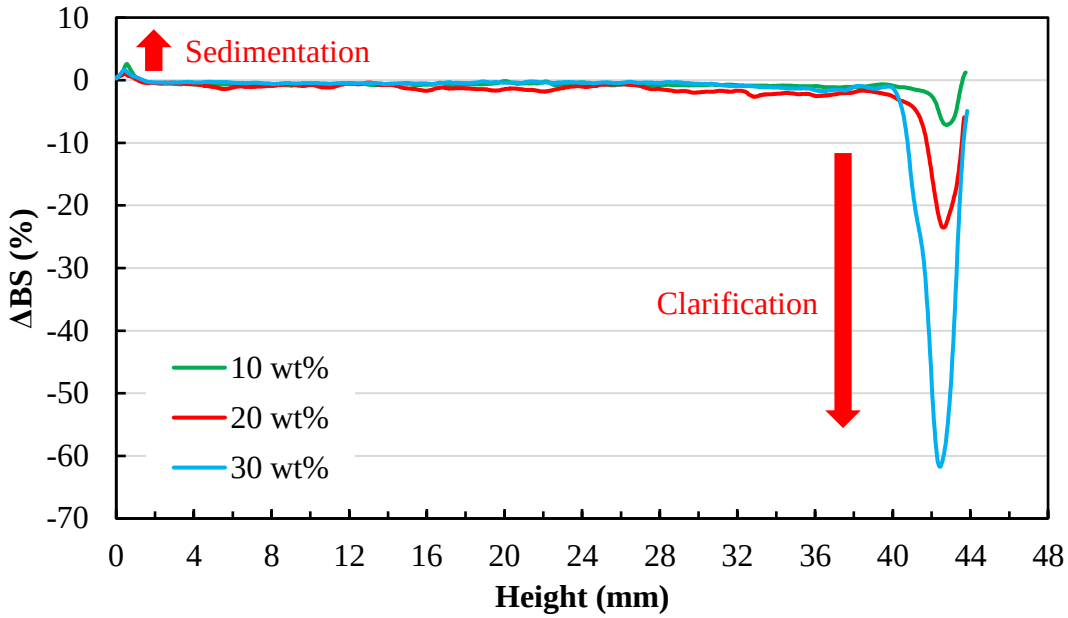

Figure 5.3 Delta backscattering values for the final turbidity scan of 10, 20 and 30 wt% slurry samples.

The graph shows the changes in the BS values for the full height of the vials. All three samples show a relatively steady BS throughout the middle part of the vial. As expected, variations are only observed on the top and bottom of the samples. This time, small backscattering increases can be observed at the bottom of the samples due to an increase in the concentration of the PAEK phase (sedimentation). However, these variations are insignificant compared to the clarification phase of all three samples. This behaviour suggests that the migration rate of the PAEK particles in the top section of the vial is possibly faster than of the migration rate in the bottom section. Another speculation could be that some or all ingredients of the L2O find their way to the top part of the vial (creaming) at a faster rate compared to the particle migration rate to the bottom.

Given the obtained and analysed results so far, it can be suggested that the blend of dispersing and water-thickening agents inside the L2O can promote homogenous suspension of PAEK particles in the slurry for prolonged periods without significant sedimentation and helps preventing particle flocculation.

For a better understanding of the extent in which L2O could be utilised as a suitable carrier for prepreg manufacture, the colloidal stability of 10 wt% PAEK slurries with

the added nanomaterials is investigated next. Figure 5.4 shows the global destabilisation kinetics for five different samples. The stability comparison of different formulations using only the raw T or BS signals can be difficult and require advanced calculations. It is possible to monitor the destabilisation kinetics in the samples versus ageing time, thanks to the Turbiscan Stability Index (TSI). TSI is a dimensionless value that is the result of summing all occurring destabilisation phenomena in the sample that can be measured by noticeable change of the BS or T signal intensity along the sample height. The higher is the TSI value, the lower the stability, as these signal variations are directly linked to any destabilisation in the sample.

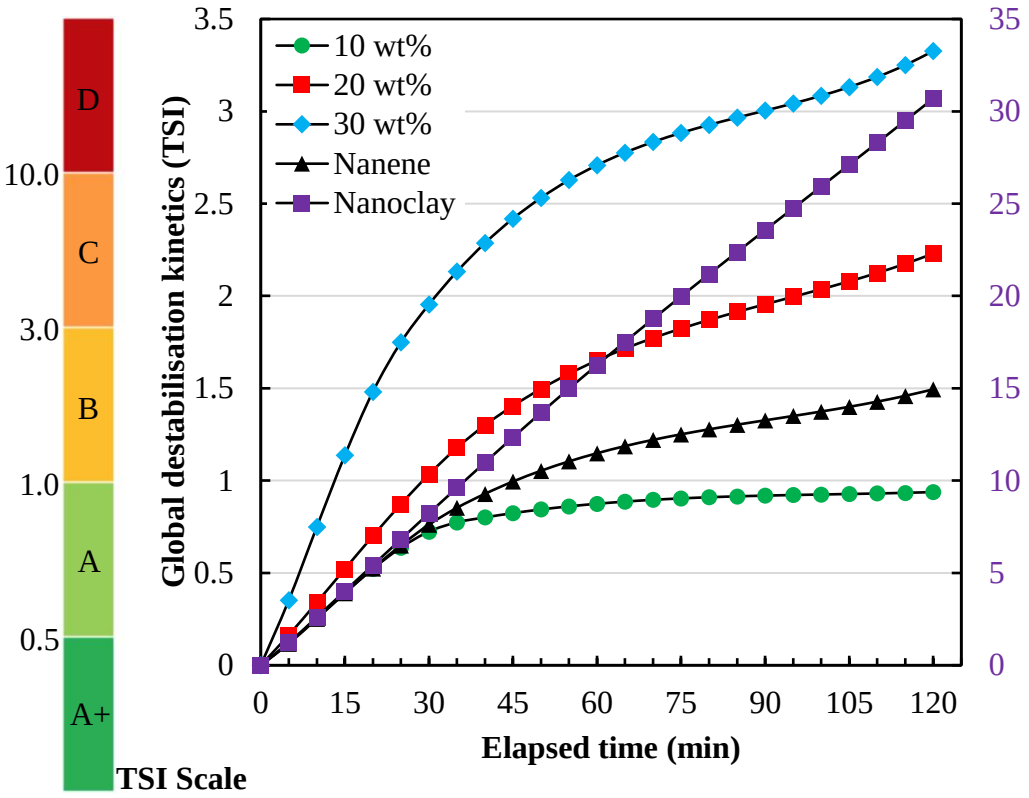

Figure 5.4 Global destabilisation kinetics versus the ageing time for different samples.

For the purpose of illustration, samples can be ranked and compared using the TSI scale, as per Table 5.2. As seen in the table and also in Figure 5.4, TSI values are associated with a colour that allows for a direct analysis of the samples. Since the TSI values obtained for slurries with the added nanoclay are very high, the results for this tier are plotted in a secondary axis (purple in colour) so to fit the graph area for comparison purposes.

Table 5.2 Interpretation of different levels of the TSI scale.

TSI Scale	Description
A+	No significant variation – not visible
A	Emerging destabilisation – not visible
B	Weak destabilisation – potentially visible
C	Significant destabilisation – visible
D	High destabilisation – visible

Figure 5.4 shows that for 120 minutes of sample ageing, the TSI values for 10 wt% PAEK samples show a steady grow for 30 minutes, and then slight increases until the TSI value reaches just below 1. Values between 0.5 and 1 indicate a visually good suspension (Band A). Destabilisations are detected but are at the very early stages. In the A ranking, no visual destabilisations are observed. Here, 20 and 30 wt% samples have a higher initial growth slope compared to 10 wt% samples and they stand at 2.23 and 3.33 after 120 minutes, respectively. This would place 20 wt% samples in category B and 30 wt% samples in category C. In band B, destabilisations remain non-visual in most cases; however, important destabilisations corresponding to large sedimentation/creaming or particle size variation can be attributed to band C.

All said, analysing the TSI data for an ageing time of 30 minutes show that all the values for 10, 20 and 30 wt% samples remain under 2, with 20 and 10 wt% even being 1 and under. Although the turbidity test was run for 120 minutes, the captured data for 30 minutes of elapsed time is a more pragmatic time scale for the impregnation process of the prepreg manufacture. This clearly indicates that for a duration of 30 minutes, no external stirring would be necessary inside the resin bath for agitating PAEK particles, and the slurry concentration remains constant during the winding for a consistent prepreg production.

The addition of 5 wt% Nanene to 10 wt% PAEK slurries did not have significant effects on the obtained TSI values. Figure 5.4 shows that the TSI stays below 1.5 for samples with Nanene, for a duration of 120 minutes. The TSI growth trend remains

similar to that of normal 10 wt% samples until 30 minutes, which indicates slurries with the added 5 wt% Nanene can also be used without need for stirring the resin bath.

TSI values for 5 wt% nanoclay samples are however significantly different compared to the rest of the samples. TSI values jump above 1 only after 5 minutes of ageing. A linear and steady growth in TSI values is observed, reaching approximately 8.22 for 30 minutes of ageing, and surpassing 30 after 120 minutes. For a better understanding, delta BS traces versus the height of the nanoclay sample is sketched in Figure 5.5 for a total of 25 scans (120 minutes).

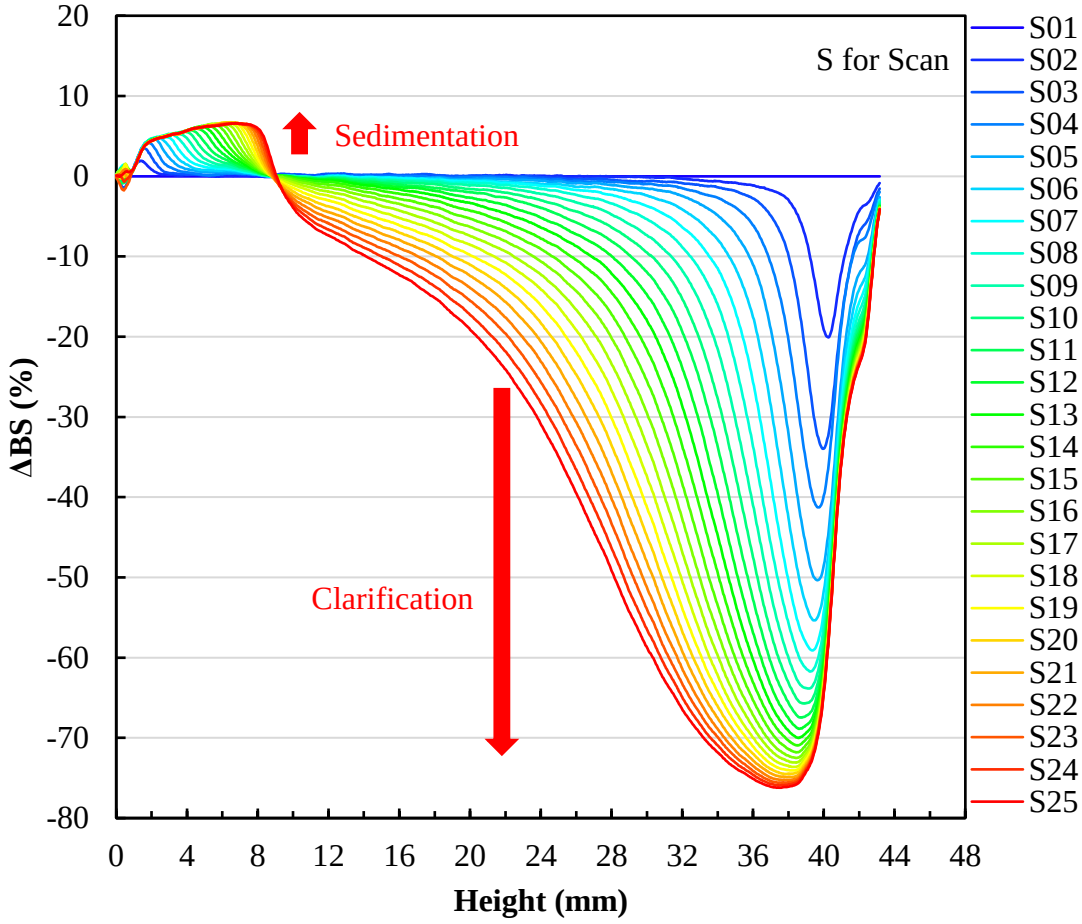

Figure 5.5 Delta backscattering values for 25 cycles of a sample with added nanoclay showing particle migration to the bottom of the vial.

Changes in the TSI can be attributed to variations in the BS light as a result of particle sedimentations. It is observed from Figure 5.5 that delta BS increases at the bottom of

the vial, while the values decline (clarification) on the top section as a result of particle sedimentation and consequently, increased light transmission through the sample.

Figure 5.6 shows the sedimentation level in a nanoclay sample after 25 cycles (120 minutes). It is clear from the image that a thick layer of particle is formed at the bottom of the vial, hence the approximately 8 % rise in the BS value captured in the last scan. At the same time, the top part of the vial starts to clarify. This phenomenon could be attributed to the hydrophilic properties of clay, leading to an increased cohesive attraction between particles and possible particle agglomeration over time. Another possible explanation to this could be the high density and shape of clay particles, and the inability of the utilised L2O concentration in successfully suspending and separating clay particles.

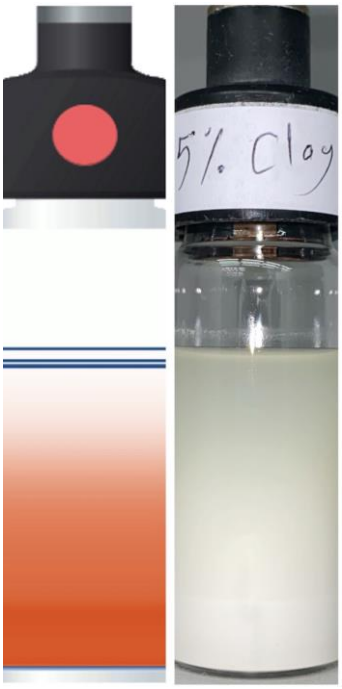

Figure 5.6 Visuals and graphics of a nanoclay sample showing sedimentation levels after 120 minutes of ageing.

5.2.2 Winding Speed and Fibre Tension Adjustment

The winding speed is one of the important settings on the prepreg rig that will affect the prepreg material. Winding speed is effectively varied from 20 to 100 %, with intervals of 10 %. This is equivalent to 0.9 to 19.0 rpm as previously listed in Table 3.8. Fibre tension is also kept constant and is initially set to option 1 (0.8 N).

Initial trials with the winding speed controller indicated that the winding drum does not start revolution at 10 % setting. This was mainly due to the presence of frictions between the bearing parts and belts, and also the low torque of the implemented DC motor. There was no attempt to address this issue as even the 20 % (0.9 rpm) speed setting was deemed too slow for the winding process.

Here, 30 % (2.6 rpm) and 40 % (4.6 rpm) speeds were tested, and it was found that such the slow speeds would result in some major problems. Firstly, the time it takes for the full transverse around the winding drum is significant. For the winding speed of 2.6 rpm, it approximately took 50 minutes for the linear actuator to complete the transverse run for a full winding. This time was reduced markedly when 4.6 rpm setting was used. However, with both settings being relatively slow, other problems emerged. As can be seen in Figure 5.7, when these slow speeds are used for winding, the PAEK slurry starts accumulating at the bottom part of the drum and subsequently drips off the winding drum. This is not ideal as considerable amount of resin slurry would be wasted. Also, the free run of slurry droplets would result in an uneven distribution of slurry and change the amount of resin dispersed on the prepreg and consequently, alter the consistency of the production.

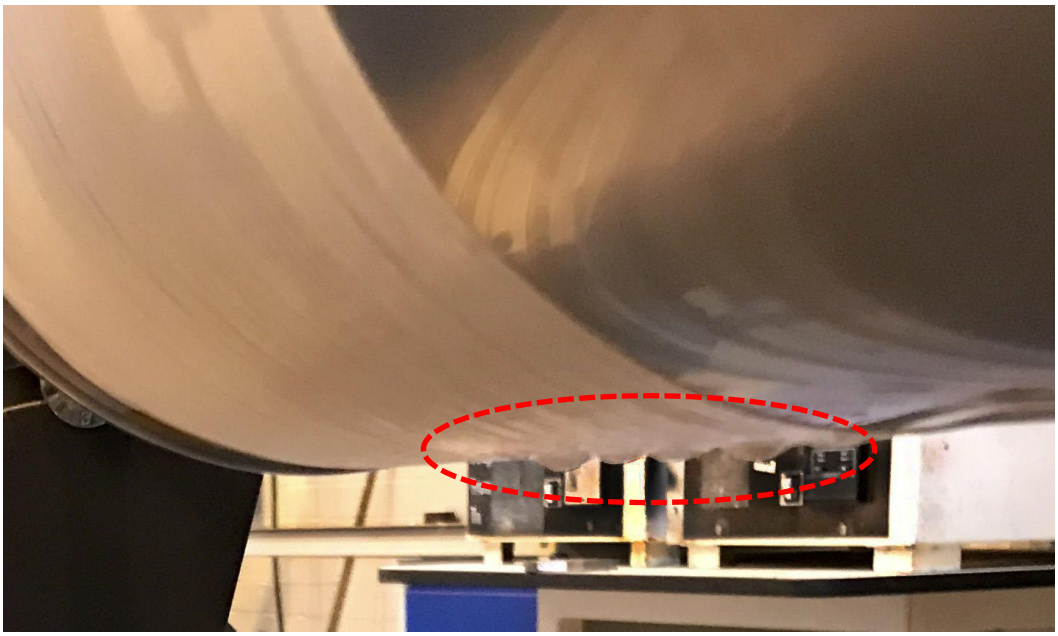

Figure 5.7 PAEK slurry dripping from winding drum for slow winding speeds.

Another problem identified while using slow winding speeds was the heavy drip of the slurry from the spreading rollers as illustrated in Figure 5.8. Although this phenomenon is beneficial in terms of discarding the excess resin off the rollers, the large amount of PAEK slurry unloaded due to the slow speed of the fibre tow would result in not enough resin being deposited on the fibre filaments. When dried, the wound prepreg had obvious signs of exposed fibres due to lack of sufficient resin.

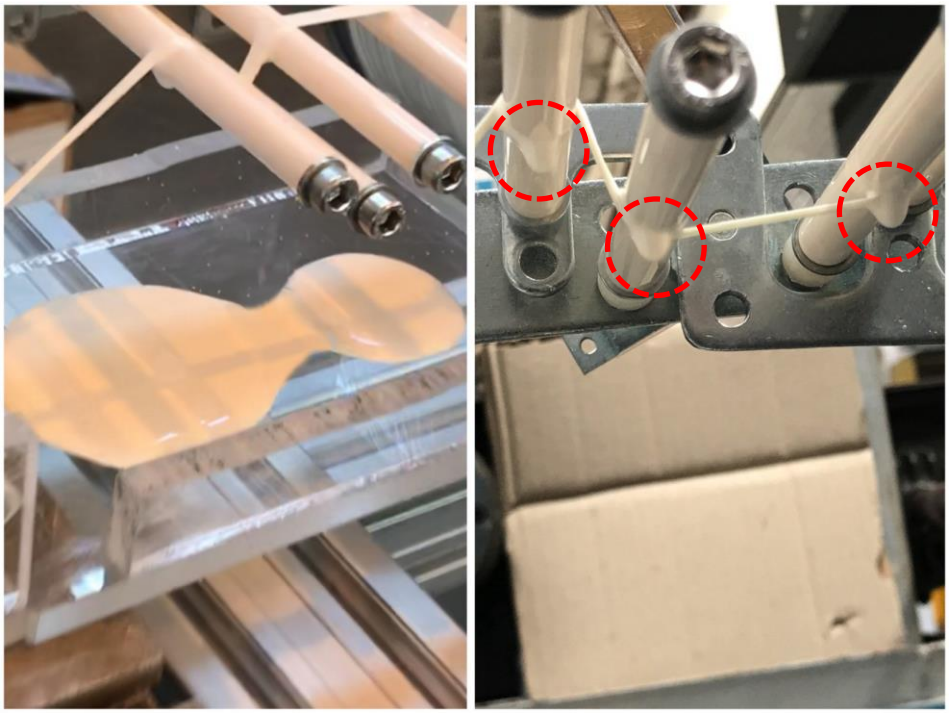

Figure 5.8 PAEK slurry dripping from spreading rollers for slow winding speeds.

Faster winding speeds were also tested. It was found that for the speed of 70 % (11.7 rpm) or more, the aforementioned dripping issues were addressed, however, numerous other problems surfaced. For such the speed, the amount of resin picked up by the fibre tow is significantly increased and the excessive PAEK slurry does not find enough time to drop back to the resin bath. Figure 5.9 illustrates an example that the drum speed of 70 % (11.7 rpm) is chosen. From Figure 5.9(a) it is evident that the PAEK resin starts running free on the drum when it is turning with high speeds. This results in high tolerances in the prepreg thickness values and an irregular surface finish. Figure 5.9(b) demonstrates the heavy resin pick-up after the winding is complete with resin moving freely on the outer surface of the prepreg. Once dried, PAEK powder was observed agglomerating in certain parts of the prepreg as per

Figure 5.9(c), creating a rough and inconsistent prepreg surface. Such situation is not desirable as the final prepreg material would have high thickness variations and consequently, the laminated composites would have resin rich areas that significantly weakens its mechanical properties.

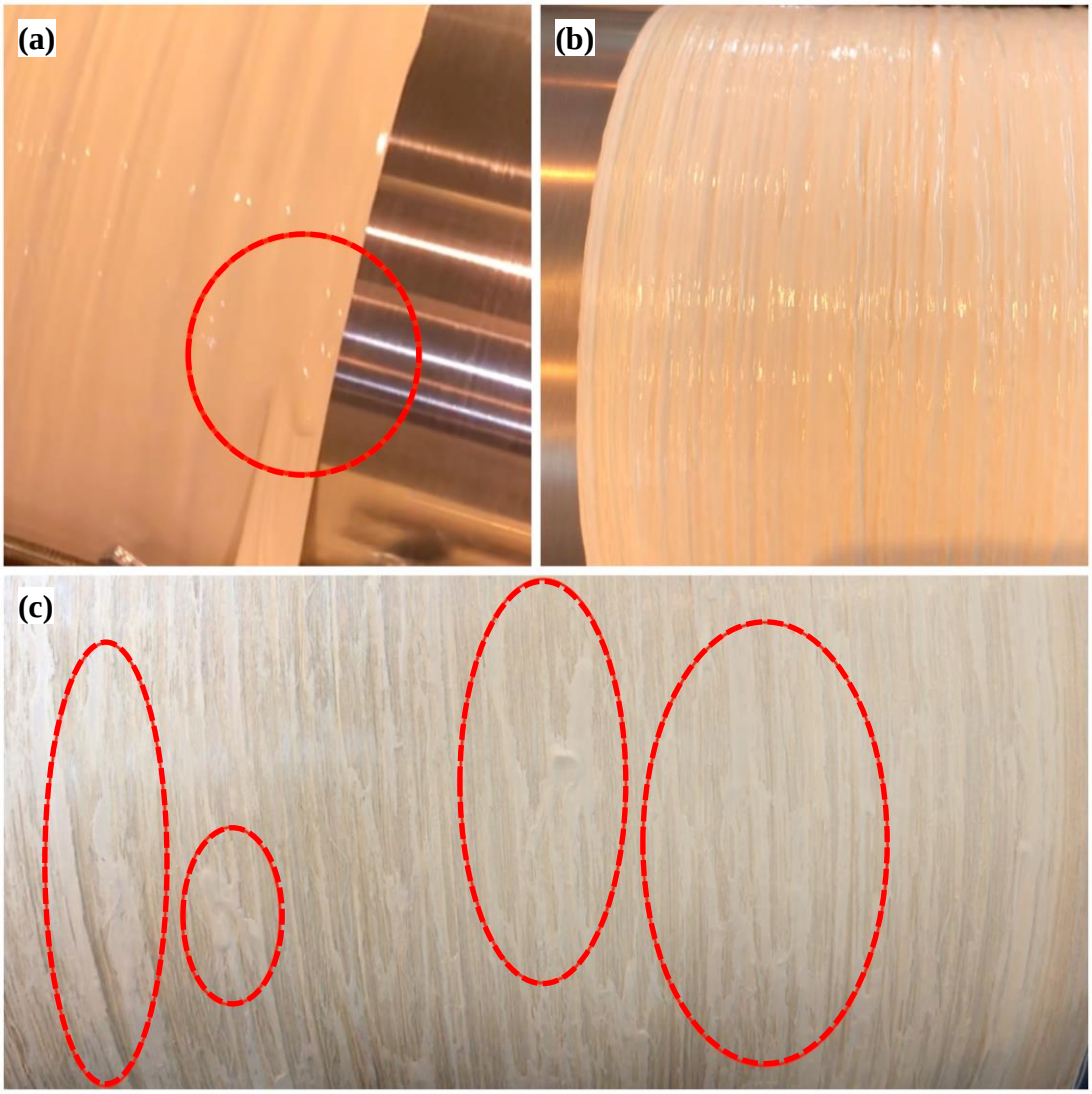

Figure 5.9 Winding problems at high winding speeds: (a) free slurry run on the drum, (b) heavy resin pick-up and (c) irregular prepreg surface after drying.

Higher winding speeds of 90 % (16.5 rpm) and 100 % (19.0 rpm) fosters additional drawbacks. As mentioned before, heavy resin pick-up by the fibre is observed during high speed winding. This is followed up by excessive build-up of PAEK powder on the spreading rollers as seen in Figure 5.10.

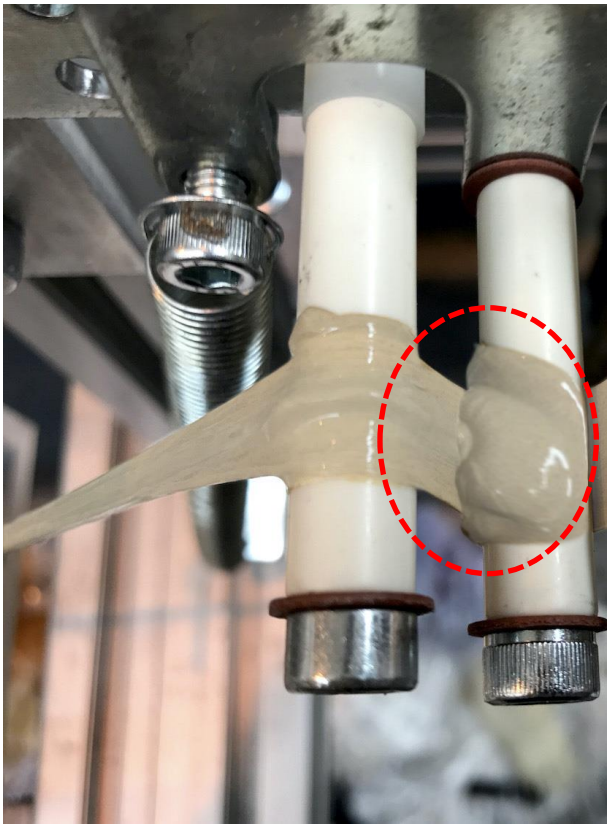

Figure 5.10 PAEK agglomeration around the rollers due to high winding speeds.

Resin agglomeration around the rollers affects the fibre spread effectiveness and also, results in fibre breakage in areas where PAEK powder is agglomerated. Fibre spread was observed to noticeably decrease when 80 % speed setting or more is employed, which basically counters the goal of increasing the width (cross-sectional length) of the impregnated fibre tow that plays an important role in PAEK penetration and prepreg thickness control. Due to this resin accumulation, shear stress and the frictional stress build-up associated with passing the fibre tow through condensed resin and spreading rollers can result in filament breakage and excessive fibre abrasion.

On the other hand, once S2-glass fibre filaments start to break, they also start tangling around the spreading rollers and consequently, creating a rough surface on the rollers. The S2-glass fibre used during this project is compatible with PAEK resin (933 sizing); however, it inherits high abrasive and brittle properties. As the glass fibres are very abrasive when they are in contact with other surfaces, the glass fibre tow that passes on another glass fibre surface (created by the fibre tangling around the rollers) is damaged, which will result in additional fibre breakage.

Previous findings indicate that very low or high speeds are not ideal. Therefore, winding speeds of 50 % (6.7 rpm) to 60 % (9.0 rpm) were tested as the golden mean. It is evident from Figure 5.11 that many of the problems associated with low and high speed windings are addressed when moderate speed setting is utilised. For instance, no obvious resin rich area was found, as a direct consequence of decreased free resin run on the drum. Also, no resin agglomeration on the rollers was observed throughout the entire winding process, which resulted in significantly less fibre breakage.

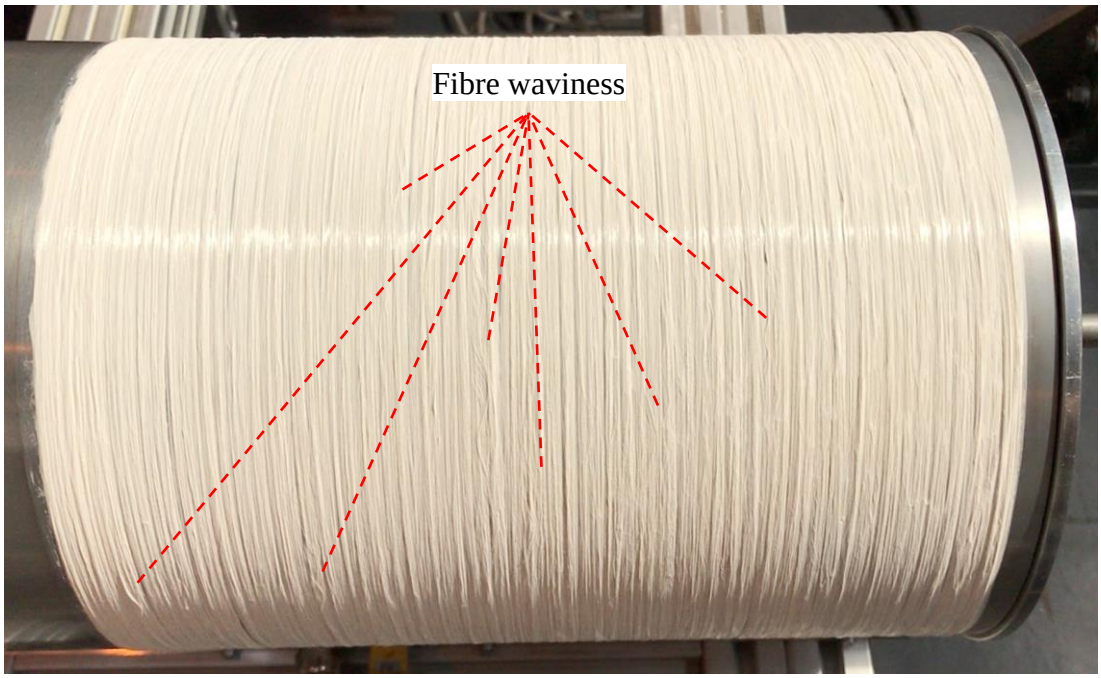

Figure 5.11 Fibre waviness observed during medium speeds and low tension settings.

It was concluded that winding speeds between 50 % (6.7 rpm) to 60 % (9.0) are the most beneficiary. Therefore, it was decided to choose the winding speed of 55 % (7.8 rpm) as the ideal speed for the winding process, for further tests, and for the manufacturing of prepregs.

All previous tests were conducted when the initial tensioning force is set to option 1 (0.8 N). One major problem that was discovered during the observations was the presence of considerable fibre waviness. As illustrated in Figure 5.11, the impregnated fibre tow displays waviness when wound on the drum. The curves in the reinforcing fibres are appalling and will considerably affect the mechanical performance of the

prepreg and consequently the laminated composite. This is because fibres tend to function better when they are held straight with less crimp. For this reason, other fibre tension settings were tested as well.

Figure 5.12 compares the quality of the winding when different tension settings are utilised. As discussed before, the fibre waviness, when the fibre tension setting is set to option 1 (0.8 N), can be attributed to the low initial tensioning force on the fibre tow and therefore, the formation of curves on the impregnated S2-glass fibres. By adjusting the initial tensioning force to setting 2 (1.3 N), the fibre waviness issue is tackled and the prepreg quality improves. Fibre breakage is also kept to a minimum with no obvious signs of resin agglomeration on the rollers or resin rich areas on the prepreg. When higher fibre tension settings, such as that 3 (2.3 N) or more is used, the fibre tow tends to wind up straight as expected. However, signs of fibre breakage were spotted on the material when the wound prepreg is dried. Increase in the initial fibre tension generates high pulling forces on the fibre roving. As the fibre passes through the rollers, this tension builds up and results in breaking of filaments. As filaments start to break (and tangle on the rollers), PAEK also gathers on the rollers, which initiates further fibre breakage. Broken filaments ultimately affect the mechanical properties of the composite such as the tensile strength.

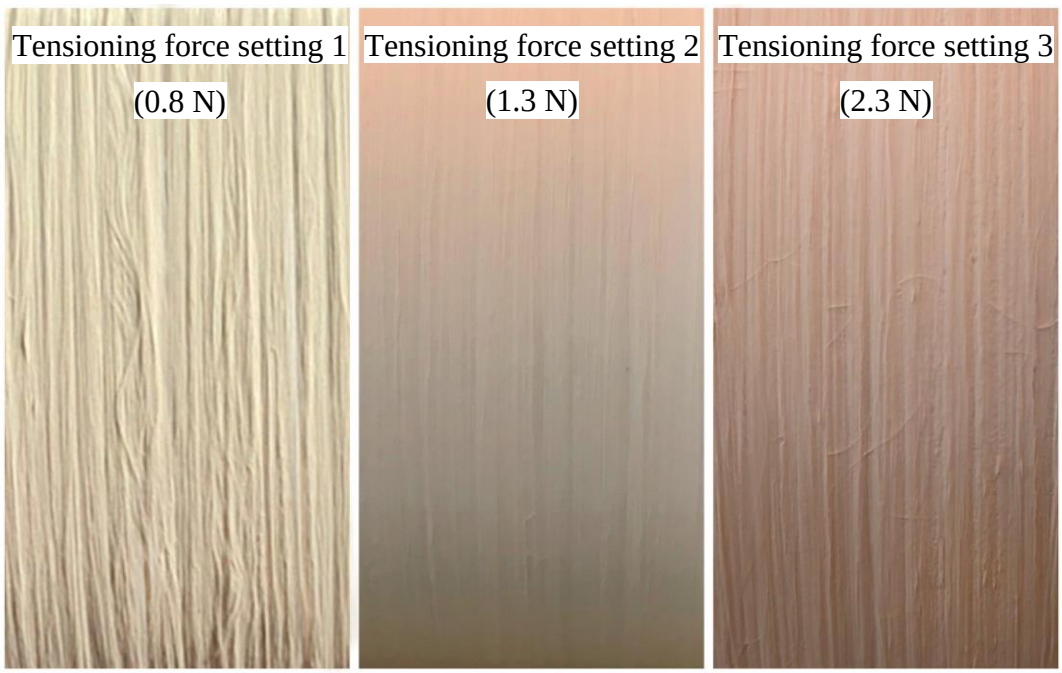

Figure 5.12 The effect of fibre tension setting on the quality of fibre winding.

It was therefore concluded that the initial tension setting on the package holder should be adjusted in a fashion to aid directing the fibre tow through different guides on the prepreg rig. Tension force should be just sufficient to hold the reinforcing fibre straight and excessive tension should be avoided. It was decided to choose setting 2 as the ideal tension for the winding process, for further tests, and for manufacturing prepregs.

5.2.3 Fibre Spread: The Effect of Frequency, Amplitude and Fixed or Rotating Roller

Fibre spread was one of the factors investigated in this study. The novel fibre spreader device is capable of spreading dry or wet fibre bundle and therefore control the thickness of the material. The main findings for the degree of fibre spread discussed below is for when the S2-glass picks up the PAEK slurry and is guided onto the fibre spreader (wet fibre spreading). However, some preliminary results from when the dry fibre is spread is essential to be discussed. Figure 5.13 showcases examples of effort to spread dry S2-glass fibres.

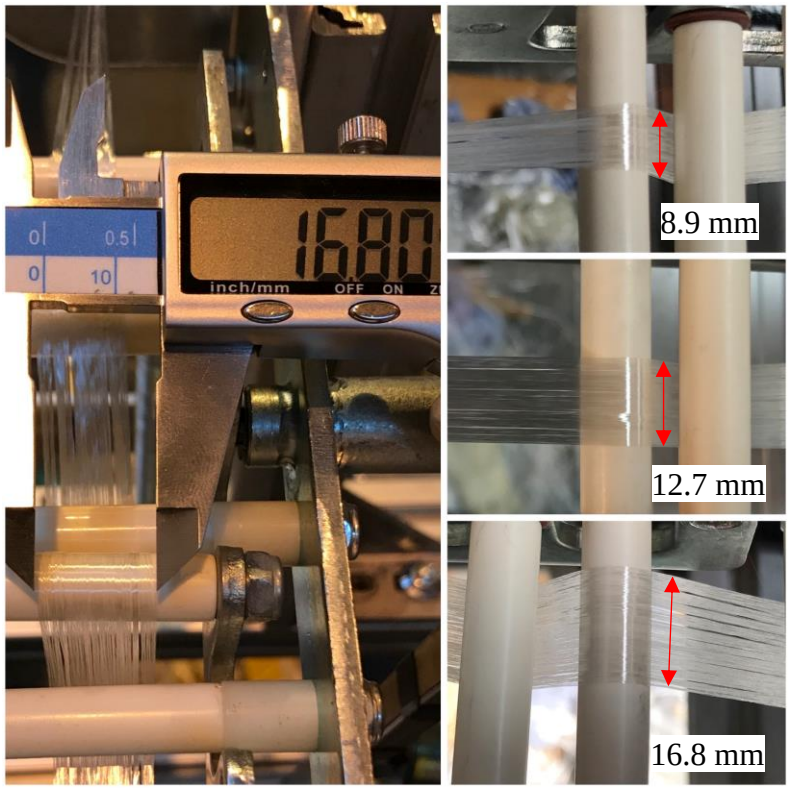

Figure 5.13 Examples of spreading S2-glass fibre bundle using the fibre spreader assembly.

As can been seen clearly in the figure, the fibre spreader is capable of spreading the S2-glass fibres to different tow widths. It is noteworthy to mention that there was no effort to thoroughly investigate the spread of dry fibre at this point and the main focus was on the effect of different fibre spreader setting in the degree of impregnated fibre spread. Regardless, testing different settings of the spreader, it was realised that fibre spreader assembly is definitely capable of completing the tension-cycles (as discussed in Section 3.6.3.2) and as the result, uniformly spreading the fibres. Fibre spread can vary depending on the factors adjustable on the spreader such as the frequency, amplitude and the type of roller used. Exercising some settings could result in a dry fibre spread, 4 to 7 times larger than the original fibre bundle width of 2.5 mm.

Wet fibre spread was studied extensively, and the results are presented in Figure 5.14. The results of the graph are for when a winding speed of 55 % (7.8 rpm) is used and the rollers are set to rotating. The average width of the fibre bundle when the fibre spreader was not in use was recorded as 3.5 mm. This is when the impregnated fibre tow only passes over the rollers with no reciprocal movements involved.

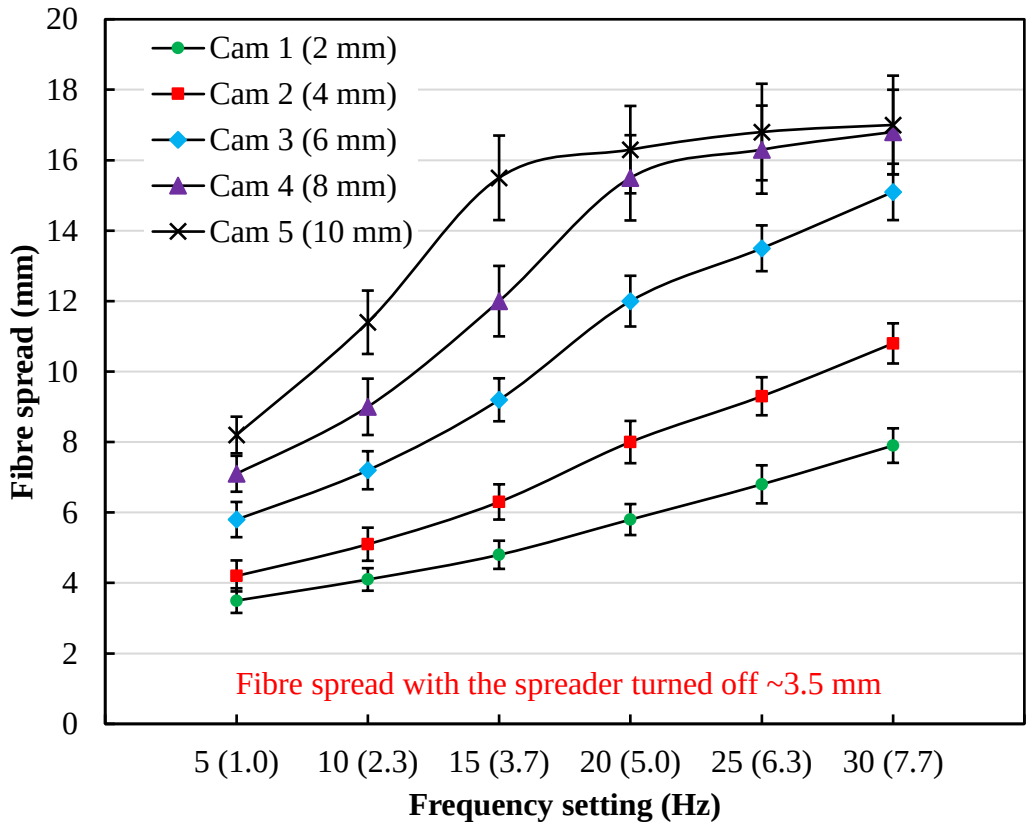

Figure 5.14 Effect of frequency and amplitude on the degree of fibre spread.

When the spreader assembly is utilised, frequency and amplitude of the vibration are subjects to change. According to the graph, the fibre spread is not significant when Cam 1 and 2 are used, which are correspondence to 2 and 4 mm amplitude, respectively. This is especially true for low frequency settings of 5 (1.0 Hz) and 10 (2.3 Hz). For instance, frequency setting 5 will result in 3.5 and 4.2 mm fibre spread when Cam 1 and 2 are implemented, respectively. For Cam 1, this value is the same as when the spreader is turned off. Trend lines of both Cam 1 and 2 indicate that both settings have a semi-linear behaviour; i.e. as the frequency increases, fibre spread degree also increases accordingly. The increase in fibre spread is observed up to the maximum frequency setting available, which is 30.

Similar trend is also visible when Cam 3 (6 mm amplitude) is utilised. One difference compared to Cam 1 and 2 is that even when low frequency settings are used, the fibre spread is noticeable. For example, the spread is 1.6 and 1.4 fold compared to when using Cam 1 and 2 respectively, with the corresponding frequency setting 5. As the frequency increases, the fibre spread also increases, however more rapidly, compared to Cam 1 and 2. At frequency setting 30 (7.7 Hz), the fibre spread can reach as high as 15.1 mm. That is 1.9 and 1.4 times more spread than when Cam 1 and 2 are used at the same frequency.

The established results from Cam 4 and 5, which are correspondence to 8 and 10 mm amplitude respectively, display a significant difference when compared to Cam 1, 2 and 3. It can be seen from Figure 5.14 that Cam 4 and 5 both have an ascending trend. However, the increase rate remarkably slows down after frequency setting 20 (5.0 Hz) for Cam 4, and after setting 15 (3.7 Hz) for Cam 5. It is evident from the graph that for frequencies more than 5.0 and 3.7 Hz for Cam 4 and 5 respectively, the fibre spread does not change much. This indicates that the degree of fibre spread apparently has reached its limit and therefore, further increase in frequency does not necessarily lead to higher fibre spreads. For instance, Cam 5 provides 15.5 mm of spread at frequency setting 15 and this values only increases by approximately 1.5 mm for when the maximum frequency is used. This clearly indicates that there is a limit to the amount of achievable fibre spread and further spreading of the fibre might not be practically possible using the existing fibre spreader or might require additional settings or tools.

Figure 5.15 exhibits examples of successful and relatively consistent fibre spread using the minimum and maximum frequency settings with Cam 3 for illustrative purposes. During the observations and data capture it was realised that for Cam 1, 2 and 3 all frequency settings could be used with no notable problem. The results indicate low variation in fibre width and no fuzz was generated on the spreading rollers as the result of the reciprocal movement. Moreover, no significant fibre breakage was observed on the winding drum.

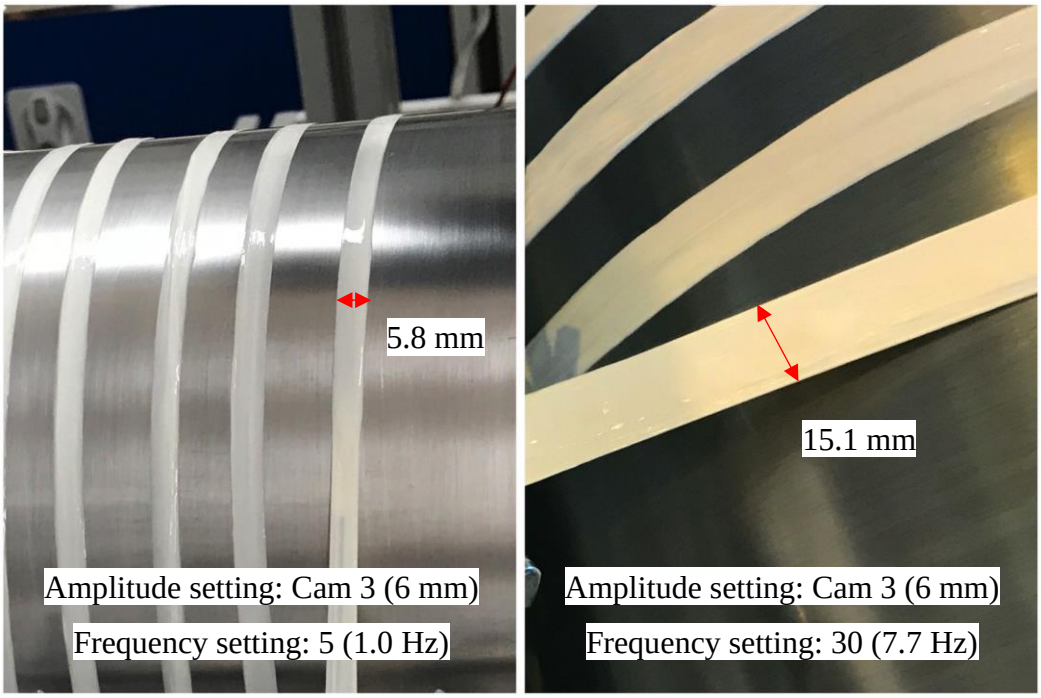

Figure 5.15 Examples of fibre spread using different frequency settings but similar amplitude setting (Cam 3).

On the other hand, Cam 4 and 5 manifest some restrictions when coupled with high frequency speeds. At frequency settings of 20 and over, the fibre bundle running throughout the winding process becomes unstable and, in some cases, impregnated fibre can deviate from the preordained fibre bundle passage. Fuzz can be created on the spreading rollers and damage to filaments is therefore inevitable. The result on the winding drum is a fibre spread with high variations, and in some cases fibre twists, creating filament entanglements and affecting the width consistency. Figure 5.16 is an example of such occurrence, in which Cam 4 was used in conjunction with frequency setting 20.

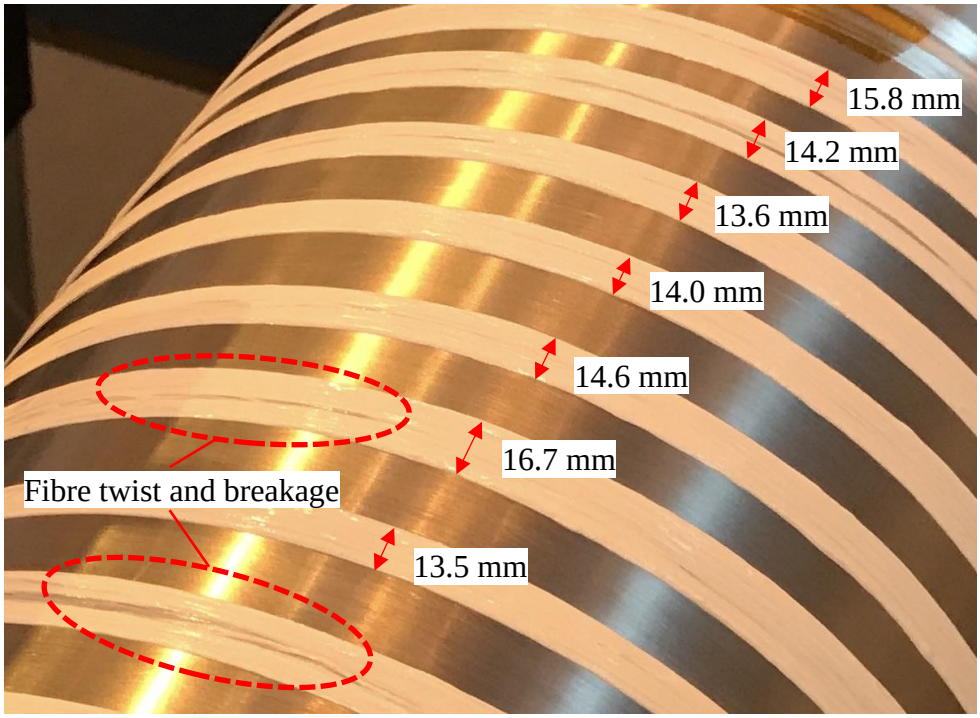

Figure 5.16 Problems with high amplitude together with high frequency settings.

Thus, it is evaluated that Cam 3 provides a good balance between fibre spread effectiveness and practicability. It provides grounds for spreading the fibre tow up to 6 times the original width. Therefore, it was decided to choose Cam 3 as the ideal amplitude on the fibre spreader for the winding process and for further tests on the manufacturing of prepregs. In the next section, the effect of fixed rollers on the level of spread is investigated, while utilising Cam 3 and only tampering the frequency.

Figure 5.17 shows the effect of static roller on the degree of fibre spread. It is evident from the chart that using fixed rollers can significantly increase the amount of fibre spread. At high frequencies such as 25 (6.3 Hz) and 30 (7.7 Hz), fibre bundle width can increase up to 57 %, with respect to the corresponding spread value of rotating rollers. This enhancement in the fibre spread is quite remarkable as it provides the basis for producing very thin ply prepregs. This trend is valid for all other frequencies; however, as the frequency increases, the grow rate of the spreading width declines. That is to say the largest growth in fibre spread corresponds to the frequency setting 5 with a 76 % increase. The highest value of fibre spread was observed during the highest frequency, in which the impregnated fibre tow was spread up to an average value of 23.5 mm, as seen in Figure 5.18.

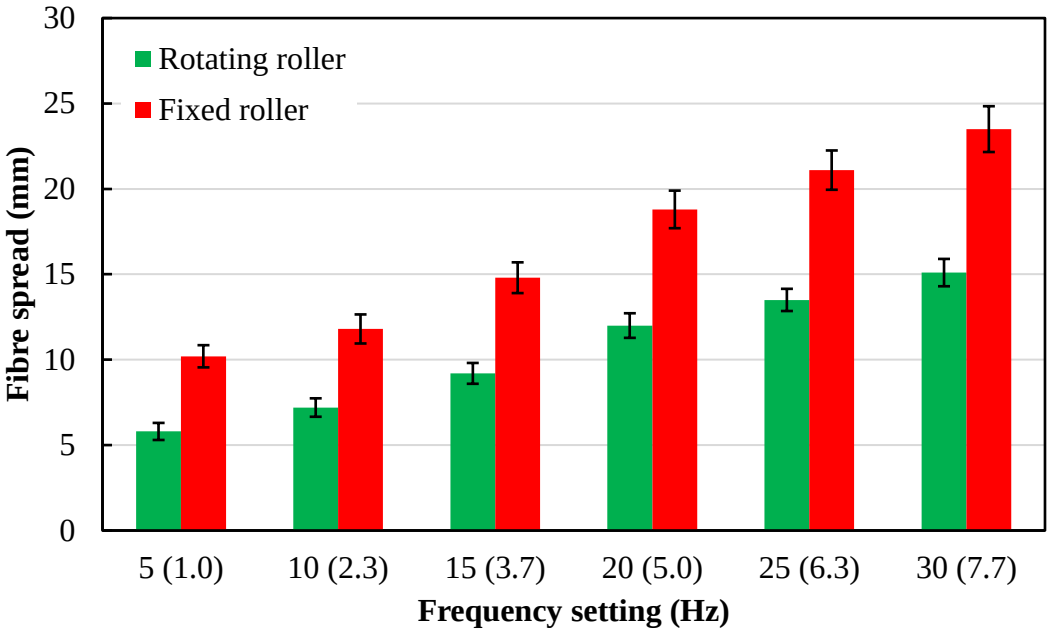

Figure 5.17 Comparison between rotating rollers vs fixed rollers in fibre spreading using Cam 3.

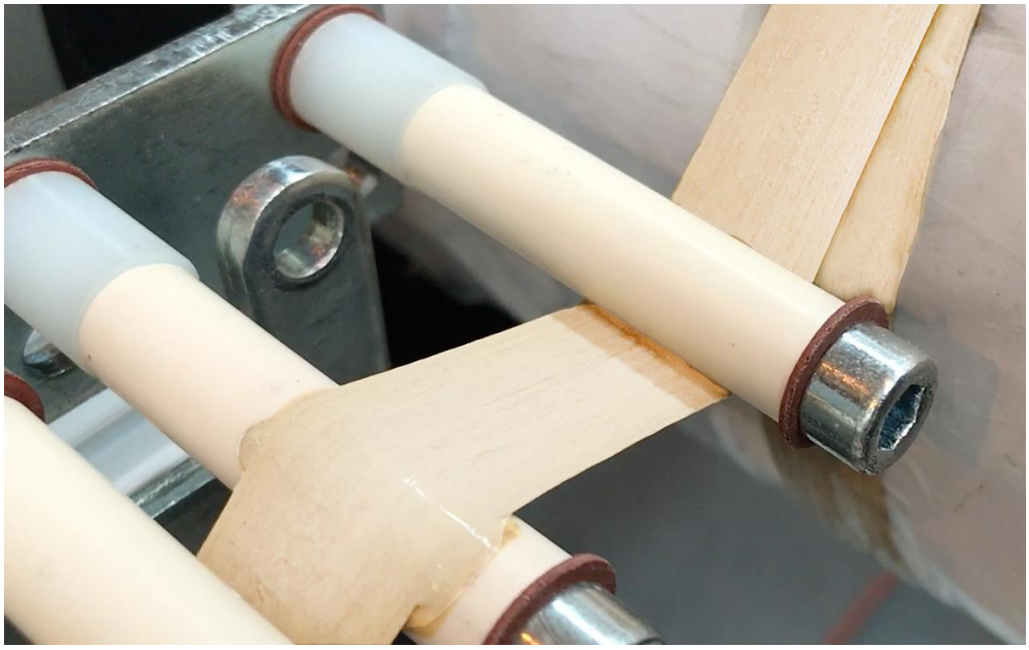

Figure 5.18 Spread of 23.5 mm achieved with fixed rollers and frequency setting 30.

The use of fixed rollers is however not without problems. As the fibre is guided on the spreading rollers, the tension increases. This increases in tension are getting higher when the rollers are set to fix rather than rotating. Higher tension results in greater forces on fibre filaments and eventually leads to fibre breakage and creation of fuzz on the rollers. Moreover, due to rollers being stationary, PAEK resin is not able to

rotate with the roller and consequently, starts building up on the rollers. This PAEK agglomeration results in further intensification of the fibre tension and also creates additional filament breakage.

In order to control the spread of the fibre and subsequently achieve a consistent and accurate fibre bundle width, grooved guide rollers can be used as the interchangeable end roller to limit the amount of fibre spread by the spreading device. Here, 5 or 10 mm grooved end rollers can be utilised, and they were implemented in the experiments as can be seen in Figure 5.19. The thickness of the prepreg, which is one of the important physical factors, can be controlled and adjusted in this way to reduce the thickness variation of the final prepreg material for a further consistent product.

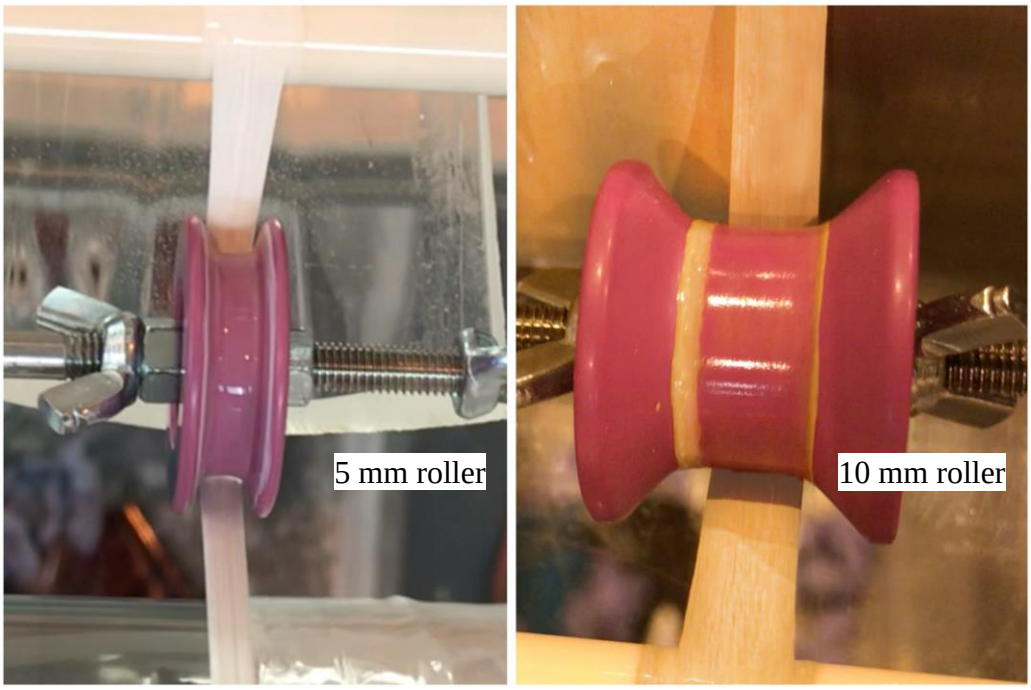

Figure 5.19 Fibre spread control by using 5 and 10 mm grooved guide rollers.

It was decided to limit the fibre spread and use the 5 mm roller for the resin pick-up tests (discussed in the next section), and also for manufacturing of prepregs. The main reason was the produced prepreg would have ultra-low thickness if high spread settings are used, which means the requirement of numerous plies for fabricating the needed number of composites laminates. In other words, this requires running the prepreg rig too many times just for producing a single laminate when the ply thickness

is too low. This problem emerges only due to the time limits of this project. In addition, the problem forecasted with using the 10 mm grooved guide for manufacturing prepregs was the uncertainty around the spread of fibre tow for lower PAEK–L2O ratio, i.e. 10 wt% PAEK slurry. As mentioned before, 20 wt% PAEK slurry was used for all aforementioned results in the fibre spread test and the effect of different PAEK–L2O ratios on the degree of fibre spread was not investigated. It is predicted that in the similar spreading settings and conditions, 10 wt% PAEK slurry fibre tow would spread less than the corresponding spreading values of 20, 30 and 40 wt% ratios. This would obviously be due to less availability of PAEK particles in 10 wt% PAEK slurry, acting as spacers to penetrate the fibre bundle and cause the fibre tow to spread.

5.2.4 Resin Pick-up Test Results

Resin pick-up test was conducted to verify the consistency of the winding process from when the fibre tow picks up the PAEK slurry and is wound on the drum. The goal would be to identify whether the fibre bundle collects a constant amount of resin up until 10 meters of rig running (approximately 16 revolutions of the drum). Here, only the PAEK–L2O ratio is changed, and other variables are kept constant. Figure 5.20 exhibits the results recorded from the four PAEK–L2O ratios that were tested.

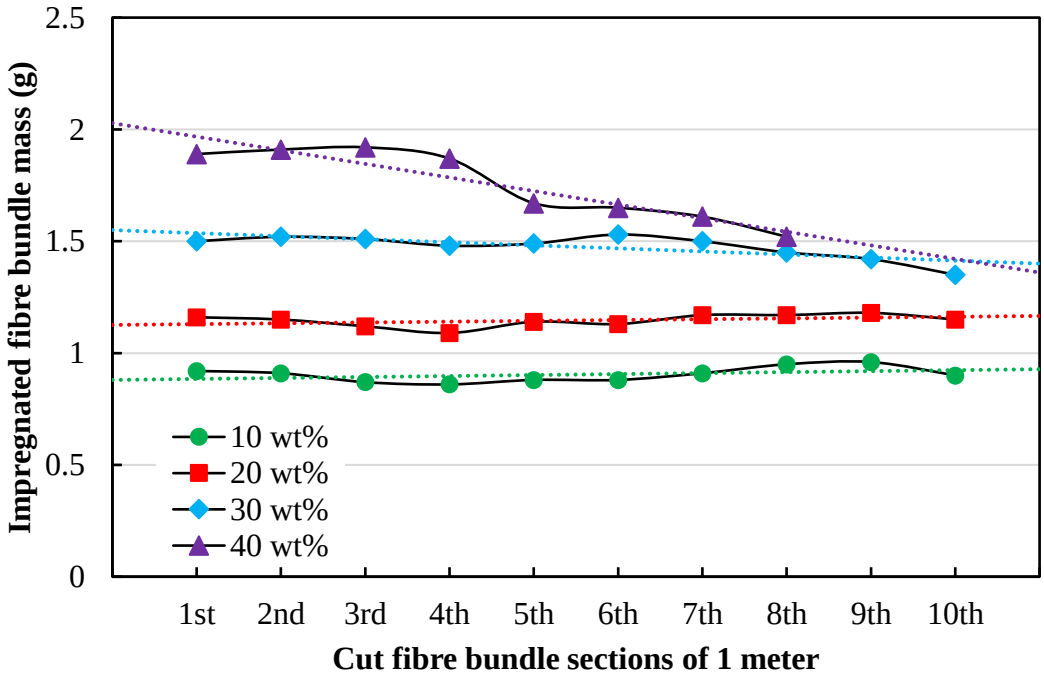

Figure 5.20 Consistency check of the impregnation process by resin pick-up test.

It is indicative from the figure that 10 and 20 wt% slurry provides a very consistent collection of PAEK slurry throughout the impregnation process. For 10 wt% slurry, the impregnated fibre mass tolerance is within ±0.05 grams with a standard deviation of 0.03. Similar trend was observed for 20 wt%, recording a standard deviation of 0.03 as well. This fashion is slightly different in 30 wt% samples and as can be seen in the figure, it has a slight downward trend. The reason of this descending order lies on the fact that for 30 and 40 wt% PAEK slurry, resin agglomeration was observed on the spreading rollers, consequently increasing the fibre tension and breaking fibre filaments. Fuzz was created on the rollers and filaments start to tangle around the rollers. Ultimately, what emerges next is less and less fibre filament being wound on the drum and the impregnated fibre bundle starts losing mass. In the extreme circumstances, fibre bundle is cut off due to high fibre loss and high fibre tensions. This circumstance is even more obvious in 40 wt% slurry trend line, as evident in Figure 5.21, heavy agglomeration is occurred when these resin systems are experimented.

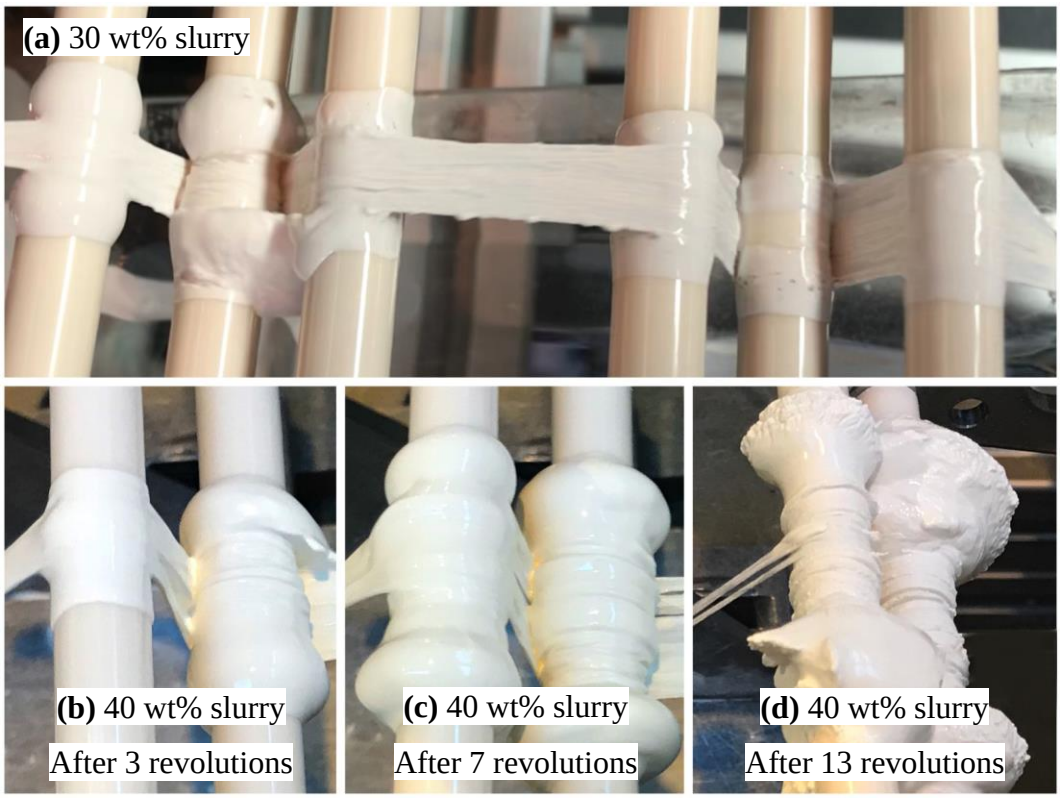

Figure 5.21 Resin agglomeration on spreading rollers: (a) 30 wt% slurry system and (b–d) 40 wt% slurry system.

As shown in Figure 5.21(a), resin agglomeration is observed throughout the winding process when 30 wt% resin is used. It is clear from the figure that the first two rollers accumulate the most amount of slurry as expected, since PAEK powder is squeezed off the fibre bundle as it travels through the impregnation rollers. Figure 5.21(b) to (d) demonstrate the same trend for 40 wt% resin system, however more aggressive. After only 3 revolutions of the drum, a heavy slurry agglomeration is observed. Fibre entanglement around the rollers and creation of fuzz leads to fabrication of a rough surface on the rollers and causes further resin gathering and filaments splitting. After approximately 13 revolutions (8 meters of winding), resin agglomeration and fibre tension become so severe that a majority of fibre filaments are broken. Hence, the winding is stopped after around 13 revolutions for the 40 wt% resin setting.

Grade 933-AA-750 S2-glass has a linear density of 675 g/1000m (TEX) and therefore, a 1-meter-long section of the dry fibre bundle would have a mass of approximately 0.68 grams, which was also confirmed in-house by experiment. Figure 5.22 shows the calculated data of the PAEK mass fraction in the impregnated fibre bundle for different resin systems.

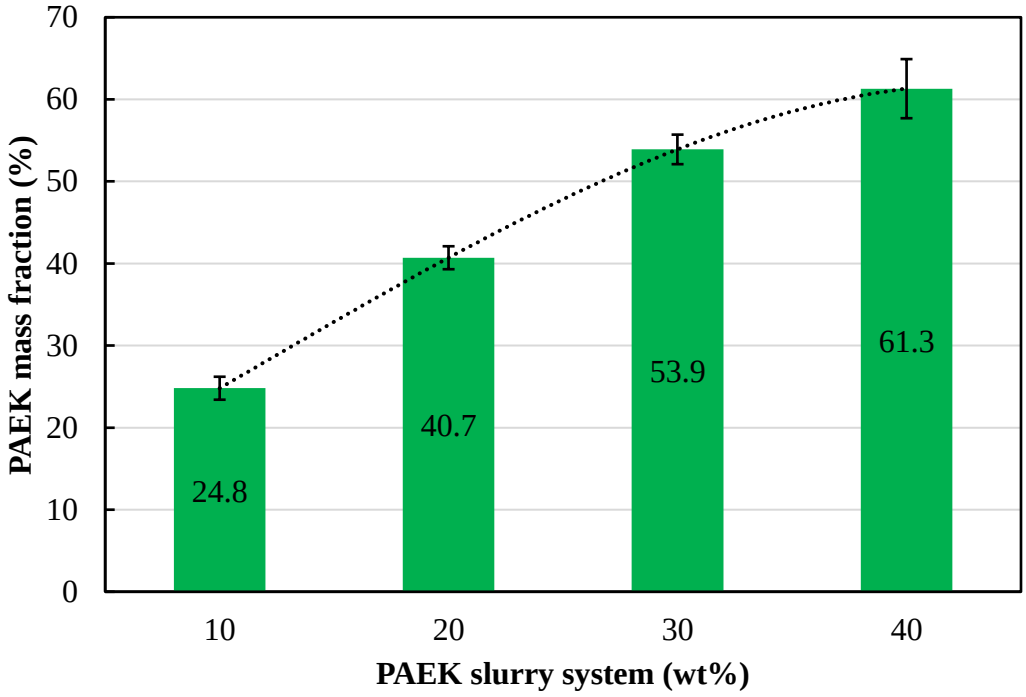

Figure 5.22 PAEK mass fraction of the impregnated fibre for different slurry systems.

The figure illustrates that in average, 1 meter of impregnated S2-glass with 10 wt% slurry would pick up approximately 0.22 grams of PAEK, which counts towards 24.8 % of the overall mass. The rise in the PAEK mass fraction seems having a relatively linear trend; however, there is a decline in gradient between 30 and 40 wt% settings. It can be presumed that the higher PAEK–L2O ratios (if practically possible to implement) will have a less effect on the amount of PAEK picked-up by the fibre.

It was concluded that 40 wt% PAEK–L2O ratio is too viscous for prepreg manufacture and would cause numerous problems as previously mentioned. This resin setting was therefore withdrawn from any further experimentation. Although the 30 wt% PAEK–L2O ratio was also found problematic with regards to resin agglomeration, it was realised that with an effort to slightly remove the accumulated resin manually from the rollers, one can proceed with the winding process for half the length of the drum and thus, manufacturing of prepreg is just made possible. The extent of consistency of the prepreg materials is realised in the following sections.

5.3 Unidirectional S2-Glass/PAEK Composite

Three tiers of S2-glass/PAEK prepregs were manufactured using the AE 250 PAEK powder as the main polymer with different PAEK–L2O ratios of 10 wt%, 20 wt% and 30 wt%, as previously agreed upon. Several attempts were also made to manufacture 20 wt% prepregs by utilising PEK grade G-PAEK 1100PF, and also a PEK/PBI blend GAZOLE 6200PF. Using carbon fibre as the reinforcing fibre was also investigated. Before moving on to the main results for the primary AE 250 resin prepregs, some preliminary results for PEK, PEK/PBI and CF are discussed.

Both PEK and PEK/PBI were discarded in early stages of the project due to problems and limitations they imposed. Although both grades are capable of being used for the preliminary tests (due to having the same particle size as the AE 250), they show some disadvantages when used for manufacturing prepregs. Having a melting point of 372 °C, their processing temperature is approximately 390–400 °C for the PEK and 420–440 °C for the PEK/PBI blend, which are much higher than AE 250 PAEK. PBI polymer has a T_g exceeding 400 °C and for this reason, it requires a very high processing temperature and pressure.

Figure 5.23 shows the first problem encountered while using PEK and PEK/PBI resins. Experiments suggested that both grades manifest releasing problems. In other words, the prepreg showed difficulty releasing from the winding drum when heat melt the polymer for permanent consolidation. This problem also persisted in the lamination stage, where the stainless steel plates sticked to the laminated composite. Employment of high-temperature Kapton film in conjunction with the release agent also did not provide a better release. As seen in the figure, laminate stuck onto both steel plates and the film and undesirable force was needed to extract the composite. This problem however might be associated with the release agent employed. Typical release agents utilised in composite industry might start cross-linking in very high temperatures, resulting in a difficult release of the sample from the moulding tool. That said, no releasing problem was observed when using AE 250 as the resin matrix.

Figure 5.23 Releasing problems associated with utilising PEK and PEK/PBI.

It is noteworthy to state that no further effort was carried out to tackle the aforementioned releasing issue as both PEK and PEK/PBI illustrates further drawbacks. Due to their very high viscosity, S2-glass laminates from both grades

contain very high void contents. Figure 5.24 is a preliminary micrograph image of a laminate sample manufactured using PEK/PBI matrix with a processing temperature of 420 °C, a processing pressure of 10.5 bar and a holding time of 20 minutes.

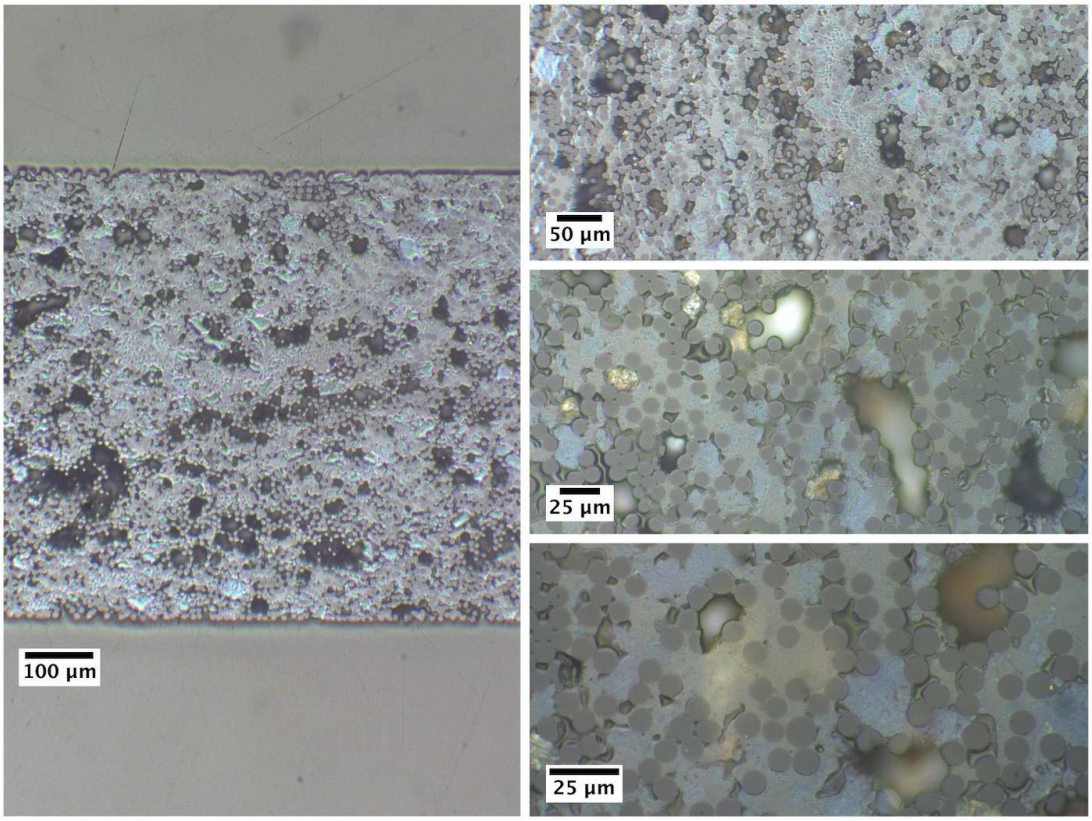

Figure 5.24 Cross-sectional micrograph of a PEK/PBI matrix laminate.

No attempts were made to measure the exact void content. However, the figure clearly demonstrates the flaws in the laminate. There exist void areas as large as 0.01 mm^2, which is not desirable and will ultimately deteriorate the mechanical performance of the composite material produced in this way.

For demonstration purpose, CF was also used as a reinforcing fibre in the prepreg rig. Figure 5.25 showcases an example of CF being processed in the prepreg rig by going through 20 wt% PAEK resin and winding on the drum before curing. Subsequently, the resulting prepreg was cut into pieces, stacked in a mould and was processed by hot compression moulding to produce the composite laminates. At this point, it is clear that the rig is capable of producing CF based composite prepregs. As this trial was only for demonstration purposes, no attempts were made to characterise the resulting

prepreg or laminates. S2-glass remains the primary reinforcement throughout this project.

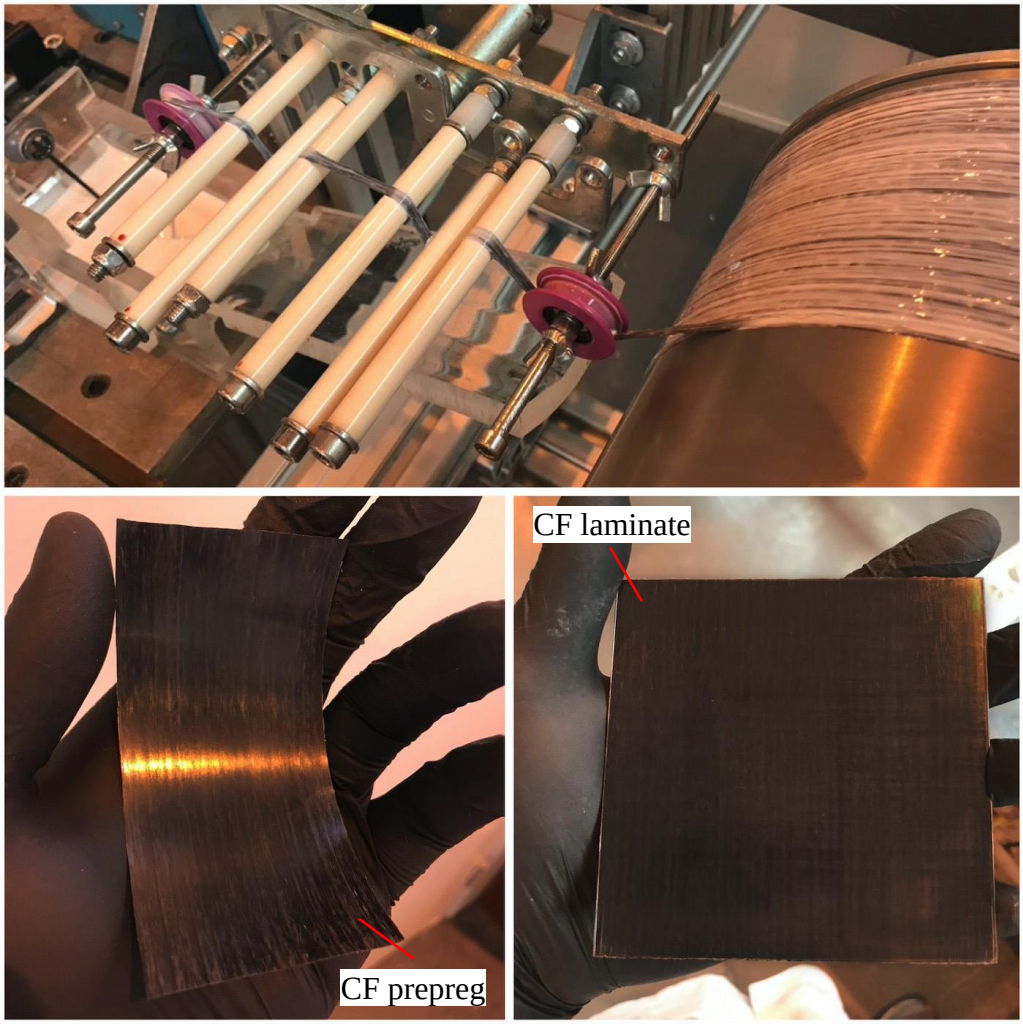

Figure 5.25 Prepreg rig trial with carbon fibre as the reinforcing fibre.

5.3.1 Physical Properties of the Prepreg

Here, 10, 20 and 30 wt% AE 250 PAEK prepregs were manufactured using S2-glass fibre as the main composite material being studied in this research. Figure 5.26 shows 100 x 100 mm prepreg specimen for each PAEK sample category. In the first instance all three sample types look visually similar, with a slight enhancement in the colour tone as the PAEK ratio increases. Between the utilised PAEK–L2O ratios, it was previously mentioned that processing 30 wt% PAEK–L2O slurry leads to a few problems, which in return, affects the prepreg produced.

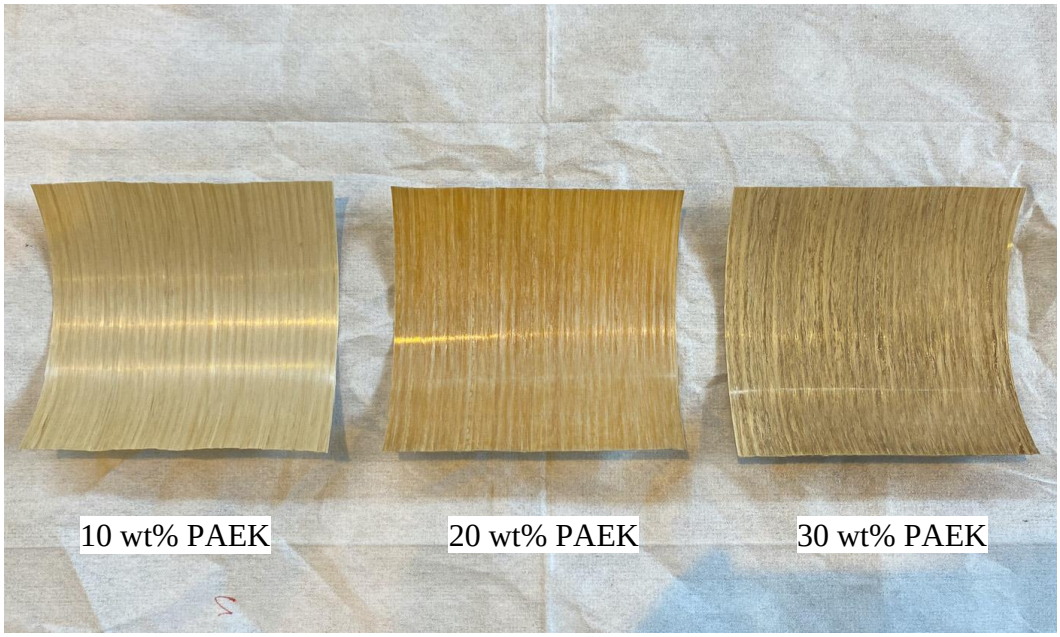

Figure 5.26 Sample 100 x 100 mm prepreg plies for each PAEK category.

By visually checking 30 wt% prepreg plies, some flaws can be noticed. Figure 5.27 demonstrates various irregularities on the surface of the prepreg. This includes fibre waviness and resin rich areas that lead to high variation of the ply thickness. Fibre breakage is also visible in some parts.

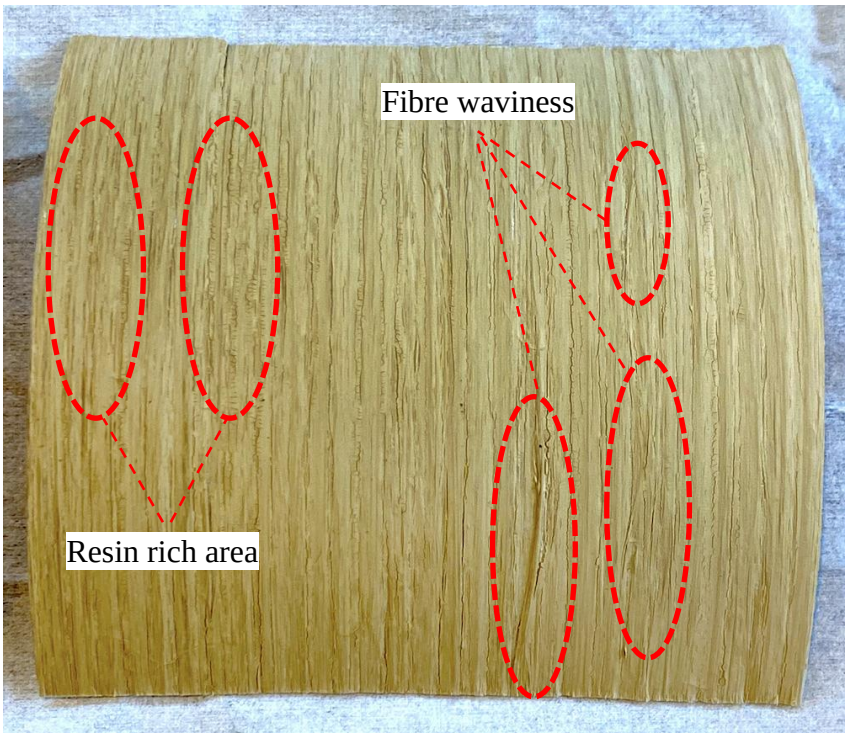

Figure 5.27 Production defects associated with 30 wt% PAEK prepregs.

It is believed that the events during the winding process lead to the abovementioned flaws in 30 wt% PAEK prepregs. Resin agglomeration on the spreading rollers during the winding process can markedly affect the quality of the prepreg manufactured and cause such defects in the final product. Regardless, 30 wt% prepregs were still employed in this study for manufacturing composite laminates and undertaking a number of physical and mechanical characterisations.

5.3.1.1 Prepreg Areal Weight and Thickness: Effect of Different PAEK–L2O Ratio

After the manufacture of prepregs, it is essential to obtain some physical characteristics of the composite. Figure 5.28 shows the average prepreg areal weight (PAW) and thickness for the three different PAEK–L2O ratios employed.

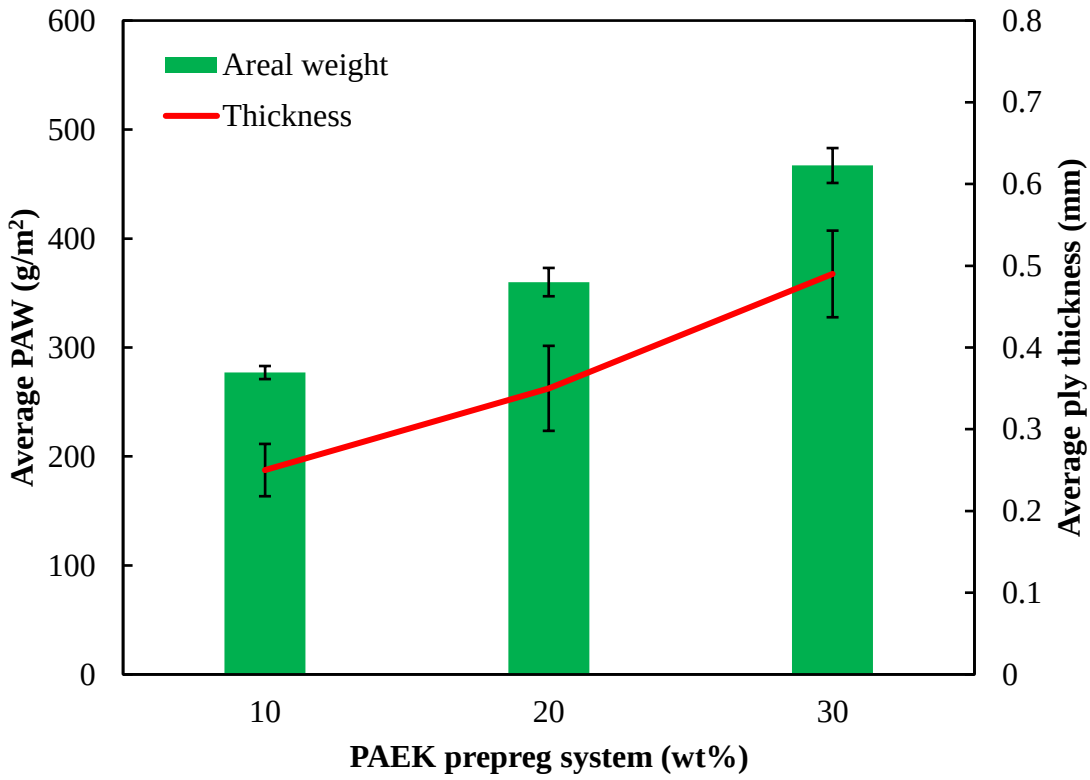

Figure 5.28 Comparison of areal weight and thickness for prepregs with different PAEK–L2O ratio.

For obtaining the results stated in Figure 5.28, the prepreg rig was used to manufacture at least 5 batches for each PAEK–L2O setting. Each batch produces a single prepreg sheet on the drum, which can be cut into a maximum of 24 prepreg specimens with a dimension of 100 x 100 mm if the winding transverse is fully completed.

It is clear from the graph that with the increase of PAEK content in the resin slurry, PAW and thickness of the prepreg increases. This growth is almost linear for both PAW and thickness as expected from the findings in Section 5.2.4. It is observed that for 10 wt% slurry prepregs, PAW and thickness variations are noticeably less than of the values for 20 and 30 wt% prepregs. Average PAW value for 10 wt% prepregs is measured at 277 (±2.2 %) g/m^2 and average thickness is recorded at 0.25 ± 0.03 mm. These variations are slightly higher for 20 and 30 wt% prepregs, however. For instance, average PAW for 30 wt% prepregs is 467 (±3.5 %) g/m^2 and average thickness is observed at 0.49 ± 0.05 mm. The higher tolerances for 30 wt% prepregs could be associated with the production problems mentioned in Section 5.3.1 regarding resin agglomeration around the spreading rollers.

Overall, the recorded values indicate a good product consistency and demonstrates the prepreg rig is reliable in this manner. It is realised that the rig benefits from a constant resin pick-up by the fibre and this consequently results in a relatively homogenous prepreg material.

5.3.1.2 Cross-sectional Micrographs

Micrographs were produced from longitudinal and transverse cross-sections of 10, 20 and 30 wt% prepreg plies to observe the extent of polymer particle infusion into the fibre bundle and homogeneity of fibre/matrix distribution. Figure 5.29 shows micrographs of three cut and stacked specimens from random parts of three prepreg plies with different PAEK ratios of 10, 20 and 30 wt%.

Obviously, gas bubbles can be observed in all three categories. The S2-glass fibre impregnated with the PAEK polymer only comes to meet with the spreading rollers as means for resin impregnation. No other impregnation assisting means such as compaction roller is used before the wet fibre tow is wound on the drum, or, after the prepreg is wound on the drum with polymer in wet or molten condition. Therefore, such void areas are inevitable unless a considerable compressive force is deployed on both sides of the prepreg plie. These void contents are slightly higher in 30 wt% prepregs, which can be attributed to high slurry viscosity and consequently, more difficult PAEK impregnation compared to 10 and 20 wt% slurries.

Another notable factor studied during the observations is the thickness variations in all three prepreg types. Thickness tolerances are unavoidable due to the nature of the manufacturing process. As discussed in Section 4.3, impregnated fibre tows are wound on the drum with slight fibre-overlap. This overlap has proved to be crucial by helping to eliminate any possible gaps between fibre tows while winding. This however will not affect the average ply thickness significantly. Regardless, some cracks and fractures observed in the prepreg micrographs can be attributed to possible mishandling of the prepreg plies when cut, or any damages tolerated during the polishing process.

As evident from Figure 5.29, top side of the prepreg plies showcases a rougher surface in comparison to the bottom surface, i.e. the lower side of the prepreg is much more flat. The reason behind the smoother side is that the lower part of the prepreg is in direct contact with the winding drum, which has a smooth and flat surface. Therefore, the prepreg would achieve a much straighter bottom surface compared to the top surface after final consolidation in the oven.

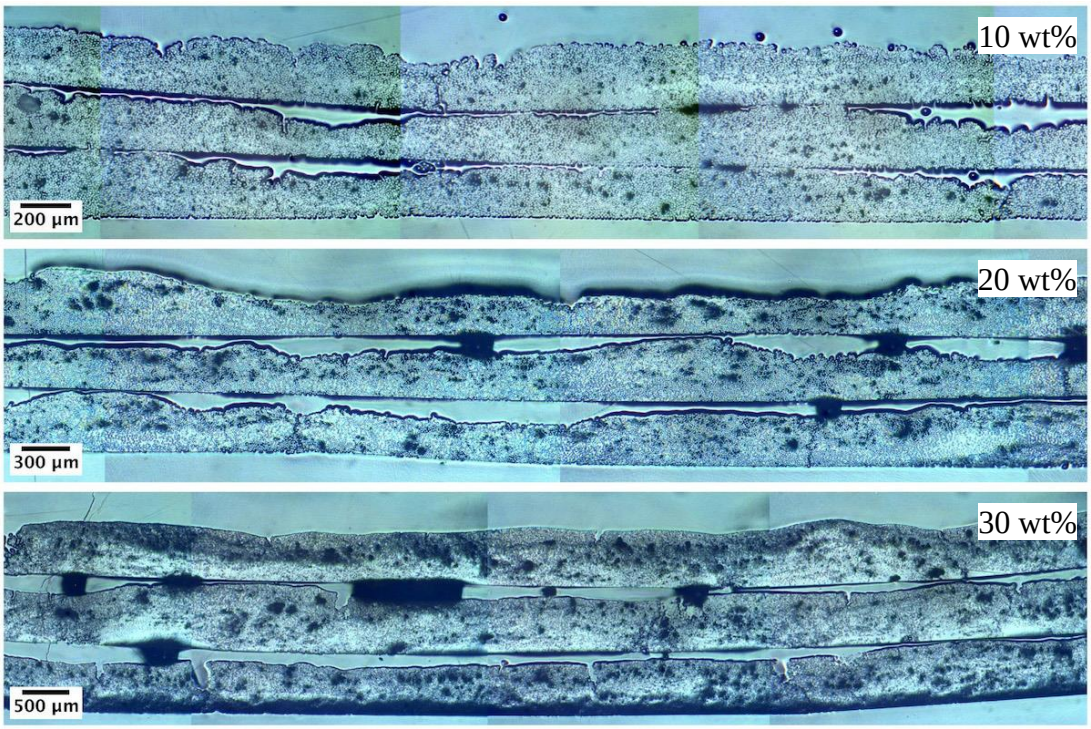

Figure 5.29 Cross-sectional micrographs of prepreg plies with different PAEK–L2O ratio.

Despite the gas bubbles observed in the prepregs cross-sections, PAEK particles are fully infused between the S2-glass fibres, as illustrated in Figure 5.30. Since the transverse cross-sections only demonstrate a 2D plane of the sample, longitudinal sections were also studied. All three categories show a great degree of powder infusion. Effective fibre impregnation is particularly important in 10 wt% prepregs, as the amount of PAEK particles in the prepared slurry is much lower than 20 and 30 wt% ratios. It is evident from the figure that PAEK particles have reached the centre of the glass fibre tow in 10 wt% prepregs. Same trend is observed in 20 and 30 wt% prepregs.

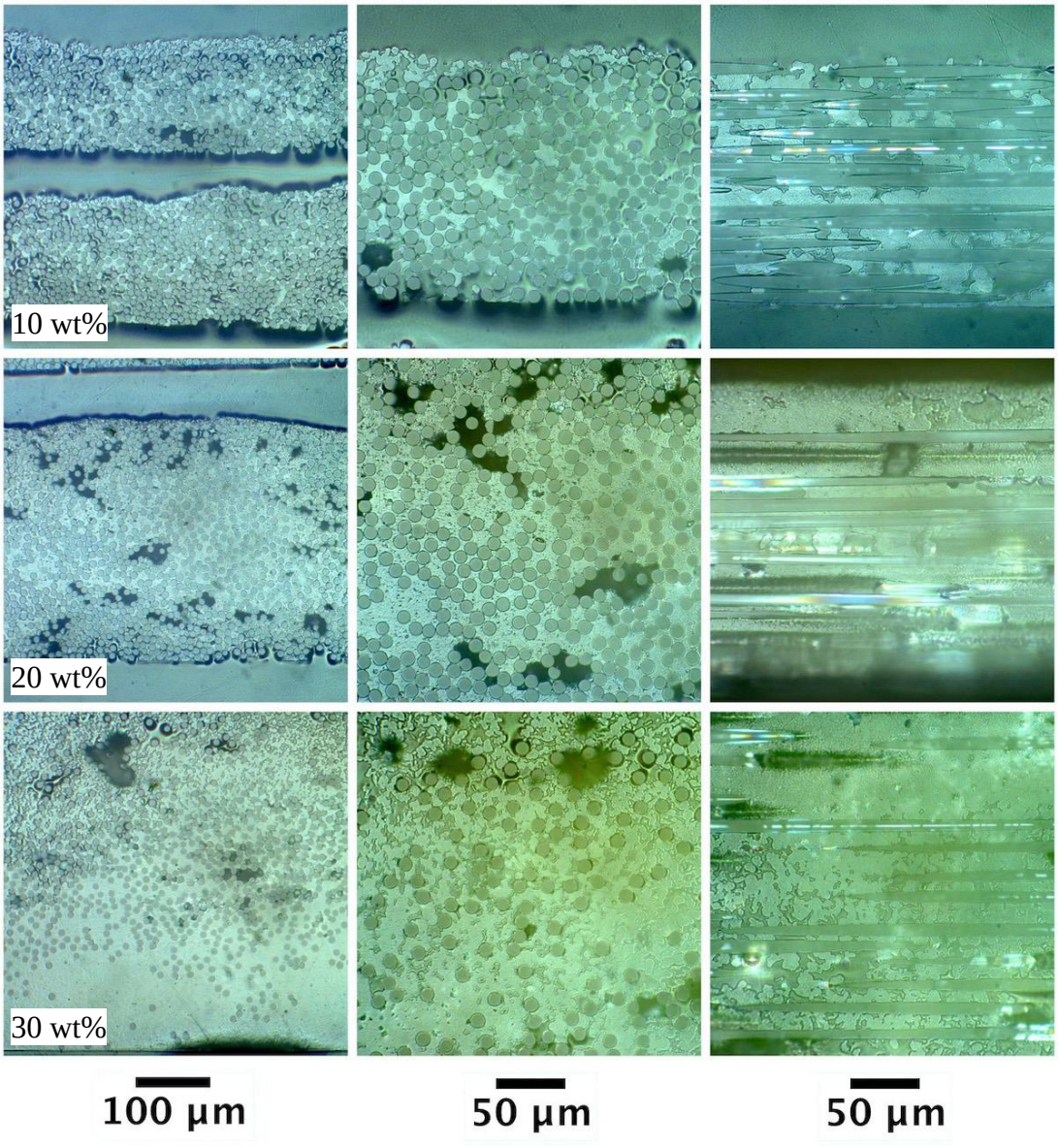

Figure 5.30 A closer look at transverse and longitudinal prepreg cross-sections to observe the degree of PAEK impregnation.

Looking closely at the pictures, it can be seen that the concentration of PAEK can sometimes be higher on the top surface of the prepreg. This can be attributed to the slight running of the resin slurry on the winding drum when the impregnated S2-glass fibre tow is processed, despite the previously mentioned efforts to tackle this problem. The tensioning force exerted from the winding drum on the impregnated fibre bundle also affects the distribution by pushing the PAEK particles towards the outer surface of the prepreg and leaving more fibres closer to the surface of the drum.

Another observable factor in higher magnification micrographs is the presence of singular and agglomerated PAEK particles between the fibre filaments. This is a good indicator that the PAEK particles are very well suspended in the liquid carrier without considerable agglomeration. Otherwise, such high degree of powder impregnation was not practical. Therefore, the use of ~10 micron PAEK particles is proved beneficiary in this instance.

Lastly, the 30 wt% prepregs show obvious resin rich areas in their cross-sections. The nature of such flaws in 30 wt% PAEK ratio prepregs is usually connected to the problems associated with the prepreg manufacturing process such as agglomeration of resin on the spreading rollers and fibre waviness. In the next sections, it is realised that the quality of 30 wt% prepregs will also affect the physical and mechanical properties of the corresponding manufactured laminates.

5.3.2 Physical Properties of the Laminate

UD laminates were produced using 10, 20 and 30 wt% PAEK prepreg plies by the method of hot compression moulding. Figure 5.31 demonstrates a sample of each laminate after extraction from the moulding tool. The 10 wt% laminates are brighter in colour compared to 20 and 30 wt% due to having higher volume of S2-glass fibre. It is worth pointing out that the surface of the moulding tool that is in direct contact with the composite (stainless steel plates), directly contributes towards the colour tone and surface finish of the laminate. After several extractions, the surface of the mould also dims and could result in colour changes in the surface of the laminate. This shall in no way affect the physical or mechanical tests undertaken and the properties.

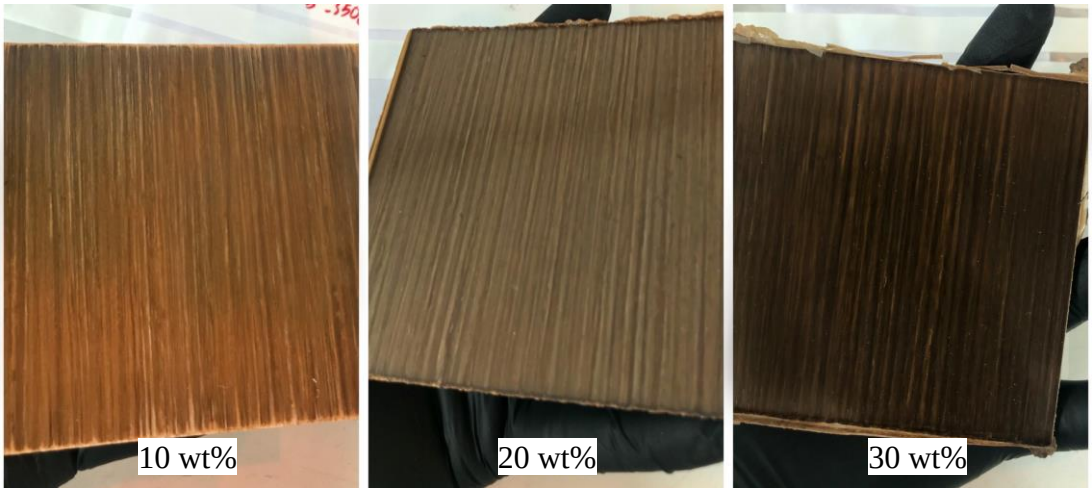

Figure 5.31 Sample 10, 20 and 30 wt% laminates.

As the manufactured composites investigated in this study are novel materials, characterisation is crucial for understanding the behaviour of the material. Physical properties are discussed in the following sections.

5.3.2.1 The Effect of Processing Pressure and Time on Fibre Volume and Void Content

Perhaps, one of the most important properties of composite laminates is the proportions of the matrix and reinforcing fibre. Usually, this ratio is assigned by considering the fibre volume content of the laminate. There always exists a fraction of the overall volume that is gas, trapped inside the matrix, although very minute. This void content can significantly affect the performance of the composite material and therefore is a factor discussed here. Thus, it is important to realise the optimum processing criteria to achieve a firm and void-free laminate for each resin setting. Figure 5.32 summarises fibre volume and void content results for 27 different laminates, comprising 3 PAEK–L2O ratio prepregs with 3 different processing pressure and 3 different processing time as discussed in Section 4.4.2. Here, typical pressure and time utilised in composite industry for processing thermoplastics are realised. A processing pressure of around 3 to 6 bar coupled with a holding time of approximately 15 minutes is usually deemed satisfactory in many cases and results in a composite part with relatively low void content. These factors can however vary significantly and are different with each polymer, fibre or prepreg setting. Therefore, a wider processing range is chosen for a thorough investigation as seen in the figure.

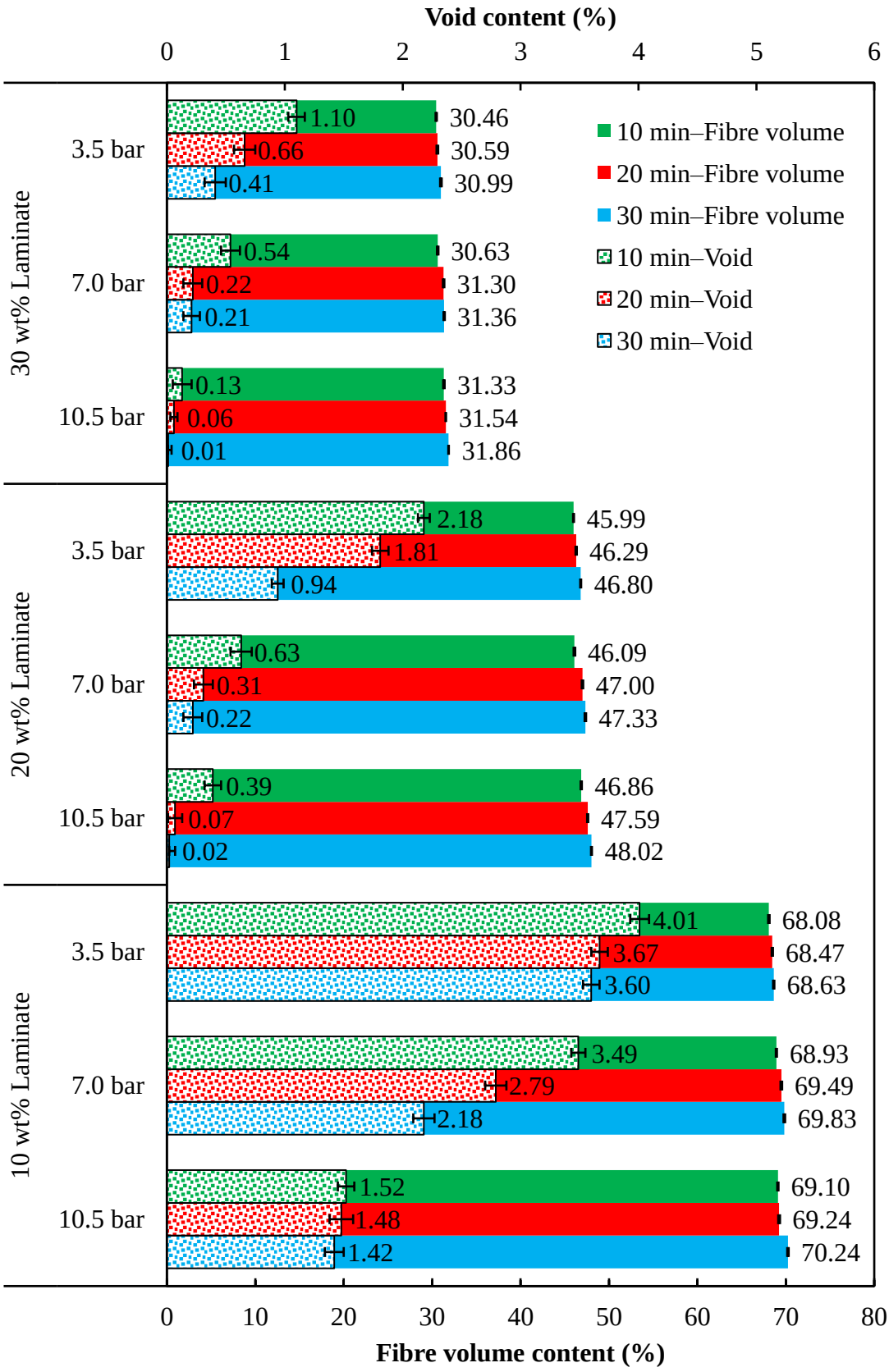

Figure 5.32 Effect of pressure and time on fibre volume and void content of laminates.

The initial impression from the figure is that 10 wt% prepreg laminates have the highest fibre volume content. As expected, as the ratio of polymer powder increases in the resin slurry bath, fibre volume content reduces. Due to uniqueness of every prepreg ply and thus every laminate, it is essential to understand that change in fibre volume and void ratio is different for each setting. In other words, fibre volume and void content are not necessarily related, and it is actually the density of the sample that significantly affects these ratios.

The density of the sample is directly associated with the processing factors during lamination. Density values can vary between 1.64–1.66 g/cm^3 for 30 wt% laminates, 1.80–1.85 g/cm^3 for 20 wt% laminates and 2.04–2.10 g/cm^3 for 10 wt% laminates. In the first glimpse, mentioned density ranges might seem insignificant but in reality, any small variation in the density will have a great impact on the proportion of constituents, substantially affecting the void content. It is evident from Figure 5.32 that increase in both processing pressure and time causes the fibre volume content to rise and reduces the void content. This trend is observed in every PAEK-L2O ratio setting.

Figure 5.32 shows that 30 wt% slurry setting results in laminates with an average 31 % fibre volume content. For 3.5 bar pressure setting, time plays a major role, with 30 minutes of holding time resulting in the lowest void content. In this instance, tripling the holding time decreases the void by almost two-third. Figure 5.33 exhibits the cross-sectional images explaining how the processing time can affect the void content in 3.5 bar pressure setting. Ten minutes is clearly not enough time coupled with the 3.5 bar pressure and results in formation of micro voids, as seen in Figure 5.33(a). PAEK polymer does not find enough time to flow though the fibre bundle and fully wet-out the fibre filaments. Enhancing the processing time to 20 minutes decreases the void content to 0.66 %. However, there still exist micro voids formed inside the matrix. Finally, 30 minutes of holding time results in a more appealing composite void content (0.41 %) and voids are only formed between areas where S2-glass filaments are denser, as seen in Figure 5.33(c). Generally, increasing the holding time and enhancing the melt pressure tend to enhance the impregnation rate. However, packed and concentrated fibres can reduce the permeability of the fibre bed [1, 2].

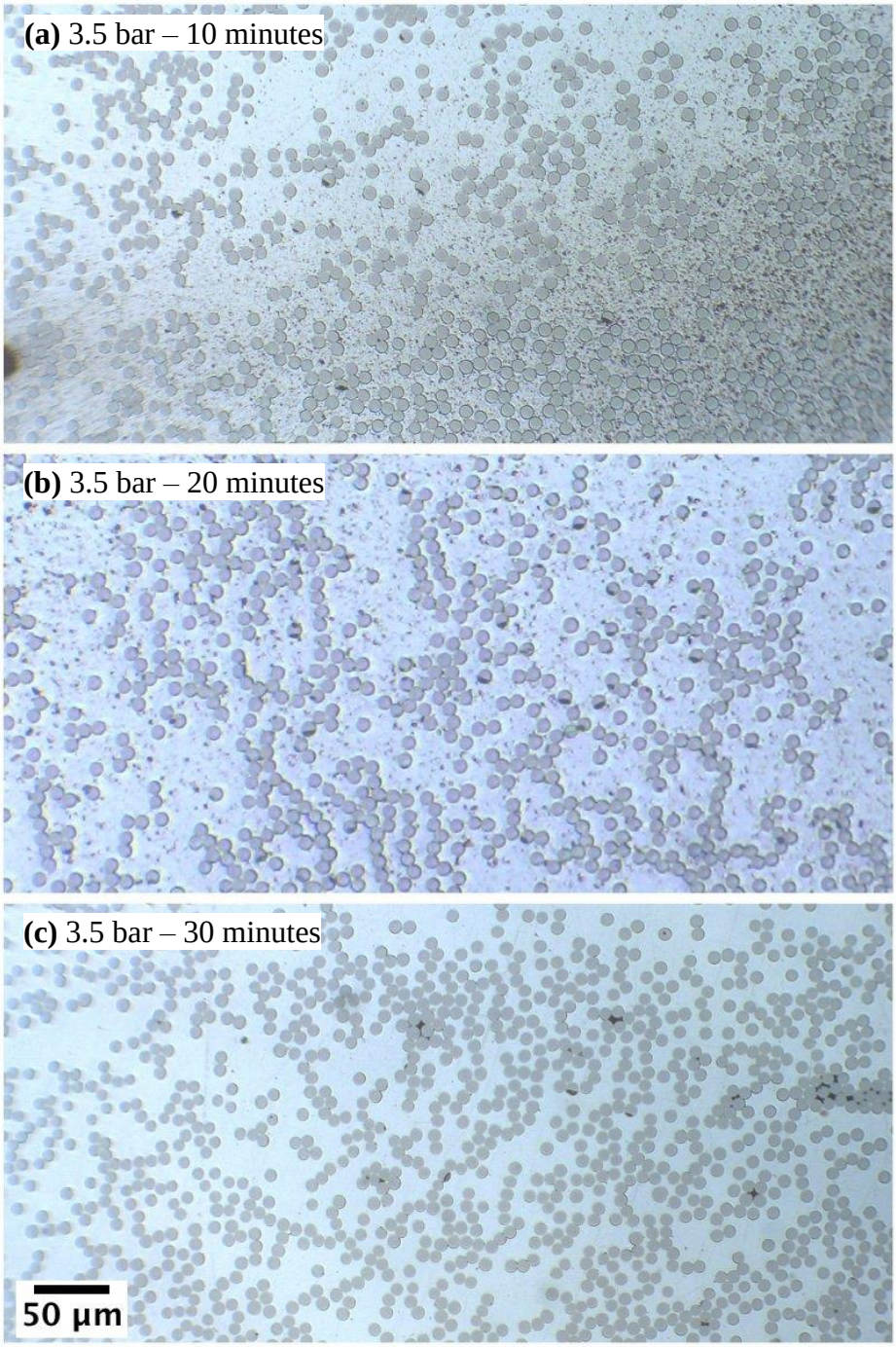

Figure 5.33 The effect of processing time on consolidation of 30 wt% laminates at low processing pressure.

The effect of higher impregnation time almost dissipates for 7.0 and 10.5 bar melt pressure, mainly from 20 to 30 minutes. For example, increasing the press time in 7.0 bar pressure from 20 to 30 minutes is almost ineffective in the void content. Although the higher pressure is beneficial in terms of eliminating gas bubbles, its effect is not significant when changing from 7.0 to 10.5 bar, compared to when using 7.0 bar

instead of 3.5. Regardless of the pressure and time setting utilised, 30 wt% laminates did not contain obvious macro voids.

Figure 5.34 illustrates example of a fully consolidated 30 wt% laminate. The settings here are 10.5 bar melt pressure with 30 minutes of press time.

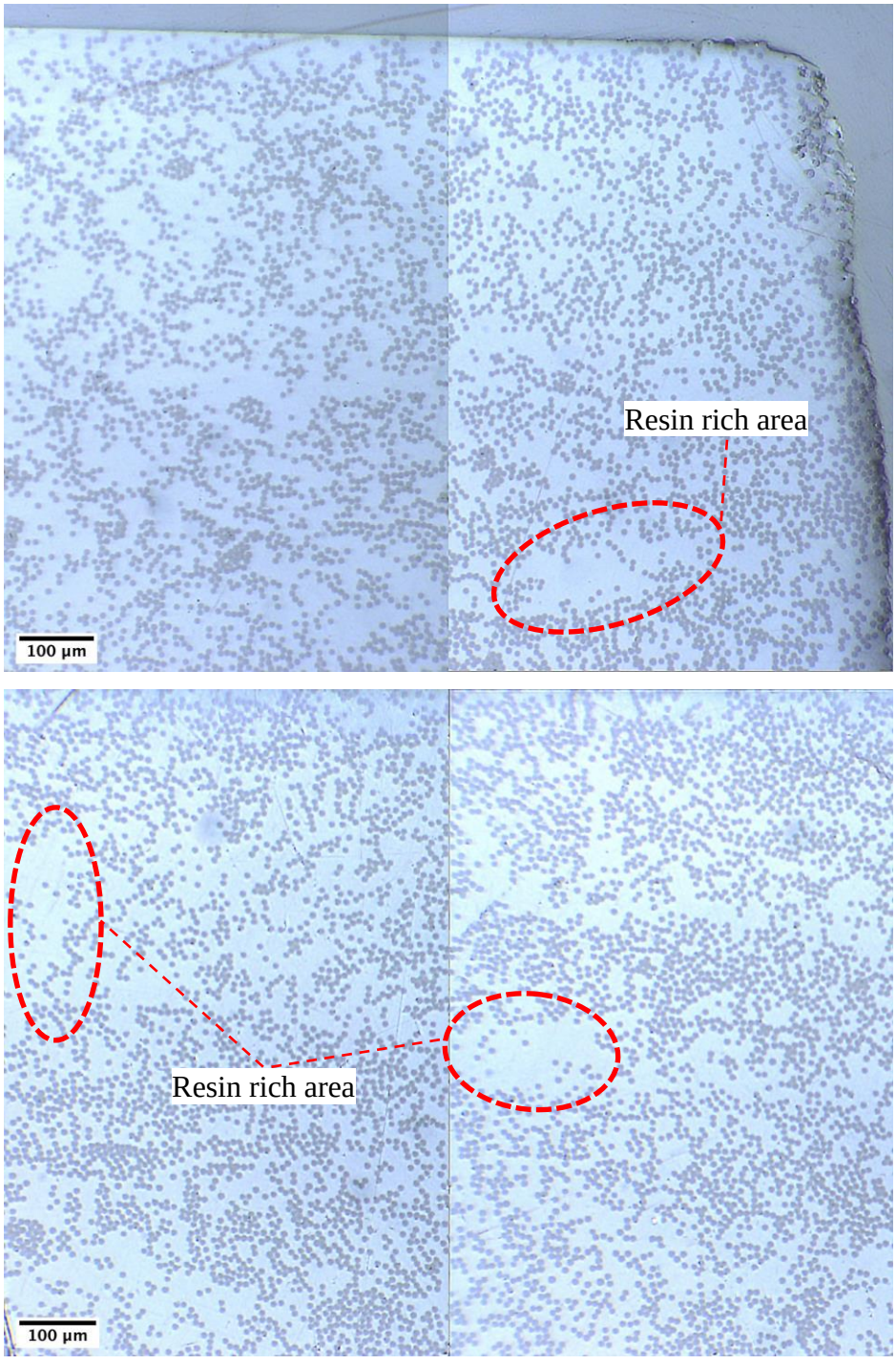

Figure 5.34 Cross-sectional example of a fully consolidated 30 wt% laminate.

As can be seen from the images and also the values recorded, such processing criterion is able to produce virtually void-free laminates. Average fibre volume content here is 31.86 % and the void content stands at 0.01 %. The overall uniformity of fibre distribution throughout the laminate is satisfactory, given the relatively low fibre volume content. One notable issue would be the presence of resin rich areas, although sparsely. These imperfections can be associated with the quality of 30 wt% prepreg plies, in which various irregularities (fibre waviness and resin rich areas) on the surface of the prepreg was observed and realised due to the problems with fibre winding using 30 wt% PAEK slurry. Nevertheless, it is noteworthy to say that it is practically impossible to produce a perfectly uniform and homogenous laminate.

Figure 5.32 also presents the results of constituents' proportion for 20 wt% laminates. Average fibre volume content for this resin setting is approximately 47 %. The 20 wt% laminates follow the same trend with respect to the change in fibre volume and void content as 30 wt% samples. In other words, higher processing pressure and time lead to an improved consolidated composite. Figure 5.32 indicates that 3.5 bar pressure is not sufficient to produce a low void composite part, even with 30 minutes of pressing time. These details are recognised in Figure 5.35(a) to (c).

Unlike 30 wt% laminates, 20 wt% settings can lead to macro voids. The formation of large gas bubbles can be clearly spotted when 3.5 bar pressure is utilised, even with 30 minutes of melt impregnation time, according to Figure 5.32. The void content is decreased drastically by doubling or tripling the pressure as seen in Figure 5.35(d) to (f) and (g) to (i), respectively. Implementing 10.5 bar of pressure shall result in the best void contents and higher fibre volume contents. The maximum fibre volume achieved was recorded at 48.02 % with a void content of 0.02 %, when laminate is pressed for 30 minutes, according to Figure 5.32.

Figure 5.35(h) indicates that 20 minutes of press time under 10.5 bar pressure is also satisfactory in terms of void content and is able to eliminate virtually all gas bubbles. Although it is preferred to have the least amount of void content, processing PAEK matrix in molten state for prolonged times can possibly lead to polymer degradation. This is not ideal as it will reduce the quality and mechanical performance of the

composite produced. Therefore, melt compressing the prepreg plies for 20 minutes might be a better and more reasonable choice in this instance. Not only the risk of polymer degradation is reduced, but processing time is also lowered for a faster production rate.

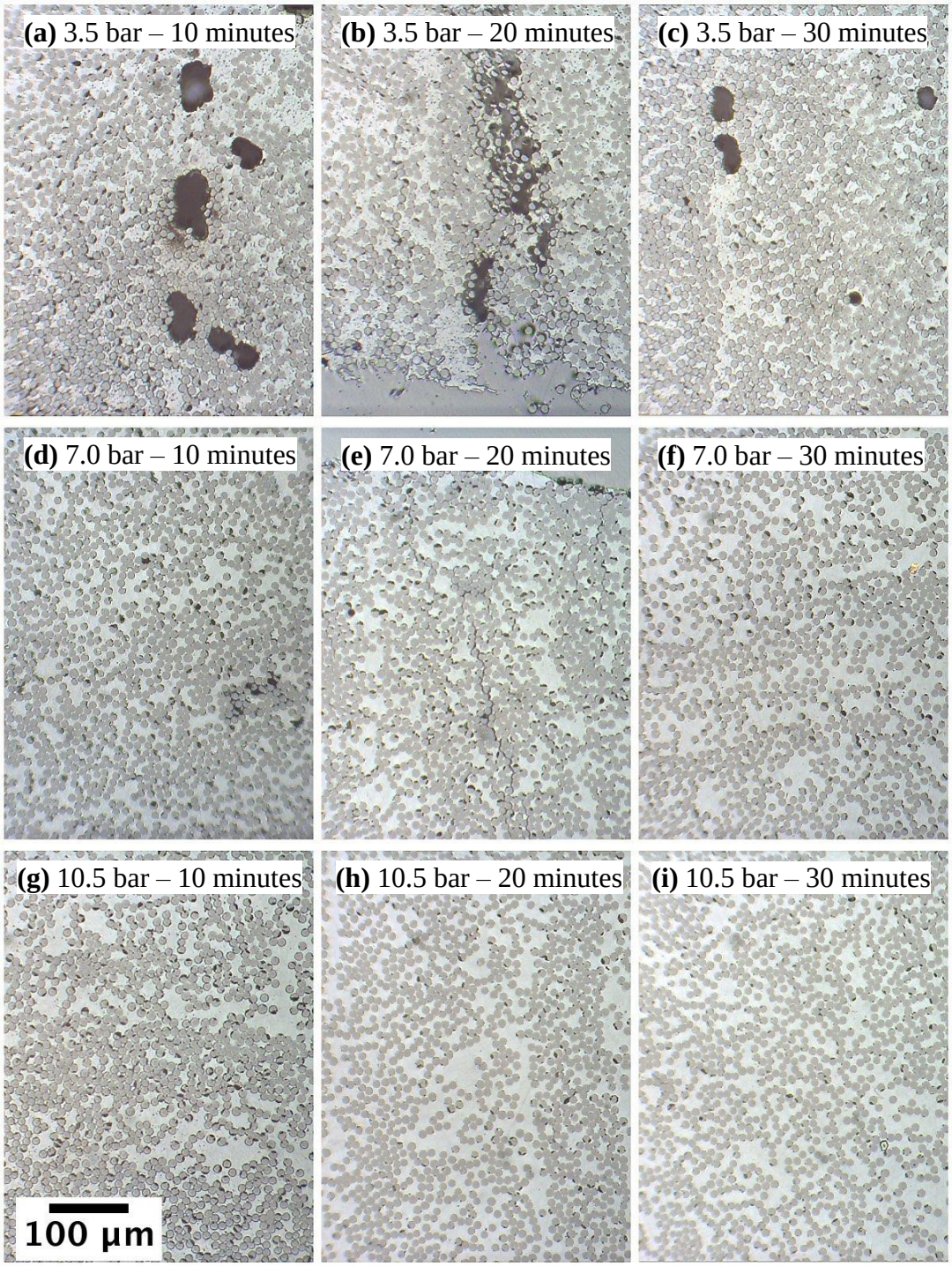

Figure 5.35 Cross-sectional examples for all 9 processing settings used for producing 20 wt% laminates.

By studying the results in Figure 5.32, it can be established that 10 wt% laminates can top an average fibre volume content of 69 %. This is an improvement of more than 122 % in fibre volume in comparison with the 30 wt% laminates. The pressing time factor for the 10 wt% laminates does not play a major role, specifically for 3.5 and 10.5 bar pressure setting. This indicates that higher pressure is more crucial than higher melt impregnation time to eliminate the gassy constituents. This phenomenon can be associated with the high fibre content. Here, molten PAEK could face a difficult flow rate for the purpose of fibre impregnation due to the high concentration of S2-glass fibres. Fibre filaments can act as a filter and slow down the flow of resin perpendicular to the fibre direction.

Figure 5.36 illustrates how a higher pressure can help better fibre impregnation and therefore, lower the void content in 10 wt% laminates with an identical processing time of 20 minutes. Comparable to 20 wt% laminates, 10 wt% laminates also develop macro voids for a 3.5 bar pressure being used. As indicated in Figure 5.32, increasing the holding time from 10 to 30 minutes, only contributes to 8.5 % reduction in the void content. Regardless of this change, 3.60 % void for 30 minutes of pressing is still considered too high. This is very similar to the results from 20 minutes holding time, leading to 3.67 % void, as illustrated in Figure 5.36(a).

After setting the pressure to 7.0 bar coupled with a processing time of 20 minutes, one can observe some significant differences in the void ratio. Figure 5.36(b) shows how the formed macro voids from 3.5 bar setting can reshape into smaller micro voids. These smaller voids are seen being formed in-between concentrated filaments and also in some resin rich areas, with some of the voids being half the cross-sectional size of a S2-glass fibre.

A pressure of 10.5 bar introduces a significant change in the void ratio as seen in Figure 5.36(c); void is kept to the minimum compared to 3.5 and 7.0 bar pressure settings. Micro voids formed inside 10.5 bar laminates were mostly noticed between tight fibre areas. Also, the processing time for 10.5 bar pressure laminates almost has no effect on gas elimination with the void content being 1.52, 1.48 and 1.42 % for 10, 20 and 30 minutes of press time, respectively.

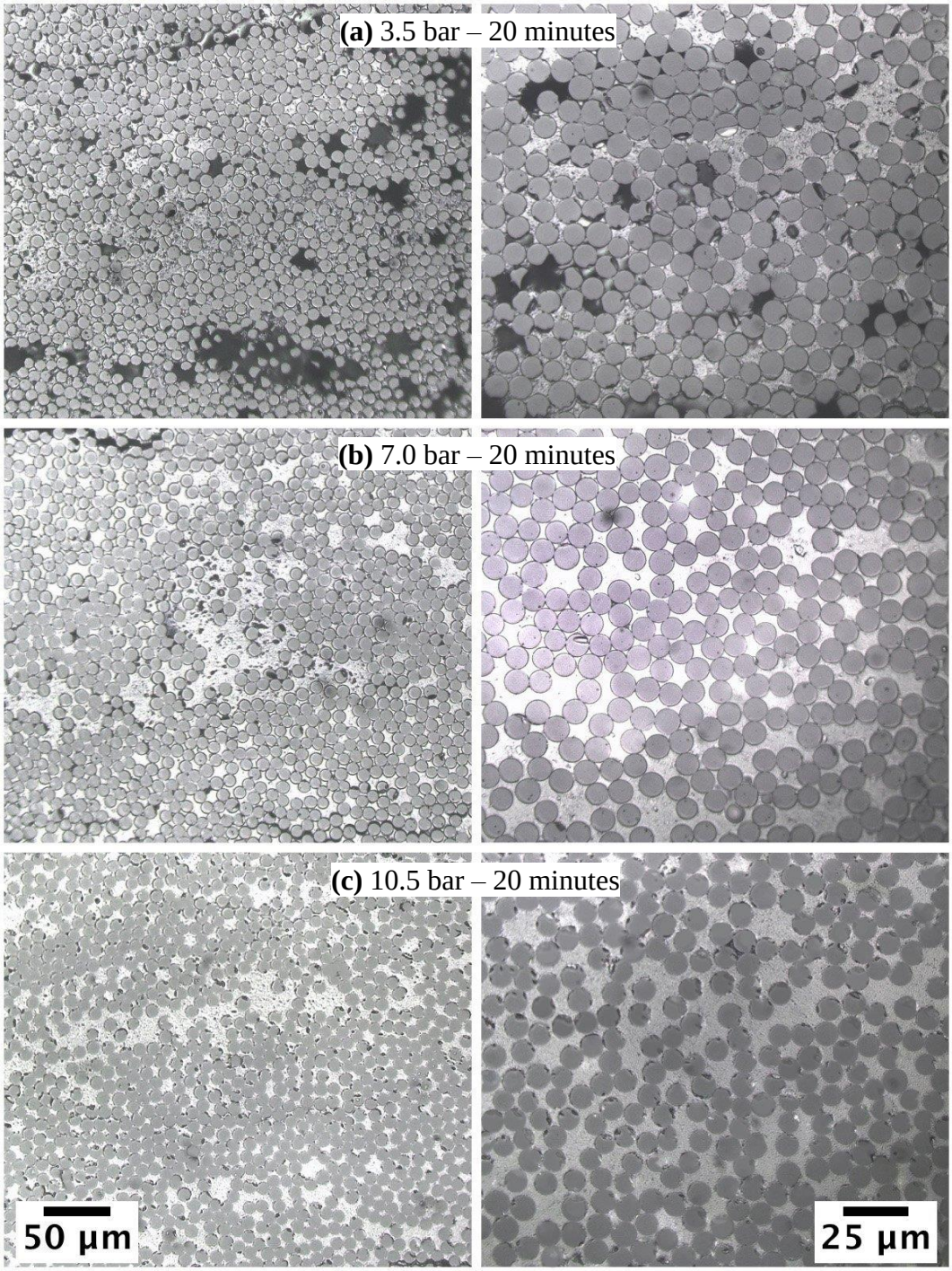

Figure 5.36 The effect of processing pressure on consolidation of 10 wt% laminates with 20 minutes of processing time.

Although increasing the pressure to 10.5 bar solves the problem of high void content in 10 wt% laminates, it was decided to implement a higher processing pressure for this tier of laminates to identify whether it is possible to decrease the void content further, while increasing the fibre volume. For this purpose, a higher processing pressure of 14.0 bar was utilised. Given the fact that extending the processing time any further

than 30 minutes might lead to unwanted polymer degradation, only the pressure was enhanced at this stage and the press time was kept at a safer value of 20 minutes. The resulting laminates utilising such settings would have a density of around 2.13 g/cm^3, an average fibre volume content of 71.67 % and a reduced void content of 0.19 %. Despite observing only 3.5 % improvement in the fibre volume content, the void content is lowered significantly by 778.9 % compared to the laminates processed with 10.5 bar pressure and 20 minutes setting. This decrease in the void content is remarkable and can improve the quality of the composite parts significantly.

Figure 5.37 compares side-by-side cross-sectional micrographs of fully consolidated laminates produced with 10, 20 and 30 PAEK–L2O ratio prepregs. Here, all laminates were processed under pressure for 20 minutes. Evidently, for all three tiers of S2-glass/PAEK prepregs, 20 minutes of processing time is deemed sufficient in order to achieve a high level of consolidation and a low void content. Lower pressing time also avoids any unnecessary polymer degradation and accelerates the production rate. Therefore, it was decided to use the 20 minute setting for processing all three prepreg types. A pressure of 10.5 bar for 20 and 30 wt% prepregs, and 14.0 bar pressure for 10 wt% prepregs is utilised and is considered satisfactory.

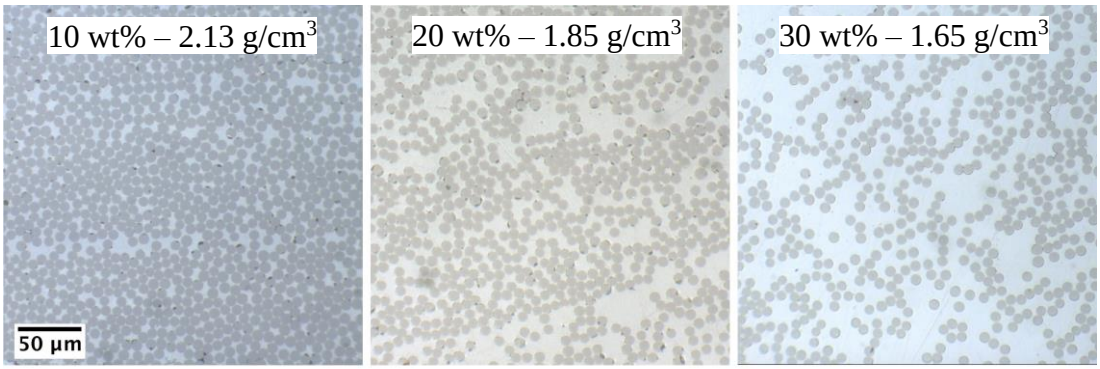

(a) 14.0 bar – 20 min **(b)** 10.5 bar – 20 min **(c)** 10.5 bar – 20 min

Figure 5.37 Comparison of fully consolidated laminates with different PAEK ratios.

Figure 5.37(a) shows the cross-sectional micrograph of the previously mentioned 10 wt% laminate processed at 14.0 bar pressure with 20 minutes of impregnation time. It is clear from the image that the fibre dispersion in the matrix is very uniform and hardly any noticeable resin rich areas can be discovered. The manufactured laminates

are also virtually void-free. It is noteworthy to state that achieving such high fibre volume content and low void ratio, with a clearly exceptional fibre impregnation level is proved to be a very difficult task. Many traditional methods of manufacturing thermoplastic prepregs (such as melt impregnation method) are simply not capable to achieve very high fibre volume contents. This clearly demonstrates the advantages of powder impregnation process and in particular, wet powder impregnation technology over conventional methods.

Both 20 and 30 wt% laminates also benefit from a uniform dispersion of S2-glass fibres with minimal resin rich areas and virtually zero void content. This is a good indicator and confirmation that the designed and manufactured prepreg rig is capable of executing such difficult tasks by producing highly impregnated prepreg plies with acceptable physical tolerances.

Figure 5.38 compares the fibre volume content achieved for fully consolidated laminates with different PAEK ratios of 10, 20 and 30 wt%. By using the estimated trend line equation stated in the figure, one is able to adjust the desired fibre volume content by altering the PAEK–L2O ratio in the resin bath slurry. For instance, in order to obtain a fully consolidated 60 % fibre volume content laminate, 14.4 wt% PAEK slurry setting shall be approximately implemented.

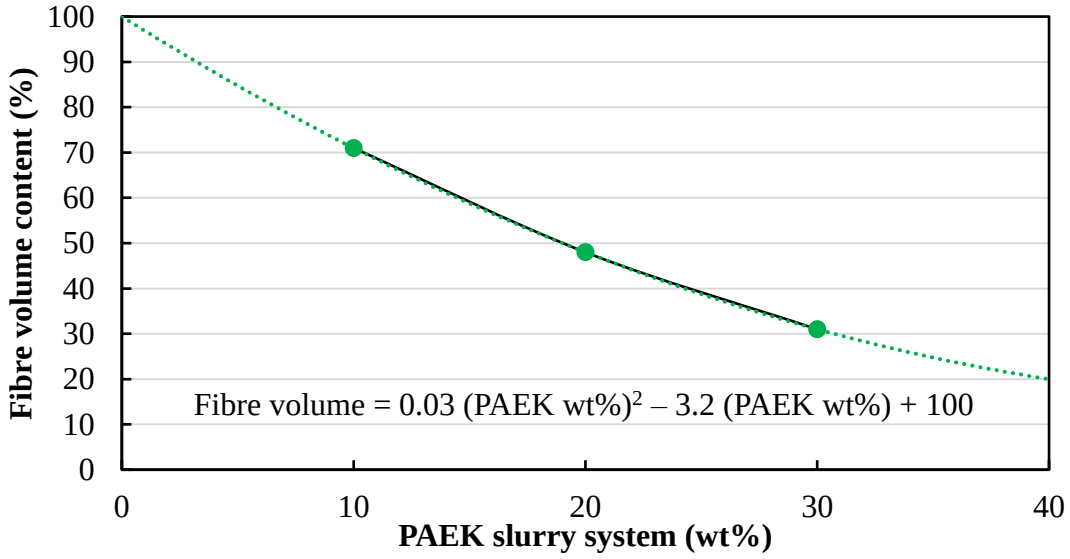

Figure 5.38 Fibre volume content for different PAEK–L2O ratios: experiment values and predictions.

5.3.2.2 Cured Ply Thickness

The thickness of prepreg ply changes when it is hot compression moulded and is measured by dividing the thickness of the fully consolidated laminate by the number of plies. Figure 5.39 compares average ply thickness for different PAEK–L2O ratios.

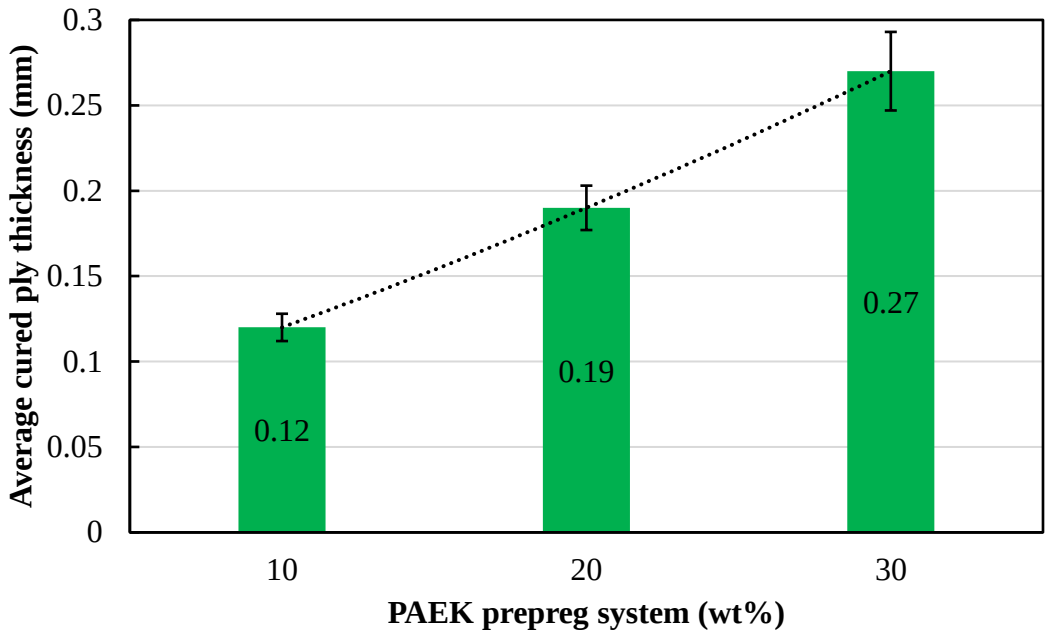

Figure 5.39 Comparison of cured ply thickness for fully consolidated laminates with different PAEK–L2O ratio.

The figure shows that 10 wt% prepreg laminates expectedly have the lowest cured ply thickness. This tier also benefits from the least amount of ply thickness tolerance, verifying low thickness variation in the utilised prepreg plies.

For 20 wt%, cured ply thickness is increased by approximately an average of 0.07 mm. On the other hand, 30 wt% laminates also show an increase of about 0.08 mm from 20 wt% laminates, hence the rather linear behaviour of the graph. The major difference between 30 wt% setting compared to 10 and 20 wt% is the relatively higher tolerance in the cured ply thickness measured. The main reason behind this situation can be traced back to the relatively higher thickness variation in 30 wt% prepreg plies and the problems associated with processing 30 wt% PAEK slurry with the prepreg rig.

Cured ply thickness provides an essential piece of information when dealing with design and manufacture of composite parts. This value is needed in order to obtain certain geometry for the final composite parts and specifically for controlling the thickness of the material. For instance, when required to produce laminates of 10 wt% prepregs to obtain a thickness of approximately 1 mm, 8 prepreg plies are required for use in hot compression moulding.

5.3.3 Mechanical Properties of the Laminate

After physical evaluation of the manufactured composite laminates, a number of mechanical properties are investigated. In this section, tensile, interlaminar shear and flexural tests are carried out. The effect of high temperatures on tensile properties of samples is also investigated.

5.3.3.1 Tensile Test

Fully consolidated 10, 20 and 30 wt% laminates were tested in order to identify their tensile properties. Tensile strength, tensile modulus and failure strain were the parameters measured. Figure 5.40 shows tensile results obtained from testing different PAEK ratio laminate settings. Tensile results were calculated to three significant figure and standard deviation was included.

It is understood from the figure that tensile strength decreases as the PAEK–L2O ratio rises. In other words, laminates with higher fibre volume content will obviously have a better tensile performance due to presence of more cross-sectional reinforcing fibres in a specified volume. Fully consolidated 10 wt% laminates have the highest fibre volume content (~72 %) and as the result, have the highest average tensile strength of 1760 MPa. As the fibre content declines, tensile strength also decreases; 20 and 30 wt% laminates have an average tensile strength of 1380 and 952 MPa, respectively. The increase rate in the tensile strength is observed to be lowered as the PAEK concentration decreases. By the means of illustration, tensile strength was enhanced by approximately 45 % when switching from the 30 to 20 wt% setting. However, this increase is 28 % when changing from the 20 to 10 wt% laminates.

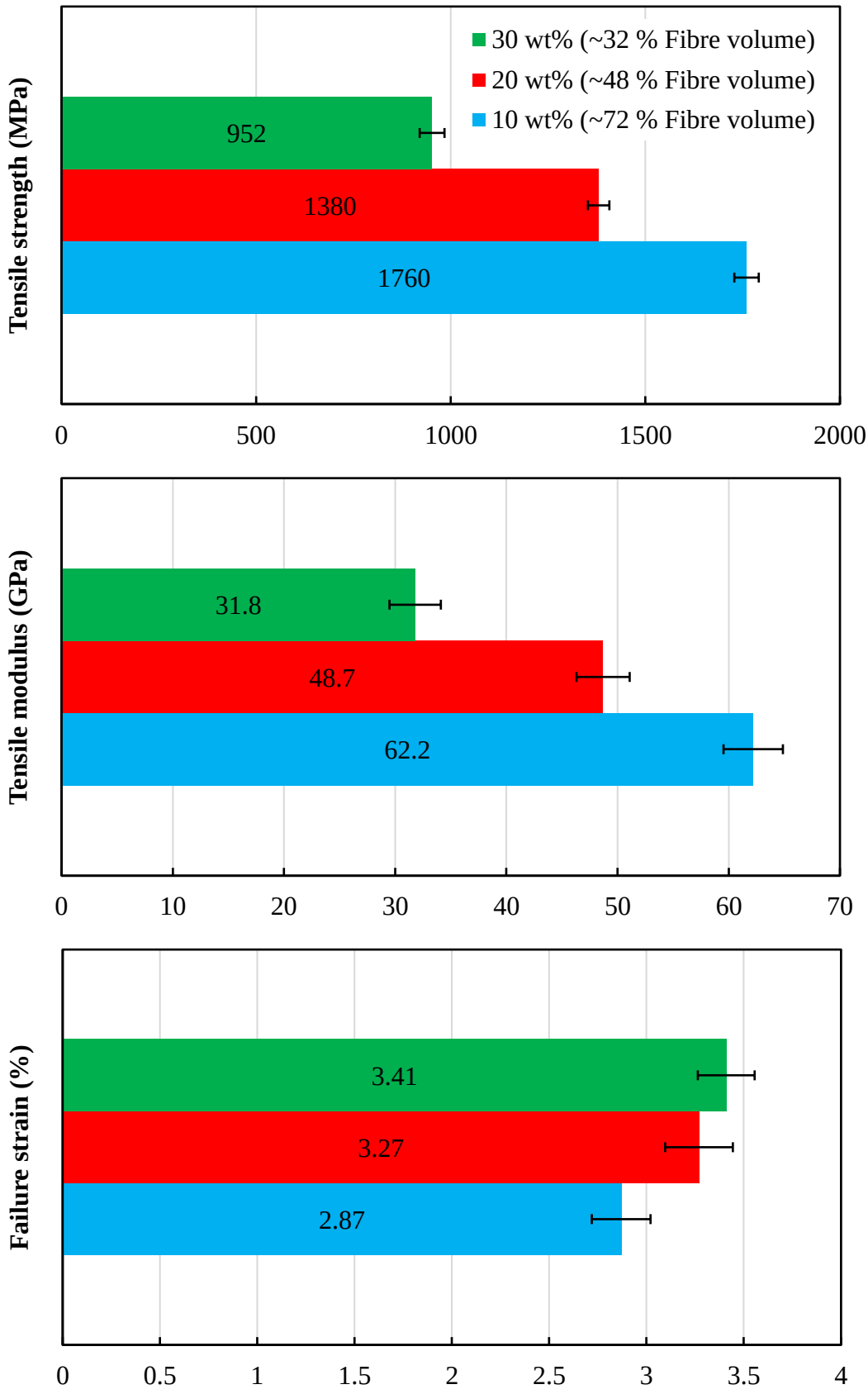

Figure 5.40 Comparison of tensile strength, tensile modulus and failure strain for fully consolidated laminates with different PAEK–L2O ratio.

Similar trend is observed for the tensile modulus. The existence of higher proportion of S2-glass in 10 wt% laminates lead to a stiffer and denser composite. Thus, 10 wt% setting has the highest tensile modulus value of approximately 62.2 GPa. As the ratio of S2-glass declines, the composite material loses stiffness and subsequently, 20 and 30 wt% composite laminates embrace lower modulus values of 48.7 and 31.8 GPa, respectively.

By implementing the rule of mixture for composites, values for tensile modulus can be predicted for 10, 20 and 30 wt% (72, 48 and 32 % fibre volume) composite samples. The rule of mixtures is a weighted mean used to predict various properties of a composite material such as the tensile modulus. The predicted tensile modulus E_c of the composite sample along the fibre direction can be calculated using the following equation:

$$E_c = E_f V_f + E_m V_m \qquad \textit{Equation 5.1}$$

where E_f is the tensile modulus of the fibre and E_m is the tensile modulus of the matrix. Figure 5.41 compares the calculated modulus with the data from experiment.

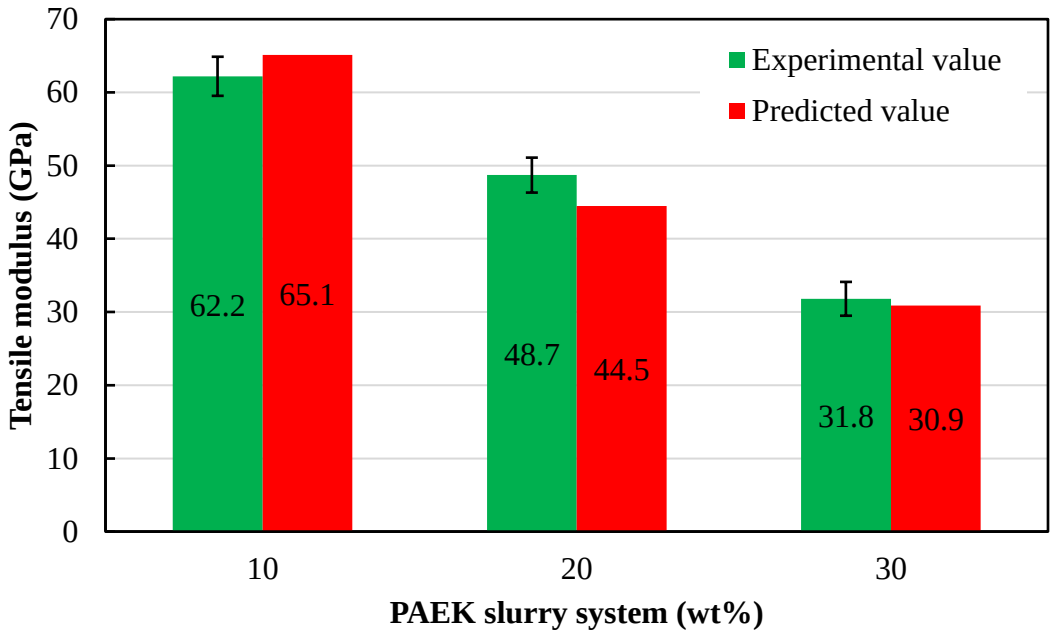

Figure 5.41 Comparison of experimental values and numerical calculations of tensile modulus for fully consolidated laminates with different PAEK–L2O ratio.

It is observed from the chart that the obtained experimental data for tensile modulus correlates well with the calculated predictions. The difference between the experimental and numerical values is approximately 4.5 % for 10 wt% (72 % fibre volume) samples, 9.4 % for 20 wt% (48 % fibre volume) samples, and 2.9 % for 30 wt% (32 % fibre volume) samples. The relatively low variation between the values suggests accurate fibre volume measurements and mechanical tests.

Figure 5.42 compares tensile strength and tensile modulus for 10, 20 and 30 wt% laminates, or in other words, for 72, 48 and 32 % fibre volume content.

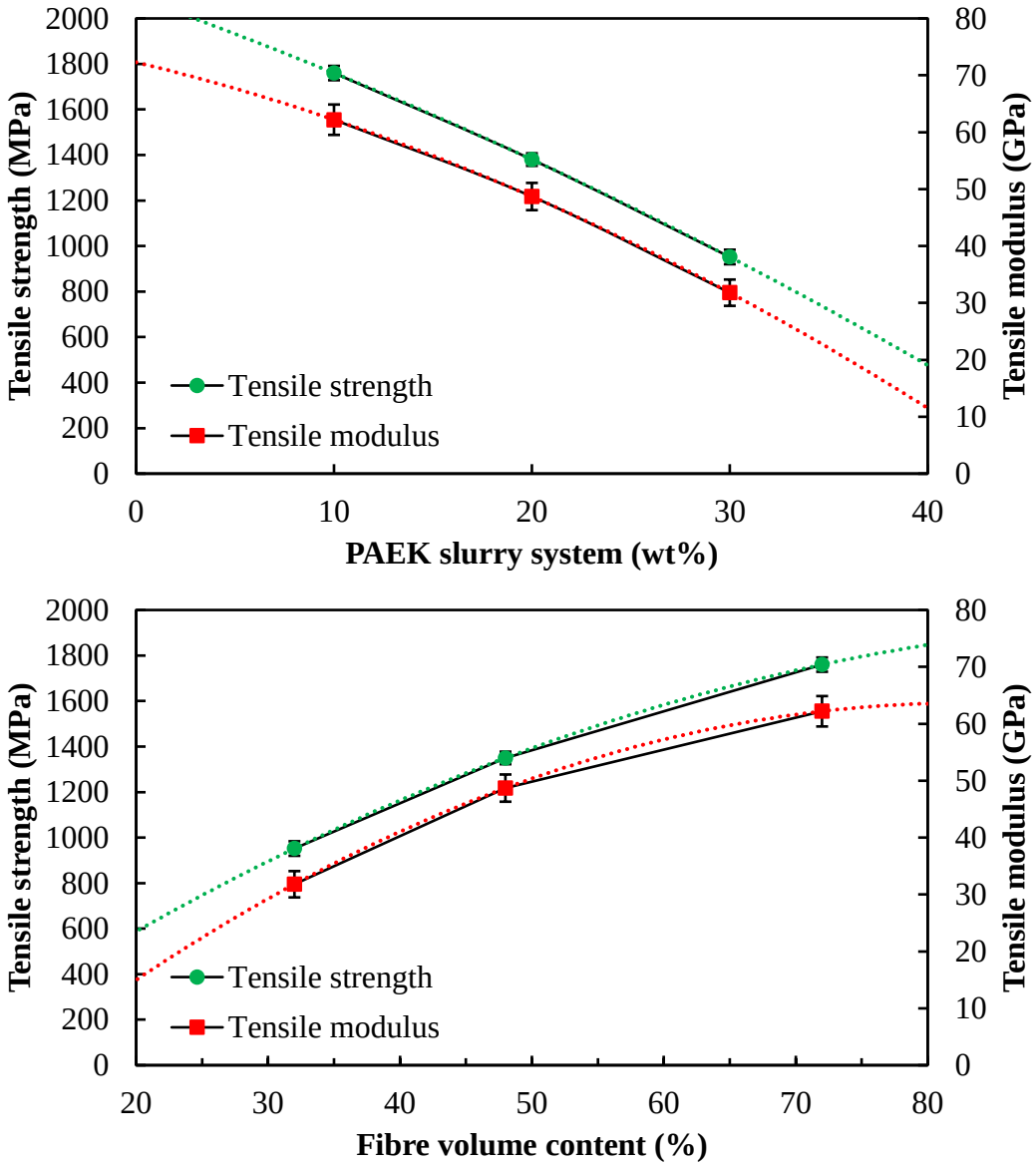

Figure 5.42 Comparison of tensile strength and tensile modulus for different PAEK–L2O ratios and different fibre volume contents.

Figure 5.42 exhibits the rate of change in both tensile strength and tensile modulus, with the enhancement of PAEK concentration (or increase in fibre volume content). Both graphs can be utilised for predicting tensile properties of laminates with different PAEK ratios or fibre volume content. As a matter of example, it is expected that a fully consolidated laminate with 60 % fibre volume content (~14.6 wt% PAEK), would incorporate a tensile strength of approximately 1590 MPa with a modulus of 56.4 GPa. The ability to forecast the properties of composite parts with different resin setting is especially essential for design, when the tensile performance needs changing or adjustments. One difference that is noticed when comparing the two graphs is that tensile strength/modulus versus the PAEK ratio is more linear than that of the tensile strength/modulus versus fibre volume content. Regardless of this difference, forecasting tensile properties using both graphs give results within acceptable tolerance.

When comparing the failure strains for different laminates from Figure 5.40, it can be seen that by increasing the fibre volume content, the composite material becomes more brittle. Obviously, a composite material will somehow represent the properties of each constituent. In this instance, S2-glass/PAEK composite is expected to have a combination of the S2-glass and PAEK polymer properties. Tensile elongation for S2-glass and PAEK is recognised from Section 3.3 as 5.7 and 15 %, respectively. Since glass fibre filaments are more brittle than the PAEK matrix, it is expected to see a decline in ductility of the composite as the fibre volume content increases. As the result, ductility decreases mildly by approximately 0.54 (strain %) from the 30 to 10 wt% laminates. This change in ductility can also affect the failure mode of tensile coupons with different PAEK to fibre ratio.

Load–displacement traces (until failure) and stress–strain curves (up to 0.5 % strain) for the 10, 20 and 30 wt% samples following tensile tests are shown in Figure 5.43(a) and (b), respectively. It is observed from the figure that typically the laminates exhibit a semi-linear behaviour up to the maximum value, at which point the samples either demonstrate a sudden and catastrophic failure (observed in 30 wt% samples) or would showcase a more progressive failure response (observed in 20 and 10 wt%).

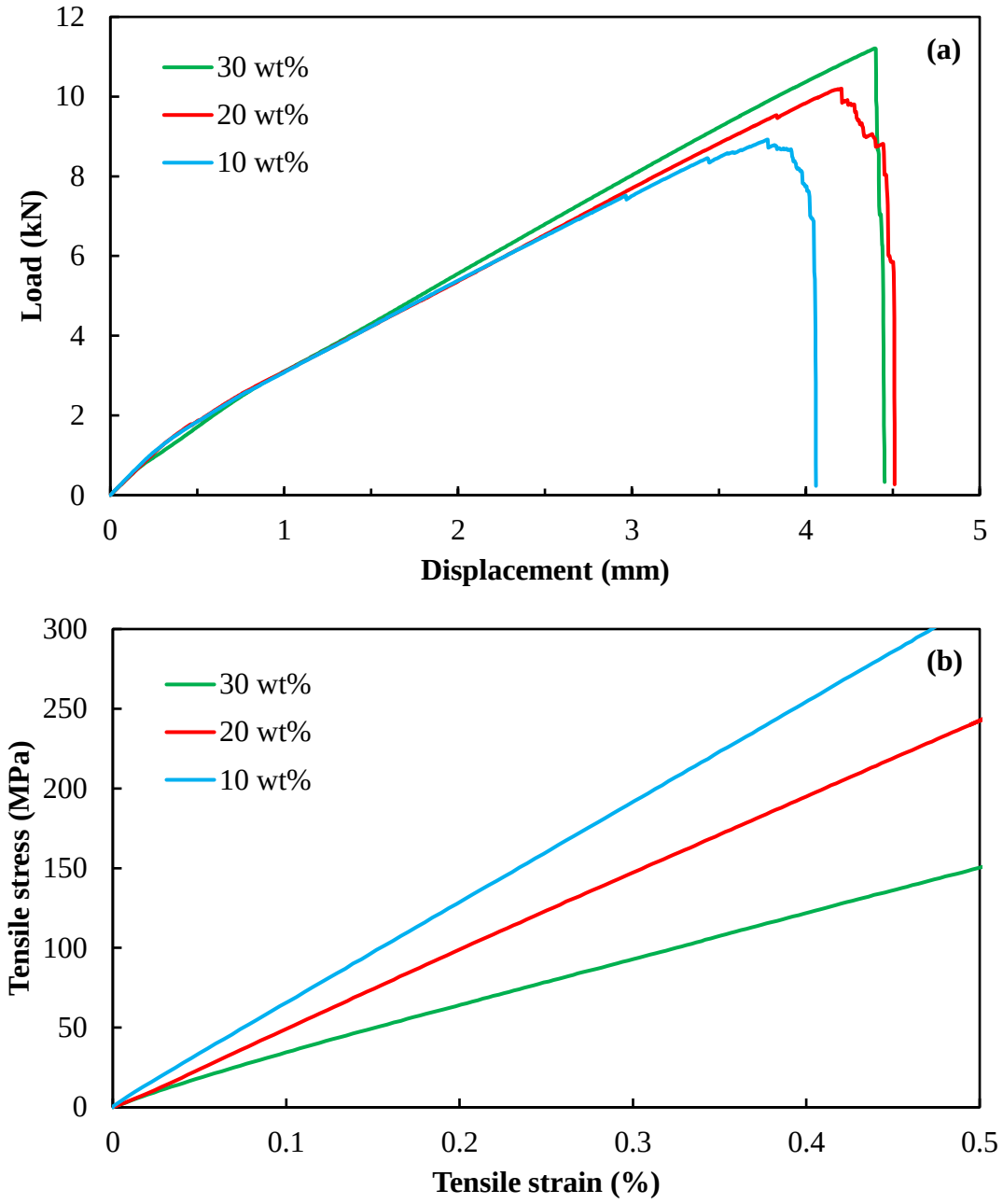

Figure 5.43 Tensile behaviour of samples with different PAEK wt%: (a) load–displacement traces until failure and (b) stress-strain curve up to 0.5 % strain.

With regards to the modulus, slope of the linear region of the stress–strain curve represents the tensile modulus. As expected, 10 wt% samples embrace the highest gradient, thus having the highest modulus.

It is evident from the graphs that the failure behaviour of 30 wt% coupons differ from 20 and 10 wt% specimens, since the samples break suddenly rather than gradually. The failure modes for some tested specimens are presented in Figure 5.44.

Figure 5.44 Comparison of tensile failure mode for samples with different PAEK–L2O ratio.

Usually, all samples start breaking from the edge of the tensile coupon. However, the failure is much more sudden in 30 wt% samples. Failure mode in 30 wt% setting is considered long splitting, in various (typically middle) locations of the gauge length section.

For 20 and 10 wt% samples, a number of interlaminar fractures can often be noticed before the full failure of the sample. This is the reason for presence of slight fluctuations in their corresponding load–displacement curves. As showed in Figure 5.44(c), 10 wt% coupons have a relatively different failure mode compared to 30 wt%. The failure mode captured to be explosive, in various (typically middle) locations of the gauge length section. On the other hand, it is understood from the failed specimens that 20 wt% samples exhibit a failure mode in-between 10 and 30 wt% laminates. Long splitting is observed to happen with slight explosion of fibres in the gauge section, as seen in Figure 5.44(b).

The aforementioned results discussed are obtained from fully consolidated laminates. Laminates with various void content were also tested and the tensile results were studied. As expected, the presence of gas bubbles inside the composite laminates degrades the mechanical properties of the samples and this instance, the tensile properties. Figure 5.45 compares results of tensile strength for 10 wt% laminates that were previously discussed in Section 5.3.2.1, for a heat press time of 20 minutes and processing pressure of 3.5, 7.0, 10.5 and 14.0 bar, resulting in an average void content of 3.67, 2.79, 1.48 and 0.19 %, respectively.

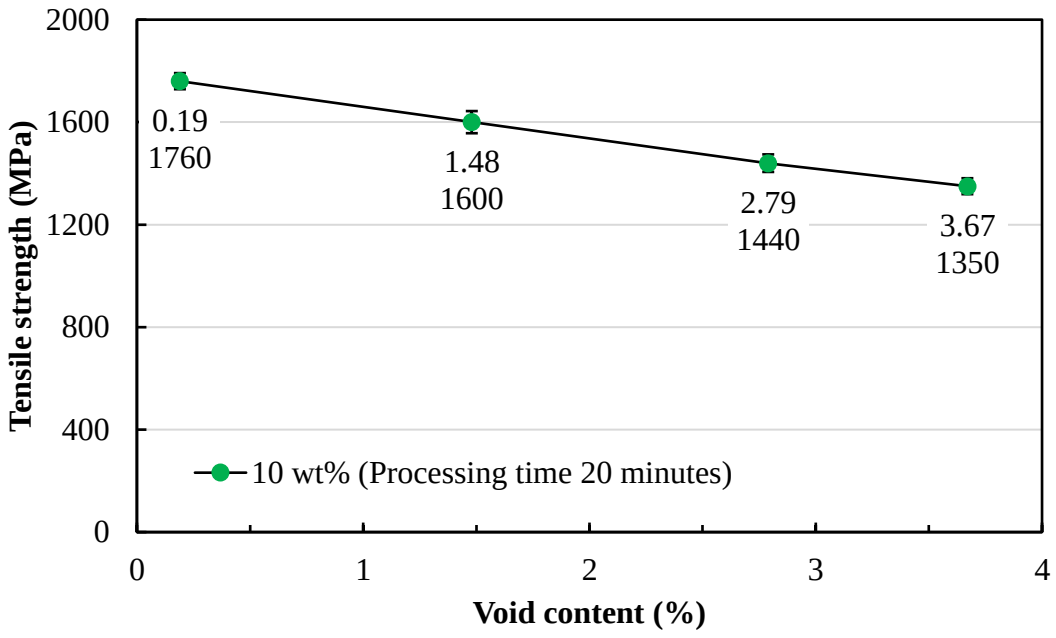

Figure 5.45 The effect of void content on tensile strength of 10 wt% laminates.

The figure maps a roughly linear relationship between tensile strength and the void content. Tensile strength decreases as the void content increases. In worst case scenario, tensile strength sees a 23.3 % decline when the laminate contains a void content of 3.67 %, in comparison to the fully consolidated laminates with an average of 0.19 % void ratio. This trend is valid for 20 and 30 wt% laminates as well.

Fibre orientation plays a very important role in determining the tensile properties of fibre-reinforced composites. Here, since the tensile tests are carried out along the fibre direction, it is important to realise the fibre orientation in the laminate and to investigate the straightness of S2-glass filaments. In order to understand the fibre architect of the manufactured UD samples, specimens from Section 4.4.3 (fibre volume determination by matrix burn-off) were observed. In this method the resin matrix of the composite is removed in a furnace by combustion. Figure 5.46 compares the fibre architect of 10, 20 and 30 wt% samples.

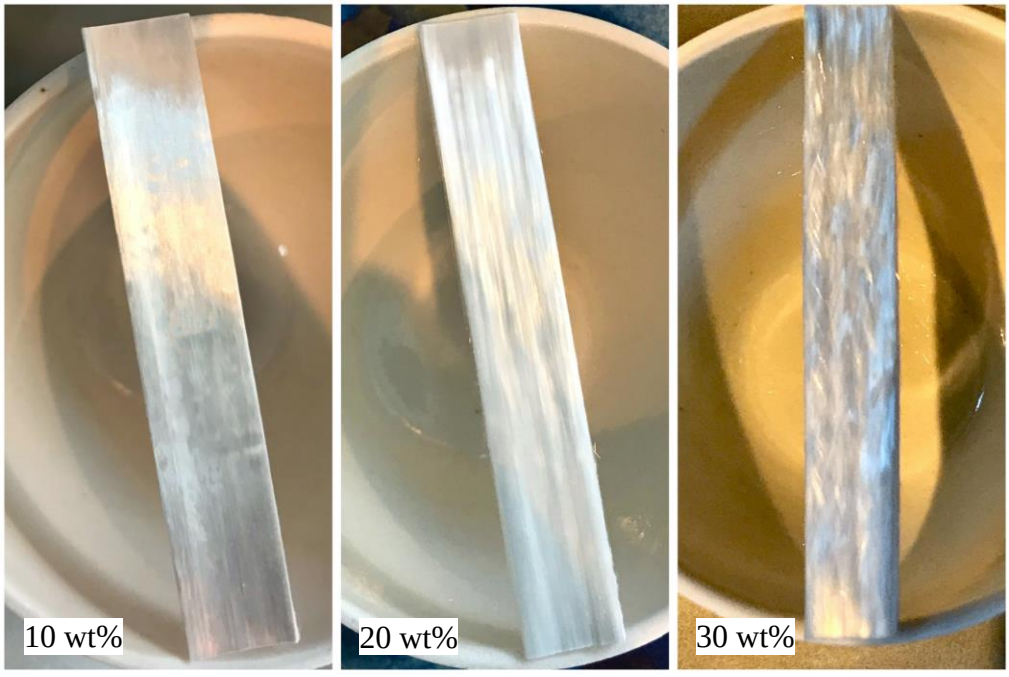

Figure 5.46 Comparison of fibre architect for 10, 20 and 30 wt% samples.

Despite some minor fibre waviness, 10 and 20 wt% samples both comprise a relatively straight fibre structure. For 30 wt% sample however, fibre waviness is more apparent. Crimp is usually not desired in high-performance composites and can adversely affect the mechanical properties of the component.

Due to the low tensile properties and also, problems associated with the production of 30 wt% prepregs, it was decided to discard this tier of laminates from further mechanical tests. Therefore, only 10 and 20 wt% samples were used for interlaminar shear and flexural tests.

5.3.3.2 Interlaminar Shear Test

Interlaminar shear tests were carried out to understand the short-beam strength of 10 and 20 wt% laminates. The shear stress in this test is developed at the specimen's mid-plane at the failure event, and the shear stress distribution only occurs, and then not exactly, on planes midway between the loading nose and support points. Due to the complexity of internal stresses, a variety of failure modes can occur, although shear is the dominant load applied in this test method. Having said that, the mid-plane interlaminar failures have to be clearly observed to attribute the short-beam strength obtained to a shear property.

Figure 5.47(a) and (b) shows the results of the tested specimens for 10 and 20 wt% samples, respectively. During the test, the specimens were not fractured into two pieces and the loading nose travel did not exceed the sample nominal thickness. Therefore, application of load on the specimens was continued until a load drop of 30 % was observed. The calculated short-beam strength results suggest close values for both 10 and 20 wt% settings. As indicated on the graphs, average interlaminar shear strength for 10 and 20 wt% laminates were calculated as 74.7 and 75.1 MPa, respectively. On the other hand, similar specimens of both settings show a similar load–displacement trace, which advises the semi-homogeneity of the laminates.

Almost identical shear value for both laminates is a clear indicator that the fibre volume content does not have much influence on the shear strength in this instance. In other words, more PAEK matrix in the 20 wt% laminates does not necessarily enhance the shear properties and fibre wet-out is good in both settings. Despite the similar shear values, the two settings showcase different mechanical behaviour. Here, 10 wt% specimens have a roughly linear behaviour up to their yield. This is then followed by a small transition region, after which the sample fails rather suddenly, positioning the fracture point on the ultimate shear point. On the contrary, 20 wt%

specimens experience an extended transition region and fail more gradually, compared to 10 wt% samples.

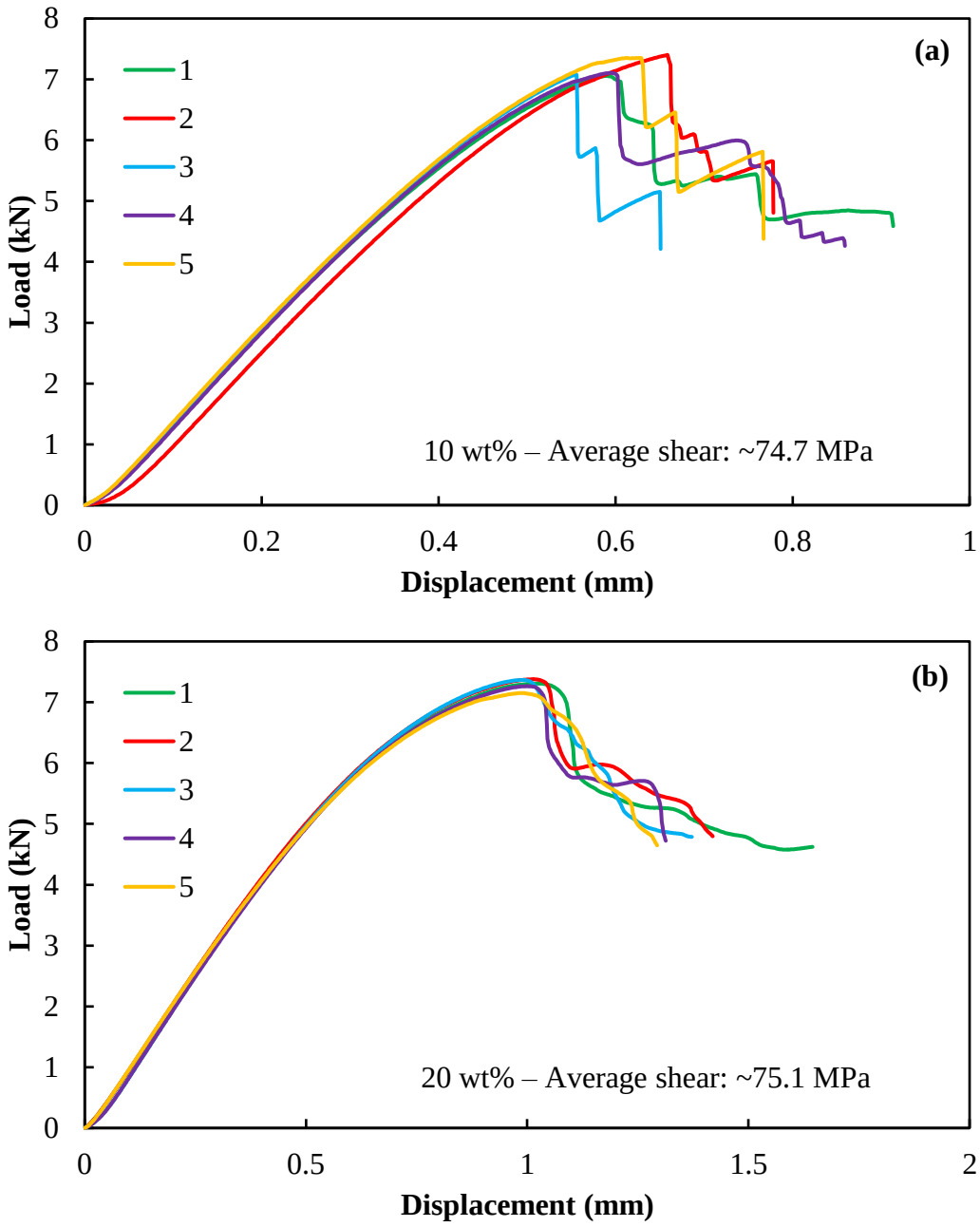

Figure 5.47 Interlaminar shear traces for: (a) 10 wt% specimens and (b) 20 wt% specimens.

Figure 5.48(a) and (b) show typical failure modes that can be identified visually for both 10 and 20 wt% samples. These failures may be preceded by less obvious, local damage modes such as trans-ply cracking. However, acceptable interlaminar shear

failure modes, akin to specimens shown in Figure 5.48(a) and (b), were observed in majority of the tested samples.

As previously mentioned, 20 wt% laminates are deemed more ductile due to having higher PAEK proportions and as the result, they show a more gradual failure. Figure 5.48(c) is an example of loaded 20 wt% specimen in the transition region. Here, inelastic deformation is observed before the shear stress delaminates the middle plies.

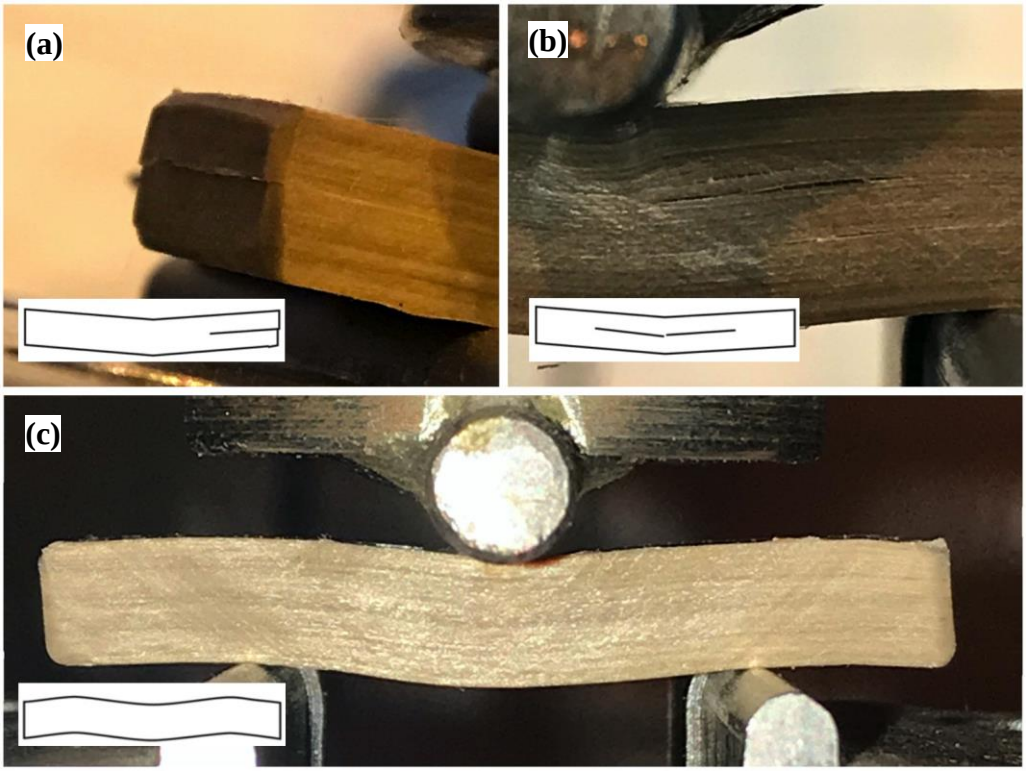

Figure 5.48 Different failure modes observed during the interlaminar shear test.

5.3.3.3 Flexural Test

Flexural tests were carried out to study the flexural strength and modulus of 10 and 20 wt% laminates. Three-point bending was utilised and initially, a span to thickness ratio of 32:1 was implemented. However, preliminary tests indicated that 32:1 setting could result in premature failure of specimens.

In order to obtain a valid flexural property, it is necessary that the specimen failure occurs on either one of its outer surfaces, without a preceding interlaminar shear failure. Failure on the compression surface may be local buckling while that on the

tension surface may be a crack. For highly orthotropic composite laminates (which is the case in this study), shear deformation can adversely reduce the apparent flexural modulus when tested at low span to thickness ratios. Additionally, the span to thickness ratio must be increased for composite laminates having relatively low out-of-plane shear strength and relatively high in-plane tensile or compressive strength parallel to the support span.

Therefore, specimens that fail in an unacceptable failure mode shall not be included in the flexural property calculations. Figure 5.49 illustrates an example of preceding interlaminar shear failure observed in 10 wt% laminates. Before an apparent force drop in load–displacement trace due to either tensile or compression failure, interlaminar shear failure was observed in lower mid-span plies, which lies in the tensile section.

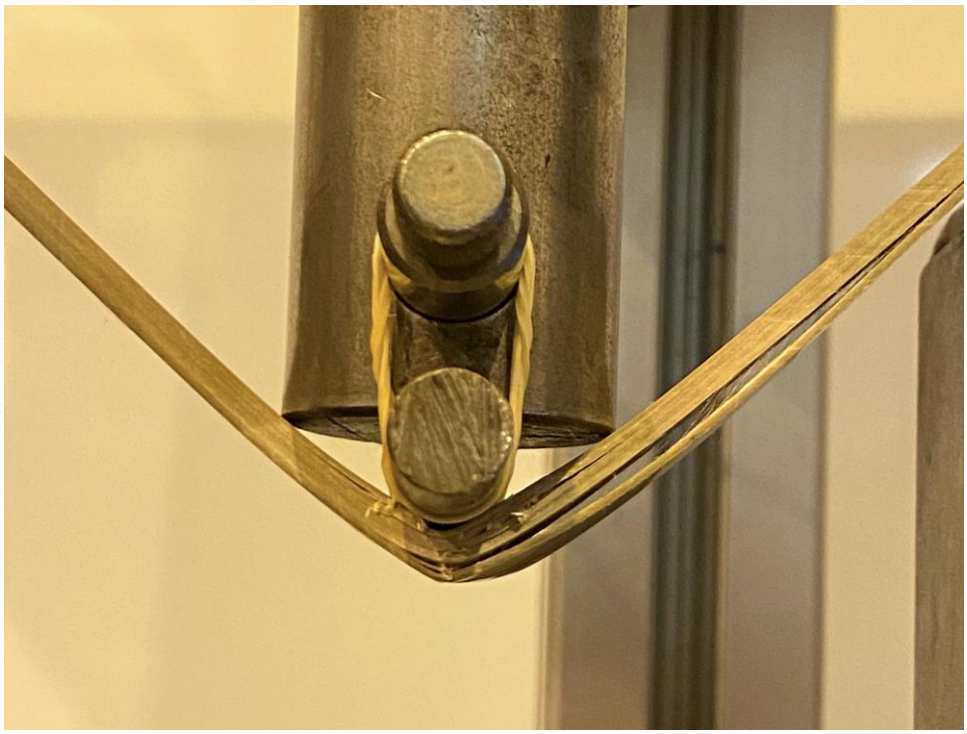

Figure 5.49 Preceding interlaminar shear failure in a 10 wt% specimen with a span to thickness ratio of 32:1.

Since a significant fraction (>50 %) of the specimens failed in an unacceptable failure mode, the span-to-thickness ratio was re-examined and an alternative ratio of 42:1 was implemented throughout the flexural experiments.

Figure 5.50 shows the flexural strength and modulus for 10 and 20 wt% laminates. Average flexural strength and modulus of 10 wt% samples were recorded as 698 MPa and 63.5 GPa, respectively. For the 20 wt% samples, flexural strength saw an increase of approximately 57.6 % and was recorded as 1100 MPa. Flexural modulus was 46.7 GPa, lower than 10 wt% category as is expected from a lower fibre volume sample.

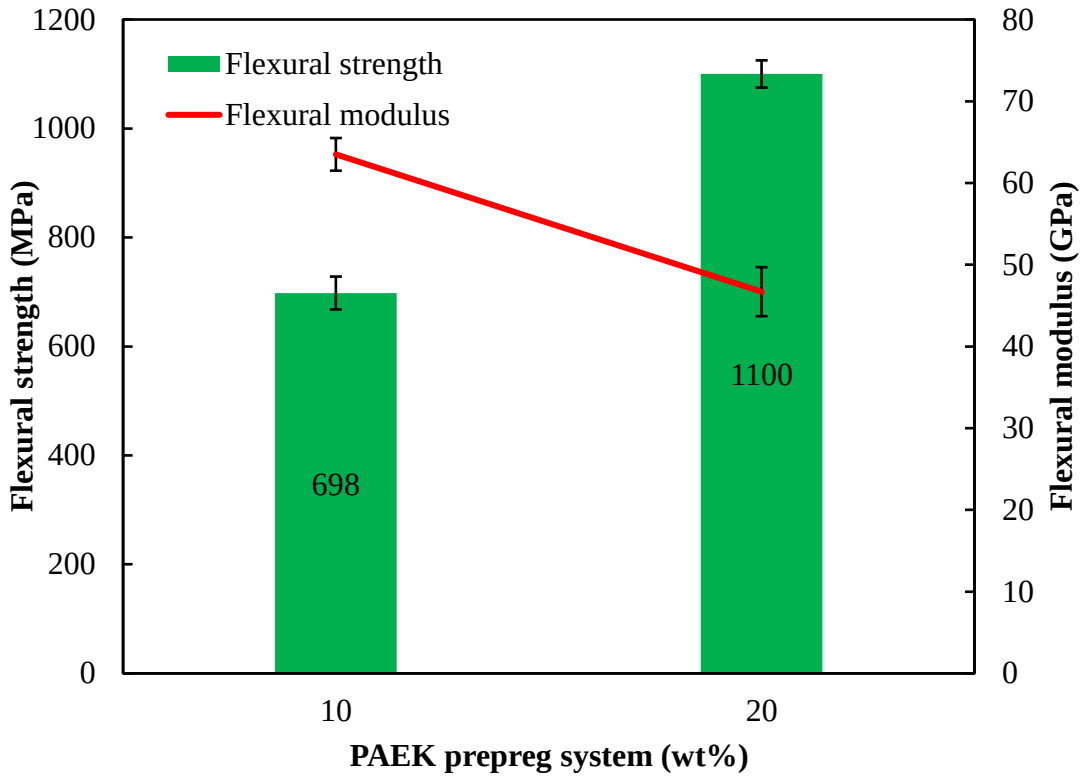

Figure 5.50 Comparison of flexural properties for 10 and 20 wt% laminates.

Due to the high fibre volume content of 10 wt% samples (~72 %), it is forecasted that the compressive strength of such samples would be lower than of 20 wt% samples with approximately 48 % fibre volume content. This is due to the fact that reinforcing fibres would have little resistance to compressive force and as a matter of fact, it is the matrix that supports the composite material in compression. Here, 10 wt% samples only have ~28 % polymer in the composite by volume and therefore, much lower assumed compressive strength compared to 20 wt% samples. Such low assumed compressive strength in 10 wt% samples consequently result in flexural failure modes through compression (due to the assumed compressive strength being much lower than tensile strength). Figure 5.51 shows images of the failure modes for both 10 and 20 wt% samples, with their corresponding flexural stress–strain traces.

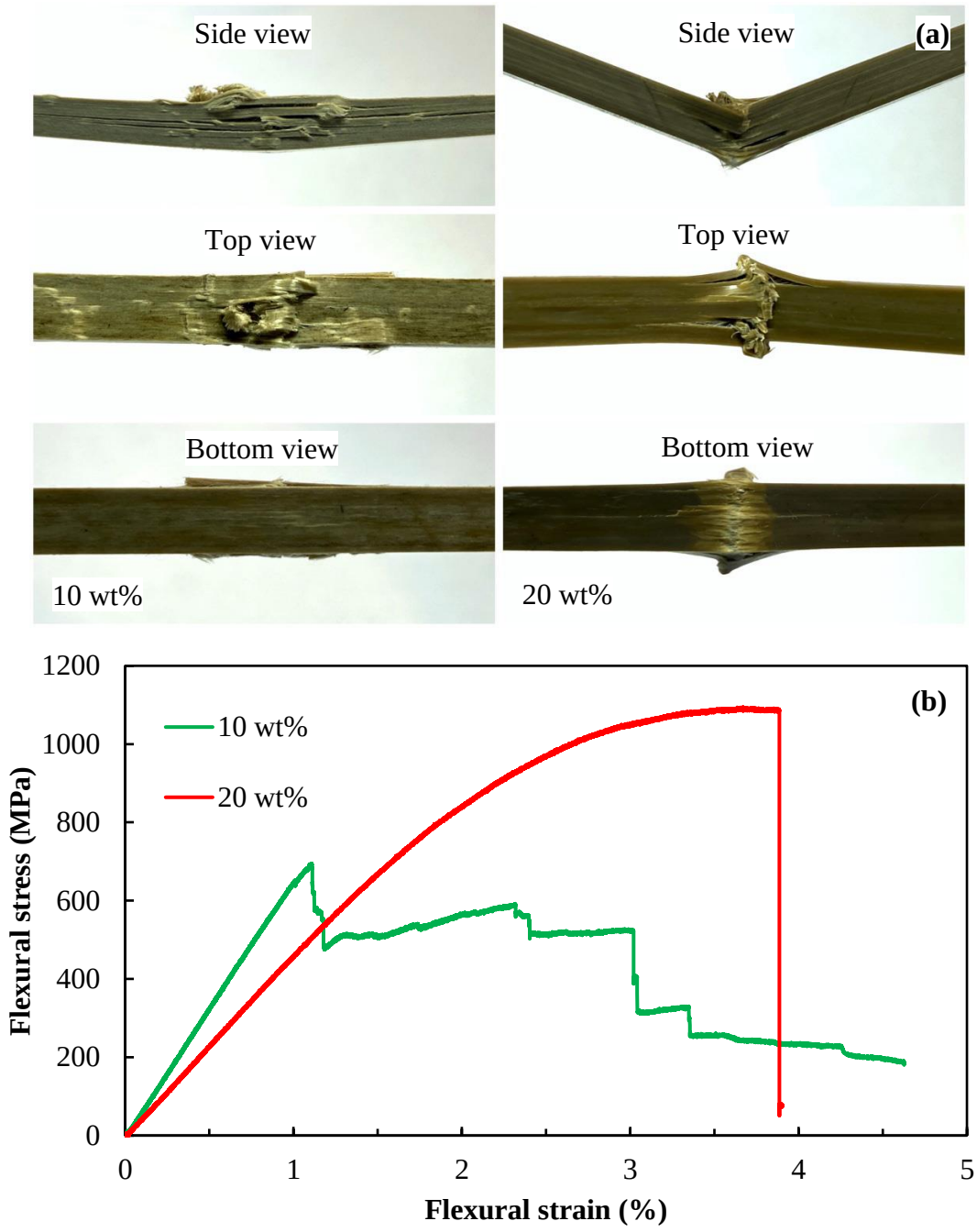

Figure 5.51 Flexural failure behaviour of 10 and 20 wt% laminates: (a) failure modes and (b) stress–strain traces.

Figure 5.51(a) for the 10 wt% sample confirms the aforementioned predictions regarding the failure mode of this category. As evident from the bottom view, no tensile failure is observed. The failure mode for 10 wt% samples are through local buckling on the compression surface. As evident from Figure 5.51(b), the failure mode of 10 wt% sample is progressive. Buckling is initially manifested as micro-buckling on numerous parts of the compression surface (as seen in top view), followed by ply-

level buckling at different levels throughout the thickness of the sample (as seen from side view). In 10 wt% samples, ply-level buckling can cause, or sometimes is preceded by delamination of the outer plies.

For a better understanding of 10 wt% samples failure modes, transverse cross-sectional micrographs of the fractured sample during the flexural test are illustrated in Figure 5.52. The maximum stress is observed just before the outer plies in the compression side of the sample experience a catastrophic ply-level buckling followed by in-plane delamination of the sample in multiple positions (this can sometimes result in complete fracture of the specimen along the delaminated plane). After which, progressive compressive failures are observed in multiple parts of the sample, as evident in the magnified examples.

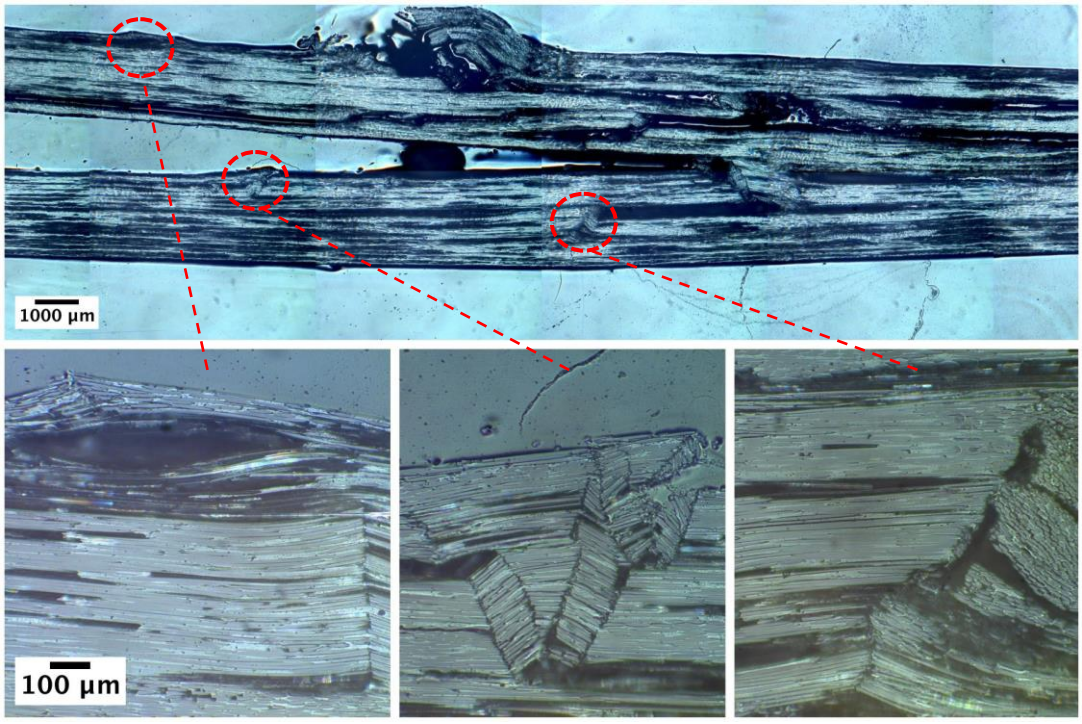

Figure 5.52 Fractographs of a 10 wt% flexural sample.

Here, 20 wt% samples have higher flexural strength due to the presence of more matrix by volume in the composite. While in compression, 20 wt% samples can better tolerate the compressive load (via PAEK matrix) and at the same time, a considerable amount of reinforcing fibre in the lower mid-span of the sample thickness is responsible for tolerating the tension force. This balance between the fibre/matrix ratio helps the 20

wt% samples to achieve a higher flexural strength compared to 10 wt% samples, by eliminating outer surface micro-buckling and preceding delamination. As illustrated in Figure 5.51(a), failure in 20 wt% sample is localised and is limited to the area under the loading nose. Stress–strain traces from Figure 5.51(b) also suggest that this category of samples experience a sudden and catastrophic failure. After the sample is fractured, failure is observed in both compression and tensile side, followed by small and localised delamination of the buckled plies. The mentioned failure mode is more obvious in the transverse cross-sectional micrographs of fractured 20 wt% sample demonstrated in Figure 5.53.

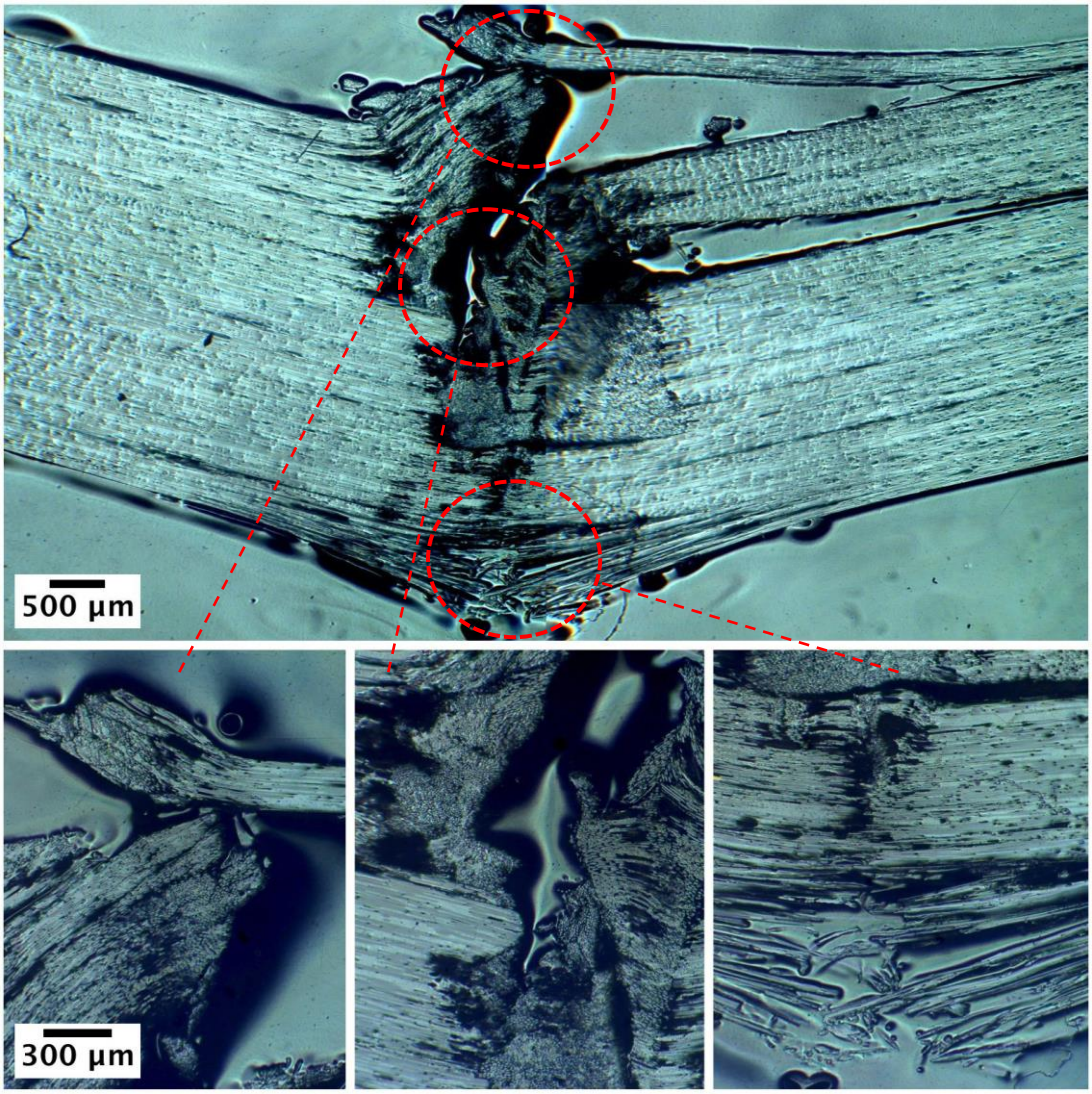

Figure 5.53 Fractographs of a 20 wt% flexural sample.

5.3.3.4 High-temperature Tensile Test

High-temperature tensile tests were carried out on 10 wt% laminates to understand the tensile performance of S2-glass/PAEK composites in elevated temperatures. Figure 5.54 shows the variation in tensile strength for 10 wt% specimens with temperature. As expected, tensile strength deteriorates with increase in temperature. The examination of the graph points out that the slope of the trend slightly sharpens at 150 °C testing temperatures; that is close to the PAEK's glass transition temperature of 149 °C. This is expected as at temperatures close to T_g, the polymer matrix starts softening and consequently, bonding strength between constituents is affected. In other words, the bonding becomes weaker, leading to reduction in composite stiffness and subsequently reduction in the tensile strength.

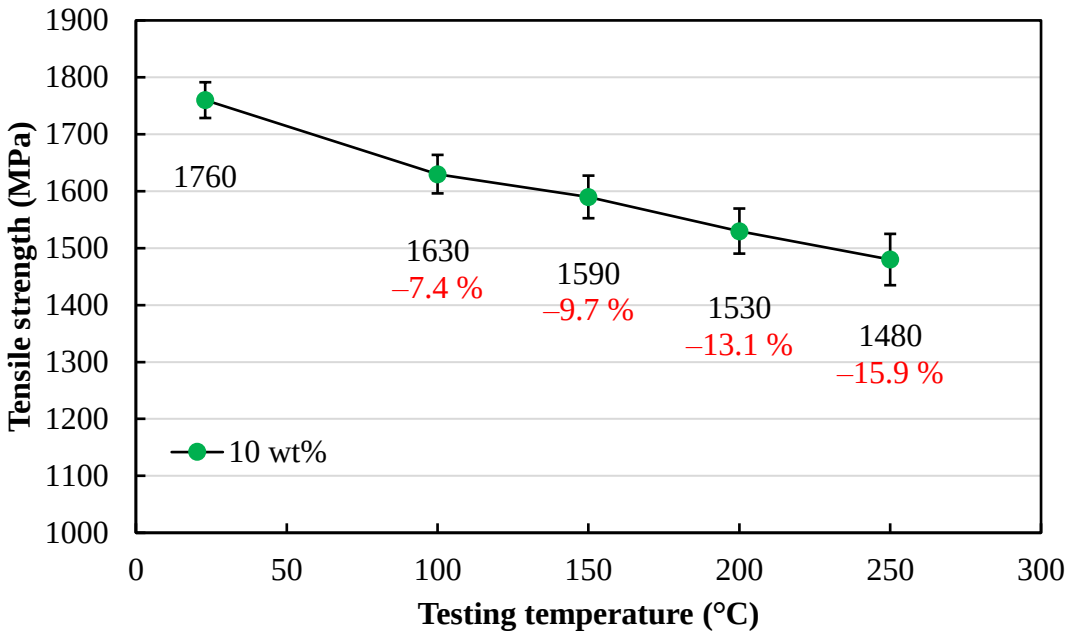

Figure 5.54 The effect of elevated testing temperature on tensile strength of 10 wt% laminates.

Nevertheless, the high-temperature performance of the S2-glass/PAEK is still maintained even at 250 °C, with only 15.9 % reduction in tensile strength compared to results from room temperature. This evidence highlights the advantages of high-temperature semi-crystalline polymers over traditional thermosetting matrices.

5.3.4 The Effect of Nanomaterials on Physical and Mechanical Properties of the Laminates

Nanomaterials were added into the 10 wt% PAEK slurry inside the resin bath in order to produce multiscale (hierarchical) fibre-reinforced nanocomposite prepregs. The goal is to understand the effect of additional nanomaterials on the mechanical properties of 10 wt% S2-glass/PAEK laminates.

5.3.4.1 Physical Properties

Figure 5.55 illustrates sample 10 wt% prepreg plies with the added nano graphene (Nanene). To allow a wide testing range and broaden the investigation, nanomaterial was added 0.5, 1.0, 2.5 and 5.0 part per hundred of PAEK by weight in the resin slurry mixture.

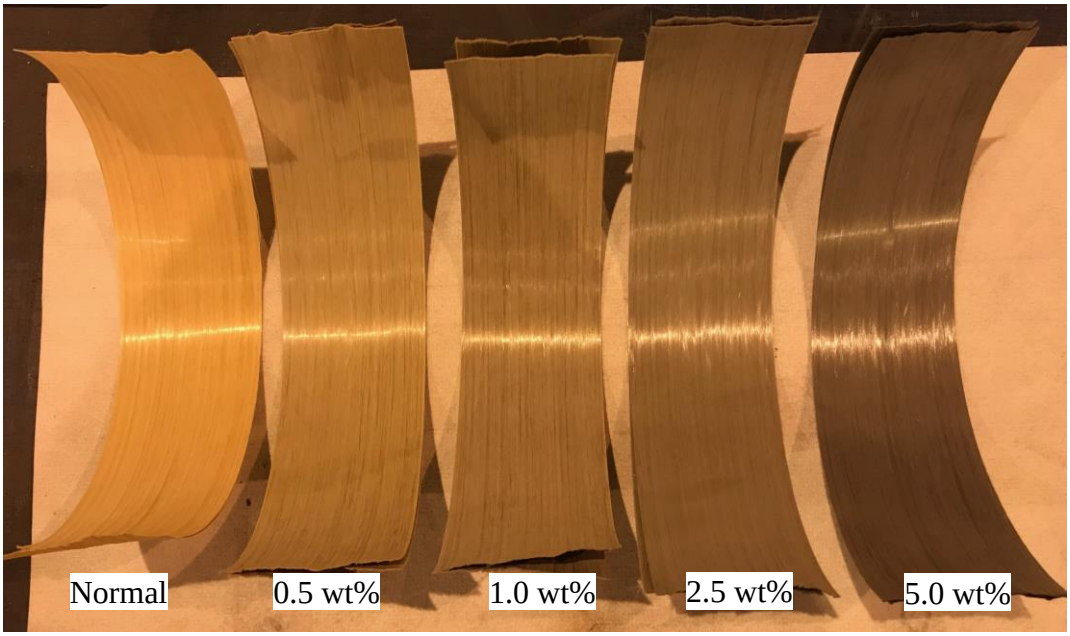

Figure 5.55 Sample hierarchical 10 wt% prepregs reinforced with 0.5, 1.0, 2.5 and 5.0 wt% Nanene.

As can be seen from the figure, when Nanene is added to the S2-glass/PAEK composite, the colour tone of the prepreg changes and becomes darker. This darkening enhances with increase in the Nanene concentration inside the resin bath, with 5.0 wt% Nanene prepregs being the darkest. Addition of nanoclay did not affect the colour of the prepreg due to having similar colour tone as the PAEK.

It is noteworthy to mention that processing 10 wt% prepregs with the added nanomaterials did not affect in anyway the use of the rig for manufacturing prepregs. Additionally, this modification in resin slurry did not change the physical properties of the prepreg such as areal weight and thickness. Physical properties of the manufactured laminates like fibre weight ratio and ply thickness also remained mostly unaffected.

Figure 5.56 demonstrates the prepreg rig being used while Nanene is added into the resin bath slurry and also, sample laminated composite manufactured using hierarchical prepregs. It is observed that the prepreg line runs similar to that when normal slurry is utilised. No PAEK build-up was observed on the spreading rollers and the 5 mm fibre width was maintained as expected. This condition was true for the 0.5 to 5.0 wt% nanomaterial slurry range. The winding process also remained unaffected, with no resin running freely on the drum or evident fibre twists. Ultimately, laminates are manufactured from the produced prepreg plies with success.

Hierarchical prepregs of Nanene and nanoclay were consequently laminated using the same processing parameters for laminating 10 wt% samples; that is, 14.0 bar processing pressure and 20 minutes of pressing time. Transverse cross-sections were cut from the laminates and were polished for optical microscopy as per instructions in Section 4.4.4.

Figure 5.57 shows the cross-sectional micrographs of 0.5, 1.0, 2.5 and 5.0 wt% Nanene and nanoclay hierarchical laminates. Figure 5.57(a) suggests virtually void-free laminates for when Nanene is used as a nanoscale reinforcement inside the composite, regardless of the weight fraction added to the slurry bath. All four categories of composites with the added Nanene show a great fibre distribution along the cross-section of the laminates with no obvious resin rich area or obvious void region. Some dark areas discovered in the cross-section can be attributed to possible stains on the samples, dirt on the microscope lens or glass fibre chipping during the polishing procedure.

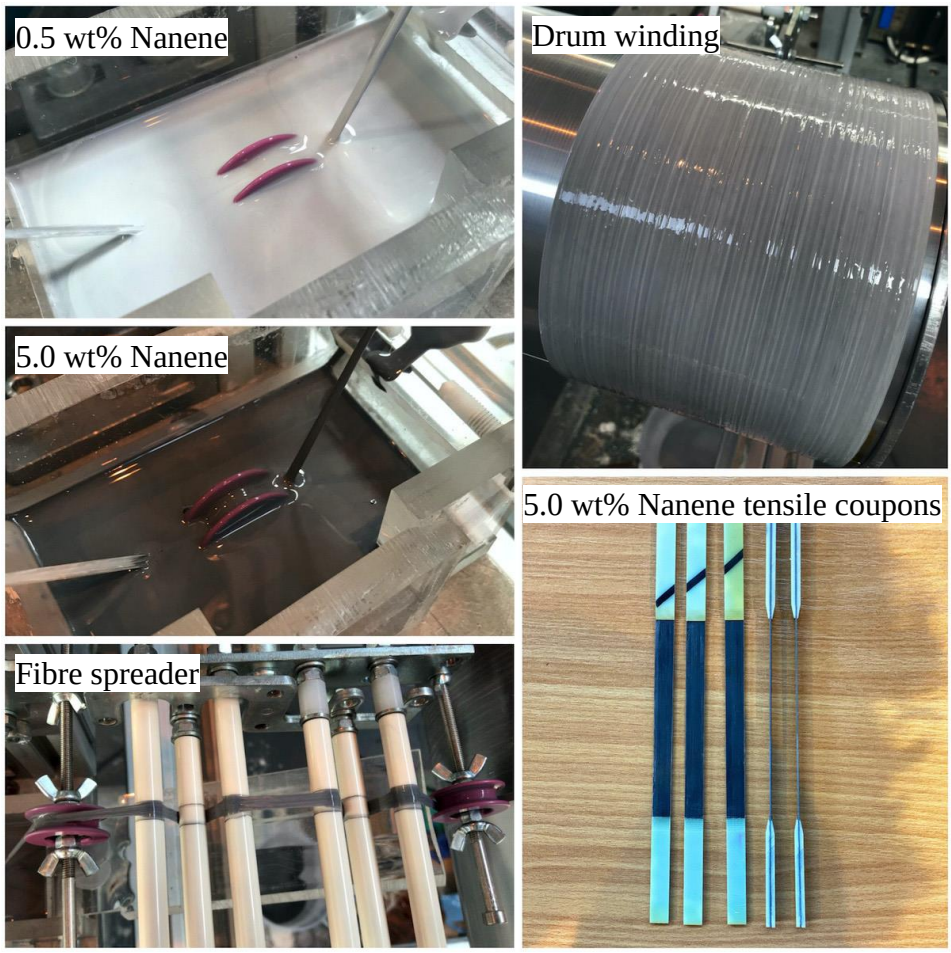

Figure 5.56 Example of incorporating Nanene as nanomaterial inside the resin slurry for prepreg manufacture and sample hierarchical composite produced.

In contrast to Nanene-reinforced samples, laminates produced with the added nanoclay comprised noticeable gas bubbles. Figure 5.57(b) indicates that as the clay content is increased in the laminate, void areas become larger and more dispersed. It has been reported that attempts to make hierarchical fibre-reinforced composites can often result in composites with more voids and lower strength compared to the refence material. It is proved difficult to achieve an adequate fibre wet-out and impregnation with many nanocomposite matrices, due to the modified melt-flow behaviours, which is attributed to a higher melt viscosity compared to the neat matrices [3, 4]. Increased weight fraction of nanomaterials in the composite matrix can potentially make the rotation and movement of aggregates more hindered, leading to a structure that can cause pseudo-solid behaviour [5].

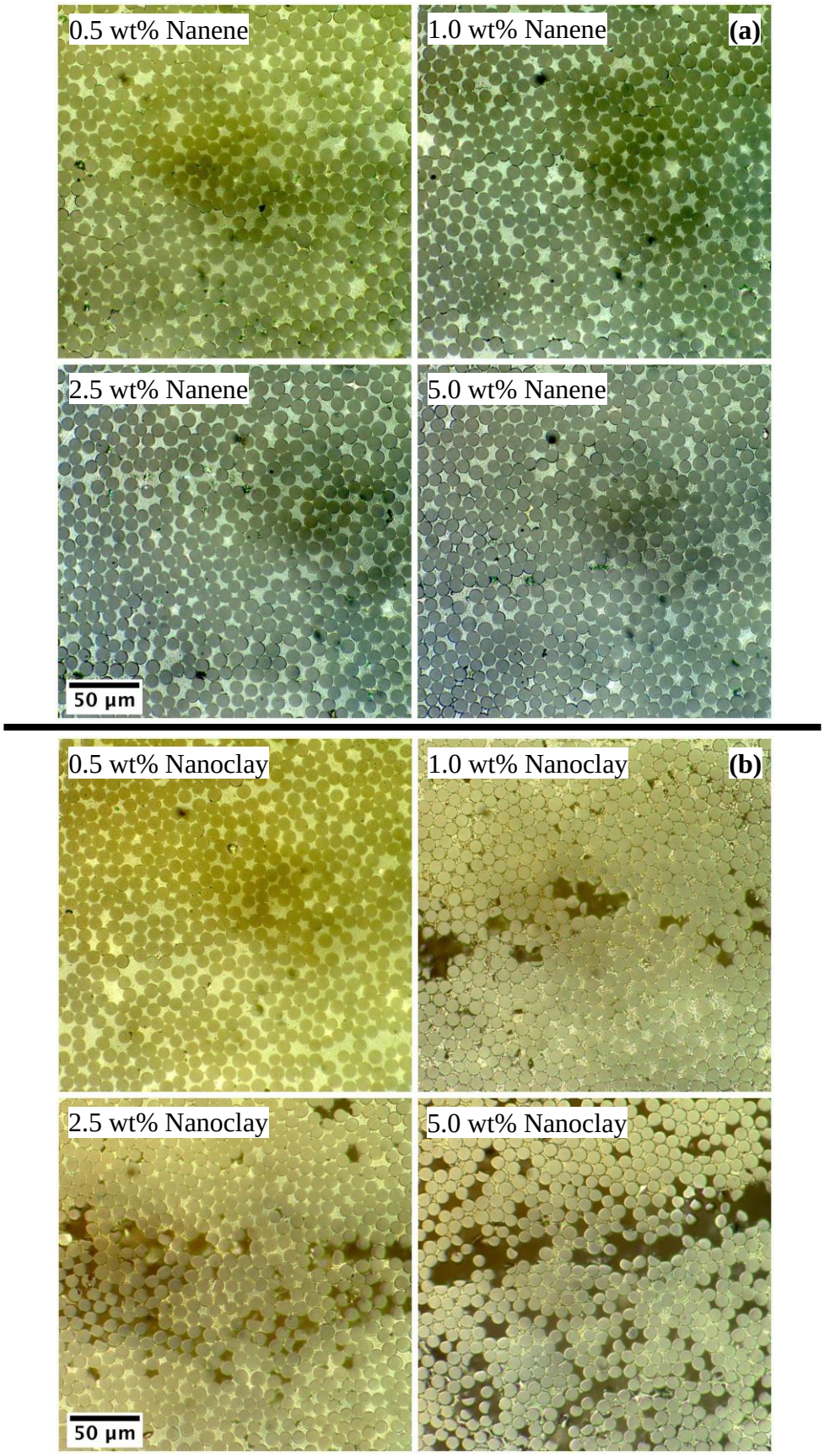

Figure 5.57 Cross-sectional micrographs of hierarchical composites: (a) laminates with added Nanene and (b) laminates with added nanoclay.

It is noteworthy to mention that processing criteria and viscosity of filled PAEK matrices with other nanomaterials such as CNTs, given the same weight ratio, could be significantly higher than when graphene is used as filler, making them more difficult to process the nanocomposites [6, 7].

Given the aforementioned factors, use of Nanene is expected to lead to enhanced reinforcement levels (as will be investigated in the next sections) without compromising the processing performance or the viscosity of the composite matrix, even at high filler ratios. At the same time, using nanoclay in the PAEK matrix is expected to have inferior implications on the mechanical performance of the manufactured composites.

5.3.4.2 Tensile Test

The effect of incorporating nanomaterials into the S2-glass/PAEK composites on the tensile strength of 10 wt% laminates was investigated. Here, 0.5, 1.0, 2.5 and 5.0 parts per hundred PAEK mass of Nanene and nanoclay were added to 10 wt% PAEK resin slurry for comparison of tensile strength with the neat 10 wt% samples, and the obtained values can be seen in Figure 5.58.

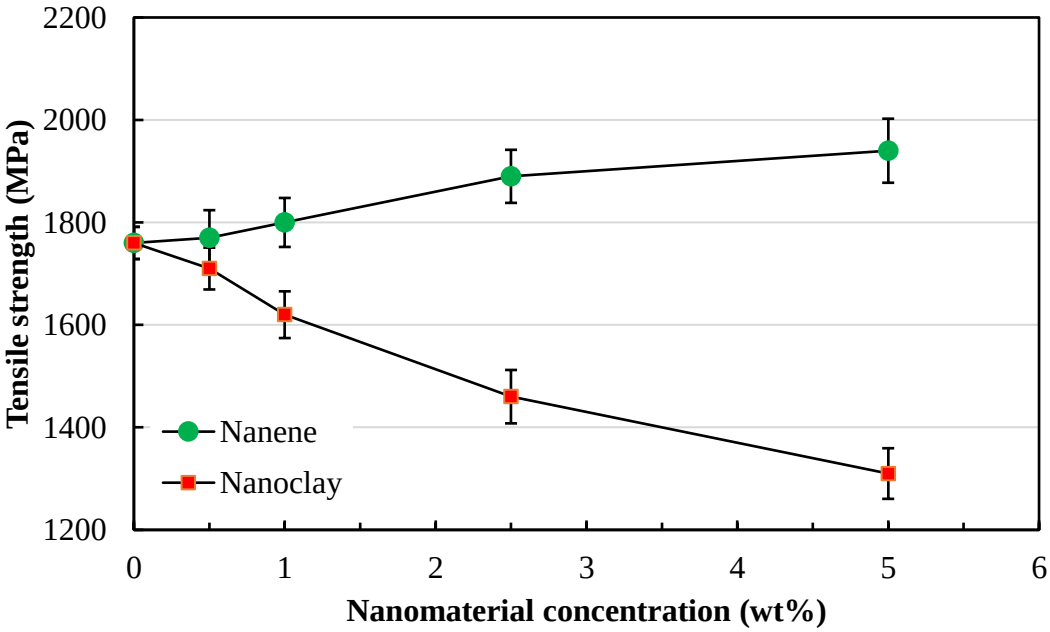

Figure 5.58 The effect of nanomaterials on tensile strength of 10 wt% laminates.

As per the results and discussion in Section 5.3.4.1, the void content in the samples reinforced by nanoclay magnifies with increase in the added weight ratio. As seen in Figure 5.58, this phenomenon has a direct impact on the tensile performance of nanoclay composite laminates. Here, tensile strength shows a steady decrease as the nanoclay concentration increases, with 5.0 wt% nanoclay samples having an average tensile strength of 1310 MPa. This is a 25.6 % reduction in tensile strength compared to the reference normal samples.

Additionally, the adhesion of clay nanocomposites with glass fibre has been shown to be occasionally weak. Critical fibre aspect ratio (critical fibre length/fibre diameter) has been reported to largely increase as a result of higher silicate concentrations, which is apparently caused by deterioration in interfacial bond strengths [8]. By studying the SEM image and micrograph of fractured tensile coupon in Figure 5.59(c), it is observed that the failed nanoclay samples contain numerous bare and exposed fibres, with smooth surfaces and occasional residual resins, which points out to a weak fibre-matrix adhesion. It should be mentioned that change in the melt flow behaviour of nanoclay matrices could potentially deteriorate the free and easy wetting of S2-glass fibres by the matrix, which might affect the quality of the interface.

In normal 10 wt% fractured samples (Figure 5.59(a)), a homogeneous and rough layer of PAEK is observed to remain on the surface of filaments after failure. This is an indication that general bonding strength between fibre and matrix constituents is strong, and sufficient for casual load transfers in the composite, and as a matter of fact, additional nanoclay could have adverse effects on the bonding energies.

A clear morphological change is observed after the introduction of Nanene in the samples. Figure 5.59(b) indicates a rough fibre surface throughout the failed sample with textured resin blocks appearing between fibres after failure. This behaviour suggests strong fibre/matrix interfacial bond and great stress share and transfer between S2-glass fibre and Nanene nanocomposite matrix.

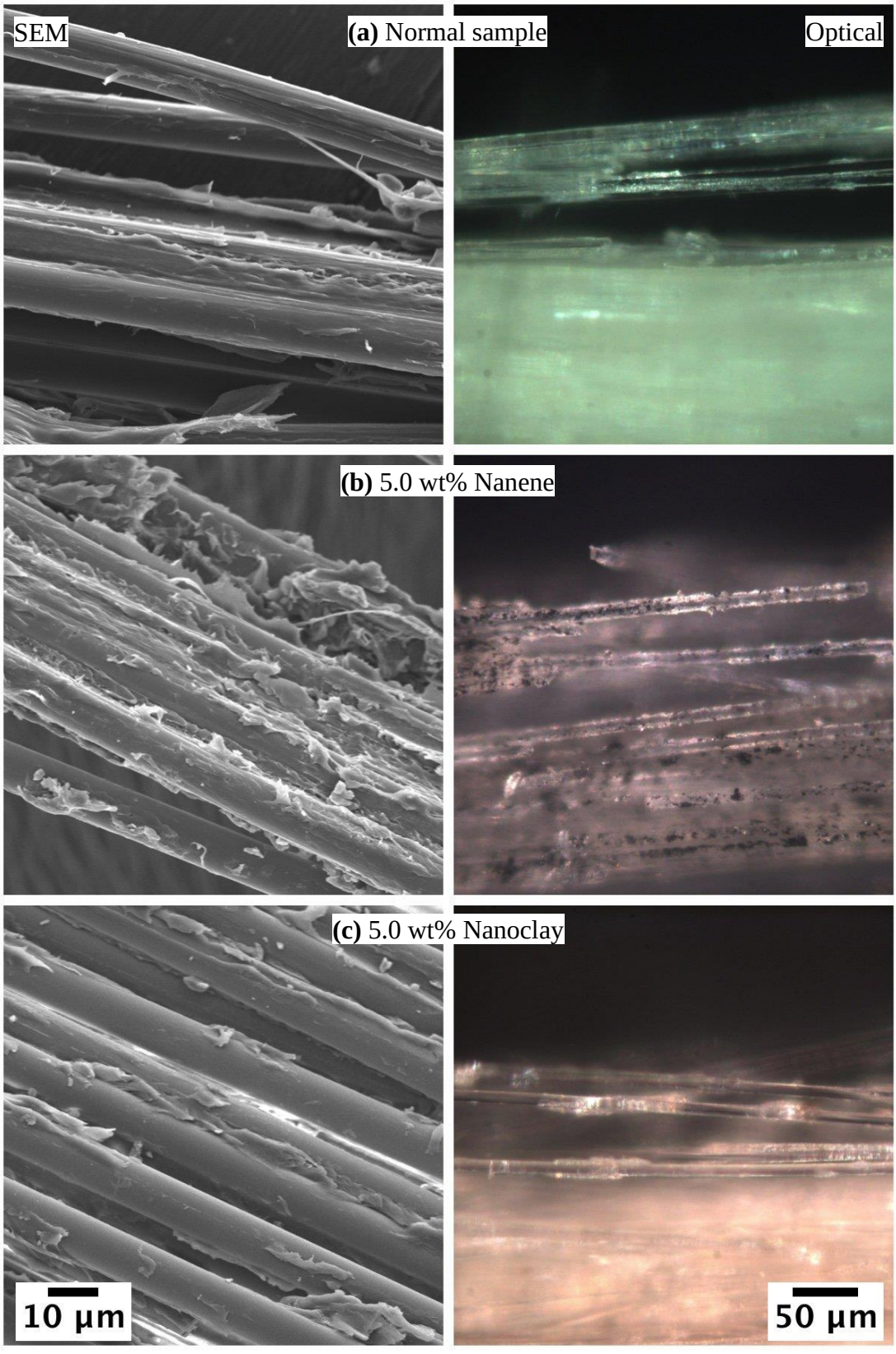

Figure 5.59 SEM images and optical micrographs of fractured 10 wt% tensile samples with: (a) no nanomaterial, (b) 5.0 wt% Nanene and (c) 5.0 wt% nanoclay.

As per the findings from Section 5.3.4.1 regarding the cross-sectional micrographs of Nanene hierarchical samples, it can be assumed that addition of Nanene to high fibre volume (~72 %) S2-glass/PAEK composites is essentially helping enhance the interfacial bonding by acting as a bridge between both constituents.

As seen in the micrograph from Figure 5.59(b), utilising the same lighting set-up and crossed-polarising filter technique in optical microscopy can shed light on the presence of the S2-glass fibre, PAEK and Nanene particles, despite the very limited depth of field. This is a particularly valuable technique since it was very difficult to identify Nanene flakes using the obtained SEM images, if at all possible. Close observation of fractured Nanene samples indicates very good dispersion of Nanene particles not only in the PAEK matrix, but also on/close to the surface of fibres as well.

Captured results of tensile samples from Figure 5.58 clearly show some enhancement in the tensile strength of Nanene-reinforced fibre composites. This increase in strength becomes more pronounced after addition of more than 2.5 wt% Nanene to the resin slurry. It is noteworthy to mention that a number of 5.0 wt% Nanene samples saw a tensile strength up to 2000 MPa, which is a considerable improvement with respect to the normal composite samples.

5.3.4.3 Interlaminar Shear Test

The addition of nanomaterials did not notably influence the short-beam strength. As seen in Figure 5.60, incorporating different weight percentage of nanoclay and Nanene had minor effects on the interlaminar shear strength values. Regardless of the type of nanomaterial or the added weight percentage, short-beam strength values approximately varied between 67.1 and 78.4 MPa for all the specimens tested.

Due to different characteristics and the uniqueness of each manufactured composite laminate and sample, it is proven difficult to make assumptions based on the small fluctuations of the recorded trend in Figure 5.60. Although these variations in the trend can be ignored by observing the error deviations, the gap between the strength values of both nanocomposites becomes larger as the nanomaterial concentration increases.

The changes in the interlaminar shear strength of 5.0 wt% samples are in the order of 4 % (increase in Nanene samples and decrease in nanoclay samples).

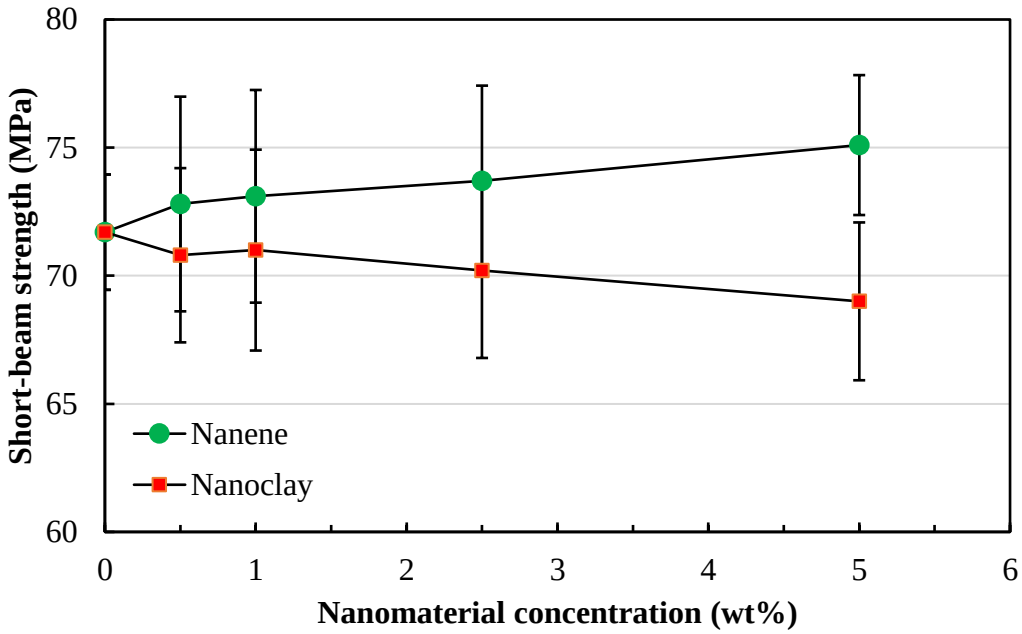

Figure 5.60 The effect of nanomaterials on short-beam strength of 10 wt% laminates.

Typical failure mode for hierarchical laminates was identical to the normal samples, i.e. mid-plane interlaminar failure with increasing the load applied on the specimens until a load drop of 30 % is observed.

5.3.4.4 Flexural Test

The effect of additional nanomaterials on the flexural strength of 10 wt% laminates was investigated. As seen in Figure 5.61, addition of Nanene and nanoclay onto the composite matrix would alter the flexural performance of the specimens. It is understood from the flexural behaviour that 0.5 and 1.0 wt% incorporation of nanoclay does not have significant effect on the performance of the composite. Similar trend is observed for Nanene, with slightly higher flexural strength in 1.0 wt% setting compared to nanoclay. Both nanomaterials see a spike in the flexural performance when added at 2.5 wt%, with an enhancement of 23.8 % for nanoclay and 35.8 % for Nanene composites.

The fact that the failure mode for the majority of 10 wt% composite samples is through compression, matrix stiffness plays an important role in providing flexural strength. This is due to the fact that the reinforcing fibres cannot provide much support while being compressed and it is the matrix in the composite that will tolerate the compressing load. The flexural strength of a continuous fibre composite is dominated by the compressive strength because failure usually starts at the compressive side due to micro buckling or kinking [3]. Stiff nanoparticles can significantly enhance the compressive properties of composite samples and in this case, increase the flexural properties.

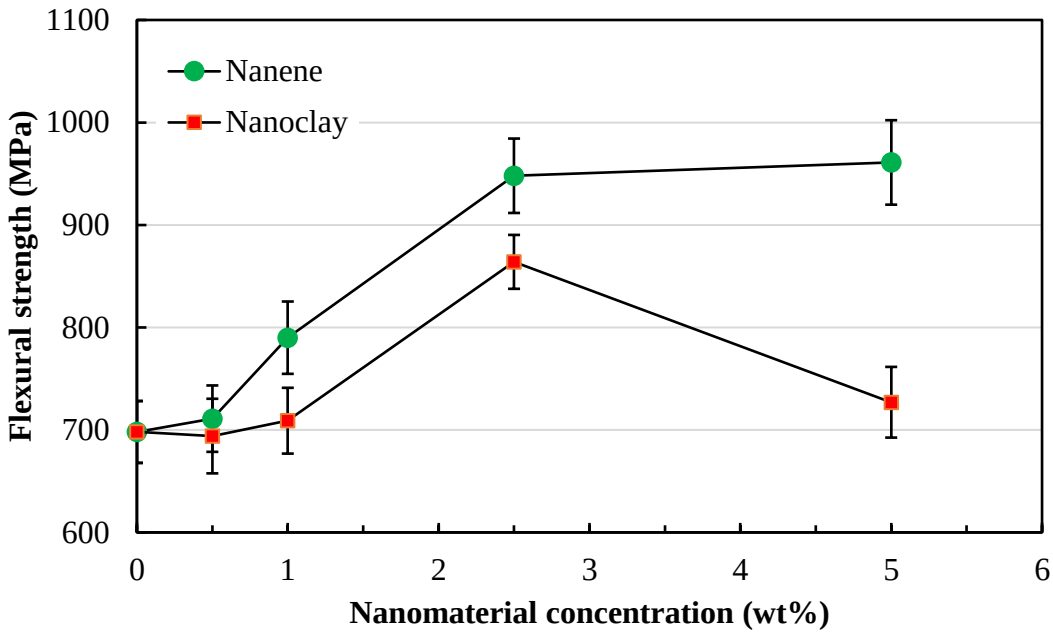

Figure 5.61 The effect of nanomaterials on flexural strength of 10 wt% laminates.

It is important to remember that the type of nanoclay utilised in this research shows severe problems with fibre wet-out, impregnation and adhesion, and it therefore, cannot represent the expected improvement of nanoclay matrix composites. At the very least, the fibre wetting problem of high concentration nanoclay PAEK matrices should be addressed for a reasonable comparison with Nanene composites. No effort was carried out to tackle the impregnation issues of nanoclay composites; however, it is expected that changes in the laminating parameters, such as increase in processing temperature, pressure or time, can potentially tackle some of these mentioned issues.

Figure 5.62 shows the failure modes of nanocomposite flexural samples with different Nanene and nanoclay ratios. When the nanomaterial concentration increases to 5.0 wt%, nanoclay composites experience a decline in their flexural strength in comparison to their corresponding 2.5 wt% samples. Here, the decline in flexural strength of 5.0 wt% nanoclay samples can be attributed to different failure modes compared to 0.5, 1.0 and 2.5 wt% samples. Due to the low tensile strength and higher void content problems associated with 5.0 wt% nanoclay samples, compression failure in their flexural test is followed by, or precedes, tensile failure in the bottom outer surface of the sample. Weak interfacial bonding between the fibre and matrix in 5.0 wt% setting also deteriorates the mechanical tolerance of the composite samples.

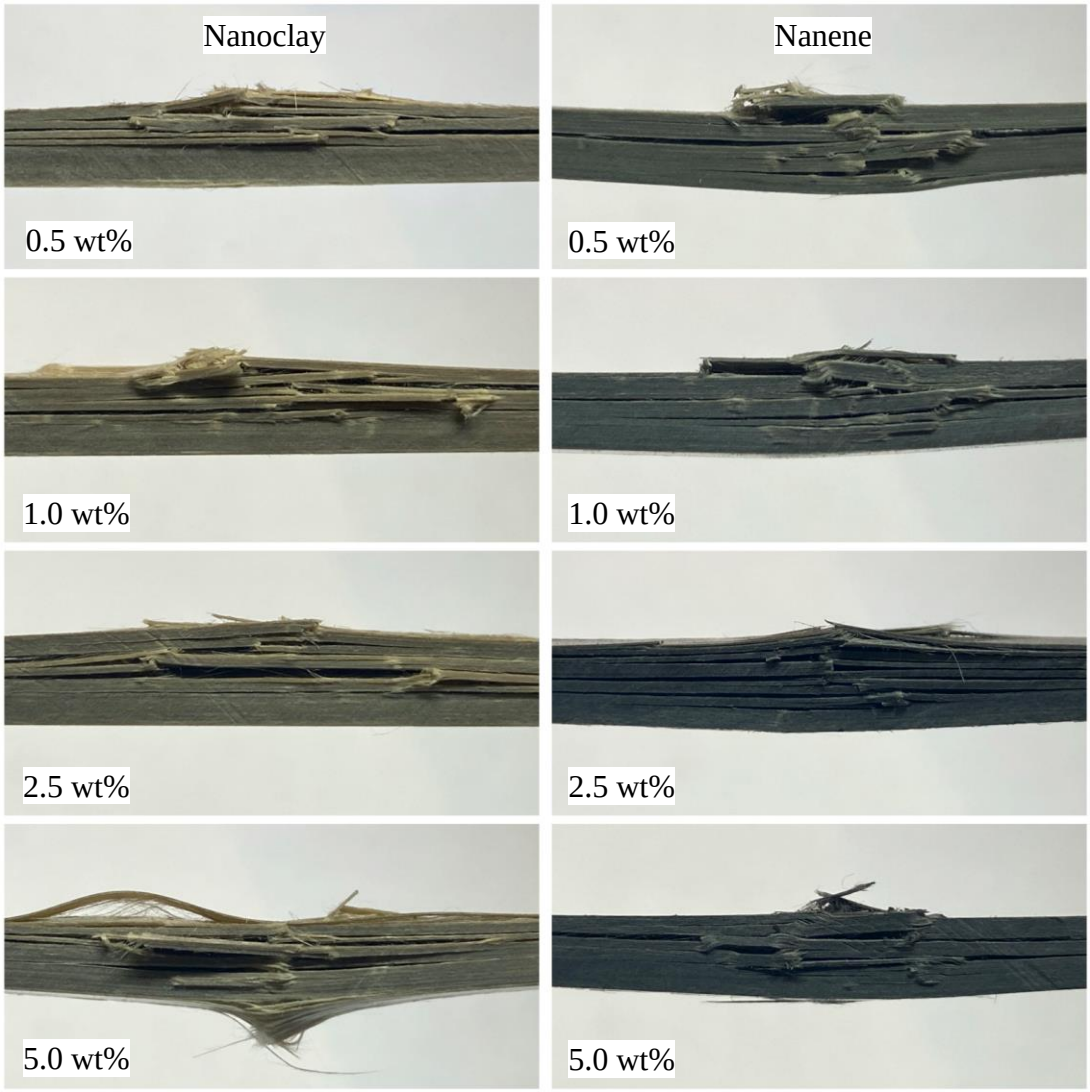

Figure 5.62 Flexural failure behaviour of Nanene and nanoclay composites with different concentrations.

Other nanoclay concentration settings undergo a different failure behaviour, which is similar to the neat composite samples (as discussed in Section 5.3.3.3). However, the matrix stiffness in 2.5 wt% samples is higher compared to lower nanoclay ratios, leading to a higher flexural strength, despite the presence of gas bubbles in the matrix. In other words, the enhancement effects in the matrix stiffness overcomes the void content problems, leading to a higher-than-normal flexural strength.

Flexural traces for samples with different Nanene concentrations shown in Figure 5.63 indicates that all Nanene samples experience similar failure modes, which are also matching that of normal 10 wt% PAEK samples. As also evident in Figure 5.62, failure is obtained through local buckling on the compression surface, followed by ply-level buckling at different levels throughout approximately two-third of the thickness of the sample. Occasionally, ply-level buckling can cause, or sometimes is preceded by delamination of the outer plies. Here, the addition of more than 2.5 wt% Nanene in the slurry does not seem to enhance the flexural properties as much, as per values in Figure 5.61. One explanation could be that in 10 wt% PAEK samples in general, preceding delamination does not allow the observation of true flexural strengths in samples and in this instance, preceding delamination prevents 5.0 wt% Nanene samples to obtain their appropriate failure mode and the strength level stays similar to 2.5 wt% specimens. Therefore, the full potential of 5.0 wt% samples is not realised.

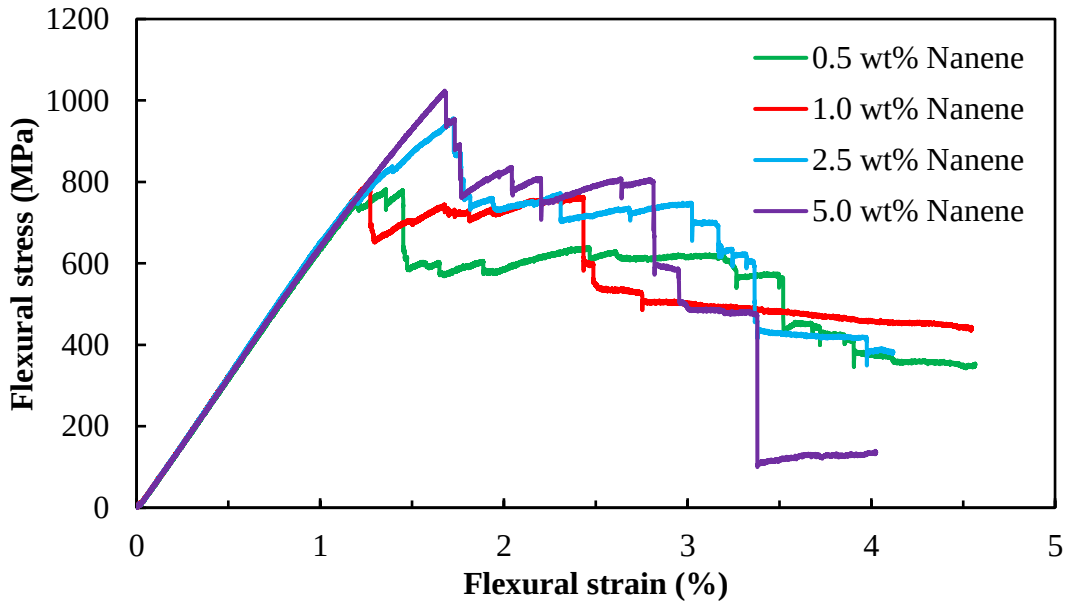

Figure 5.63 Stress-strain behaviour of samples with different Nanene concentration.

5.4 Summary

In this chapter, results from all the experimental works were presented, followed by relevant discussions for different findings. It was found that L2O is a suitable carrier for suspending and dispersing PAEK particles. PSD results indicated that PAEK is suspended better in L2O compared to water, with a higher degree of particle separation. Over 90 % of scanned PAEK particles were found to be around 20 microns or less, which is particularly important for the prepreg impregnation stage. Further tests were carried out on colloidal stability of PAEK slurries with different concentrations and it was found that L2O is capable of suspending 10 to 30 wt% PAEK slurries, without serious sedimentations, at least for the duration of fibre winding. Apart from nanoclay slurries, other samples showed good stability, without the need of external stirring in the resin bath.

Medium winding speeds in the order of approximately 7.8 rpm was found to give the best balance between processing speed and resin handling problems. Additionally, the tension exerted on the fibre bundle should be chosen in a way to provide only sufficient force in order for the fibre filaments not to deviate from their predefined path and to stay straight.

The novel fibre spreader assembly was found capable of spreading both dry and wet fibre bundle. It was realised that higher frequency and motion amplitude of the spreading rollers can lead to higher degree of fibre spread. However, very high vibrations can cause fibre twists and breakage. Usually, 6 mm of motion amplitude along with 5 Hz of frequency provides considerable fibre spread, up to 5 times greater than the original fibre bundle width. Fibre spread degree can further be enhanced by implementing fixed rollers; however, can cause resin agglomeration on the rollers and consequently results in fibre breakage.

By completing a number of preliminary tests, it was realised that the prepreg rig is consistent in the amount of resin pick-up by the fibre bundle. Utilising optimum parameter for each setting, S2-glass/PAEK prepregs were successfully produced using the AE 250 PAEK as the prime polymer grade. Three tiers of thermoplastic prepreg with different fibre and resin ratios were manufactured for comparison.

All three 10, 20 and 30 wt% PAEK prepregs showed an excellent degree of polymer powder impregnation between the fibre filaments, thanks to different design elements of the novel prepreg rig and its impregnation procedure. Further tests revealed that temperature, pressure and time are the three important factors in manufacturing composite laminates. High pressure and processing times paved the way for producing virtually void-free laminates. It was realised that as the polymer ratio is reduced in the prepreg, higher processing pressure becomes more critical. Typically, a processing pressure of 10.5 bar along with 20 minutes of pressing times could eliminate the majority of gas bubbles inside the laminates.

Laminates with a fibre volume content ranging from 32 to 72 % were successfully manufactured and tested for their mechanical properties. Tensile strength values varied depending on the ratio of constituents and could reach 1760 MPa for high fibre volume content settings (72 %). Other tensile properties such as tensile modulus and failure strain was also recorded and compared. Additionally, testing 10 wt% PAEK laminates for their tensile strength in elevated temperatures, up to 250 °C, revealed only a reduction of approximately 15.9 %. Further mechanical tests such as interlaminar shear strength and flexural strength was carried out and the results for different laminate settings were compared.

Finally, the effect of additional nanomaterials, namely Nanene (graphene) and nanoclay, on the mechanical performance of 10 wt% composite laminates was investigated. The addition of Nanene in the PAEK slurry was found beneficial with regards to tensile strength of samples, with some samples reaching a strength of approximately 2000 MPa with 5.0 wt% loading of Nanene inside the resin bath. The use of nanoclay however leaded to difficulties with ideal glass fibre wet-out by the nanocomposite matrix and deteriorated the fibre/matrix interfacial adhesion. This phenomenon had an impact on an effective investigation of nanoclay composites and comparing them to their Nanene counterparts. That said, the use of nanoclay in 2.5 wt% concentrations enhanced the flexural properties of the composite.

5.5 References

[1] Gibson, A. G., and Månson, J. A., 1992, "Impregnation technology for thermoplastic matrix composites," Composites Manufacturing, 3(4), pp. 223-233.

[2] Xian, G., Pu, H.-T., Yi, X.-S., and Pan, Y., 2006, "Parametric Optmisation of Pin-assisted-melt Impregnation of Glass Fiber/Polypropylene by Taguchi Method," Journal of Composite Materials, 40(23), pp. 2087-2097.

[3] Vlasveld, D. P. N., Daud, W., Bersee, H. E. N., and Picken, S. J., 2007, "Continuous fibre composites with a nanocomposite matrix: Improvement of flexural and compressive strength at elevated temperatures," Composites Part A: Applied Science and Manufacturing, 38(3), pp. 730-738.

[4] Vlasveld, D. P. N., Bersee, H. E. N., and Picken, S. J., 2005, "Nanocomposite matrix for increased fibre composite strength," Polymer, 46(23), pp. 10269-10278.

[5] Vlasveld, D. P. N., de Jong, M., Bersee, H. E. N., Gotsis, A. D., and Picken, S. J., 2005, "The relation between rheological and mechanical properties of PA6 nano- and micro-composites," Polymer, 46(23), pp. 10279-10289.

[6] Papageorgiou, D. G., Liu, M., Li, Z., Vallés, C., Young, R. J., and Kinloch, I. A., 2019, "Hybrid poly(ether ether ketone) composites reinforced with a combination of carbon fibres and graphene nanoplatelets," Composites Science and Technology, 175, pp. 60-68.

[7] Bangarusampath, D. S., Ruckdäschel, H., Altstädt, V., Sandler, J. K. W., Garray, D., and Shaffer, M. S. P., 2009, "Rheology and properties of melt-processed poly(ether ether ketone)/multi-wall carbon nanotube composites," Polymer, 50(24), pp. 5803-5811.

[8] Vlasveld, D. P. N., Parlevliet, P. P., Bersee, H. E. N., and Picken, S. J., 2005, "Fibre–matrix adhesion in glass-fibre reinforced polyamide-6 silicate nanocomposites," Composites Part A: Applied Science and Manufacturing, 36(1), pp. 1-11.

CHAPTER VI: CONCLUSIONS AND RECOMMENDATIONS FOR FUTURE WORK

6.1 Introduction

In this study, an experimental investigation on manufacturing high-temperature and high-performance glass fibre/PAEK thermoplastic prepreg have been presented. The experiments undertaken were discussed in two parts. The first part exploring the novel thermoplastic prepreg rig and method of manufacturing prepregs using an aqueous wet powder impregnation method. Then, a series of physical and mechanical tests were carried out on the manufactured S2-glass fibre/PAEK composite materials with different constituent ratios to evaluate the efficiency of the production line and quality of the achieved materials.

6.2 Major Conclusions

Based on the outputs of the current research work, the following conclusions can be drawn:

- The proposed thermoplastic prepreg manufacturing method utilising wet powder impregnation method is capable of producing thermoplastic composites.
- The designed and manufactured drum winding prepreg rig provides grounds for a very effective thermoplastic prepreg production in terms of costs, scale and suitability.
- The prepreg rig is compact in size, easily maintained and suitable for laboratory scale research where rapid prepreg production is required. The rig can be used with wide range of thermoplastic powders and reinforcing fibres.
- The prepreg rig is comprised of different parts including fibre guides, rollers, package holder, resin bath, fibre spreader, linear actuator, winding drum and heating unit.
- L2O is an effective liquid carrier, capable of dispersing and segregating 10, 20 and 30 wt% AE 250 PAEK polymer concentrations. No considerable sedimentation is observed for 20–30 minutes, which is the duration of the prepreg winding process.
- Winding speed can be varied from 0.9 to 19.0 rpm. Winding speeds lower than 4.6 rpm can result in a high processing time and slurry accumulation at the bottom of the drum, leading to uneven distribution of resin. Winding speeds

faster than 11.7 rpm can cause excessive slurry pick-up by the fibre tow, free resin run on drum, and fibre breakage. Winding speeds between 6.7 to 9.0 rpm are ideal and can tackle a majority of the issues.

- The optimum fibre tensioning force is found to be achieved with setting number 2 (1.3 N). Lower tensions such as 0.8 N can lead to fibre waviness in the prepreg, while higher tensions such as 2.3 N can cause fibre breakage.
- The designed and manufactured fibre spreader assembly is capable of effectively spreading dry or wet fibre bundle via a reciprocating motion of spreading rollers. It can spread impregnated S2-glass tow up to 7 times (~17 mm) the original dry fibre bundle width when rotating rollers are used, and up to 10 times (~24 mm) when fixed rollers are mounted.
- Rotating rollers are recommended for prepreg winding process, particularly for 20 and 30 wt% PAEK slurries to avoid resin agglomeration on rollers. The use of fixed rollers can result in high tensions in the fibre bundle, creating fuzz on the rollers due to filament breakage. Polymer agglomeration on rollers can follow.
- The degree of the spread can be controlled by changing the frequency and amplitude of the vibration. Cam 3, providing 6 mm of motion amplitude, was found to provide good balance between fibre spread effectiveness and practicability.
- The amount of PAEK pick up by the fibre bundle usually remains constant throughout the winding for 10, 20 and 30 wt% slurries. For 40 wt% slurry setting, heavy resin agglomeration occurs on the rollers, and in extreme cases, results in complete fibre cut off from the winding drum.
- AE 250 PAEK is chosen as the primary polymer grade due to its particle size distribution, compatibility with L2O carrier, processing temperature and mechanical performance.
- By changing the ratio of the constituents in the resin bath, prepregs with different physical properties can be produced. Prepregs with 10, 20 and 30 wt% PAEK slurry and S2-glass are prepared. Measured thickness and areal weight vary from 0.25 to 0.49 mm and 277 to 467 g/m^2, respectively.

- The proposed impregnation method exhibits very effective infusion of polymer powders into the fibre filaments. PAEK with average particle size of 10 microns is found satisfactory.
- Fibre volume content of fully consolidated 10, 20 and 30 wt% prepreg laminates are measured as 72, 48 and 32 %, respectively. Higher processing pressure and time results in lower void content. The void content for 72 % fibre volume content laminates can be as low as 0.19 %. The effect of processing time on void content diminishes for holding times of more than 20 minutes.
- Tensile strength for virtually void-free 32, 48 and 72 % fibre volume content samples were recorded as 952, 1380 and 1760 MPa, respectively. Measured tensile modulus of the samples closely matches the predictions from the rule of mixture calculations; 31.8 GPa compared to the estimated 30.9 GPa for 32 %, 48.7 GPa compared to the estimated 44.5 GPa for 48 % and 62.2 GPa compared to the estimated 65.1 GPa for 72 % fibre volume content samples.
- Tensile properties, apart from failure strain, decline as the matrix content increases. Failure strain shifts from 3.41 to 2.87 % for when ductility is decreased because of a higher fibre volume content.
- Increased void contents can proportionally lead to deterioration of tensile strengths, with 3.67 % of void reducing the tensile strength of 10 wt% PAEK samples to 1350 MPa, which is a 23.3 % decrease.
- S2-glass/PAEK laminates showcase an impressive tensile performance in elevated temperatures, with only 15.9 % reduction in tensile strength for 10 wt% slurry laminates, lowering from 1760 MPa in room temperature to 1480 MPa at 250 °C.
- Change in the fibre volume content does not have a significant effect on interlaminar shear strength for both 10 and 20 wt% laminate samples, with recorded average shear values of 74.7 and 75.1 MPa, respectively.
- Flexural strength for 20 wt% samples is approximately 1100 MPa, which is almost double the values of 10 wt% samples at 698 MPa. The flexural modulus for 10 and 20 wt% samples are 63.5 and 46.7 GPa, respectively. Failure mode for 10 wt% samples are complex, and the failure occurs on multiple levels and locations. Preceding interlaminar failure is observed in 10 wt% samples occasionally.

- Nanomaterials can easily be incorporated in the resin bath for manufacturing of hierarchical composites without affecting the prepreg process. Graphene and nanoclay was successfully added to the resin bath.
- The use of graphene can enhance the tensile strength of the samples by up to 14 %, often reaching over 2000 MPa. It can also increase the flexural strenght by up to 38 %. Adding nanoclay deteriorates the tensile strength due to introduction of void in the composite. While graphene is found to increase the bonding energies between the fibre and matrix, nanoclay is found to reduce it.

6.3 Recommendations for Future Work

Based on the results and findings of the current study, the following recommendations are proposed:

- To further optimise the prepreg rig for a more effective heating unit and a larger prepreg ply production. The resin bath can benefit from a live magnetic stirrer to prevent possible particle settling. Compaction rollers need to be implemented after fibre impregnation for a better resin infusion, and a reduced thickness variation. Also, to utilise longer impregnation length to avoid excessive slurry running on the drum for faster winding speeds.
- To design and develop a continuous thermoplastic prepreg production line based on the proposed fibre spreading and wet powder impregnation technologies.
- To investigate other high-temperature thermoplastic polymers such as PEKK, PEI and PPS in manufacture of high-performance prepregs, and determine suitability with the L2O carrier.
- To investigate other reinforcing fibres such as carbon fibre in manufacture of high-performance prepregs and to determine combability of the prepreg rig and the manufacturing procedure for use with different reinforcements.
- To study other physical properties of the prepreg samples including measurable fibre breakage and fibre waviness.
- To carry out extended mechanical tests on the manufactured composites including compression, in-plane shear and impact tests. Such tests should be

carried out in different directions for a better understanding of the mechanical behaviour of the material.

- To consider and evaluate other experiments, with regards to the suitability of the manufactured composites for use in fuselage production, such as smoke emission and fire retardancy tests.
- To further study the effect of Nanene and nanoclay on physical and mechanical properties of the nanocomposites. Other prepregs such as 20 wt% slurry setting to be investigated with the addition of nanomaterials and compared to 10 wt% setting.
- To incorporate other nanomaterials like CNTs in the manufactured prepregs to understand their effects on physical and mechanical properties of composites.
- To produce thin-ply prepreg sheets using the proposed fibre spreader assembly for manufacture of ultra-light composite laminates and explore possible enhancements in their mechanical properties compared to casual laminates.
- To develop new composite structures, such as fibre metal laminates with different alloys, using the manufactured thermoplastic prepregs and examine their potential for use in high-temperature fuselage parts.